Density Model for Sperm Whale (*Physeter macrocephalus*) for the U.S. East Coast: Supplementary Report

Duke University Marine Geospatial Ecology Lab*

Model Version 6.4 - 2016-04-21

Citation

When referencing our methodology or results generally, please cite our open-access article:

Roberts JJ, Best BD, Mannocci L, Fujioka E, Halpin PN, Palka DL, Garrison LP, Mullin KD, Cole TVN, Khan CB, McLellan WM, Pabst DA, Lockhart GG (2016) Habitat-based cetacean density models for the U.S. Atlantic and Gulf of Mexico. Scientific Reports 6: 22615. doi: 10.1038/srep22615

To reference this specific model or Supplementary Report, please cite:

Roberts JJ, Best BD, Mannocci L, Fujioka E, Halpin PN, Palka DL, Garrison LP, Mullin KD, Cole TVN, Khan CB, McLellan WM, Pabst DA, Lockhart GG (2016) Density Model for Sperm Whale (*Physeter macrocephalus*) for the U.S. East Coast Version 6.4, 2016-04-21, and Supplementary Report. Marine Geospatial Ecology Lab, Duke University, Durham, North Carolina.

Copyright and License

Revision History

Version	Date	Description of changes
1	2014-05-12	Initial version.
2	2014-09-02	Added surveys: NJ-DEP, Virginia Aquarium, NARWSS 2013, UNCW 2013. Extended study area up Scotian Shelf. Added SEAPODYM predictors. Switched to mgcv estimation of Tweedie p parameter (family=tw()). Switched to year-round model.
3	2014-10-13	Added Palka (2006) survey-specific g(0) estimates. Updated distance to eddy predictors using Chelton et al.'s 2014 database. Removed distance to eddy predictors from shelf model; added distance to canyon predictor. Removed wind speed predictor from all models. Fixed missing pixels in several climatological predictors, which led to not all segments being utilized. Eliminated Cape Cod Bay subregion (combined it with Shelf).
4	2014-11-21	Reconfigured detection hierarchy and adjusted NARWSS detection functions based on additional information from Tim Cole. Removed CumVGPM180 predictor. Updated documentation.
5	2014-12-04	Fixed bug that applied the wrong detection function to segments NE_narwss_1999_widgeon_hapo dataset. Refitted Shelf model. Updated documentation.
6	2014-01-18	Switched from DistToCanyon to DistToCanyonOrSeamount predictor, to reduce edge effects with AFTT model.

*For questions, or to offer feedback about this model or report, please contact Jason Roberts (jason.roberts@duke.edu)

6.1	2015-02-02	Updated the documentation. No changes to the model.
6.2	2015-05-14	Updated calculation of CVs. Switched density rasters to logarithmic breaks. No changes to the model.
6.3	2015-09-21	Updated the documentation. No changes to the model.
6.4	2016-04-21	Switched calculation of monthly 5% and 95% confidence interval rasters to the method used to produce the year-round rasters. (We intended this to happen in version 6.2 but I did not implement it properly.) No changes to the other rasters or the model itself.

Survey Data

Survey	Period	Length (1000 km)	Hours	Sightings
NEFSC Aerial Surveys	1995-2008	70	412	20
NEFSC NARWSS Harbor Porpoise Survey	1999-1999	6	36	0
NEFSC North Atlantic Right Whale Sighting Survey	1999-2013	432	2330	73
NEFSC Shipboard Surveys	1995-2004	16	1143	245
NJDEP Aerial Surveys	2008-2009	11	60	0
NJDEP Shipboard Surveys	2008-2009	14	836	0
SEFSC Atlantic Shipboard Surveys	1992-2005	28	1731	137
SEFSC Mid Atlantic Tursiops Aerial Surveys	1995-2005	35	196	0
SEFSC Southeast Cetacean Aerial Surveys	1992-1995	8	42	0
UNCW Cape Hatteras Navy Surveys	2011-2013	19	125	16
UNCW Early Marine Mammal Surveys	2002-2002	18	98	1
UNCW Jacksonville Navy Surveys	2009-2013	66	402	1
UNCW Onslow Navy Surveys	2007-2011	49	282	0
UNCW Right Whale Surveys	2005-2008	114	586	8
Virginia Aquarium Aerial Surveys	2012-2014	9	53	0
Total		895	8332	501

Table 2: Survey effort and sightings used in this model. Effort is tallied as the cumulative length of on-effort transects and hours the survey team was on effort. Sightings are the number of on-effort encounters of the modeled species for which a perpendicular sighting distance (PSD) was available. Off effort sightings and those without PSDs were omitted from the analysis.

Season	Months	Length (1000 km)	Hours	Sightings
All_Year	All	897	8332	501

Table 3: Survey effort and on-effort sightings having perpendicular sighting distances.

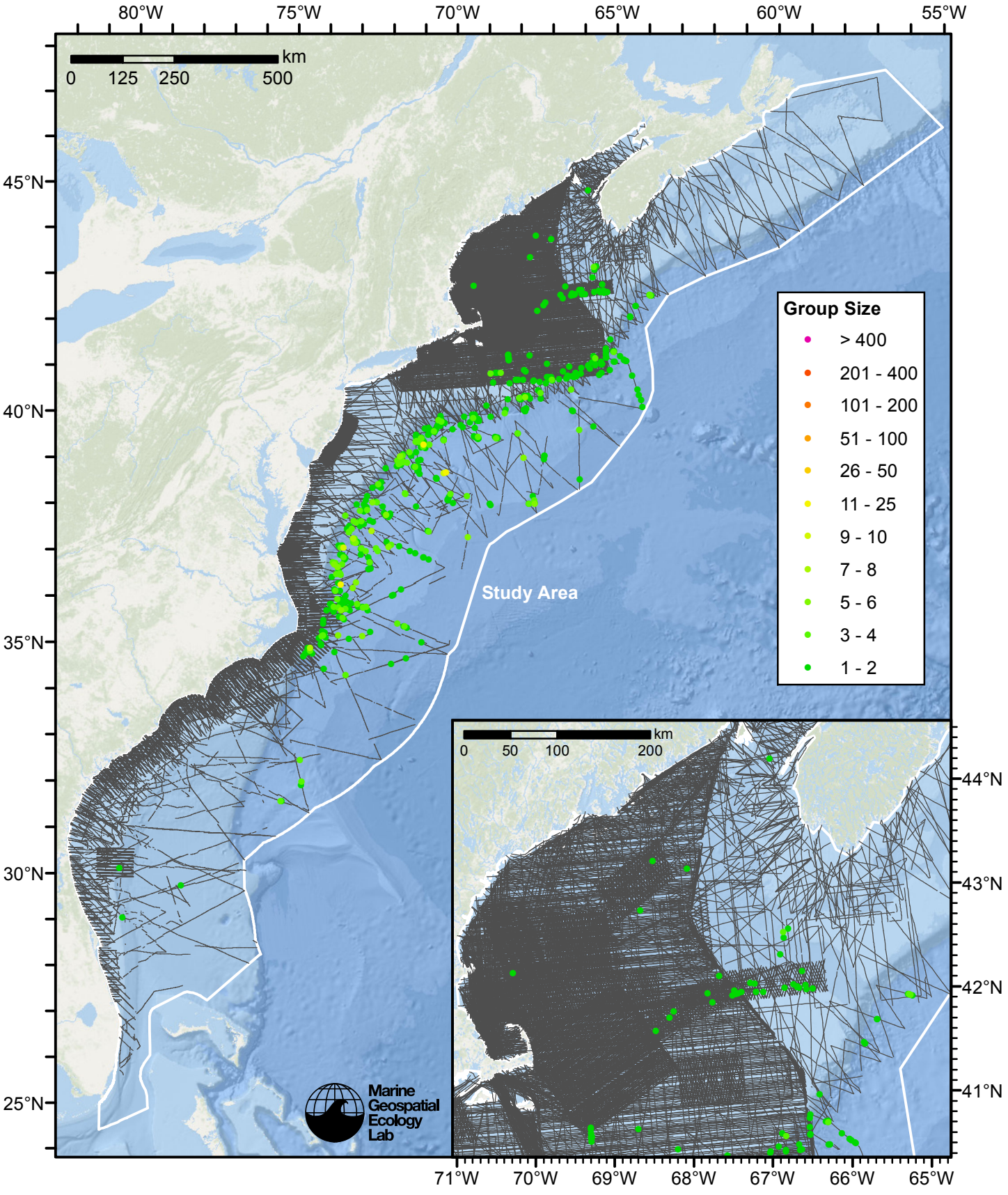

Figure 1: Sperm whale sightings and survey tracklines.

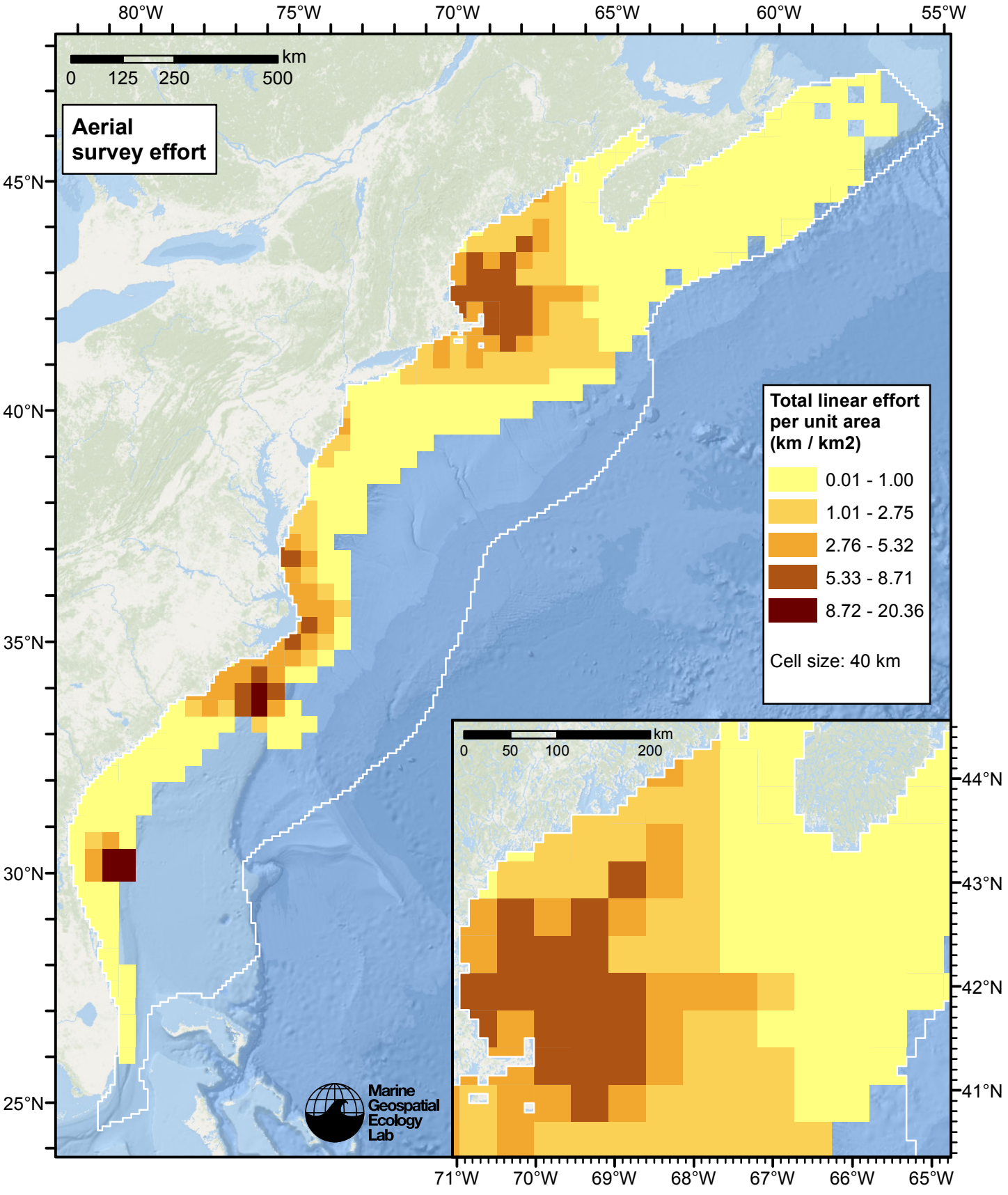

Figure 2: Aerial linear survey effort per unit area.

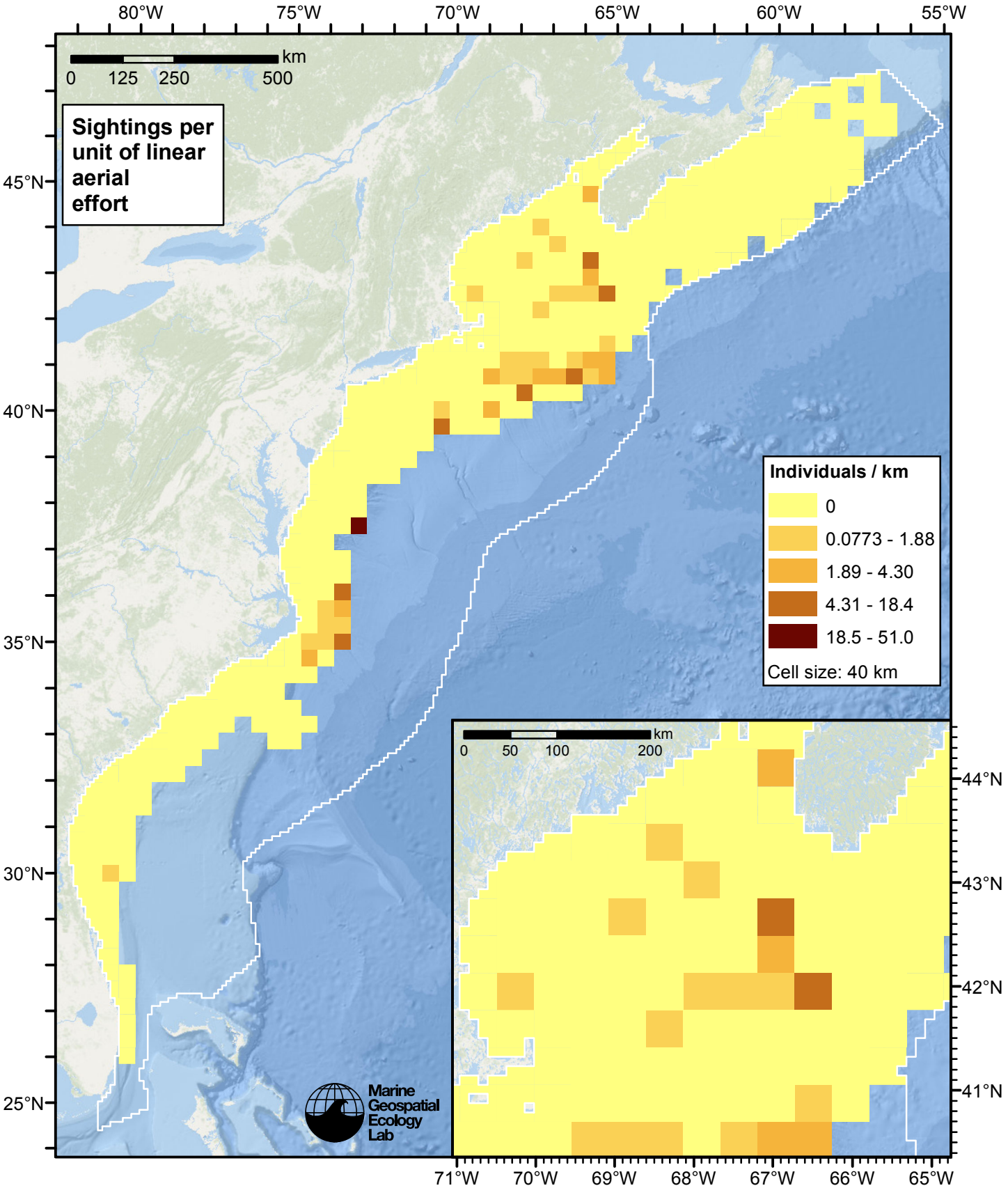

Figure 3: Sperm whale sightings per unit aerial linear survey effort.

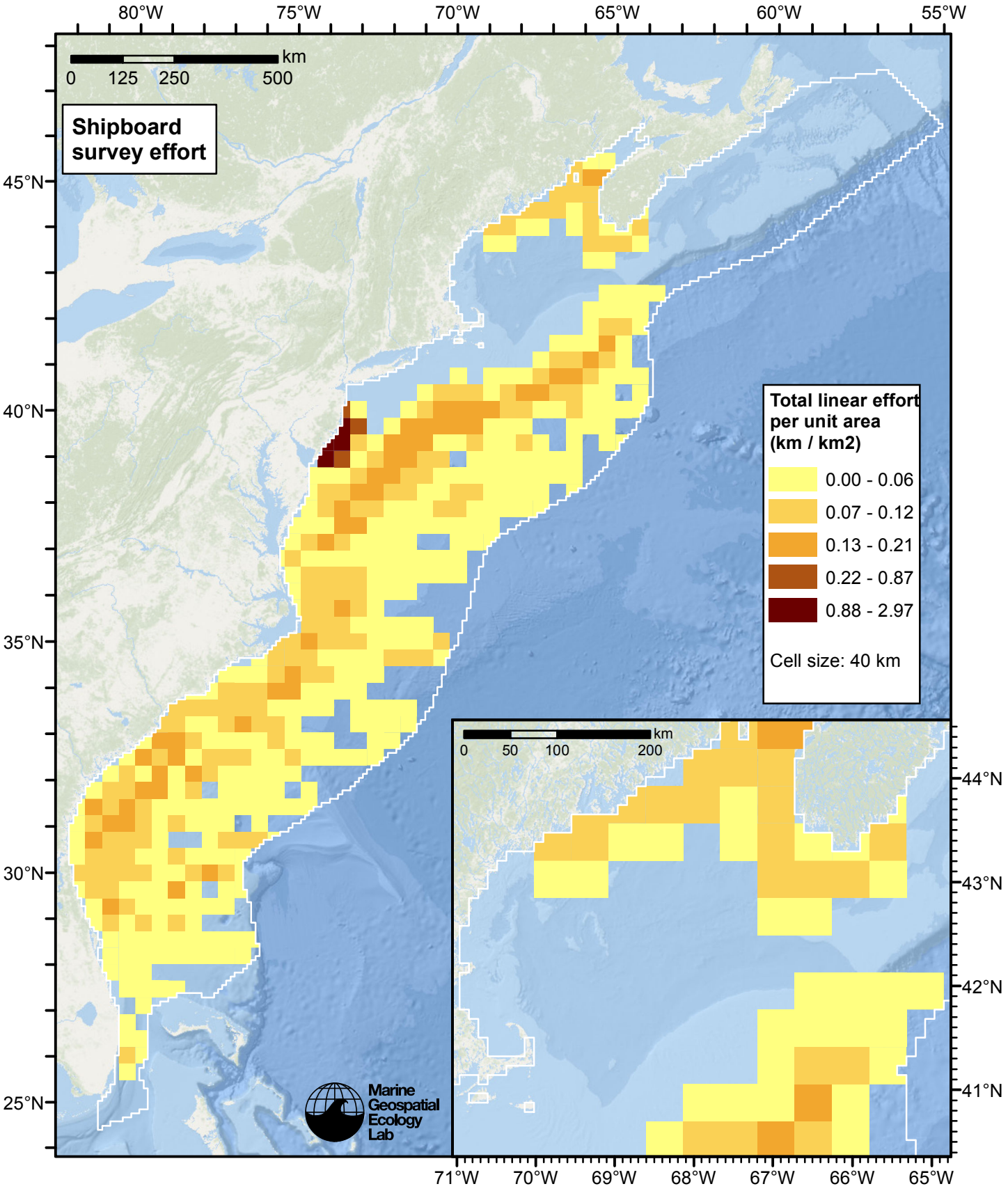

Figure 4: Shipboard linear survey effort per unit area.

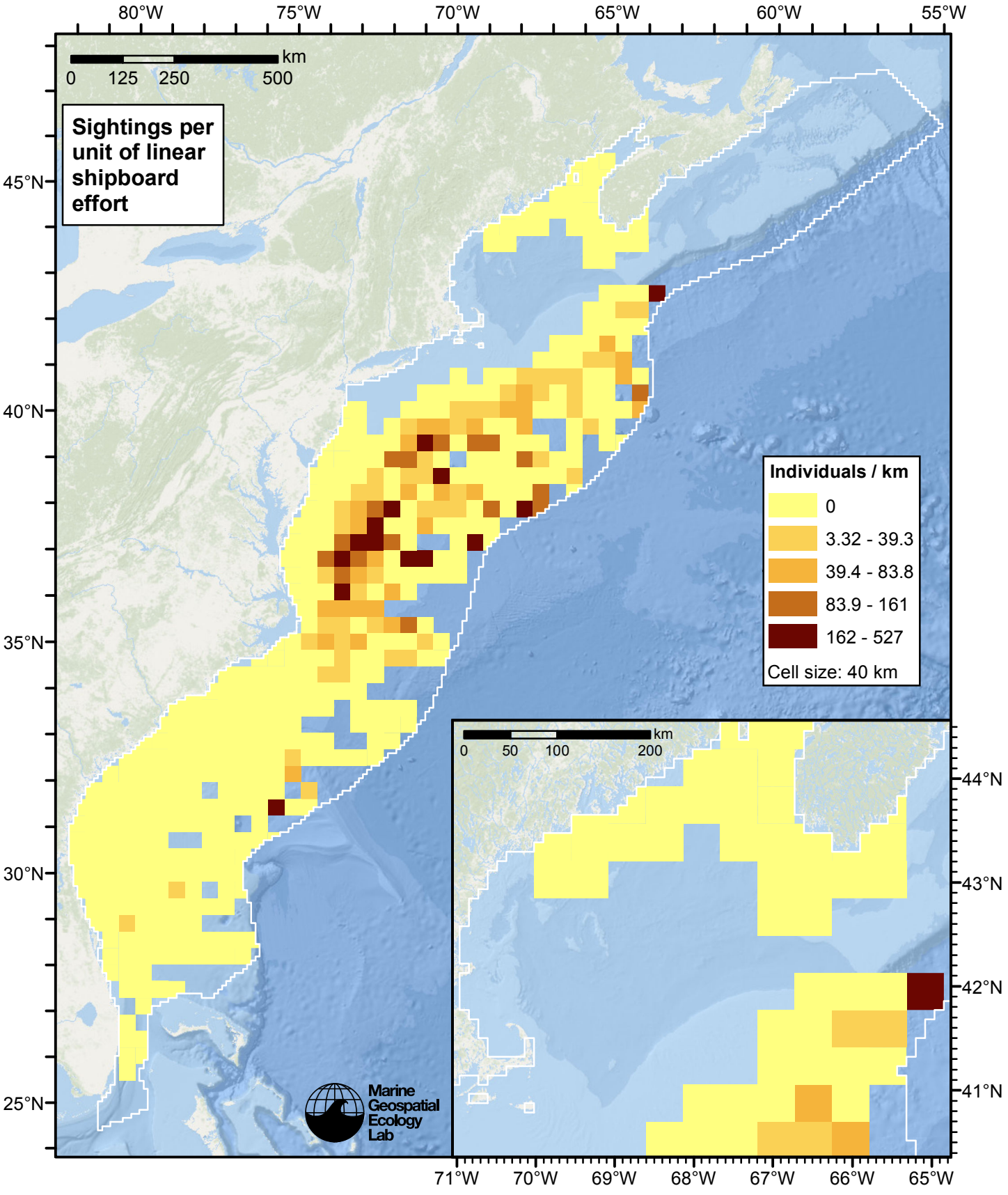

Figure 5: Sperm whale sightings per unit shipboard linear survey effort.

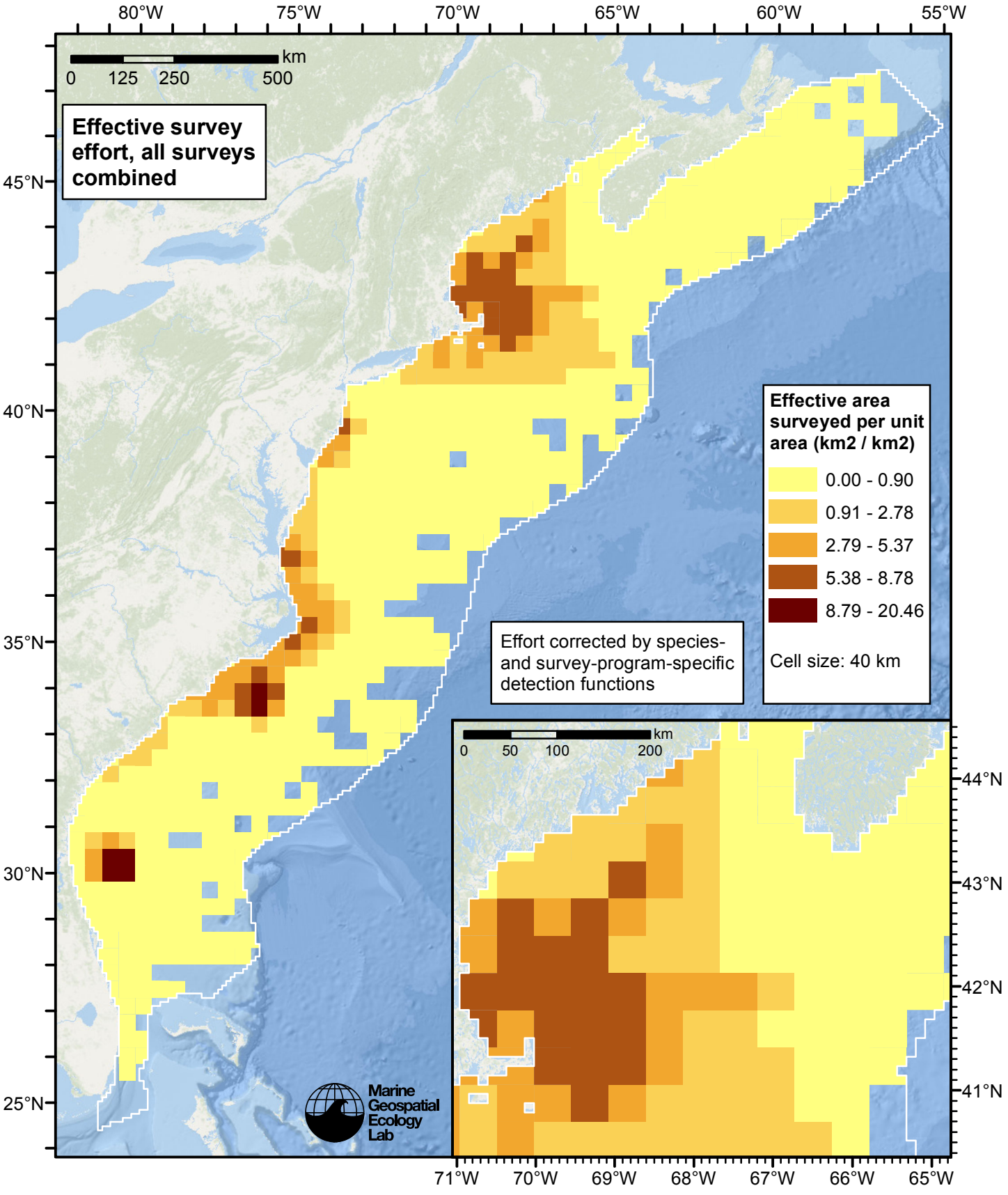

Figure 6: Effective survey effort per unit area, for all surveys combined. Here, effort is corrected by the species- and survey-program-specific detection functions used in fitting the density models.

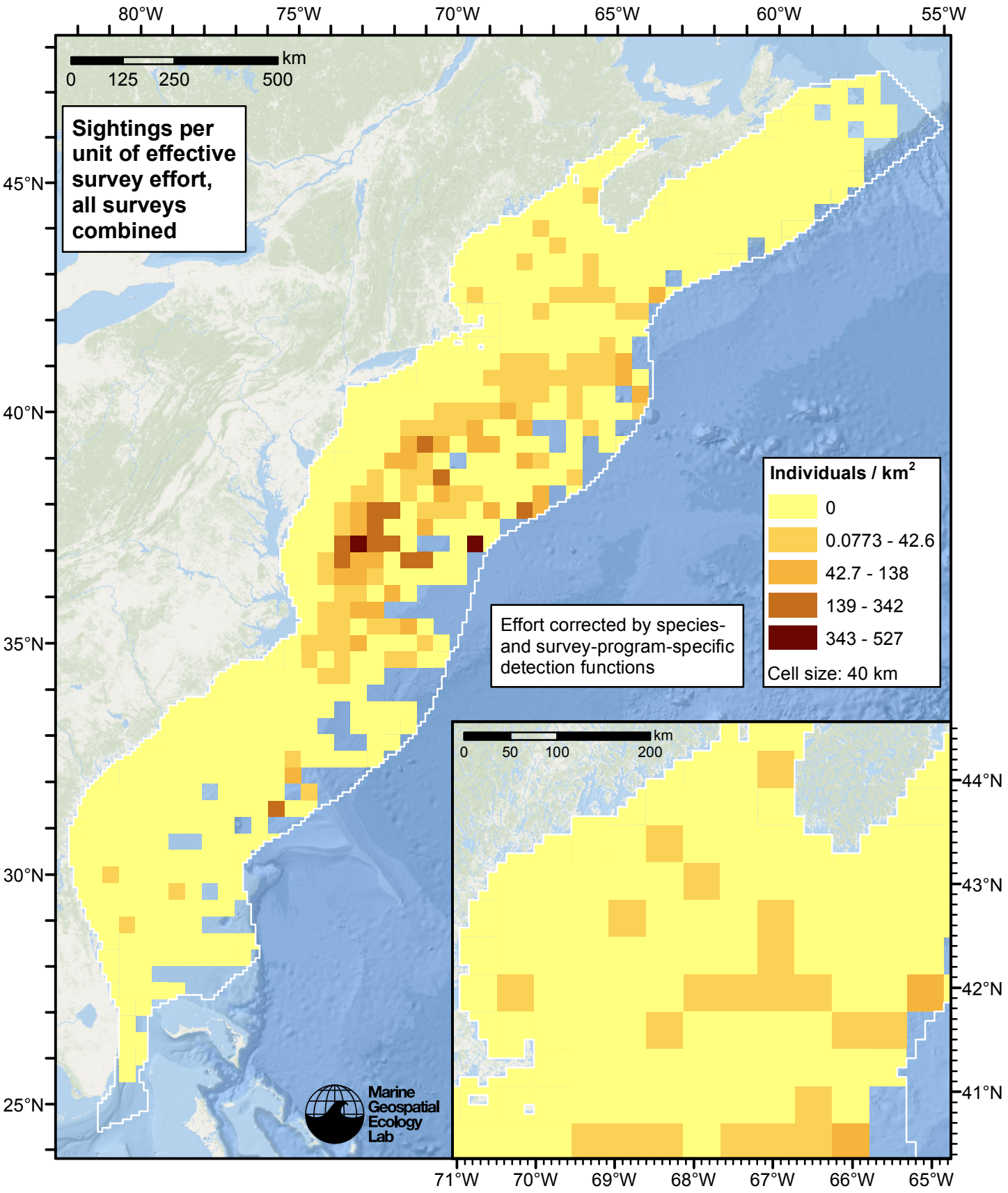

Figure 7: Sperm whale sightings per unit of effective survey effort, for all surveys combined. Here, effort is corrected by the species- and survey-program-specific detection functions used in fitting the density models.

Detection Functions

The detection hierarchy figures below show how sightings from multiple surveys were pooled to try to achieve Buckland et. al's (2001) recommendation that at least 60-80 sightings be used to fit a detection function. Leaf nodes, on the right, usually represent individual surveys, while the hierarchy to the left shows how they have been grouped according to how similar we believed the surveys were to each other in their detection performance.

At each node, the red or green number indicates the total number of sightings below that node in the hierarchy, and is colored green if 70 or more sightings were available, and red otherwise. If a grouping node has zero sightings–i.e. all of the surveys within it had zero sightings–it may be collapsed and shown as a leaf to save space.

Each histogram in the figure indicates a node where a detection function was fitted. The actual detection functions do not appear in this figure; they are presented in subsequent sections. The histogram shows the frequency of sightings by perpendicular sighting distance for all surveys contained by that node. Each survey (leaf node) recieves the detection function that is closest to it up the hierarchy. Thus, for common species, sufficient sightings may be available to fit detection functions deep in the hierarchy, with each function applying to only a few surveys, thereby allowing variability in detection performance between surveys to be addressed relatively finely. For rare species, so few sightings may be available that we have to pool many surveys together to try to meet Buckland's recommendation, and fit only a few coarse detection functions high in the hierarchy.

A blue Proxy Species tag indicates that so few sightings were available that, rather than ascend higher in the hierarchy to a point that we would pool grossly-incompatible surveys together, (e.g. shipboard surveys that used big-eye binoculars with those that used only naked eyes) we pooled sightings of similar species together instead. The list of species pooled is given in following sections.

Shipboard Surveys

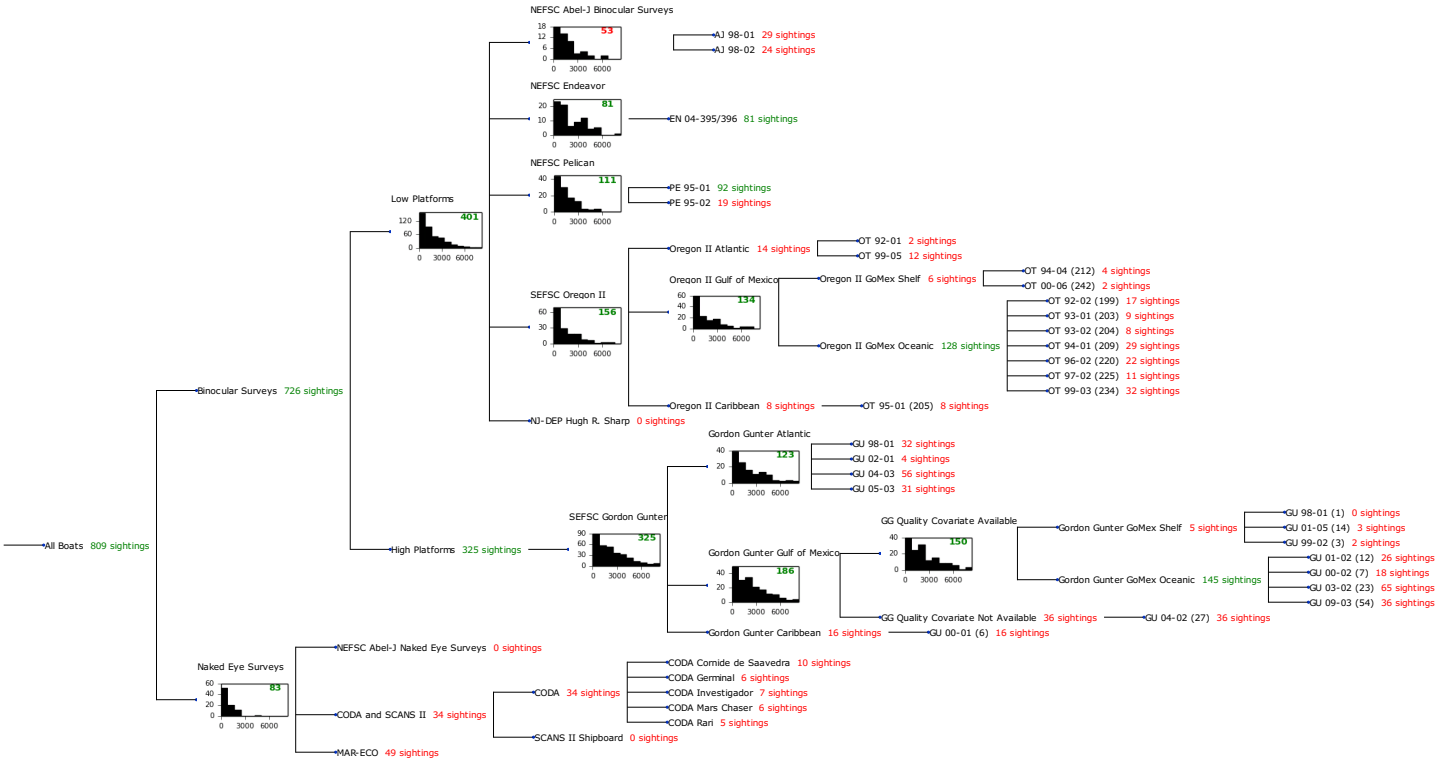

Figure 8: Detection hierarchy for shipboard surveys

Low Platforms

The sightings were right truncated at 8000m.

Covariate	Description
beaufort	Beaufort sea state.
size	Estimated size (number of individuals) of the sighted group.
vessel	Vessel from which the observation was made. This covariate allows the detection function to account for vessel-specific biases, such as the height of the survey platform.

Table 4: Covariates tested in candidate "multi-covariate distance sampling" (MCDS) detection functions.

Key	Adjustment	Order	Covariates	Succeeded	Δ AIC	Mean ESHW (m)
hr	poly	2		Yes	0.00	1988
hr	poly	4		Yes	3.32	2055
hn			beaufort, vessel	Yes	9.05	2809
hr			vessel	Yes	14.40	2298
hn			beaufort	Yes	14.44	2823
hr			vessel, size	Yes	14.99	2278
hn			vessel	Yes	15.40	2820
hr			beaufort, vessel	Yes	16.30	2312
hr				Yes	16.42	2209
hr			beaufort, vessel, size	Yes	16.94	2288
hr			beaufort	Yes	17.78	2241
hr			size	Yes	17.98	2194
hr			beaufort, size	Yes	19.35	2227
hn				Yes	19.65	2833
hn	cos	3		Yes	21.55	2830
hn	cos	2		Yes	21.59	2831
hn	cos	1		Yes	21.65	2832
hn	herm	4		Yes	21.65	2833
hn			size	No		
hn			beaufort, size	No		
hn			vessel, size	No		
hn			beaufort, vessel, size	No		

Table 5: Candidate detection functions for Low Platforms. The first one listed was selected for the density model.

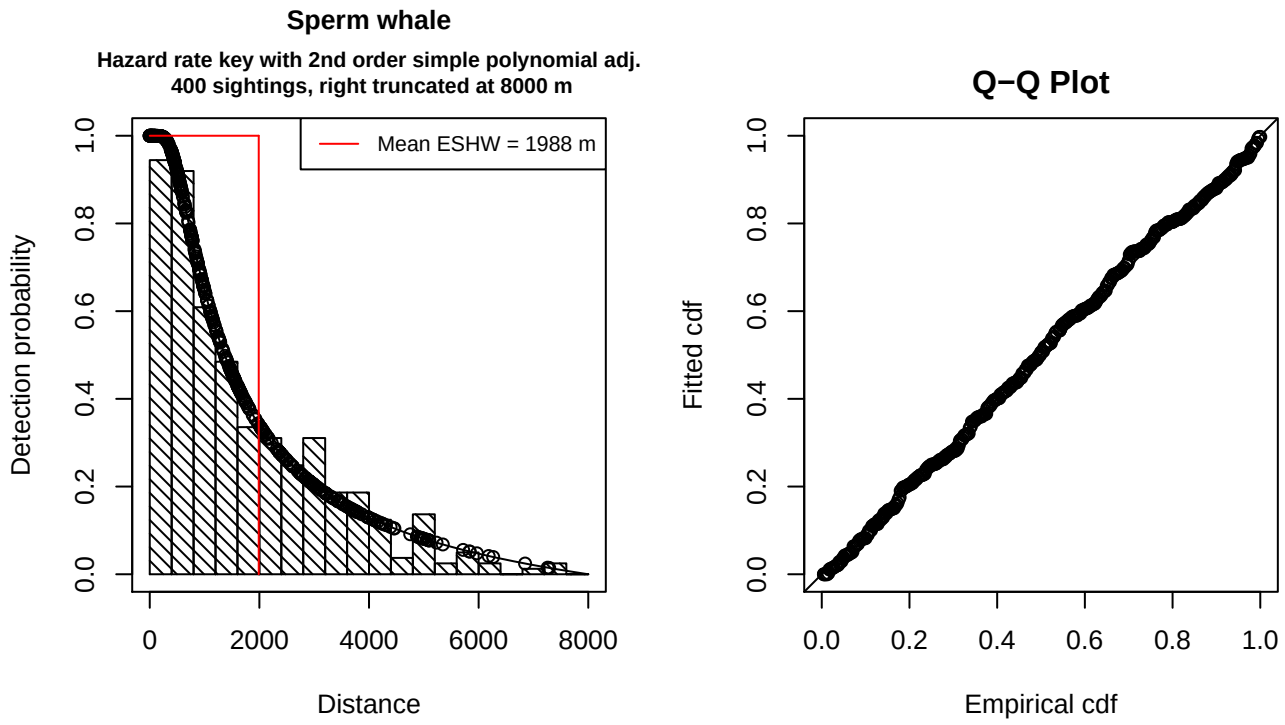

Figure 9: Detection function for Low Platforms that was selected for the density model

Statistical output for this detection function:

```
Summary for ds object
Number of observations :  400
Distance range         :  0  -  8000
AIC                    :  6739.341

Detection function:
 Hazard-rate key function with simple polynomial adjustment term of order 2

Detection function parameters
Scale Coefficients:
            estimate       se
(Intercept) 6.962142 0.2011639

Shape parameters:
             estimate        se
(Intercept) 0.2250844 0.1487208

Adjustment term parameter(s):
                estimate        se
poly, order 2 -0.9999962 0.1562196


Strict monotonicity constraints were enforced.
                         Estimate           SE         CV
Average p               0.2485251   0.02403792 0.09672232
N in covered region 1609.4955405 170.59054831 0.10599007

Strict monotonicity constraints were enforced.
```

Additional diagnostic plots:

Figure 10: Scatterplots showing the relationship between Beaufort sea state and perpendicular sighting distance, for all sightings (left) and only those not right truncated (right). The line is a simple linear regression.

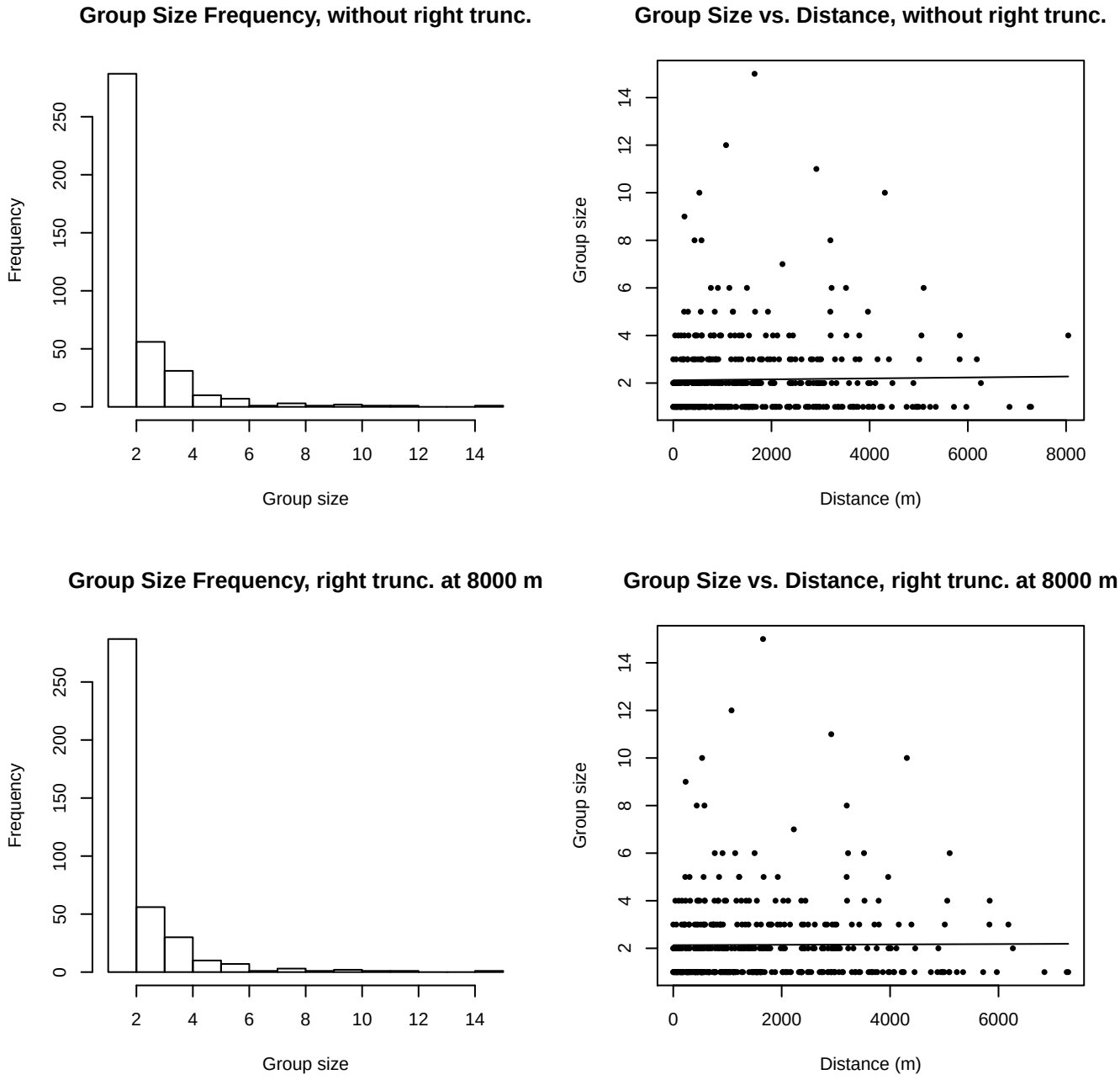

Figure 11: Histograms showing group size frequency and scatterplots showing the relationship between group size and perpendicular sighting distance, for all sightings (top row) and only those not right truncated (bottom row). In the scatterplot, the line is a simple linear regression.

NEFSC Abel-J Binocular Surveys

The sightings were right truncated at 5000m.

Covariate	Description
beaufort	Beaufort sea state.
quality	Survey-specific index of the quality of observation conditions, utilizing relevant factors other than Beaufort sea state (see methods).
size	Estimated size (number of individuals) of the sighted group.

Table 6: Covariates tested in candidate "multi-covariate distance sampling" (MCDS) detection functions.

Key	Adjustment	Order	Covariates	Succeeded	Δ AIC	Mean ESHW (m)
hn				Yes	0.00	2549
hr				Yes	1.61	2647
hn			quality	Yes	1.80	2547
hn			size	Yes	1.91	2553
hn	cos	2		Yes	2.00	2548
hn	cos	3		Yes	2.00	2549
hn	cos	1		Yes	2.00	2549
hn	herm	4		Yes	2.00	2549
hr			quality	Yes	2.53	2669
hr			quality, size	Yes	2.86	2481
hr			size	Yes	3.30	2529
hn			quality, size	Yes	3.45	2581
hr	poly	2		Yes	3.61	2637
hr	poly	4		Yes	3.61	2646
hr			beaufort, size	Yes	3.75	2321
hn			beaufort, quality	Yes	3.80	2547
hr			beaufort, quality, size	Yes	4.49	2482
hn			beaufort, quality, size	Yes	5.13	2694
hr			beaufort	No		
hn			beaufort	No		
hr			beaufort, quality	No		
hn			beaufort, size	No		

Table 7: Candidate detection functions for NEFSC Abel-J Binocular Surveys. The first one listed was selected for the density model.

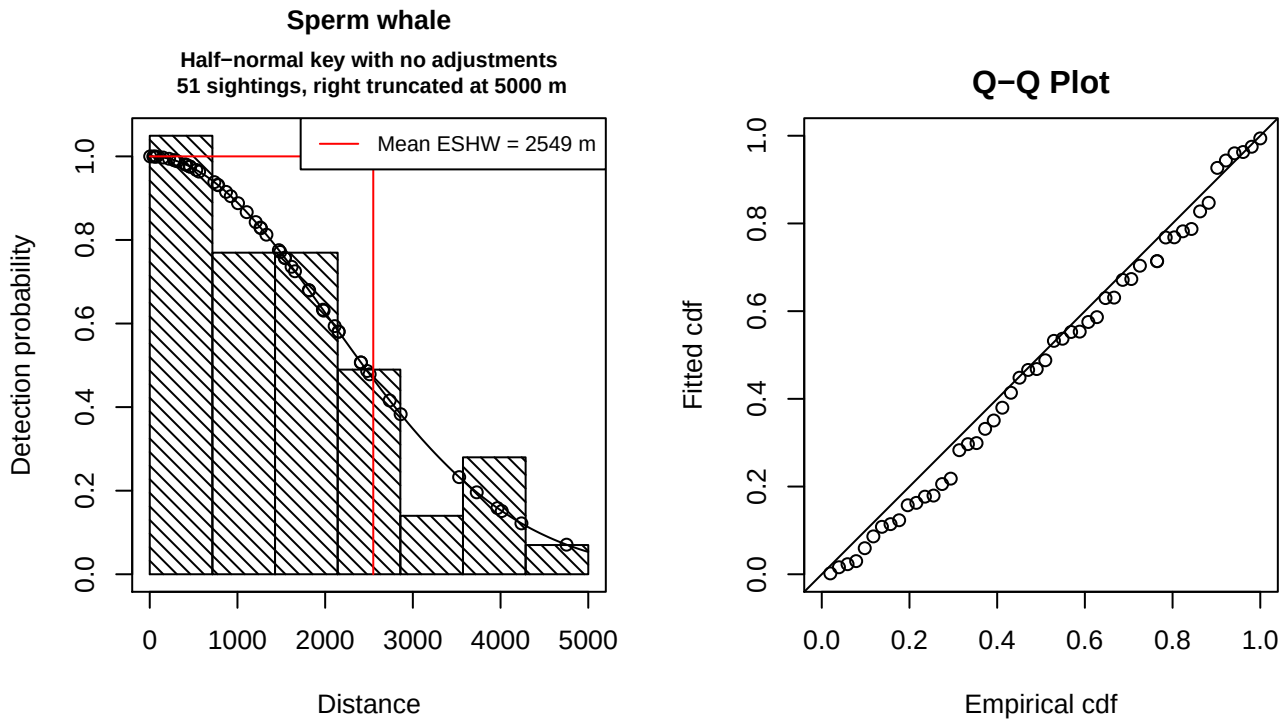

Figure 12: Detection function for NEFSC Abel-J Binocular Surveys that was selected for the density model

Statistical output for this detection function:

```
Summary for ds object
Number of observations :  51
Distance range         :  0  -  5000
AIC                    :  847.6728

Detection function:
 Half-normal key function

Detection function parameters
Scale Coefficients:
            estimate        se
(Intercept) 7.633101 0.1149616

                       Estimate         SE        CV
Average p             0.5097075  0.0524591 0.1029200
N in covered region 100.0573845 14.2229752 0.1421482
```

Additional diagnostic plots:

Figure 13: Scatterplots showing the relationship between Beaufort sea state and perpendicular sighting distance, for all sightings (left) and only those not right truncated (right). The line is a simple linear regression.

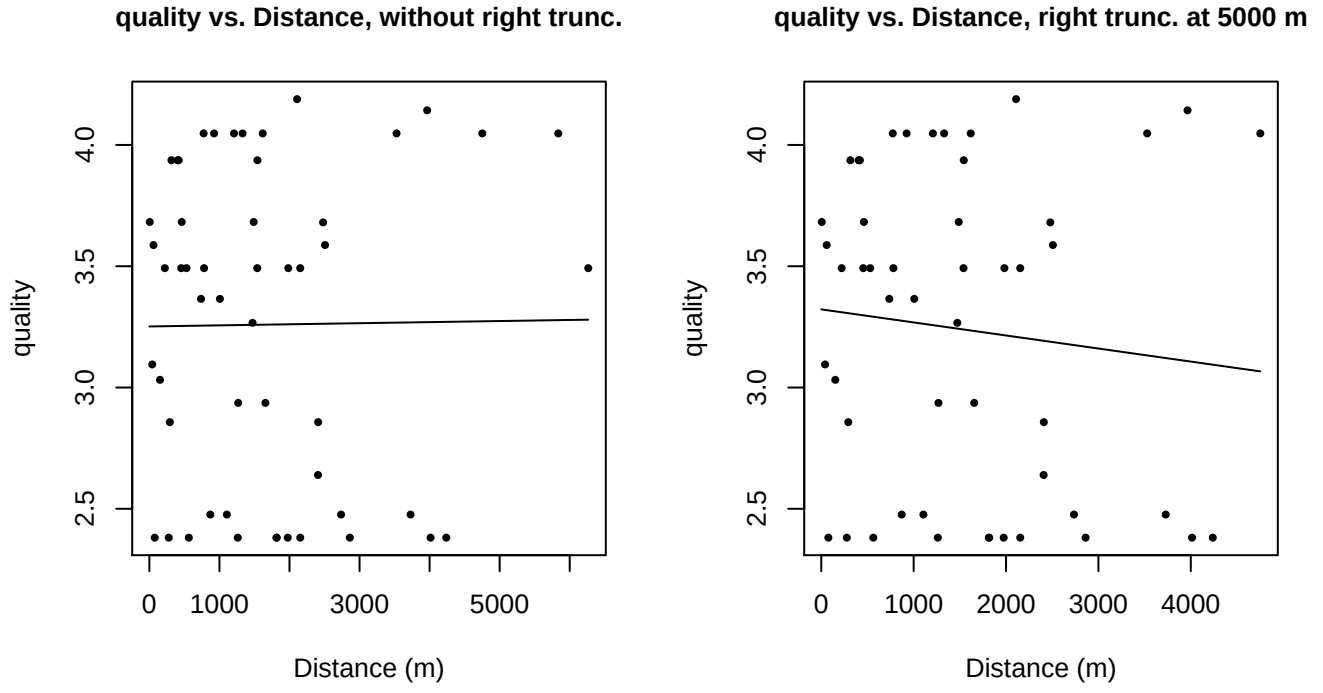

Figure 14: Scatterplots showing the relationship between the survey-specific index of the quality of observation conditions and perpendicular sighting distance, for all sightings (left) and only those not right truncated (right). Low values of the quality index correspond to better observation conditions. The line is a simple linear regression.

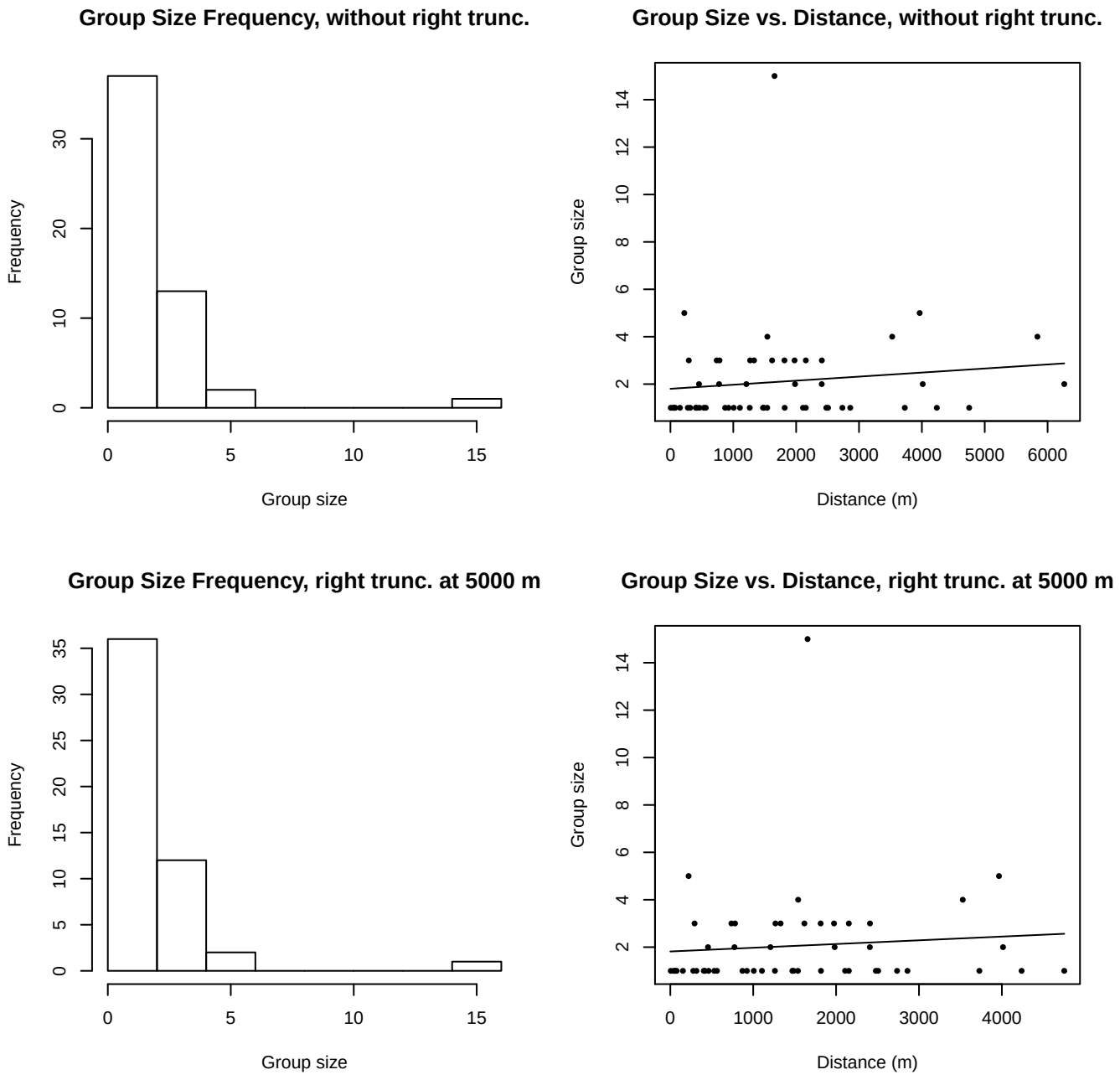

Figure 15: Histograms showing group size frequency and scatterplots showing the relationship between group size and perpendicular sighting distance, for all sightings (top row) and only those not right truncated (bottom row). In the scatterplot, the line is a simple linear regression.

NEFSC Endeavor

The sightings were right truncated at 6000m.

Covariate	Description
beaufort	Beaufort sea state.
quality	Survey-specific index of the quality of observation conditions, utilizing relevant factors other than Beaufort sea state (see methods).
size	Estimated size (number of individuals) of the sighted group.

Table 8: Covariates tested in candidate "multi-covariate distance sampling" (MCDS) detection functions.

Key	Adjustment	Order	Covariates	Succeeded	Δ AIC	Mean ESHW (m)
hn			beaufort	Yes	0.00	3761
hr			beaufort	Yes	1.55	2528
hn			beaufort, size	Yes	1.66	3743
hr				Yes	1.76	2410
hr			size	Yes	2.11	2609
hn				Yes	2.80	3543
hr			beaufort, size	Yes	2.99	2599
hn			size	Yes	4.21	3546
hn	cos	3		Yes	4.80	3542
hn	cos	2		Yes	4.80	3542
hn	cos	1		Yes	4.80	3543
hn	herm	4		Yes	4.80	3543
hr	poly	2		No		
hr	poly	4		No		
hr			quality	No		
hn			quality	No		
hr			beaufort, quality	No		
hn			beaufort, quality	No		
hr			quality, size	No		
hn			quality, size	No		
hr			beaufort, quality, size	No		
hn			beaufort, quality, size	No		

Table 9: Candidate detection functions for NEFSC Endeavor. The first one listed was selected for the density model.

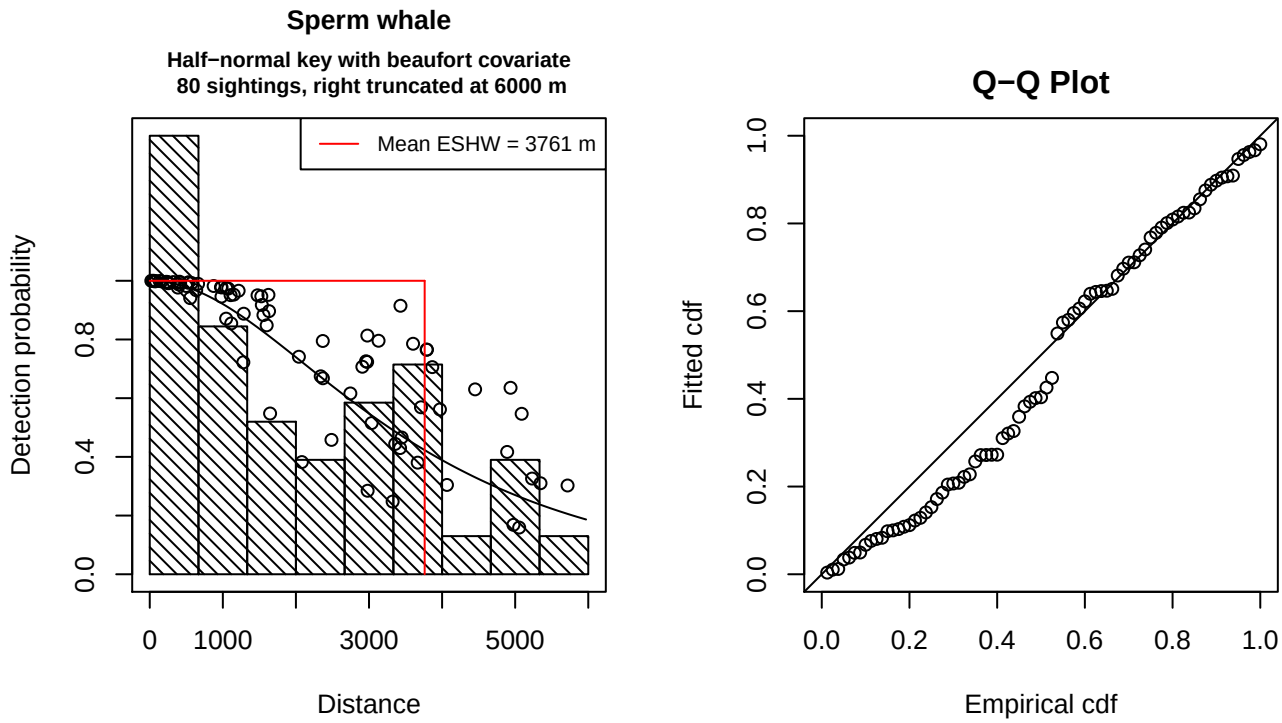

Figure 16: Detection function for NEFSC Endeavor that was selected for the density model

Statistical output for this detection function:

```
Summary for ds object
Number of observations :  80
Distance range         :  0  -  6000
AIC                    :  1369.688

Detection function:
 Half-normal key function

Detection function parameters
Scale Coefficients:
             estimate        se
(Intercept)  9.5673532 0.7776364
beaufort    -0.5633648 0.2585903

                      Estimate          SE        CV
Average p             0.5774728  0.06045764 0.1046935
N in covered region 138.5346618 17.98819815 0.1298462
```

Additional diagnostic plots:

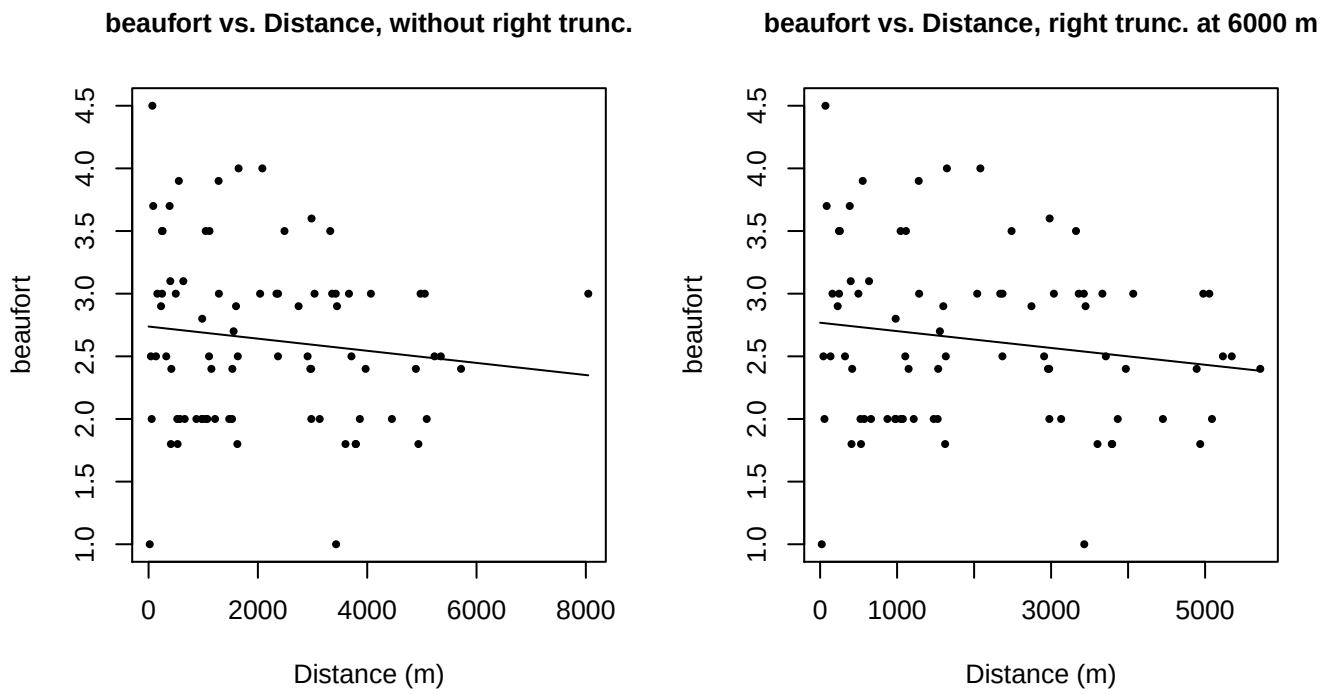

Figure 17: Scatterplots showing the relationship between Beaufort sea state and perpendicular sighting distance, for all sightings (left) and only those not right truncated (right). The line is a simple linear regression.

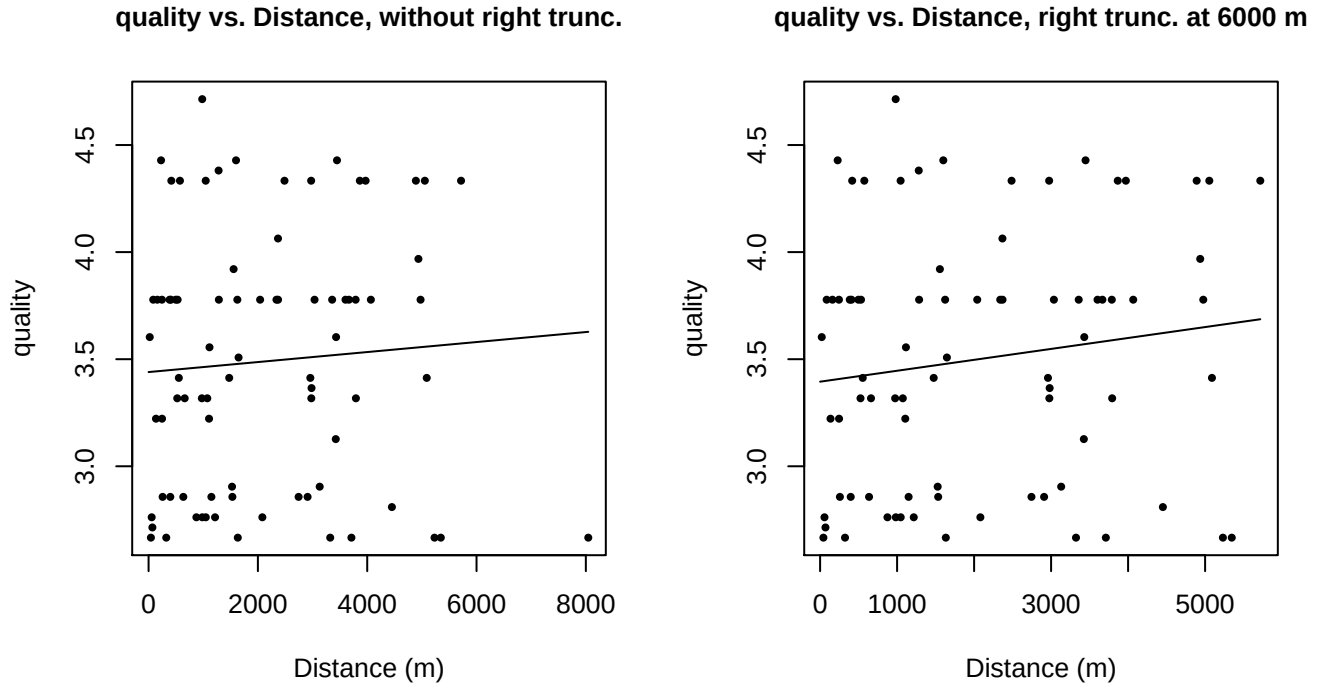

Figure 18: Scatterplots showing the relationship between the survey-specific index of the quality of observation conditions and perpendicular sighting distance, for all sightings (left) and only those not right truncated (right). Low values of the quality index correspond to better observation conditions. The line is a simple linear regression.

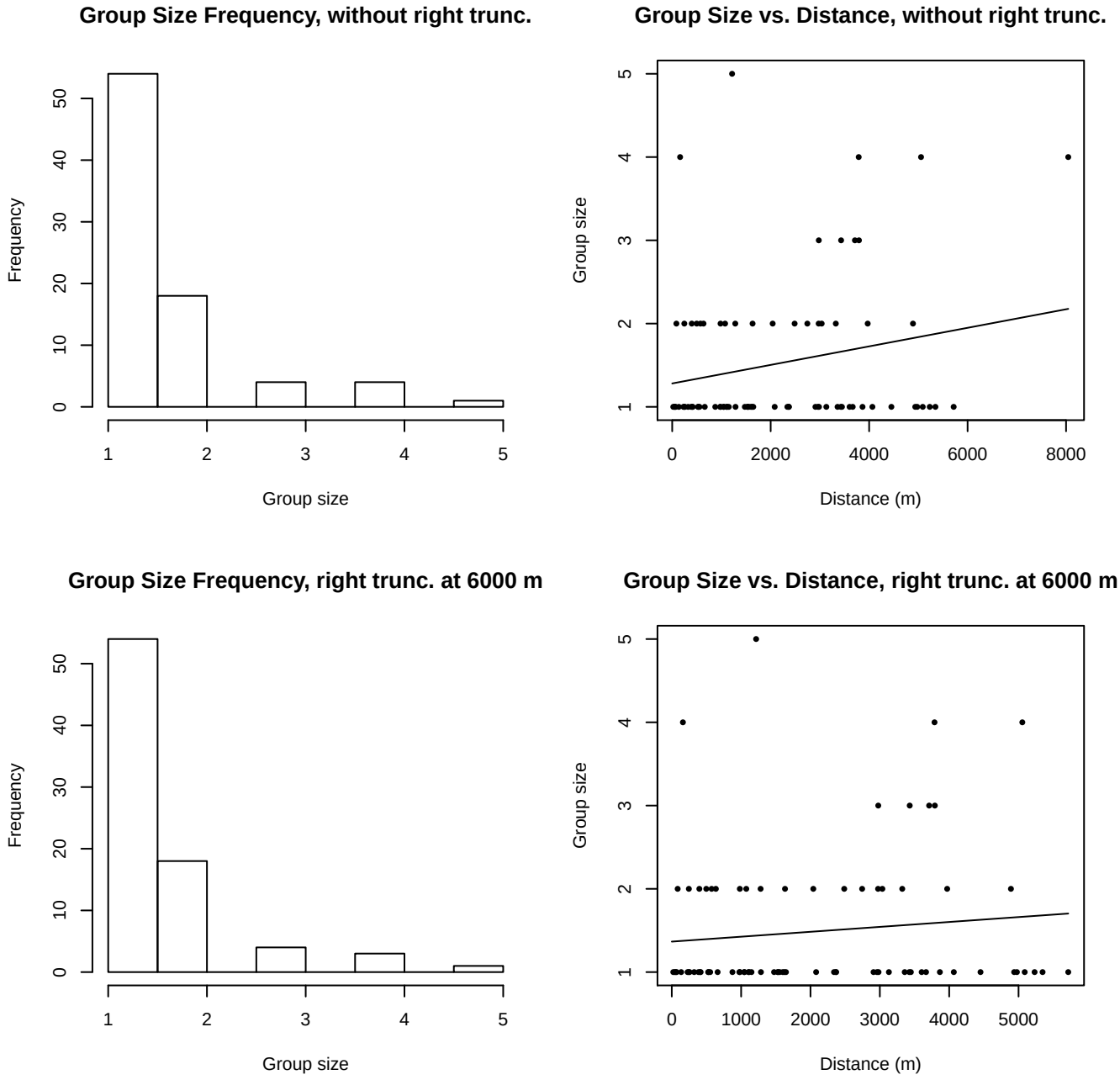

Figure 19: Histograms showing group size frequency and scatterplots showing the relationship between group size and perpendicular sighting distance, for all sightings (top row) and only those not right truncated (bottom row). In the scatterplot, the line is a simple linear regression.

NEFSC Pelican

The sightings were right truncated at 4500m.

Covariate	Description
beaufort	Beaufort sea state.
size	Estimated size (number of individuals) of the sighted group.

Table 10: Covariates tested in candidate "multi-covariate distance sampling" (MCDS) detection functions.

Key	Adjustment	Order	Covariates	Succeeded	Δ AIC	Mean ESHW (m)
hn				Yes	0.00	2154
hn	cos	3		Yes	2.00	2154
hn	cos	2		Yes	2.00	2154
hn	cos	1		Yes	2.00	2154
hn	herm	4		Yes	2.00	2154
hr				Yes	2.84	2090
hr	poly	4		Yes	2.93	2041
hr	poly	2		Yes	3.08	2028
hr			beaufort	No		
hn			beaufort	No		
hr			size	No		
hn			size	No		
hr			beaufort, size	No		
hn			beaufort, size	No		

Table 11: Candidate detection functions for NEFSC Pelican. The first one listed was selected for the density model.

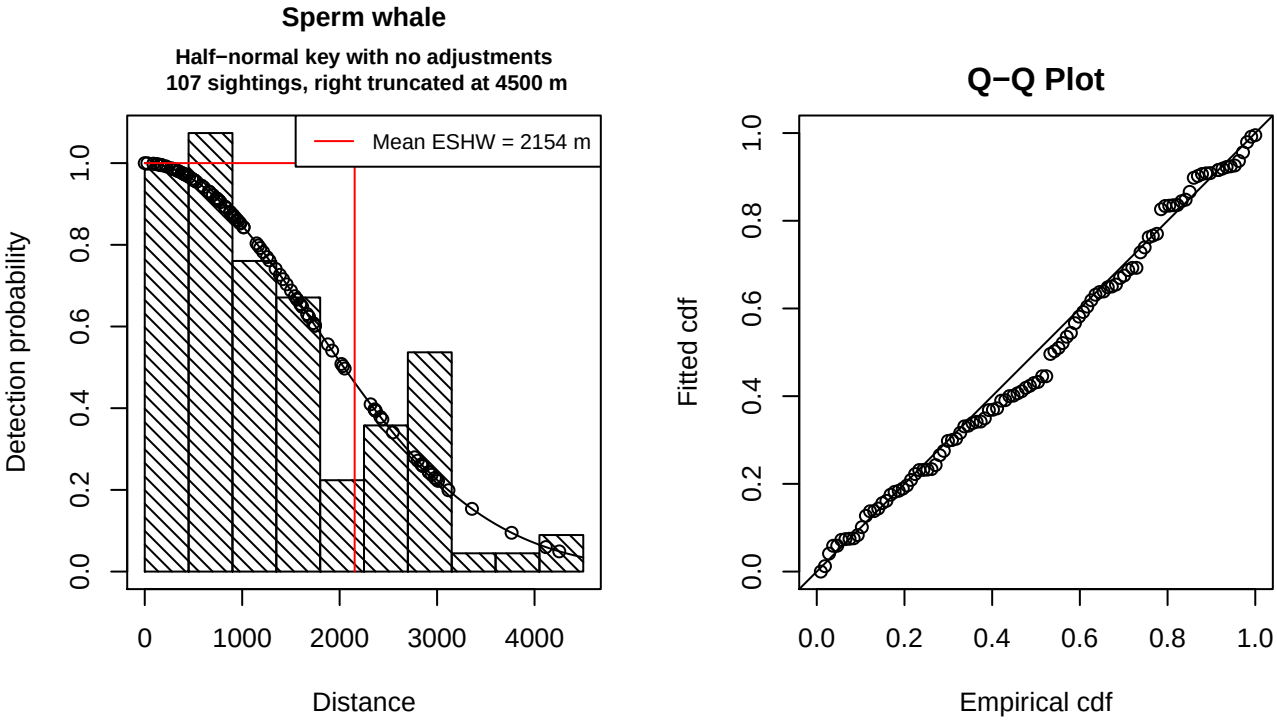

Figure 20: Detection function for NEFSC Pelican that was selected for the density model

Statistical output for this detection function:

```
Summary for ds object
Number of observations :  107
Distance range         :  0  -  4500
AIC                    :  1743.719

Detection function:
 Half-normal key function

Detection function parameters
Scale Coefficients:
            estimate         se
(Intercept) 7.458787 0.07899864

                        Estimate          SE         CV
Average p              0.4786468  0.03506846 0.07326585
N in covered region 223.5468985 22.62173632 0.10119459
```

Additional diagnostic plots:

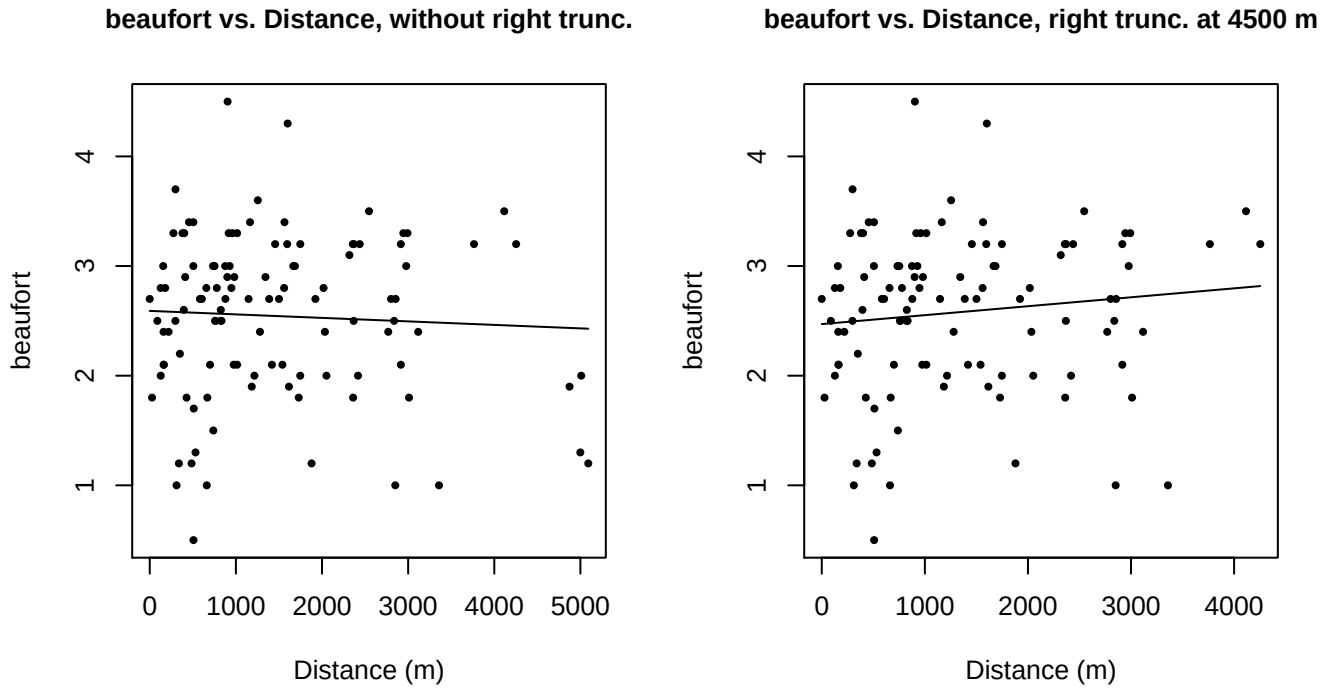

Figure 21: Scatterplots showing the relationship between Beaufort sea state and perpendicular sighting distance, for all sightings (left) and only those not right truncated (right). The line is a simple linear regression.

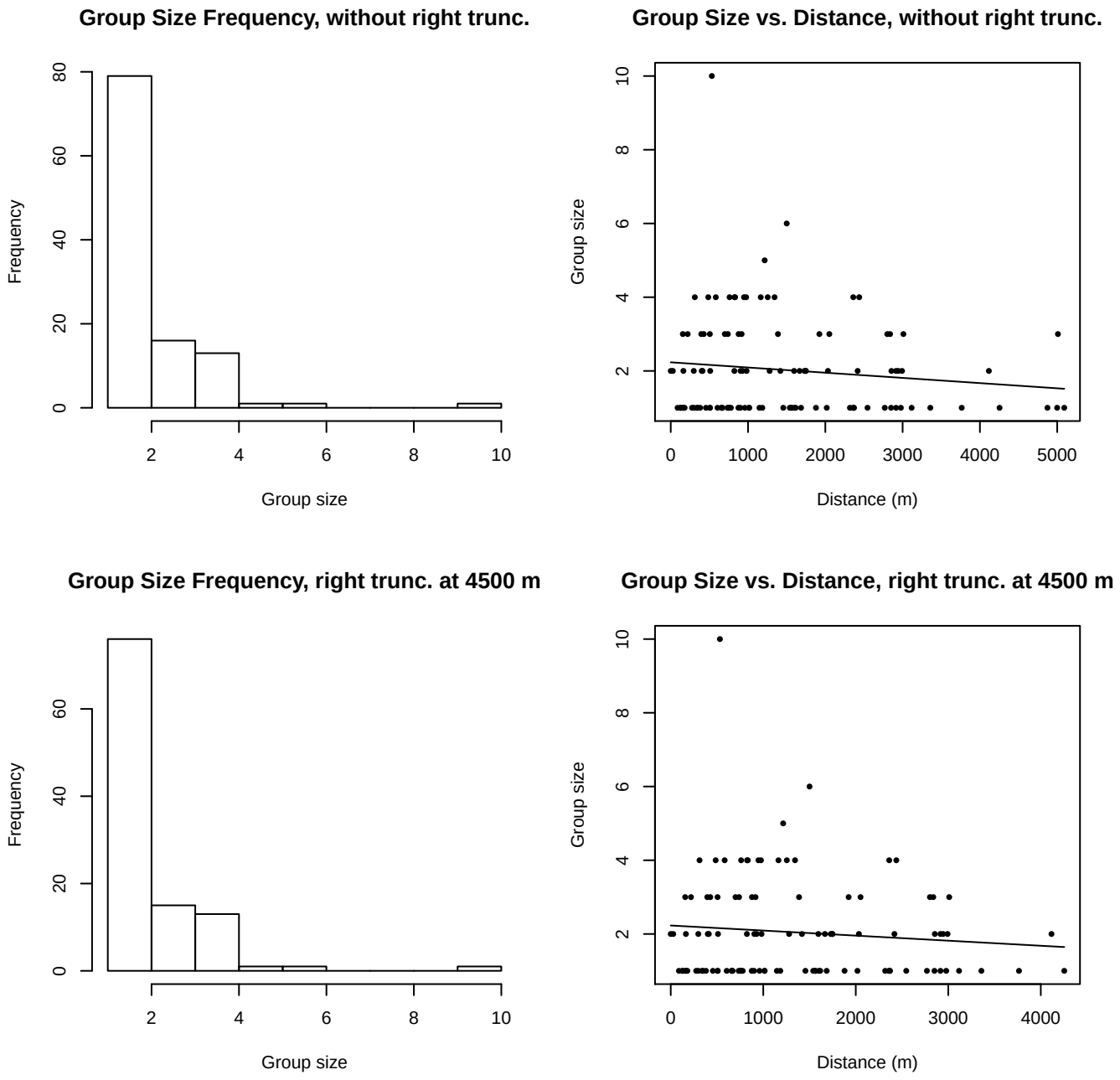

Figure 22: Histograms showing group size frequency and scatterplots showing the relationship between group size and perpendicular sighting distance, for all sightings (top row) and only those not right truncated (bottom row). In the scatterplot, the line is a simple linear regression.

SEFSC Oregon II

The sightings were right truncated at 7000m.

Covariate	Description
beaufort	Beaufort sea state.
quality	Survey-specific index of the quality of observation conditions, utilizing relevant factors other than Beaufort sea state (see methods).
size	Estimated size (number of individuals) of the sighted group.

Table 12: Covariates tested in candidate "multi-covariate distance sampling" (MCDS) detection functions.

Key	Adjustment	Order	Covariates	Succeeded	Δ AIC	Mean ESHW (m)
hr			quality	Yes	0.00	1865
hr			quality, size	Yes	0.81	1857
hr	poly	4		Yes	6.23	1521
hr				Yes	7.40	1643
hr			size	Yes	7.50	1662
hn			beaufort, quality	Yes	8.70	2717
hn			beaufort, quality, size	Yes	9.31	2742
hr	poly	2		Yes	9.40	1643
hn			quality	Yes	9.86	2742
hn			quality, size	Yes	10.13	2772
hn			beaufort	Yes	20.18	2707
hn			beaufort, size	Yes	22.08	2706
hn				Yes	22.49	2715
hn			size	Yes	24.23	2714
hn	cos	3		Yes	24.45	2712
hn	cos	2		Yes	24.46	2713
hn	cos	1		Yes	24.49	2714
hn	herm	4		Yes	24.49	2714
hr			beaufort	No		
hr			beaufort, quality	No		
hr			beaufort, size	No		
hr			beaufort, quality, size	No		

Table 13: Candidate detection functions for SEFSC Oregon II. The first one listed was selected for the density model.

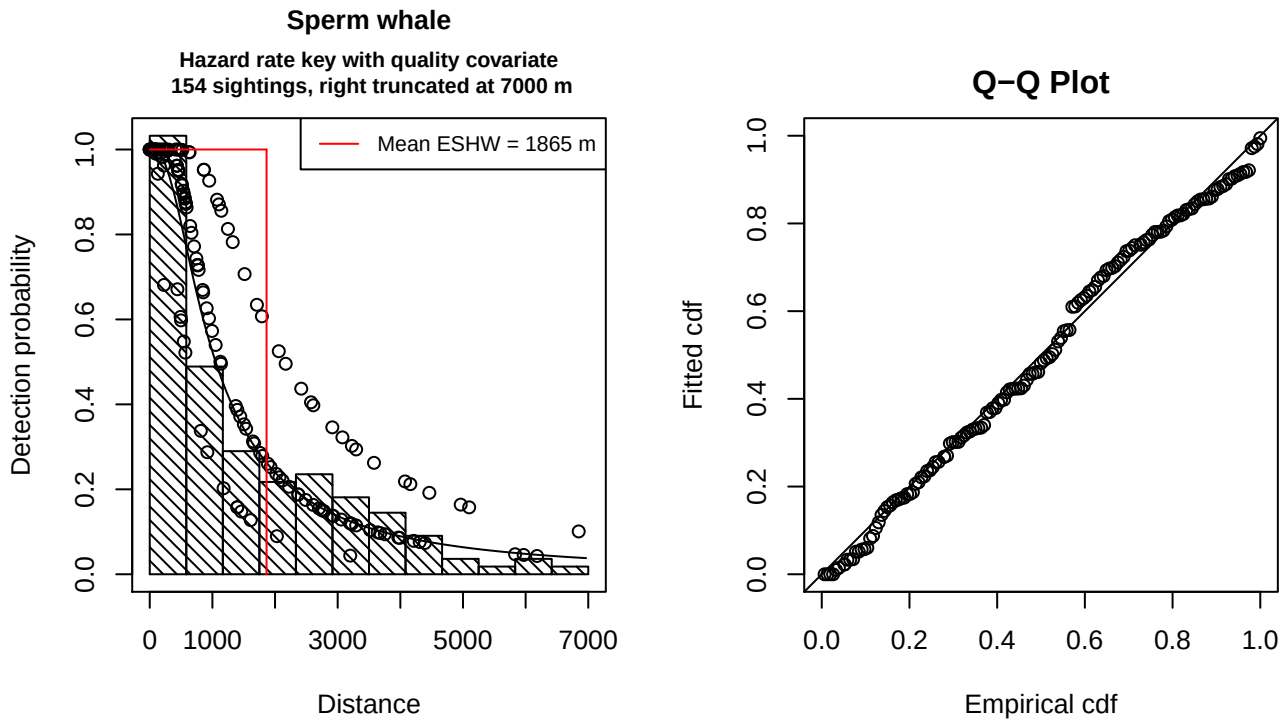

Figure 23: Detection function for SEFSC Oregon II that was selected for the density model

Statistical output for this detection function:

```
Summary for ds object
Number of observations :  154
Distance range         :  0  -  7000
AIC                    :  2566.498

Detection function:
 Hazard-rate key function

Detection function parameters
Scale Coefficients:
             estimate        se
(Intercept)  7.4486213 0.2731057
quality     -0.3878499 0.1248331

Shape parameters:
            estimate        se
(Intercept) 0.4824541 0.1535195

                       Estimate           SE        CV
Average p             0.2324495   0.03427634 0.1474572
N in covered region 662.5095157 108.75642514 0.1641583
```

Additional diagnostic plots:

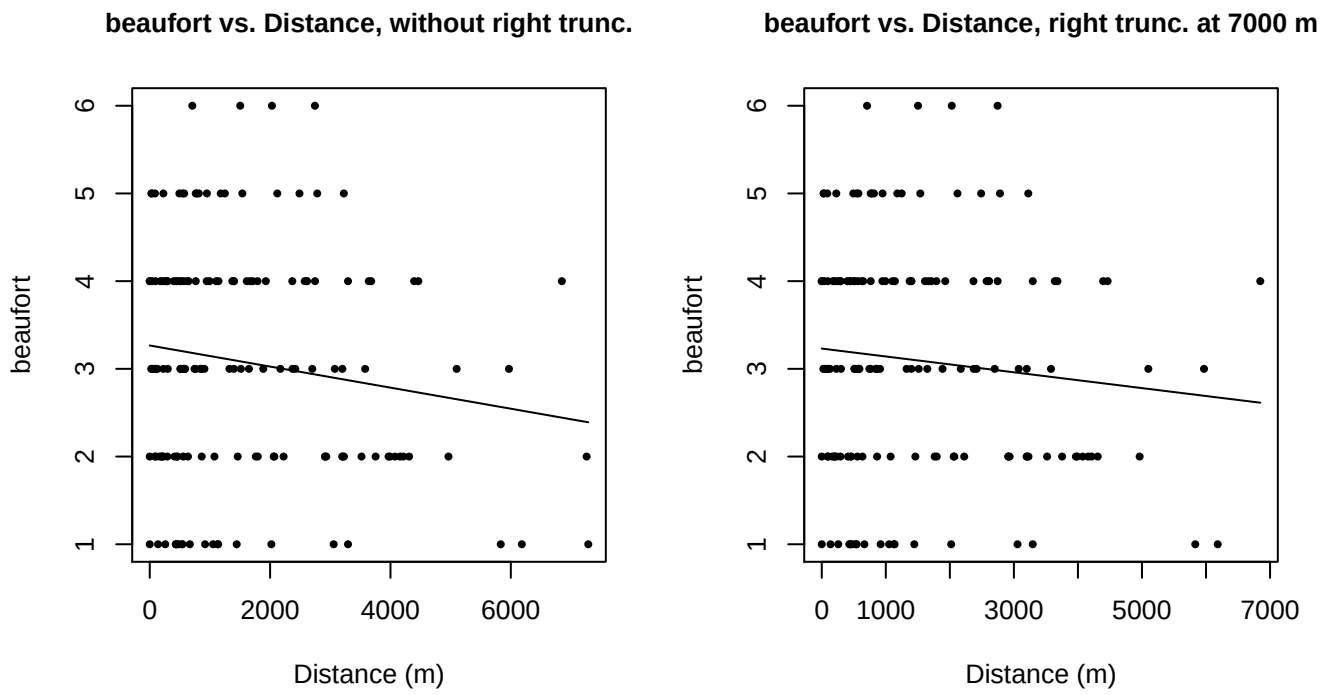

Figure 24: Scatterplots showing the relationship between Beaufort sea state and perpendicular sighting distance, for all sightings (left) and only those not right truncated (right). The line is a simple linear regression.

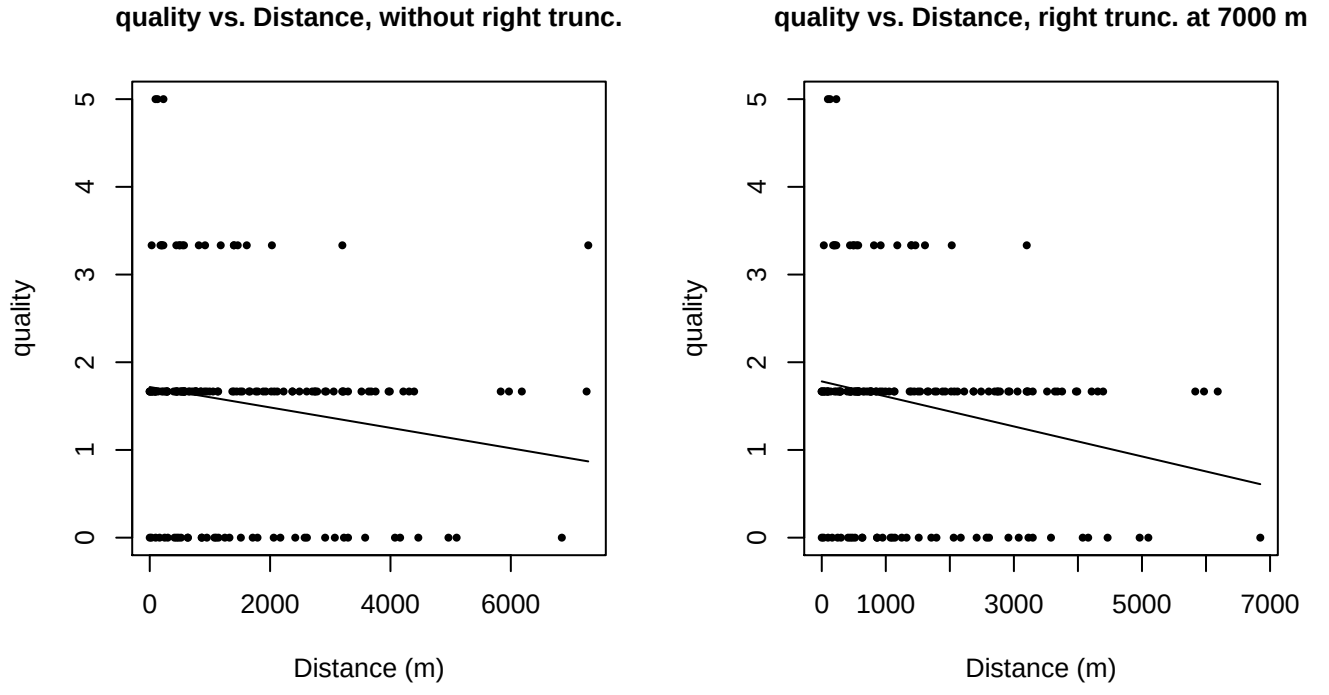

Figure 25: Scatterplots showing the relationship between the survey-specific index of the quality of observation conditions and perpendicular sighting distance, for all sightings (left) and only those not right truncated (right). Low values of the quality index correspond to better observation conditions. The line is a simple linear regression.

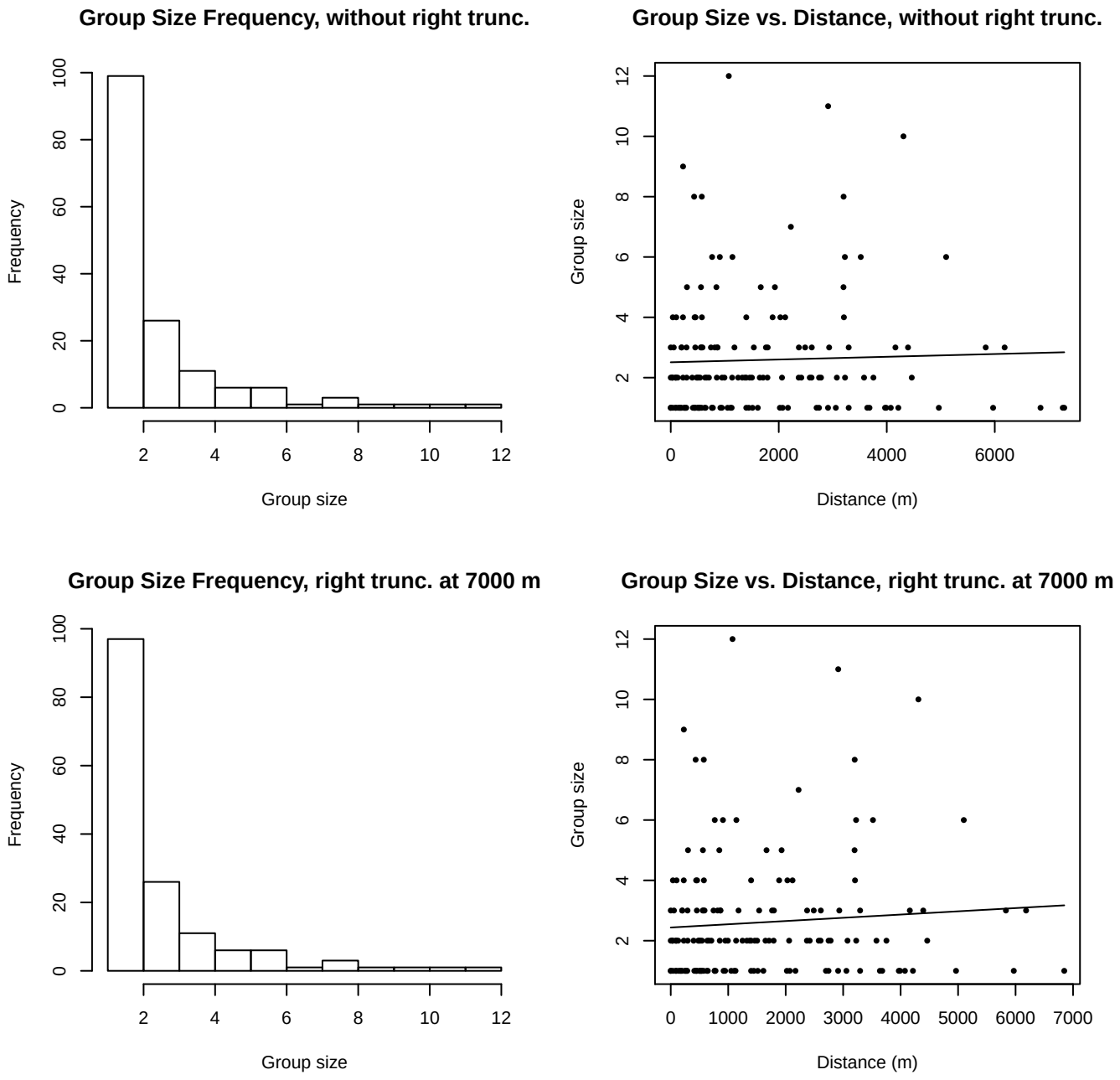

Figure 26: Histograms showing group size frequency and scatterplots showing the relationship between group size and perpendicular sighting distance, for all sightings (top row) and only those not right truncated (bottom row). In the scatterplot, the line is a simple linear regression.

Oregon II Gulf of Mexico

The sightings were right truncated at 7000m.

Covariate	Description
beaufort	Beaufort sea state.
quality	Survey-specific index of the quality of observation conditions, utilizing relevant factors other than Beaufort sea state (see methods).
size	Estimated size (number of individuals) of the sighted group.

Table 14: Covariates tested in candidate "multi-covariate distance sampling" (MCDS) detection functions.

Key	Adjustment	Order	Covariates	Succeeded	Δ AIC	Mean ESHW (m)
hr			quality, size	Yes	0.00	2083
hr			quality	Yes	0.49	2007
hn			quality, size	Yes	5.53	2864
hn			beaufort, quality, size	Yes	5.97	2835
hn			beaufort, quality	Yes	6.61	2808
hr	poly	4		Yes	6.64	1627
hn			quality	Yes	6.69	2835
hr				Yes	6.81	1696
hr			size	Yes	6.83	1809
hr	poly	2		Yes	8.81	1696
hn			beaufort	Yes	18.51	2790
hn				Yes	19.60	2794
hn			beaufort, size	Yes	19.98	2786
hn			size	Yes	20.72	2791
hn	cos	3		Yes	21.57	2792
hn	cos	2		Yes	21.58	2793
hn	cos	1		Yes	21.60	2794
hn	herm	4		Yes	21.60	2794
hr			beaufort	No		
hr			beaufort, quality	No		
hr			beaufort, size	No		
hr			beaufort, quality, size	No		

Table 15: Candidate detection functions for Oregon II Gulf of Mexico. The first one listed was selected for the density model.

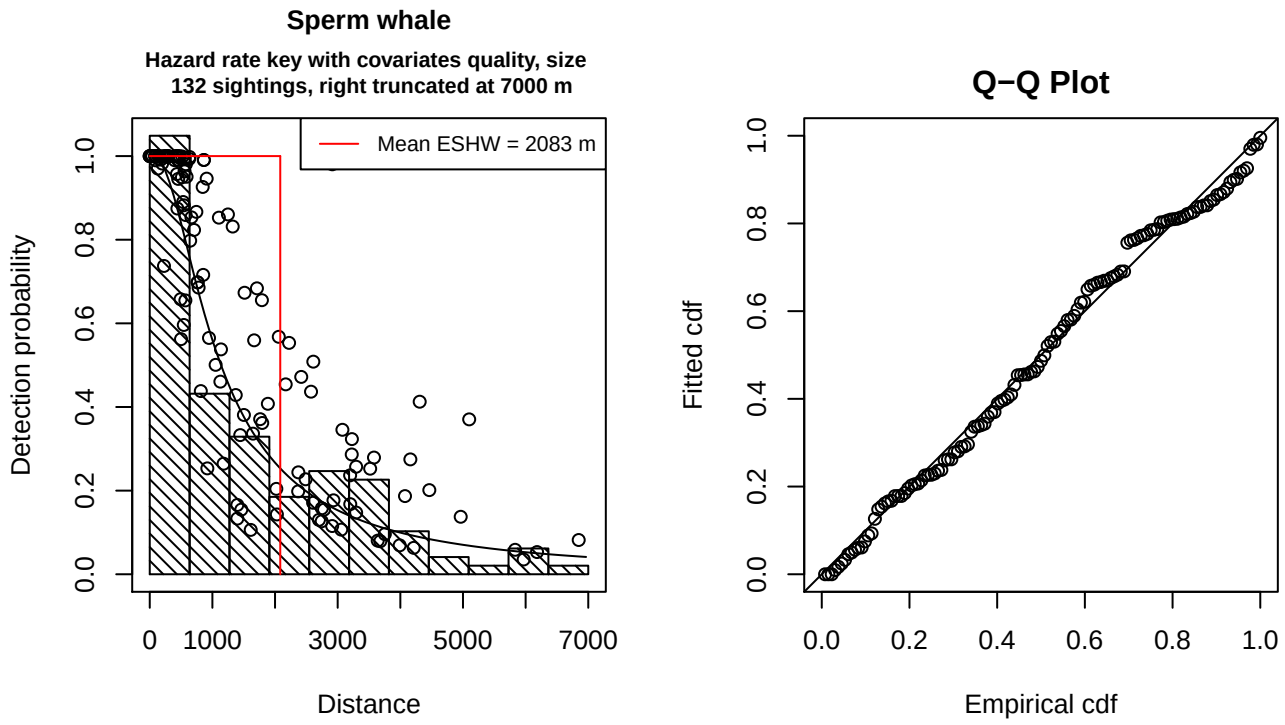

Figure 27: Detection function for Oregon II Gulf of Mexico that was selected for the density model

Statistical output for this detection function:

```
Summary for ds object
Number of observations :  132
Distance range         :  0  -  7000
AIC                    :  2206.877

Detection function:
 Hazard-rate key function

Detection function parameters
Scale Coefficients:
             estimate         se
(Intercept)  7.2488888 0.33367096
quality     -0.3860532 0.12127773
size         0.1392861 0.07772271

Shape parameters:
            estimate        se
(Intercept) 0.532807 0.1715144

                       Estimate          SE        CV
Average p              0.2467392  0.03846843 0.1559073
N in covered region 534.9779303 93.27509888 0.1743532
```

Additional diagnostic plots:

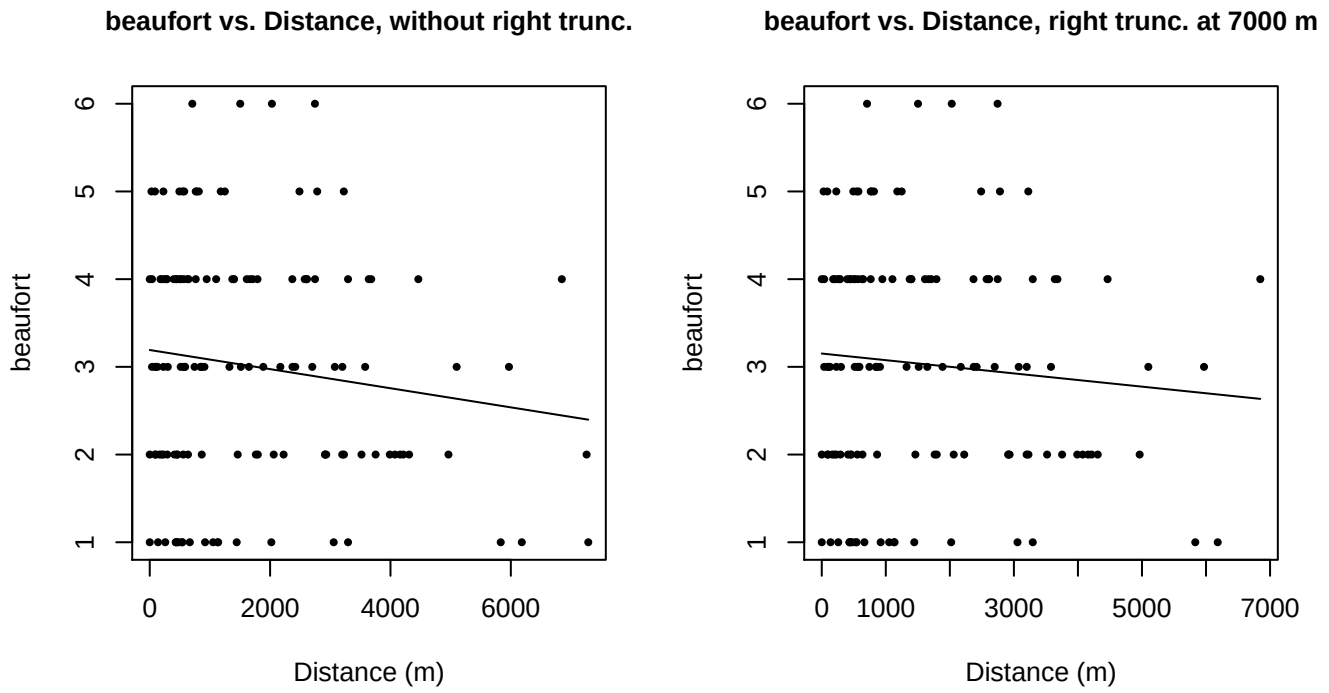

Figure 28: Scatterplots showing the relationship between Beaufort sea state and perpendicular sighting distance, for all sightings (left) and only those not right truncated (right). The line is a simple linear regression.

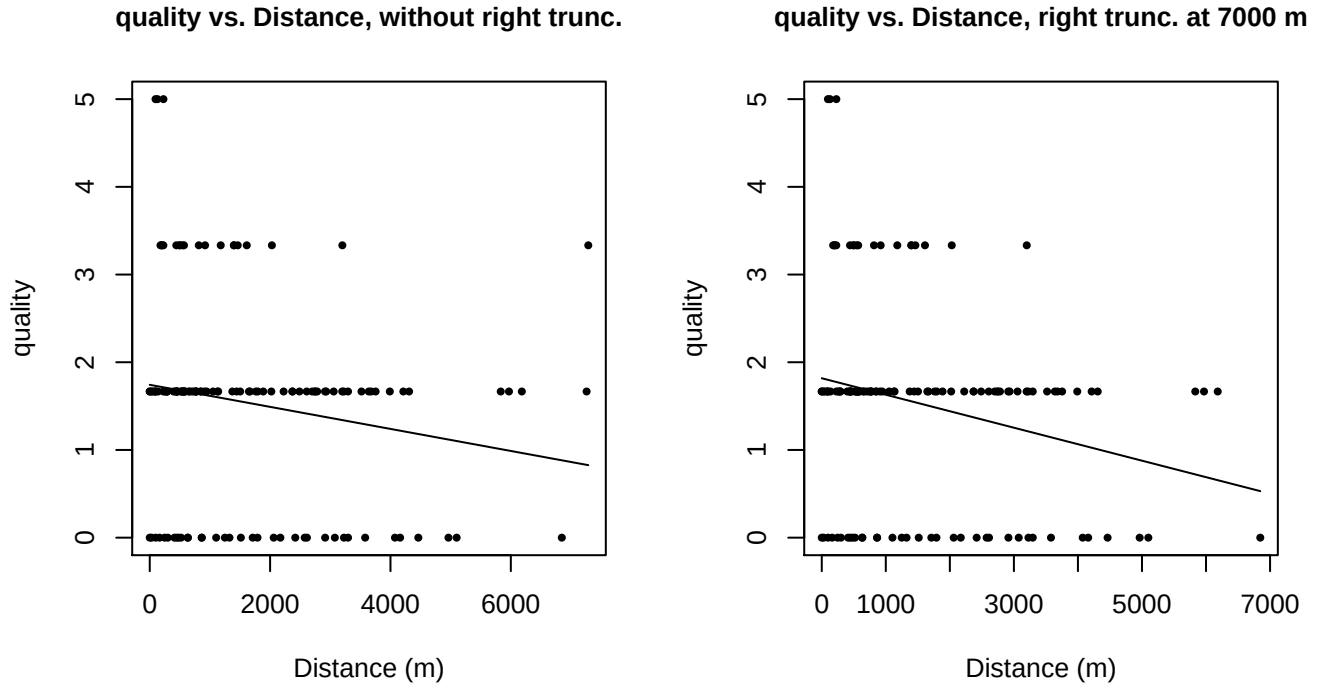

Figure 29: Scatterplots showing the relationship between the survey-specific index of the quality of observation conditions and perpendicular sighting distance, for all sightings (left) and only those not right truncated (right). Low values of the quality index correspond to better observation conditions. The line is a simple linear regression.

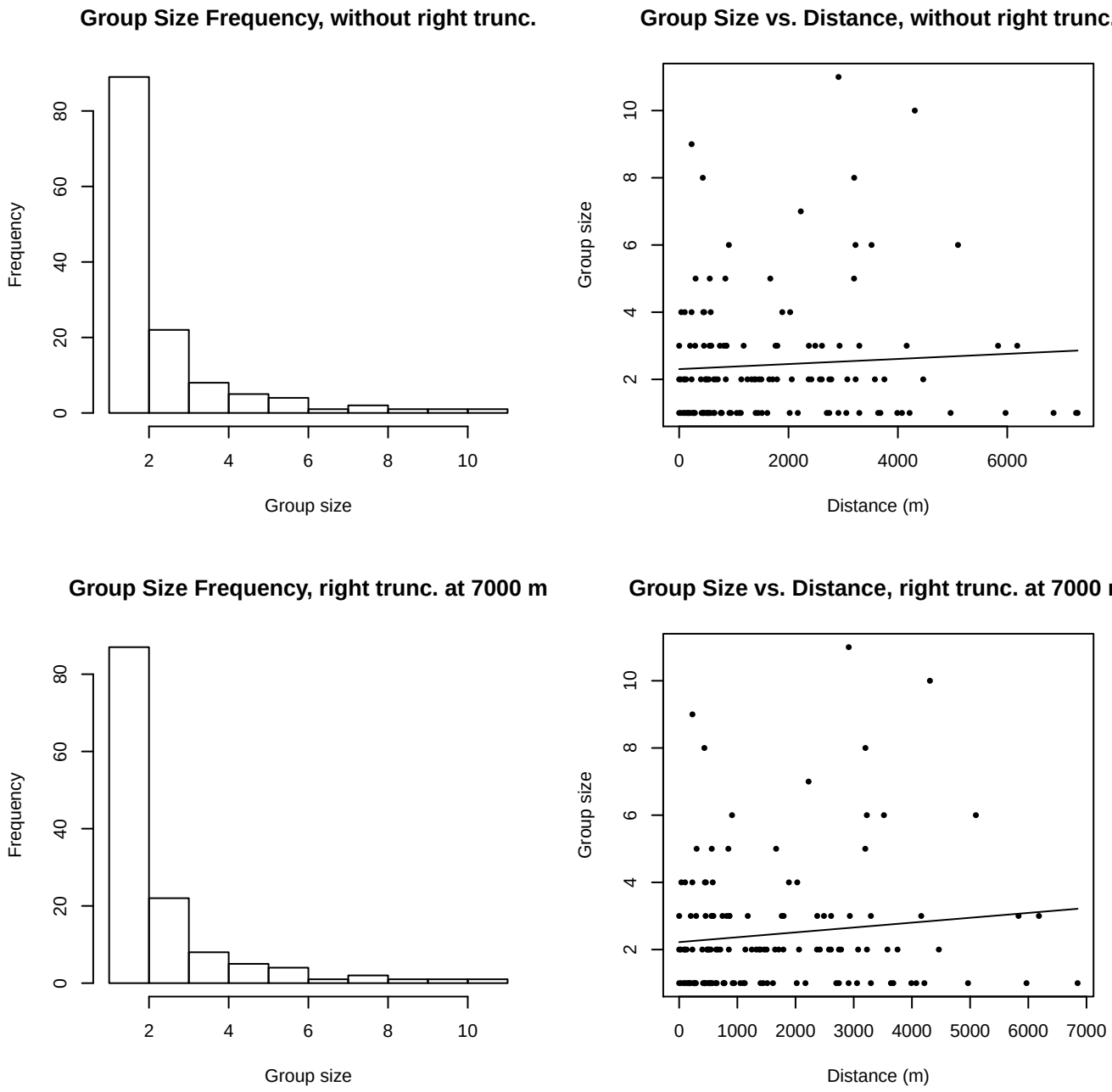

Figure 30: Histograms showing group size frequency and scatterplots showing the relationship between group size and perpendicular sighting distance, for all sightings (top row) and only those not right truncated (bottom row). In the scatterplot, the line is a simple linear regression.

SEFSC Gordon Gunter

The sightings were right truncated at 8000m.

Covariate	Description
beaufort	Beaufort sea state.
quality	Survey-specific index of the quality of observation conditions, utilizing relevant factors other than Beaufort sea state (see methods).
size	Estimated size (number of individuals) of the sighted group.

Table 16: Covariates tested in candidate "multi-covariate distance sampling" (MCDS) detection functions.

Key	Adjustment	Order	Covariates	Succeeded	Δ AIC	Mean ESHW (m)
hn			quality	Yes	0.00	3690
hr	poly	2		Yes	0.34	2990
hr	poly	4		Yes	0.45	2946
hn				Yes	3.00	3689
hn	cos	3		Yes	4.97	3688
hn	cos	2		Yes	4.98	3688
hn	cos	1		Yes	5.00	3689
hn	herm	4		Yes	5.00	3689
hr				Yes	7.71	3228
hr			quality	Yes	8.79	3346
hr			beaufort	Yes	8.93	3227
hr			size	Yes	9.40	3221
hr			beaufort, quality	Yes	10.20	3355
hr			quality, size	Yes	10.43	3334
hr			beaufort, size	Yes	10.75	3223
hr			beaufort, quality, size	Yes	11.97	3350
hn			beaufort	No		
hn			size	No		
hn			beaufort, quality	No		
hn			beaufort, size	No		
hn			quality, size	No		
hn			beaufort, quality, size	No		

Table 17: Candidate detection functions for SEFSC Gordon Gunter. The first one listed was selected for the density model.

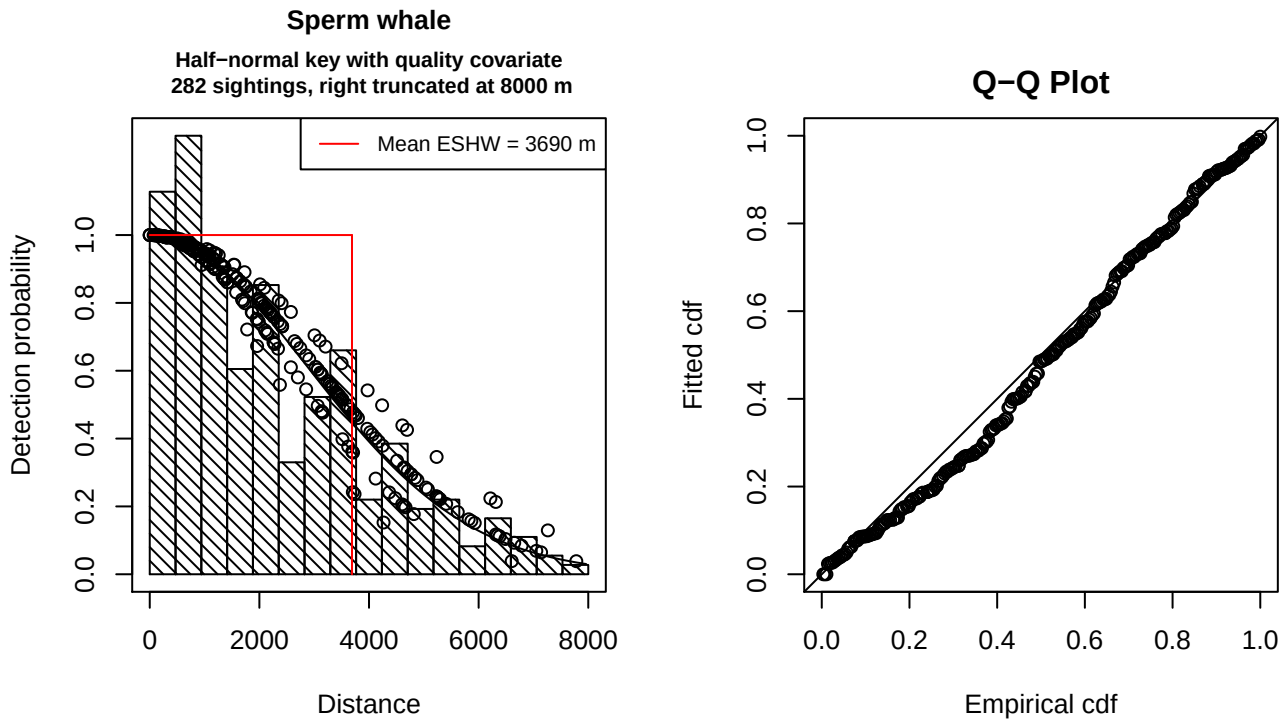

Figure 31: Detection function for SEFSC Gordon Gunter that was selected for the density model

Statistical output for this detection function:

```
Summary for ds object
Number of observations :  282
Distance range         :  0  -  8000
AIC                    :  4897.229

Detection function:
 Half-normal key function

Detection function parameters
Scale Coefficients:
               estimate         se
(Intercept)  8.18629222 0.10270182
quality     -0.09801003 0.04510844

                       Estimate          SE         CV
Average p             0.4562755  0.02057357 0.04509023
N in covered region 618.0476192 38.98476332 0.06307728
```

Additional diagnostic plots:

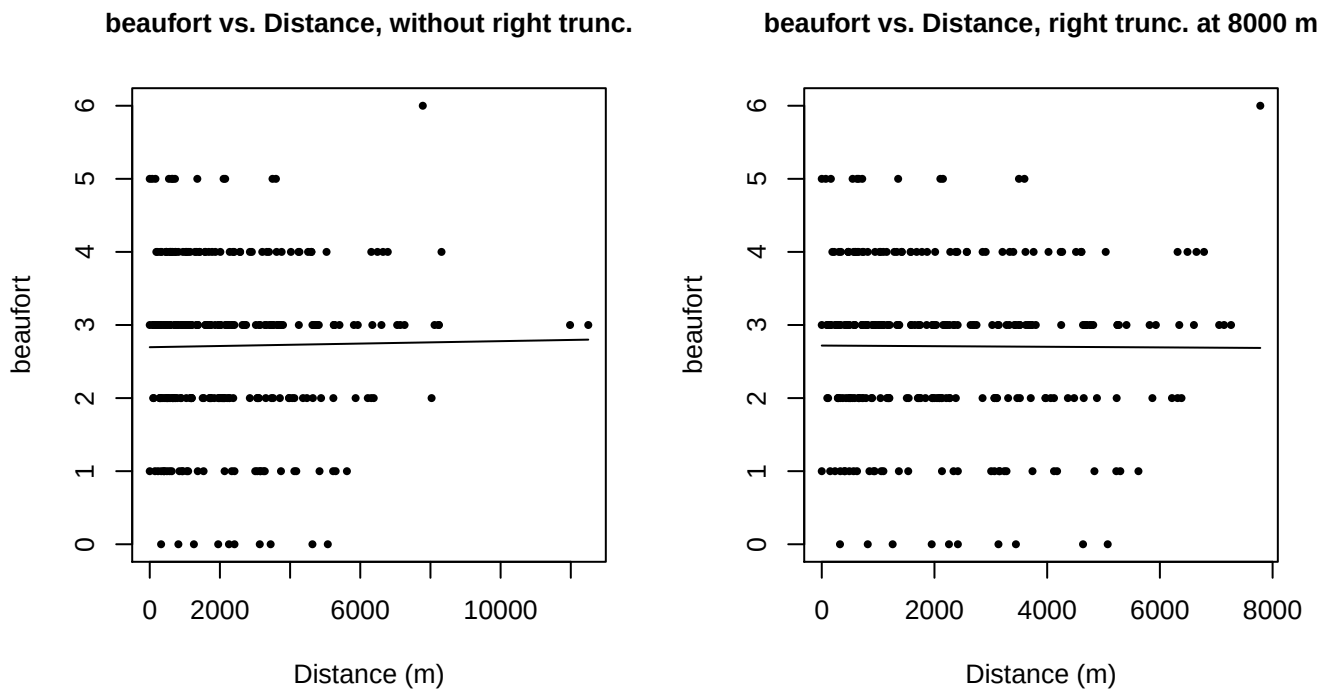

Figure 32: Scatterplots showing the relationship between Beaufort sea state and perpendicular sighting distance, for all sightings (left) and only those not right truncated (right). The line is a simple linear regression.

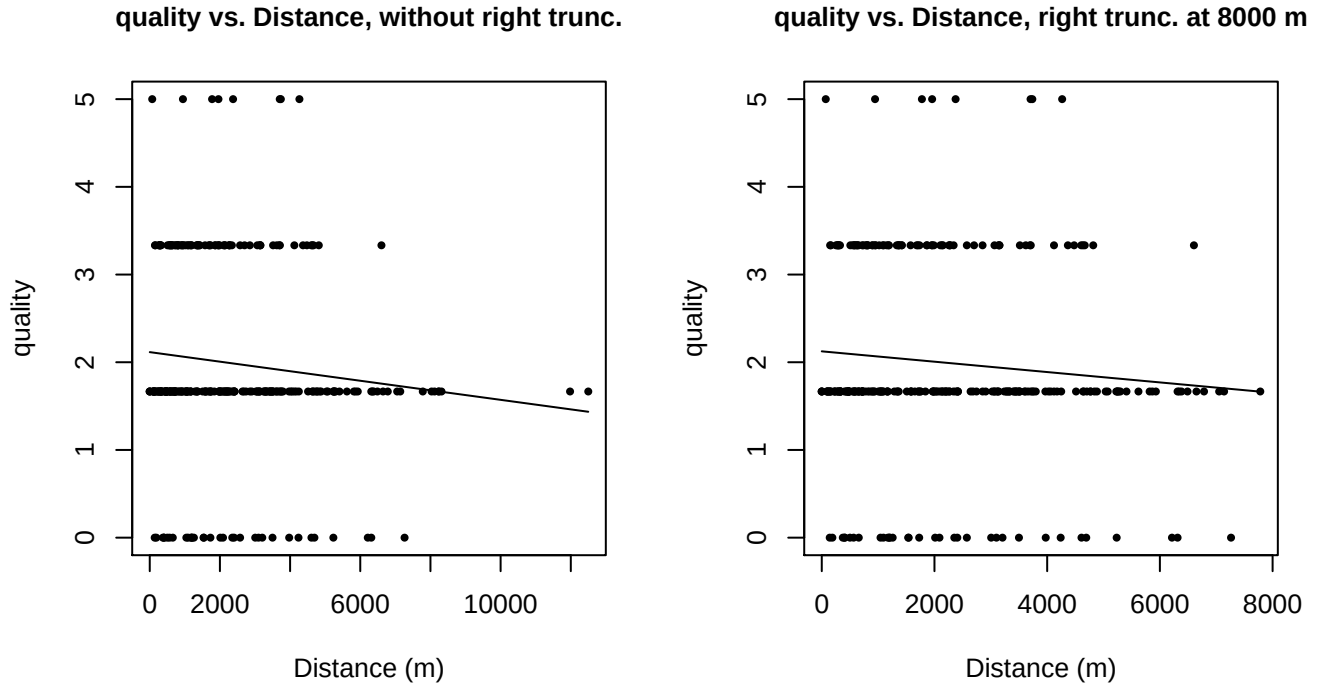

Figure 33: Scatterplots showing the relationship between the survey-specific index of the quality of observation conditions and perpendicular sighting distance, for all sightings (left) and only those not right truncated (right). Low values of the quality index correspond to better observation conditions. The line is a simple linear regression.

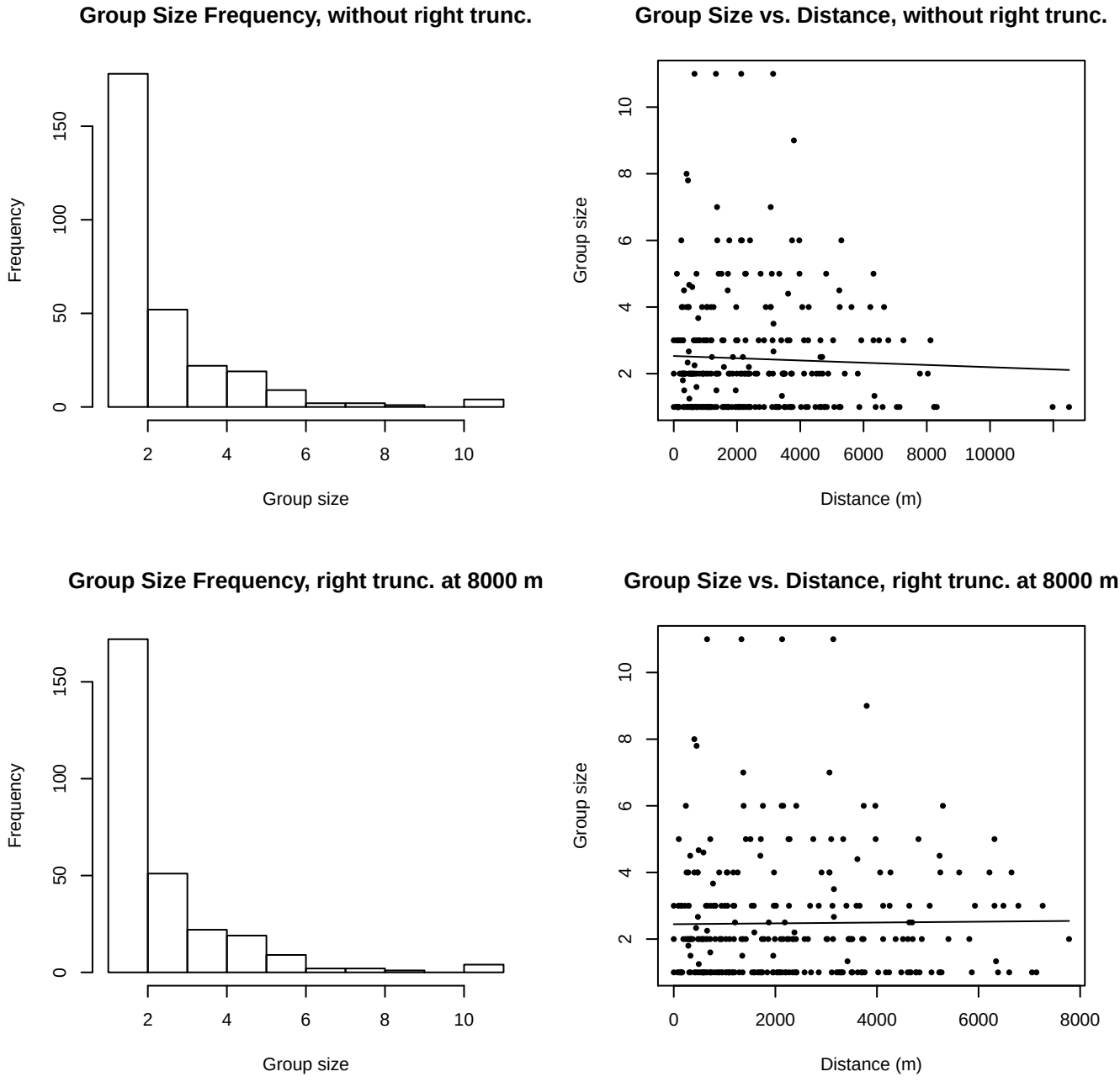

Figure 34: Histograms showing group size frequency and scatterplots showing the relationship between group size and perpendicular sighting distance, for all sightings (top row) and only those not right truncated (bottom row). In the scatterplot, the line is a simple linear regression.

Gordon Gunter Atlantic

The sightings were right truncated at 8000m.

Covariate	Description
beaufort	Beaufort sea state.
quality	Survey-specific index of the quality of observation conditions, utilizing relevant factors other than Beaufort sea state (see methods).
size	Estimated size (number of individuals) of the sighted group.

Table 18: Covariates tested in candidate "multi-covariate distance sampling" (MCDS) detection functions.

Key	Adjustment	Order	Covariates	Succeeded	Δ AIC	Mean ESHW (m)
hr	poly	4		Yes	0.00	2697
hr	poly	2		Yes	0.23	2708
hn				Yes	1.27	3535
hr				Yes	1.86	2838
hn	cos	3		Yes	3.25	3533
hn	cos	2		Yes	3.26	3533
hn			quality	Yes	3.27	3534
hn	cos	1		Yes	3.27	3535
hn	herm	4		Yes	3.27	3535
hr			beaufort	Yes	3.69	2868
hr			size	Yes	3.86	2838
hn			beaufort	No		
hr			quality	No		
hn			size	No		
hr			beaufort, quality	No		
hn			beaufort, quality	No		
hr			beaufort, size	No		
hn			beaufort, size	No		
hr			quality, size	No		
hn			quality, size	No		
hr			beaufort, quality, size	No		
hn			beaufort, quality, size	No		

Table 19: Candidate detection functions for Gordon Gunter Atlantic. The first one listed was selected for the density model.

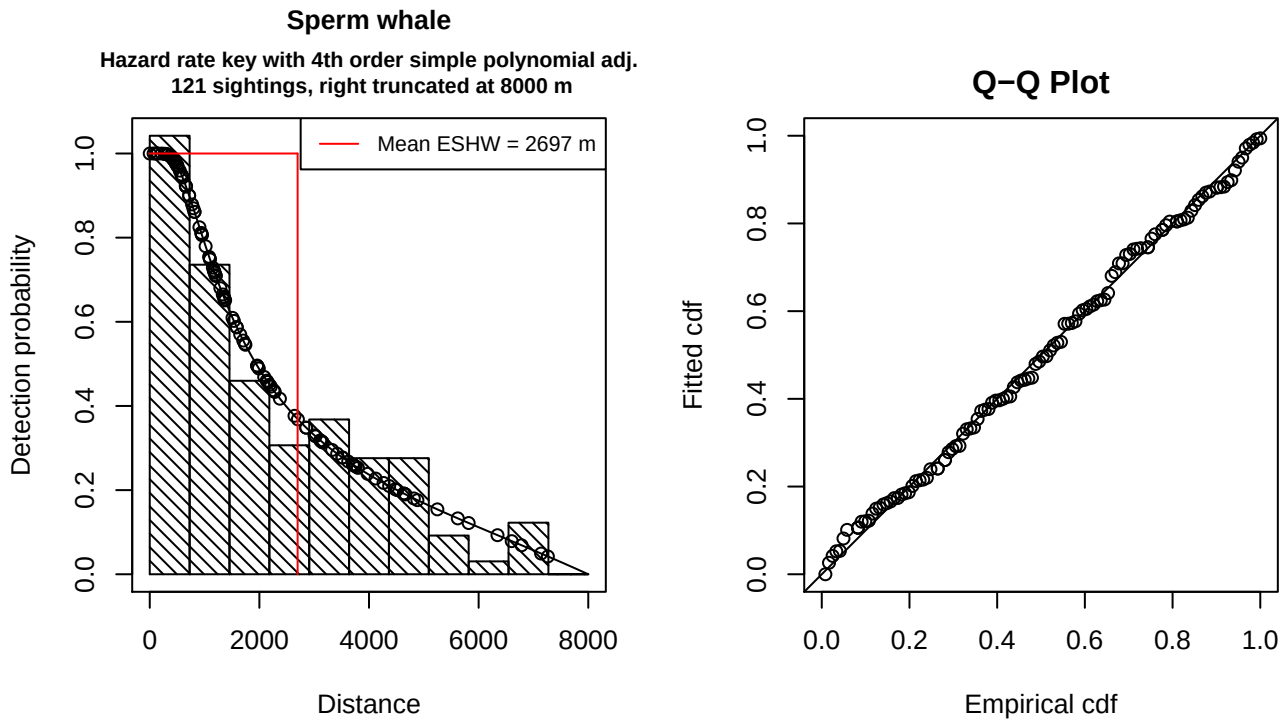

Figure 35: Detection function for Gordon Gunter Atlantic that was selected for the density model

Statistical output for this detection function:

```
Summary for ds object
Number of observations :  121
Distance range         :  0  -  8000
AIC                    :  2093.869

Detection function:
 Hazard-rate key function with simple polynomial adjustment term of order 4

Detection function parameters
Scale Coefficients:
            estimate       se
(Intercept) 7.270181 0.408596

Shape parameters:
            estimate        se
(Intercept) 0.186902 0.3170671

Adjustment term parameter(s):
                estimate        se
poly, order 4 -0.9999964 0.4155061


Strict monotonicity constraints were enforced.
                       Estimate          SE        CV
Average p              0.3371848  0.06347358 0.1882457
N in covered region 358.8536221 72.58628812 0.2022727

Strict monotonicity constraints were enforced.
```

Additional diagnostic plots:

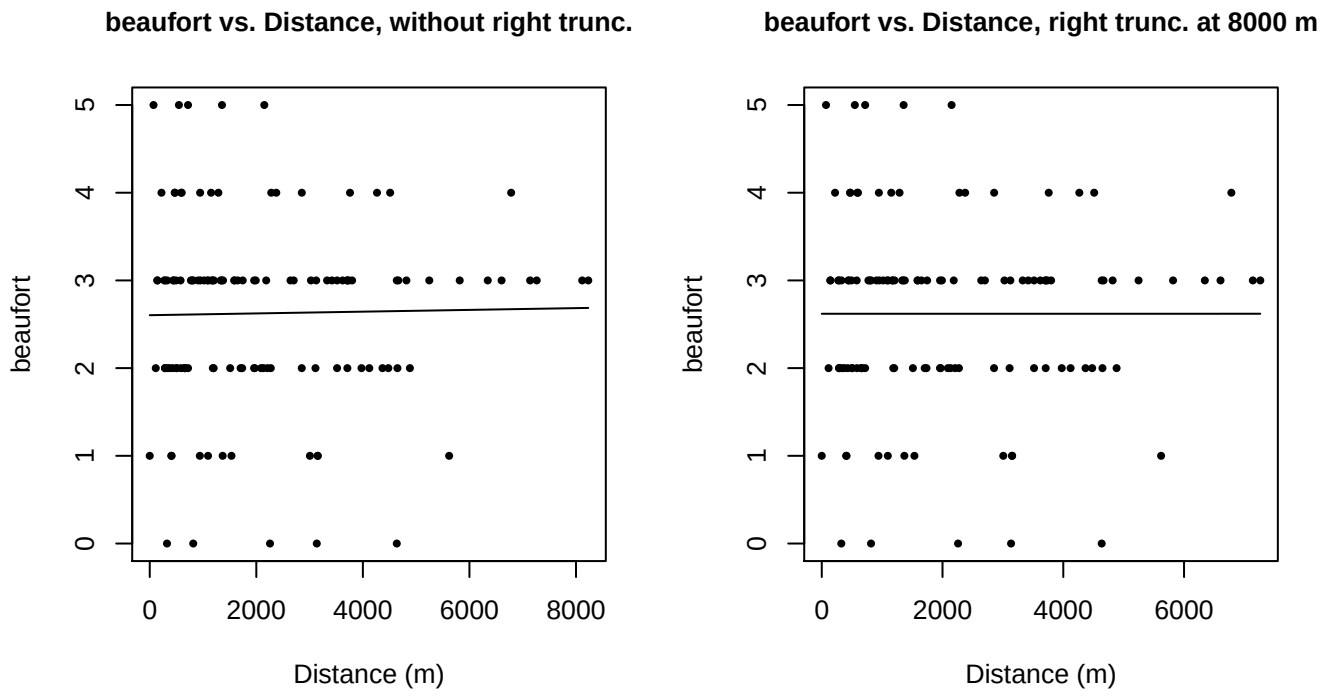

Figure 36: Scatterplots showing the relationship between Beaufort sea state and perpendicular sighting distance, for all sightings (left) and only those not right truncated (right). The line is a simple linear regression.

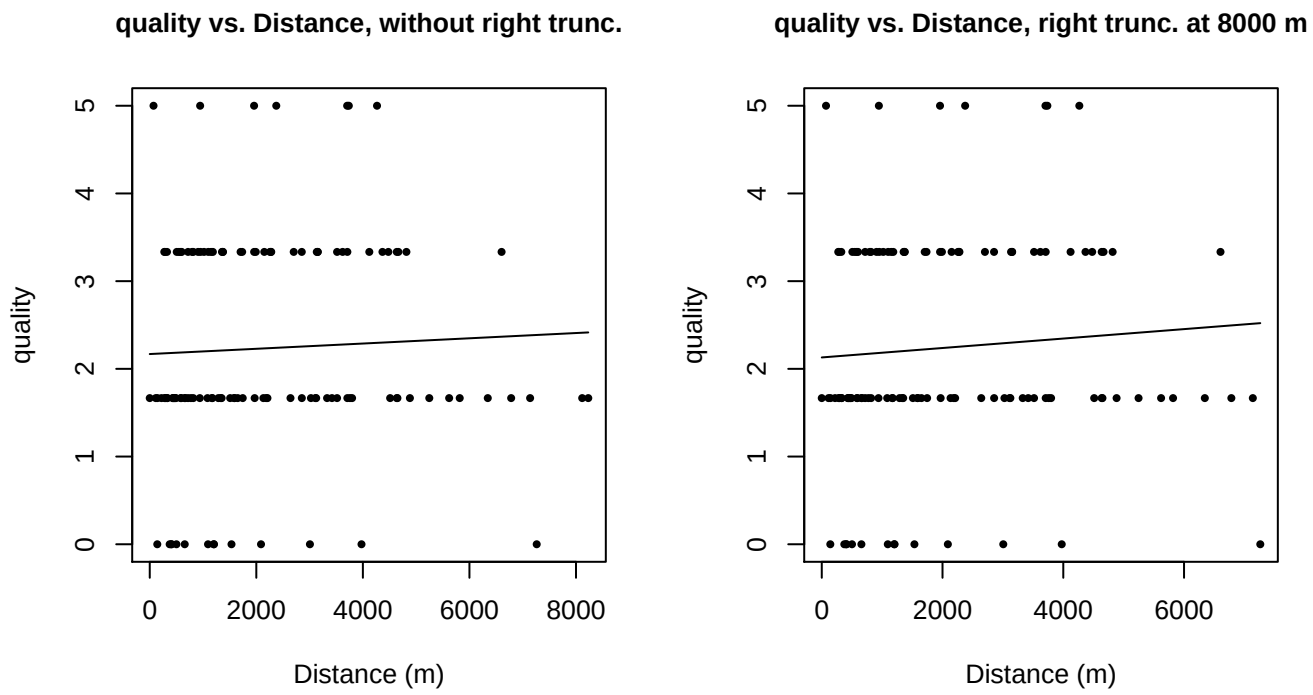

Figure 37: Scatterplots showing the relationship between the survey-specific index of the quality of observation conditions and perpendicular sighting distance, for all sightings (left) and only those not right truncated (right). Low values of the quality index correspond to better observation conditions. The line is a simple linear regression.

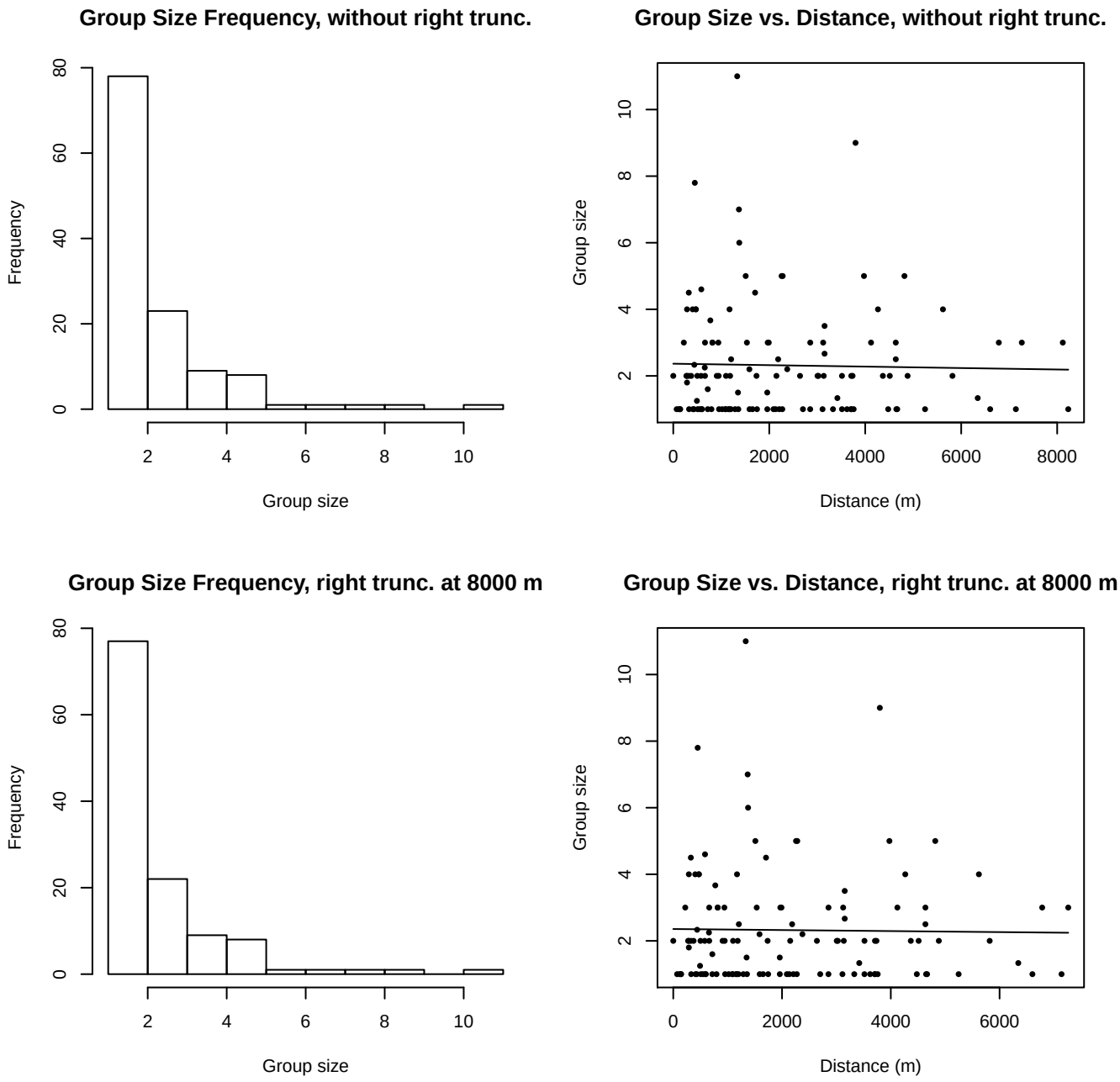

Figure 38: Histograms showing group size frequency and scatterplots showing the relationship between group size and perpendicular sighting distance, for all sightings (top row) and only those not right truncated (bottom row). In the scatterplot, the line is a simple linear regression.

Gordon Gunter Gulf of Mexico

The sightings were right truncated at 8000m.

Covariate	Description
beaufort	Beaufort sea state.
size	Estimated size (number of individuals) of the sighted group.

Table 20: Covariates tested in candidate "multi-covariate distance sampling" (MCDS) detection functions.

Key	Adjustment	Order	Covariates	Succeeded	Δ AIC	Mean ESHW (m)
hn			beaufort	Yes	0.00	3806
hn				Yes	1.00	3791
hn			beaufort, size	Yes	1.41	3811
hn			size	Yes	2.60	3792
hn	cos	3		Yes	3.00	3791
hn	cos	2		Yes	3.00	3791
hn	cos	1		Yes	3.00	3791
hn	herm	4		Yes	3.00	3791
hr	poly	2		Yes	3.37	3203
hr			beaufort	Yes	4.09	3813
hr	poly	4		Yes	4.12	3222
hr			beaufort, size	Yes	5.05	3772
hr				Yes	5.85	3846
hr			size	Yes	6.94	3759

Table 21: Candidate detection functions for Gordon Gunter Gulf of Mexico. The first one listed was selected for the density model.

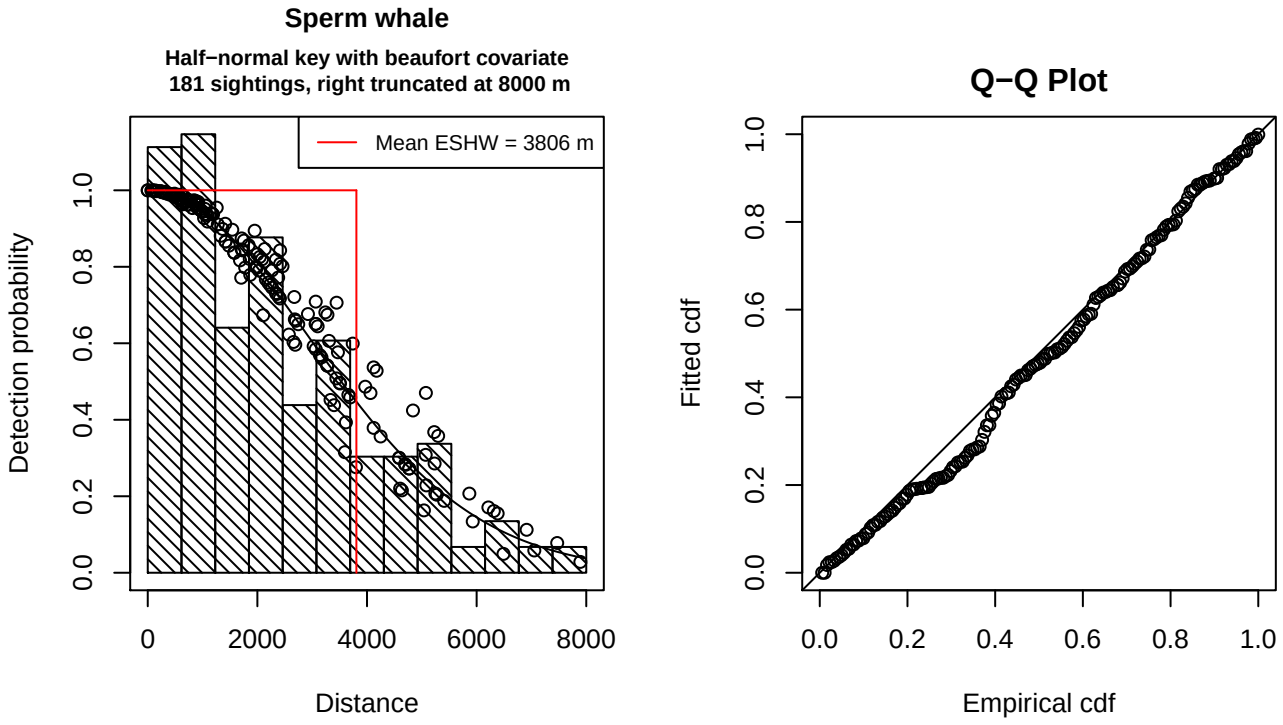

Figure 39: Detection function for Gordon Gunter Gulf of Mexico that was selected for the density model

Statistical output for this detection function:

```
Summary for ds object
Number of observations :  181
Distance range         :  0  -  8000
AIC                    :  3152.754

Detection function:
 Half-normal key function

Detection function parameters
Scale Coefficients:
             estimate         se
(Intercept)  8.3262140 0.20375291
beaufort    -0.1113671 0.06722417

                       Estimate          SE         CV
Average p              0.4695499  0.02583324 0.05501703
N in covered region 385.4755452 29.83876617 0.07740768
```

Additional diagnostic plots:

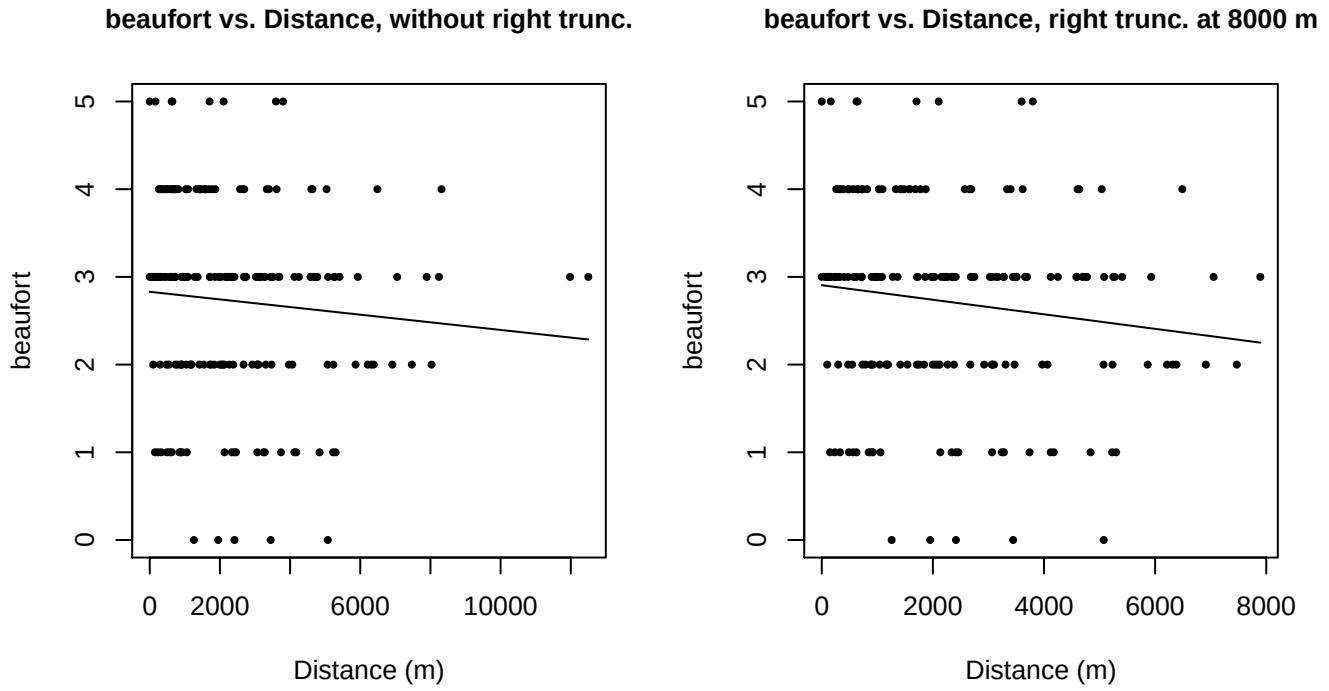

Figure 40: Scatterplots showing the relationship between Beaufort sea state and perpendicular sighting distance, for all sightings (left) and only those not right truncated (right). The line is a simple linear regression.

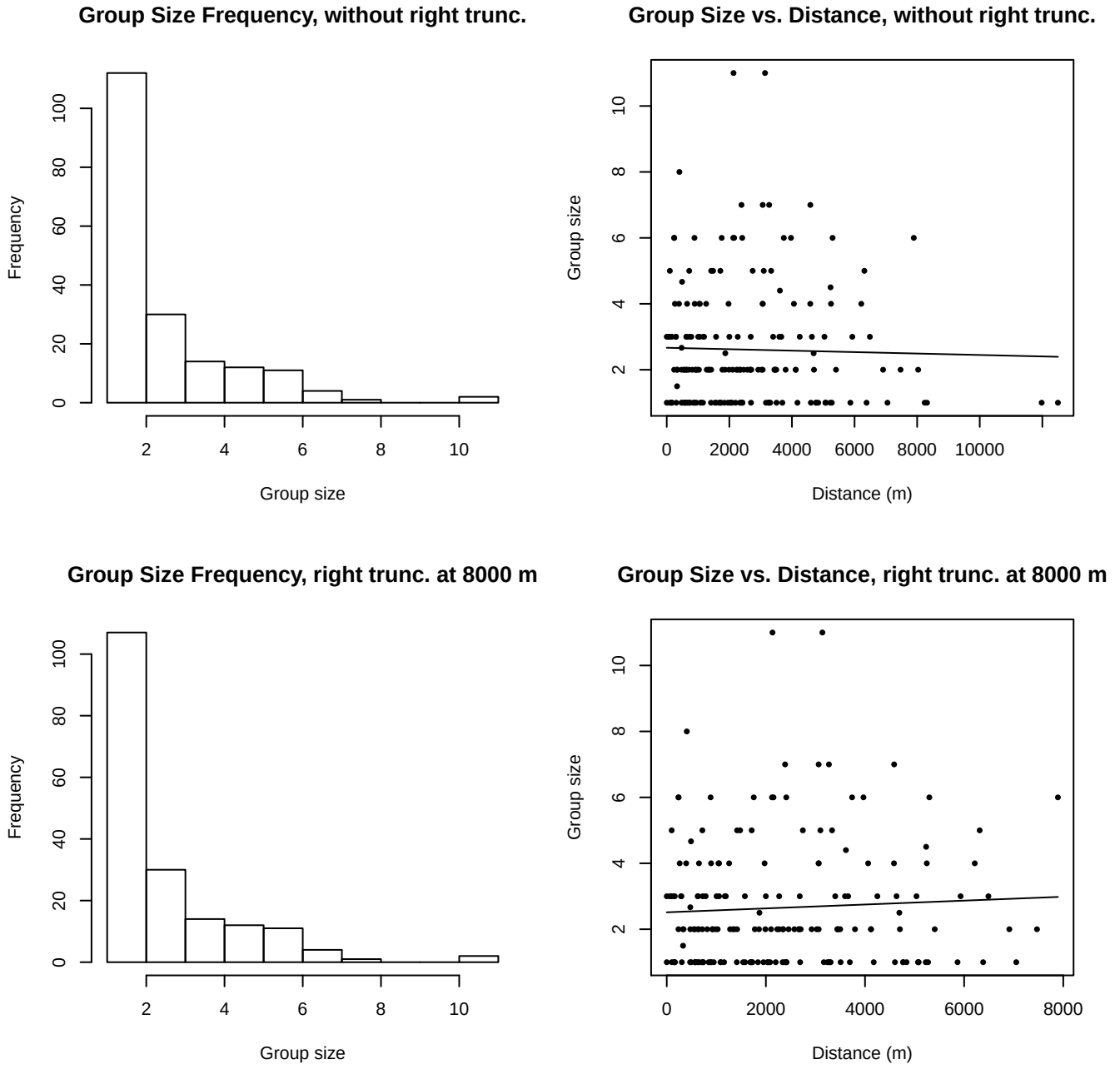

Figure 41: Histograms showing group size frequency and scatterplots showing the relationship between group size and perpendicular sighting distance, for all sightings (top row) and only those not right truncated (bottom row). In the scatterplot, the line is a simple linear regression.

GG Quality Covariate Available

The sightings were right truncated at 8000m.

Covariate	Description
beaufort	Beaufort sea state.
quality	Survey-specific index of the quality of observation conditions, utilizing relevant factors other than Beaufort sea state (see methods).
size	Estimated size (number of individuals) of the sighted group.

Table 22: Covariates tested in candidate "multi-covariate distance sampling" (MCDS) detection functions.

Key	Adjustment	Order	Covariates	Succeeded	Δ AIC	Mean ESHW (m)
hn			quality	Yes	0.00	3614
hn			beaufort, quality	Yes	1.76	3612
hn			quality, size	Yes	1.99	3614
hn			beaufort, quality, size	Yes	3.75	3612
hr			quality	Yes	7.06	4315
hr			beaufort, quality	Yes	8.39	4246
hr			quality, size	Yes	8.74	4184
hn				Yes	9.02	3610
hn			beaufort	Yes	9.15	3614
hr	poly	2		Yes	9.83	3090
hr			beaufort, quality, size	Yes	9.91	4076
hr	poly	4		Yes	10.37	3116
hn			size	Yes	10.84	3610
hn			beaufort, size	Yes	10.96	3616
hn	cos	3		Yes	11.00	3608
hn	cos	2		Yes	11.02	3610
hn	cos	1		Yes	11.02	3610
hn	herm	4		Yes	11.02	3610
hr			beaufort	Yes	13.18	3688
hr			beaufort, size	Yes	13.74	3648
hr				Yes	14.93	3673
hr			size	Yes	15.60	3500

Table 23: Candidate detection functions for GG Quality Covariate Available. The first one listed was selected for the density model.

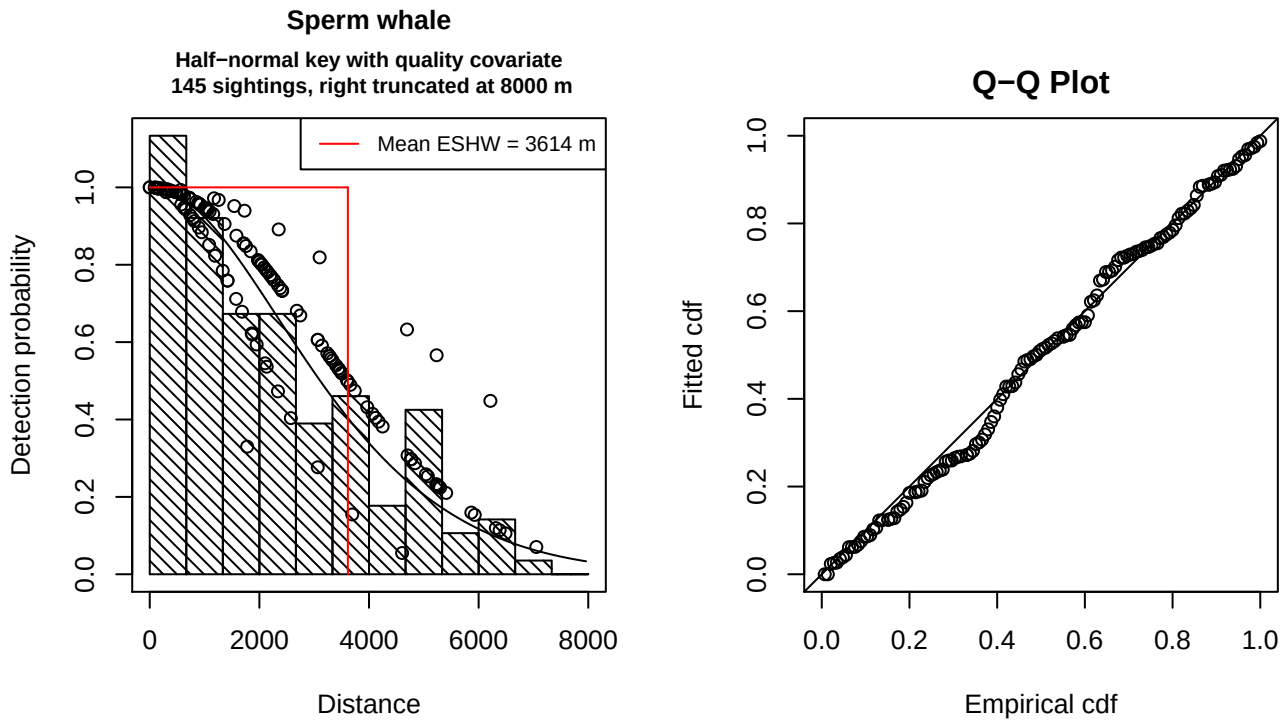

Figure 42: Detection function for GG Quality Covariate Available that was selected for the density model

Statistical output for this detection function:

```
Summary for ds object
Number of observations :  145
Distance range         :  0  -  8000
AIC                    :  2506.408

Detection function:
 Half-normal key function

Detection function parameters
Scale Coefficients:
             estimate         se
(Intercept)  8.4981362 0.19796972
quality     -0.2827478 0.09024415

                      Estimate          SE         CV
Average p             0.4279984  0.02992985 0.06992981
N in covered region 338.7863375 32.13847439 0.09486355
```

Additional diagnostic plots:

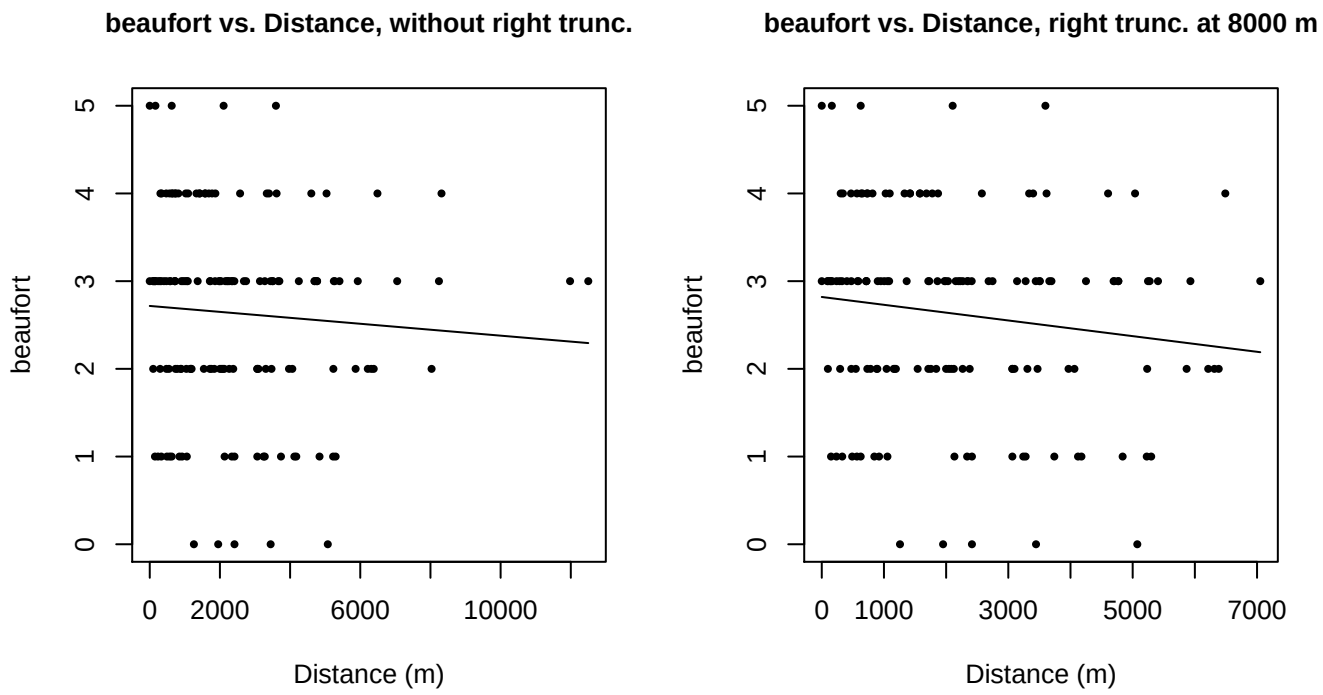

Figure 43: Scatterplots showing the relationship between Beaufort sea state and perpendicular sighting distance, for all sightings (left) and only those not right truncated (right). The line is a simple linear regression.

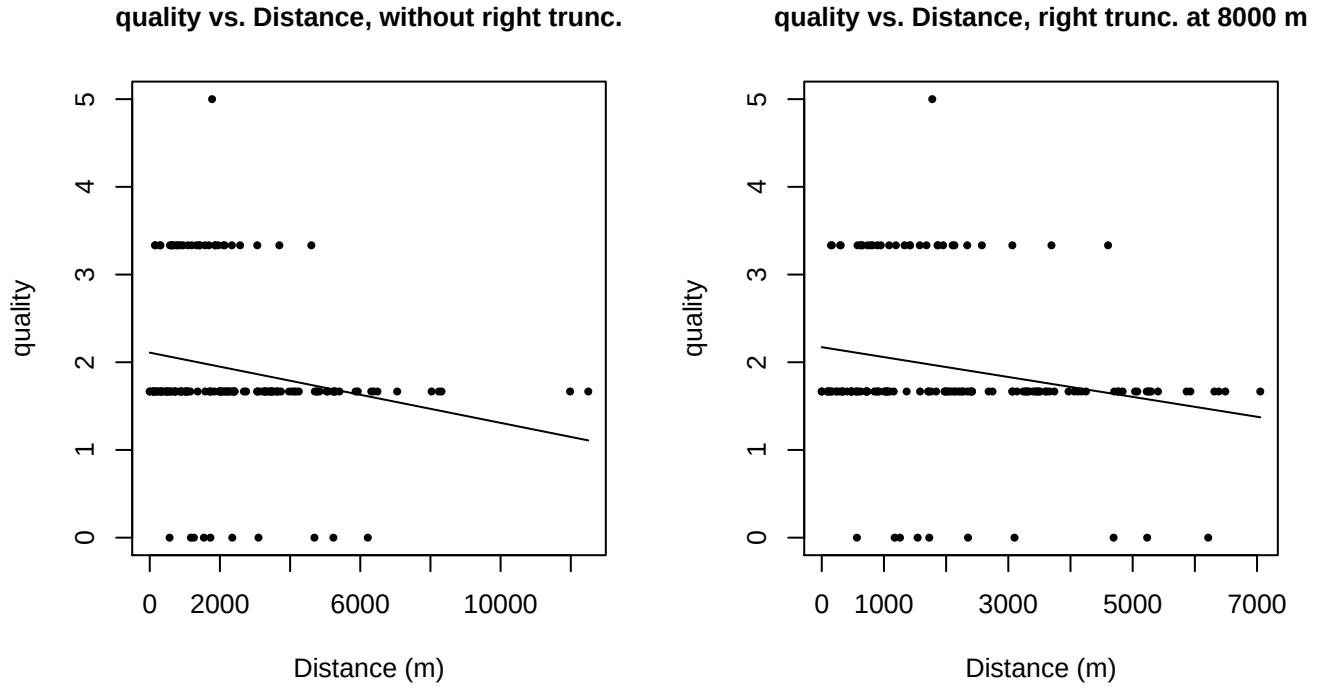

Figure 44: Scatterplots showing the relationship between the survey-specific index of the quality of observation conditions and perpendicular sighting distance, for all sightings (left) and only those not right truncated (right). Low values of the quality index correspond to better observation conditions. The line is a simple linear regression.

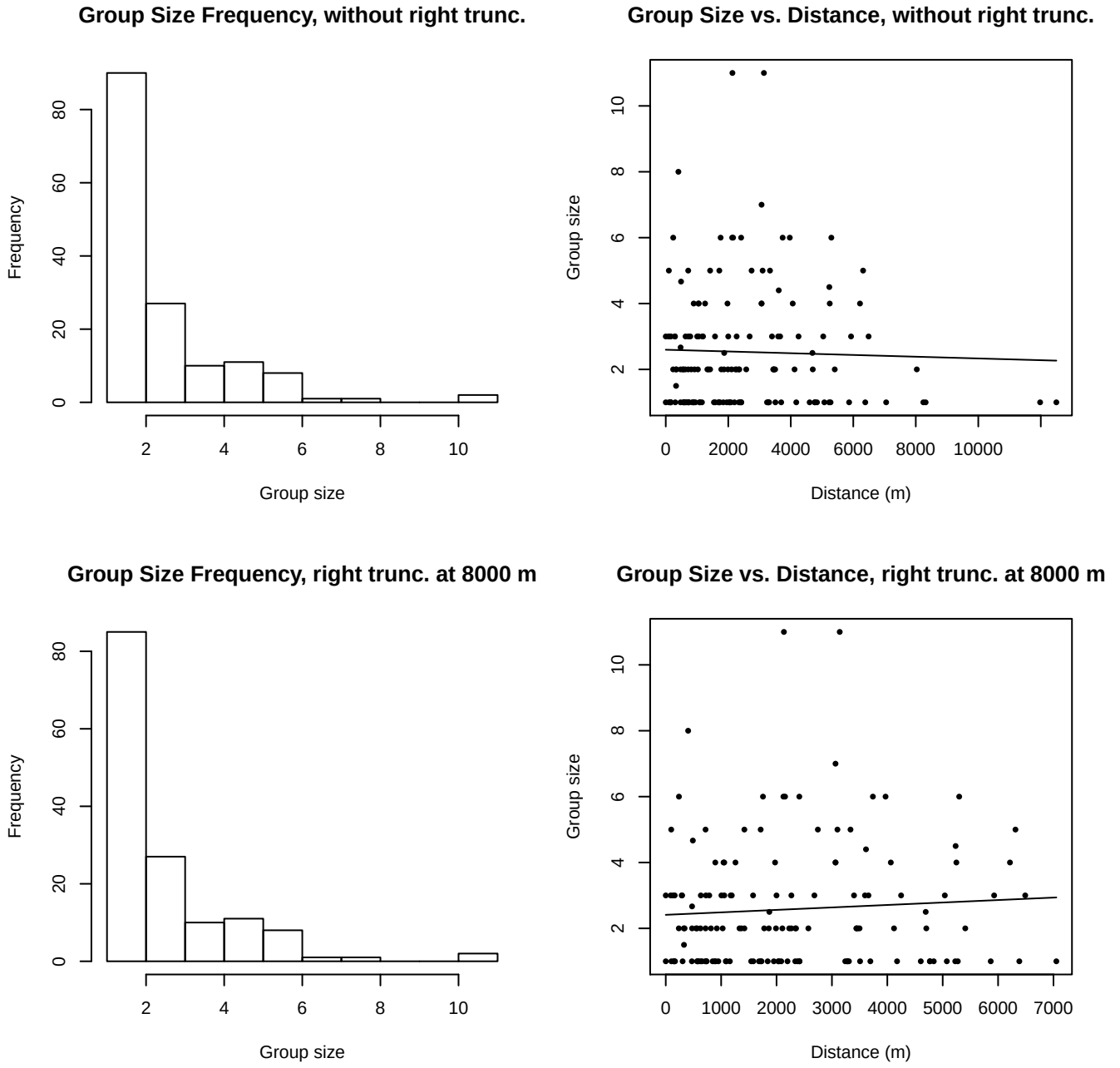

Figure 45: Histograms showing group size frequency and scatterplots showing the relationship between group size and perpendicular sighting distance, for all sightings (top row) and only those not right truncated (bottom row). In the scatterplot, the line is a simple linear regression.

Naked Eye Surveys

The sightings were right truncated at 3000m.

Covariate	Description
beaufort	Beaufort sea state.
size	Estimated size (number of individuals) of the sighted group.

Table 24: Covariates tested in candidate "multi-covariate distance sampling" (MCDS) detection functions.

Key	Adjustment	Order	Covariates	Succeeded	Δ AIC	Mean ESHW (m)
hn			beaufort	Yes	0.00	1340
hr			beaufort	Yes	2.59	1485
hn				Yes	5.48	1329
hn	cos	3		Yes	7.48	1329
hn	cos	2		Yes	7.48	1329
hn	herm	4		Yes	7.48	1329
hn	cos	1		Yes	7.48	1329
hr	poly	4		Yes	8.05	1283
hr				Yes	8.76	1342
hr	poly	2		Yes	169.37	1511
hr			size	No		
hn			size	No		
hr			beaufort, size	No		
hn			beaufort, size	No		

Table 25: Candidate detection functions for Naked Eye Surveys. The first one listed was selected for the density model.

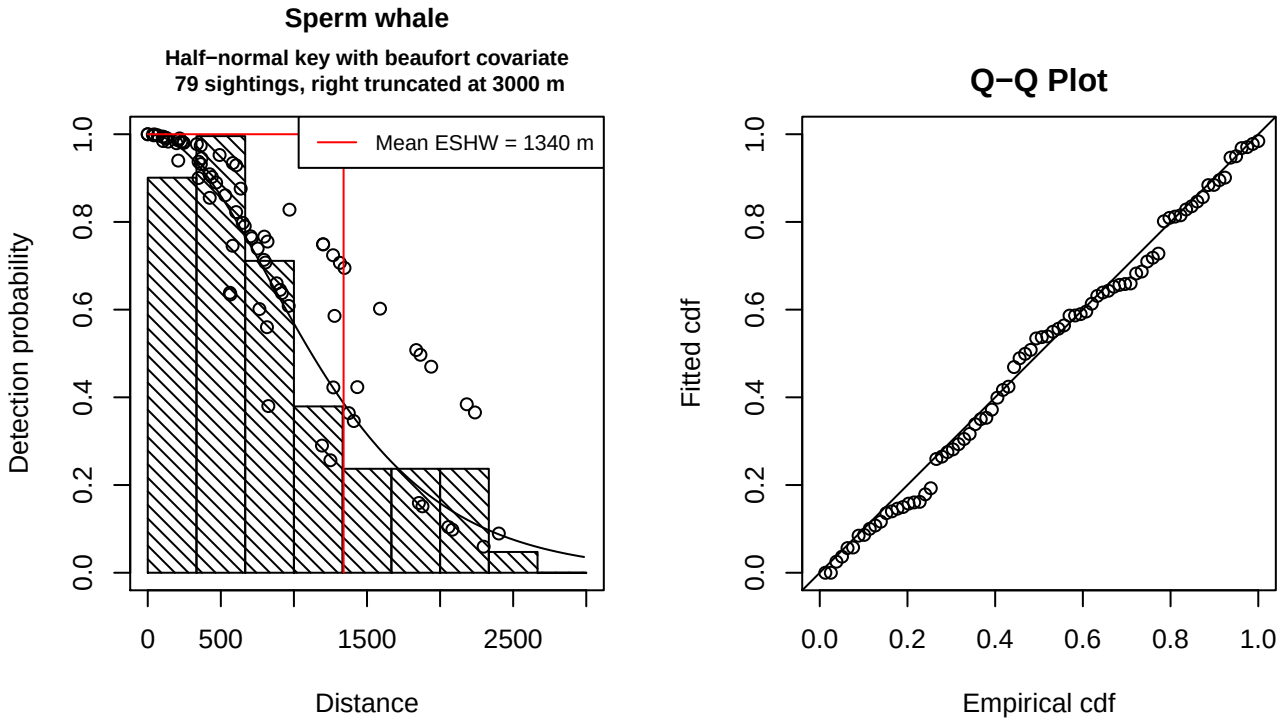

Figure 46: Detection function for Naked Eye Surveys that was selected for the density model

Statistical output for this detection function:

```
Summary for ds object
Number of observations :  79
Distance range         :  0  -  3000
AIC                    :  1208.519

Detection function:
 Half-normal key function

Detection function parameters
Scale Coefficients:
             estimate        se
(Intercept)  7.6084064 0.3815366
beaufort    -0.2445849 0.1281781

                       Estimate          SE         CV
Average p              0.4161873  0.03850659 0.09252226
N in covered region 189.8183930 24.26076178 0.12781038
```

Additional diagnostic plots:

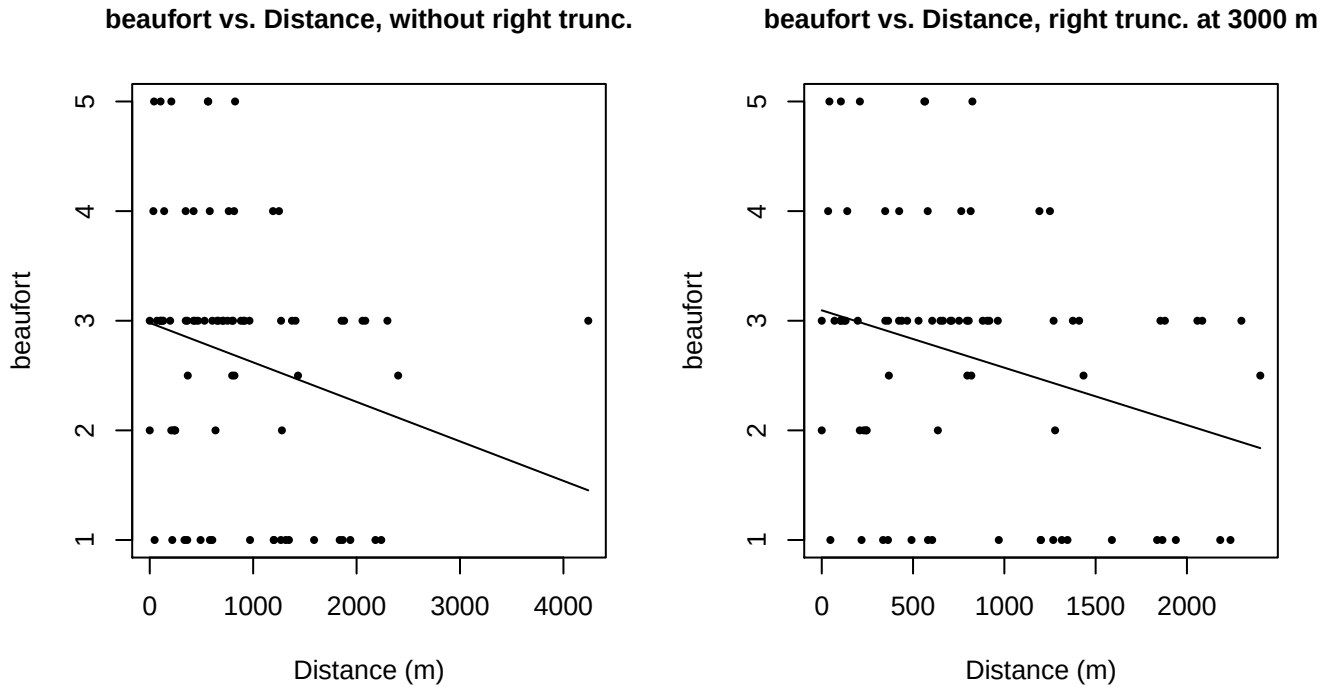

Figure 47: Scatterplots showing the relationship between Beaufort sea state and perpendicular sighting distance, for all sightings (left) and only those not right truncated (right). The line is a simple linear regression.

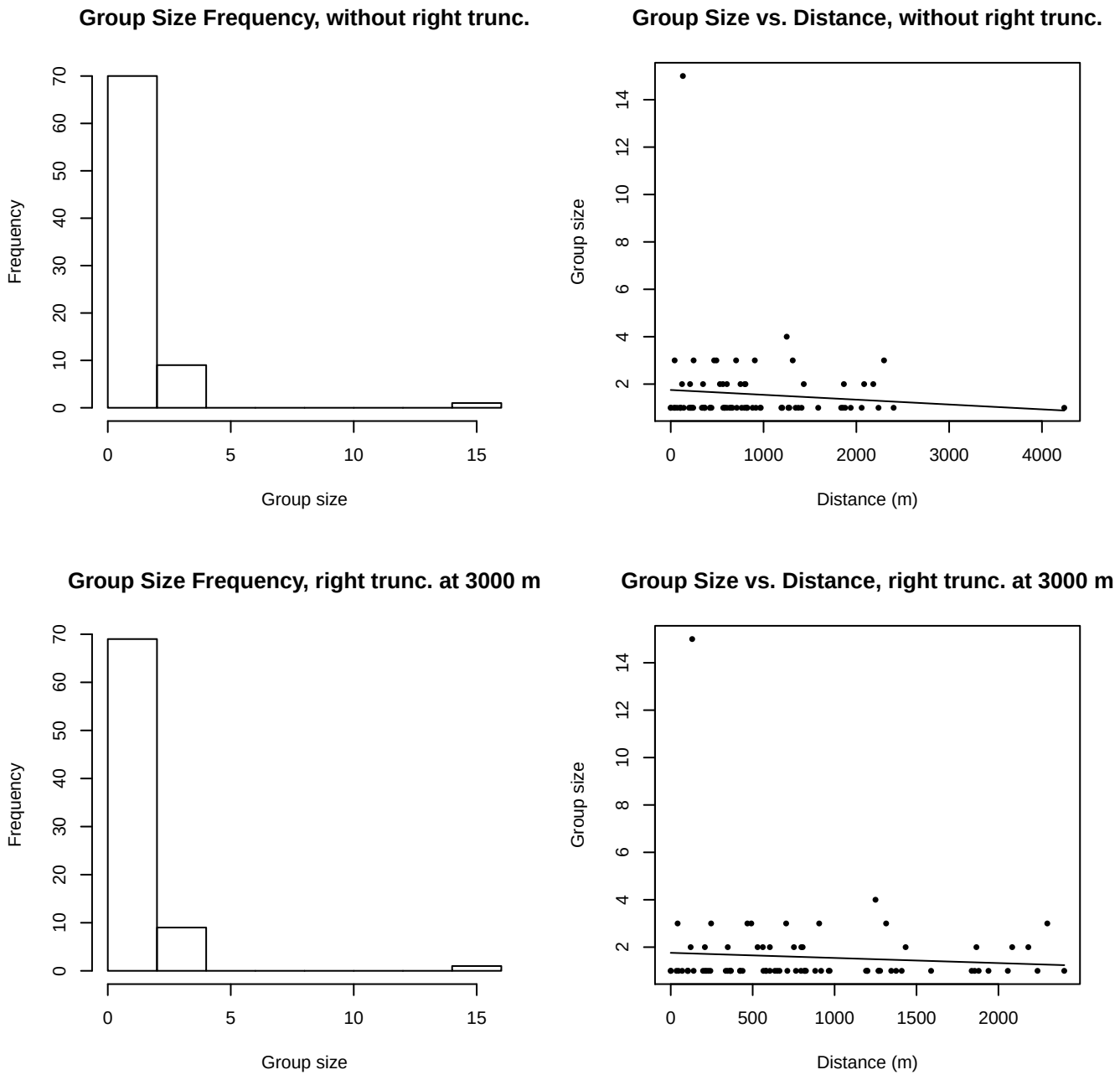

Figure 48: Histograms showing group size frequency and scatterplots showing the relationship between group size and perpendicular sighting distance, for all sightings (top row) and only those not right truncated (bottom row). In the scatterplot, the line is a simple linear regression.

Aerial Surveys

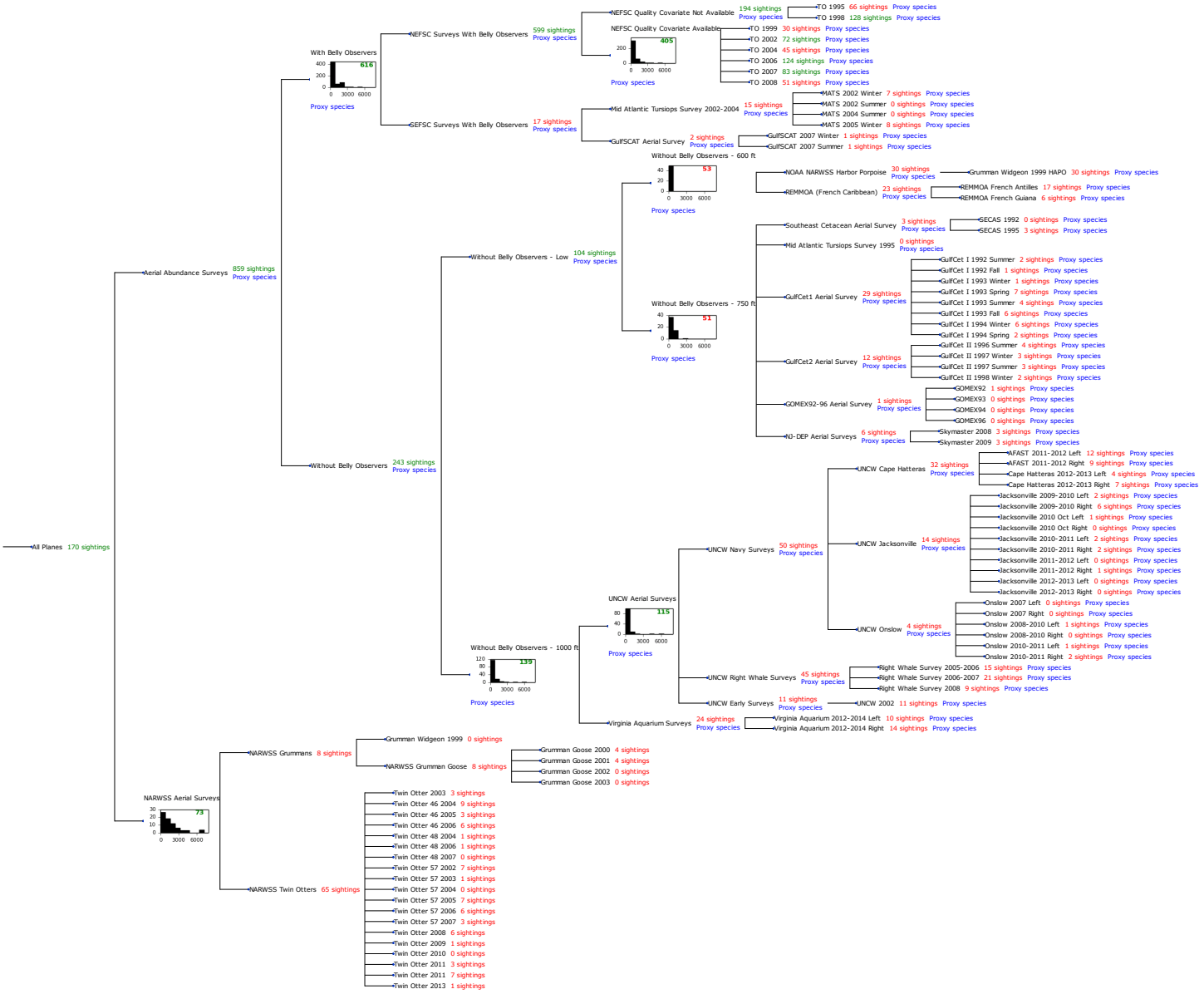

Figure 49: Detection hierarchy for aerial surveys

With Belly Observers

Because this taxon was sighted too infrequently to fit a detection function to its sightings alone, we fit a detection function to the pooled sightings of several other species that we believed would exhibit similar detectability. These "proxy species" are listed below.

Reported By Observer	Common Name	n
Balaenoptera	Balaenopterid sp.	2
Balaenoptera acutorostrata	Minke whale	97
Balaenoptera borealis	Sei whale	14
Balaenoptera borealis/edeni	Sei or Bryde's whale	0
Balaenoptera borealis/physalus	Fin or Sei whale	0

Balaenoptera edeni	Bryde's whale	2
Balaenoptera musculus	Blue whale	1
Balaenoptera physalus	Fin whale	235
Eubalaena glacialis	North Atlantic right whale	43
Eubalaena glacialis/Megaptera novaeangliae	Right or humpback whale	0
Megaptera novaeangliae	Humpback whale	198
Physeter macrocephalus	Sperm whale	24
Total		616

Table 26: Proxy species used to fit detection functions for With Belly Observers. The number of sightings, n, is before truncation.

The sightings were right truncated at 2000m.

Covariate	Description
beaufort	Beaufort sea state.
size	Estimated size (number of individuals) of the sighted group.

Table 27: Covariates tested in candidate "multi-covariate distance sampling" (MCDS) detection functions.

Key	Adjustment	Order	Covariates	Succeeded	Δ AIC	Mean ESHW (m)
hn	cos	2		Yes	0.00	593
hr	poly	4		Yes	2.46	609
hr			size	Yes	6.54	633
hr				Yes	8.64	629
hr	poly	2		Yes	10.64	629
hn	cos	3		Yes	11.17	586
hn			size	Yes	21.95	700
hn				Yes	22.65	698
hn	herm	4		Yes	24.22	697
hr			beaufort	No		
hn			beaufort	No		
hr			beaufort, size	No		
hn			beaufort, size	No		

Table 28: Candidate detection functions for With Belly Observers. The first one listed was selected for the density model.

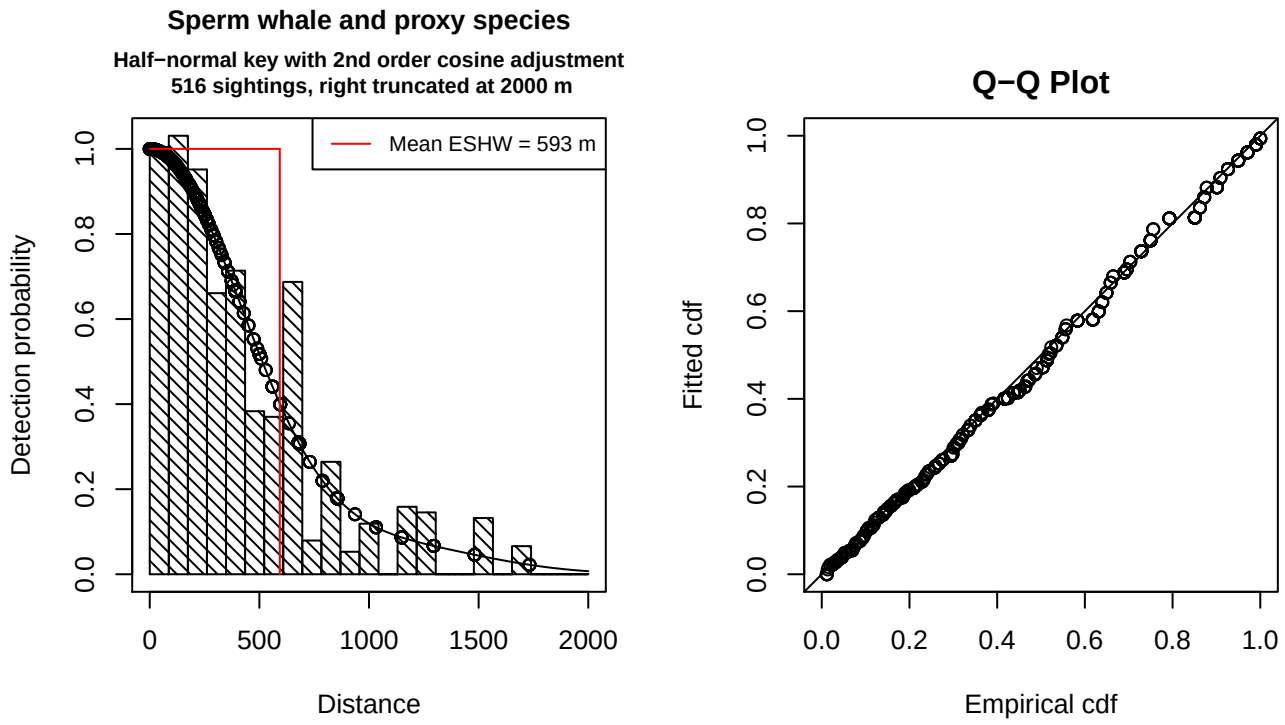

Figure 50: Detection function for With Belly Observers that was selected for the density model

Statistical output for this detection function:

```
Summary for ds object
Number of observations :  516
Distance range         :  0  -  2000
AIC                    :  7251.083

Detection function:
 Half-normal key function with cosine adjustment term of order 2

Detection function parameters
Scale Coefficients:
            estimate         se
(Intercept) 6.456112 0.04236696

Adjustment term parameter(s):
             estimate         se
cos, order 2  0.41854 0.07899307


Monotonicity constraints were enforced.
                        Estimate          SE         CV
Average p              0.2965255  0.01114114 0.03757228
N in covered region 1740.1541496 91.66829334 0.05267826

Monotonicity constraints were enforced.
```

Additional diagnostic plots:

Figure 51: Scatterplots showing the relationship between Beaufort sea state and perpendicular sighting distance, for all sightings (left) and only those not right truncated (right). The line is a simple linear regression.

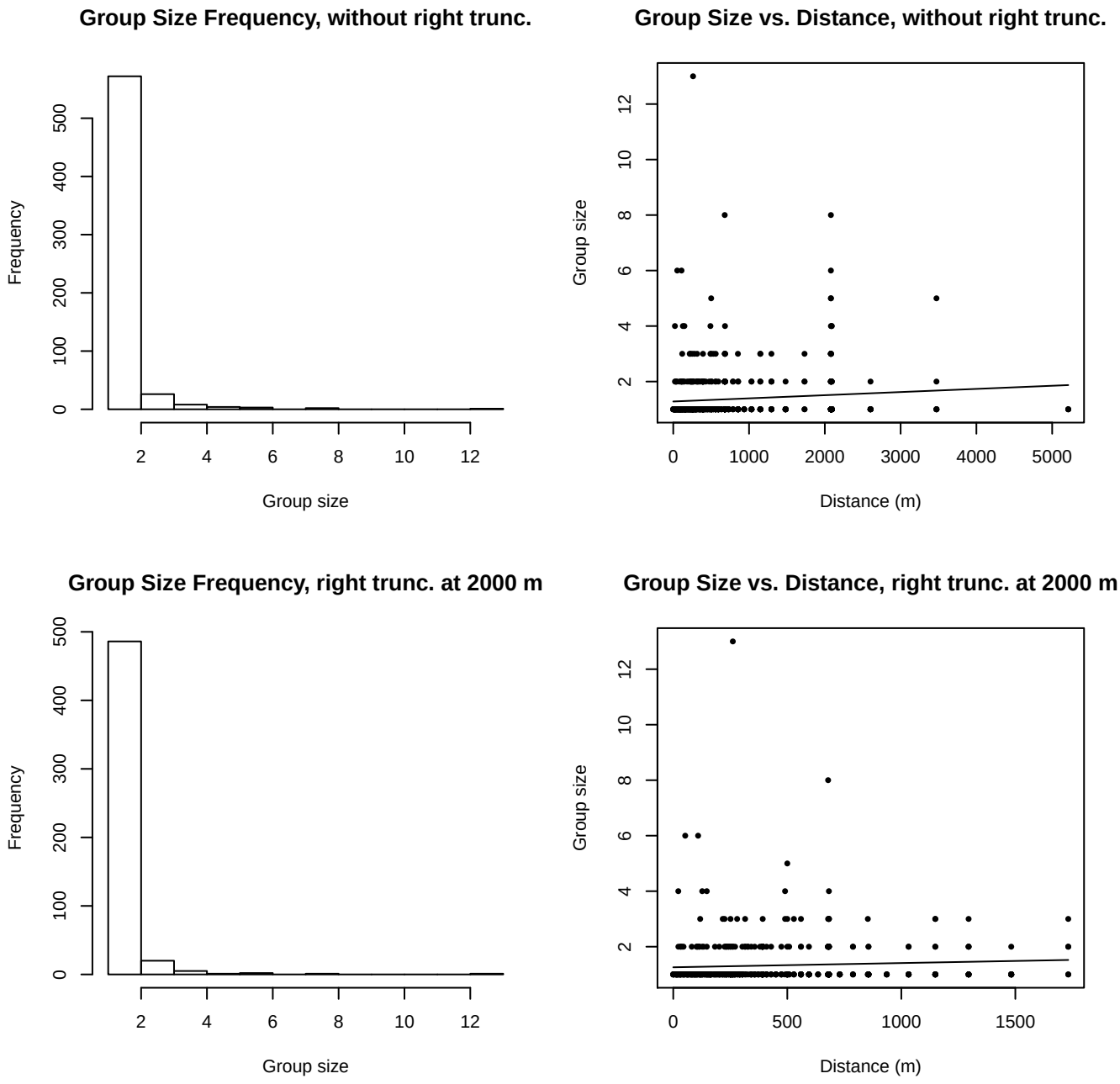

Figure 52: Histograms showing group size frequency and scatterplots showing the relationship between group size and perpendicular sighting distance, for all sightings (top row) and only those not right truncated (bottom row). In the scatterplot, the line is a simple linear regression.

NEFSC Quality Covariate Available

Because this taxon was sighted too infrequently to fit a detection function to its sightings alone, we fit a detection function to the pooled sightings of several other species that we believed would exhibit similar detectability. These "proxy species" are listed below.

Reported By Observer	Common Name	n
Balaenoptera	Balaenopterid sp.	0
Balaenoptera acutorostrata	Minke whale	68

Balaenoptera borealis	Sei whale	13
Balaenoptera borealis/edeni	Sei or Bryde's whale	0
Balaenoptera borealis/physalus	Fin or Sei whale	0
Balaenoptera edeni	Bryde's whale	0
Balaenoptera musculus	Blue whale	0
Balaenoptera physalus	Fin whale	147
Eubalaena glacialis	North Atlantic right whale	30
Eubalaena glacialis/Megaptera novaeangliae	Right or humpback whale	0
Megaptera novaeangliae	Humpback whale	130
Physeter macrocephalus	Sperm whale	17
Total		405

Table 29: Proxy species used to fit detection functions for NEFSC Quality Covariate Available. The number of sightings, n, is before truncation.

The sightings were right truncated at 2000m.

Covariate	Description
beaufort	Beaufort sea state.
quality	Survey-specific index of the quality of observation conditions, utilizing relevant factors other than Beaufort sea state (see methods).
size	Estimated size (number of individuals) of the sighted group.

Table 30: Covariates tested in candidate "multi-covariate distance sampling" (MCDS) detection functions.

Key	Adjustment	Order	Covariates	Succeeded	Δ AIC	Mean ESHW (m)
hr			size	Yes	0.00	623
hr	poly	4		Yes	1.19	579
hr	poly	2		Yes	2.57	568
hn	cos	2		Yes	3.69	605
hr				Yes	5.20	599
hn	cos	3		Yes	6.71	558
hn			size	Yes	25.74	751
hn				Yes	31.90	745
hn	herm	4		Yes	33.49	744
hr			beaufort	No		
hn			beaufort	No		
hr			quality	No		
hn			quality	No		
hr			beaufort, quality	No		

hn	beaufort, quality	No
hr	beaufort, size	No
hn	beaufort, size	No
hr	quality, size	No
hn	quality, size	No
hr	beaufort, quality, size	No
hn	beaufort, quality, size	No

Table 31: Candidate detection functions for NEFSC Quality Covariate Available. The first one listed was selected for the density model.

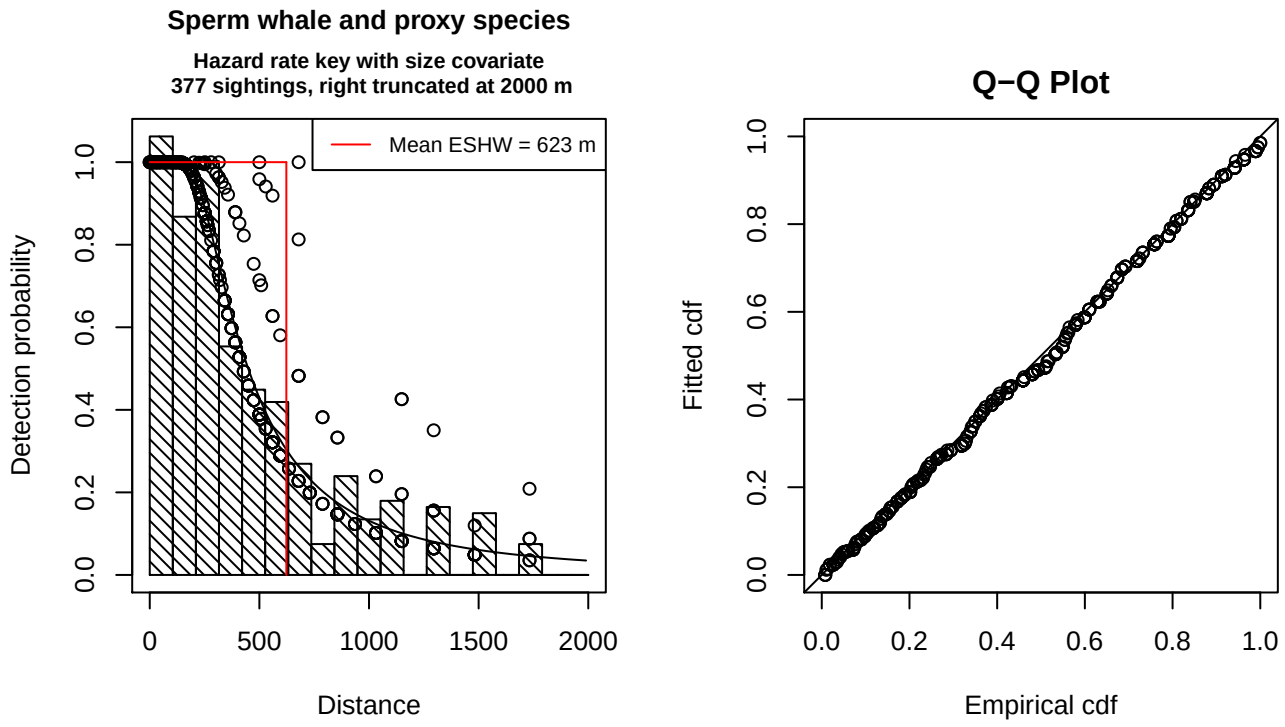

Figure 53: Detection function for NEFSC Quality Covariate Available that was selected for the density model

Statistical output for this detection function:

```
Summary for ds object
Number of observations :  377
Distance range         :  0  -  2000
AIC                    :  5330.388

Detection function:
 Hazard-rate key function

Detection function parameters
Scale Coefficients:
             estimate        se
(Intercept) 5.4325057 0.2042132
size        0.4446325 0.1425199
```

```
Shape parameters:
             estimate         se
(Intercept) 0.7426058 0.09605544

                         Estimate           SE         CV
Average p                0.2968991   0.01971228 0.06639386
N in covered region 1269.7915360 100.88087285 0.07944680
```

Additional diagnostic plots:

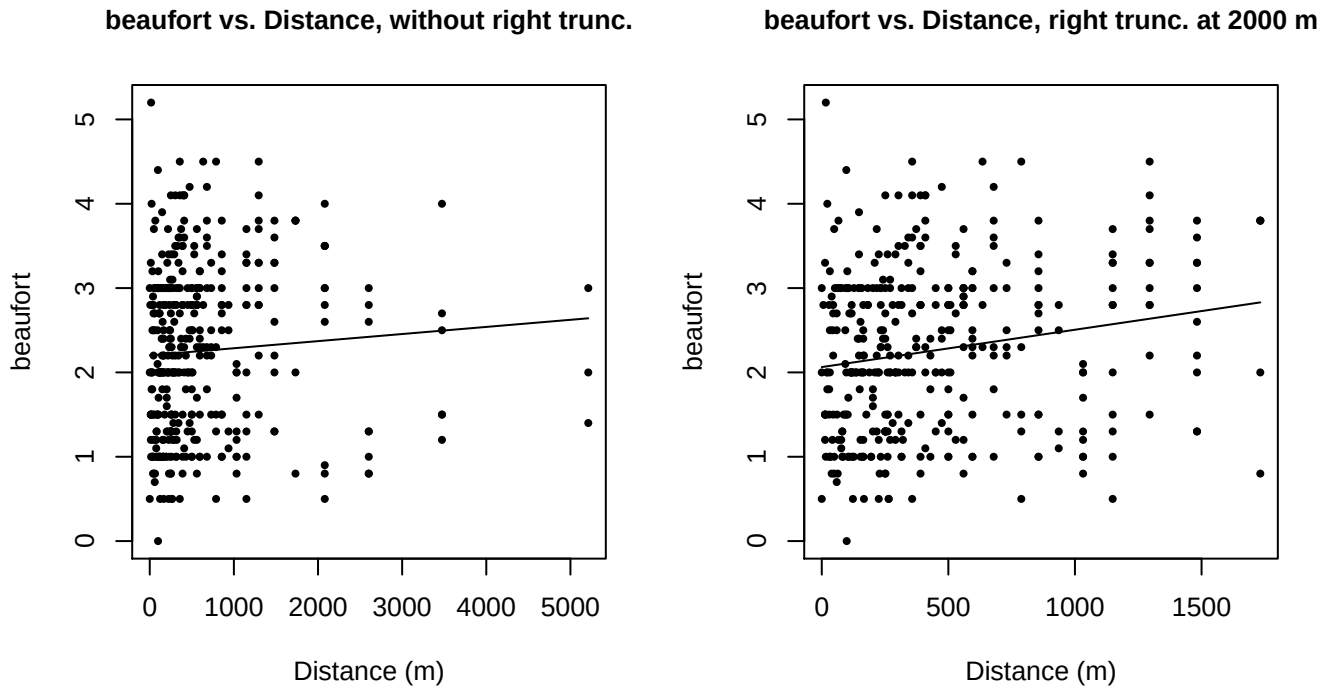

Figure 54: Scatterplots showing the relationship between Beaufort sea state and perpendicular sighting distance, for all sightings (left) and only those not right truncated (right). The line is a simple linear regression.

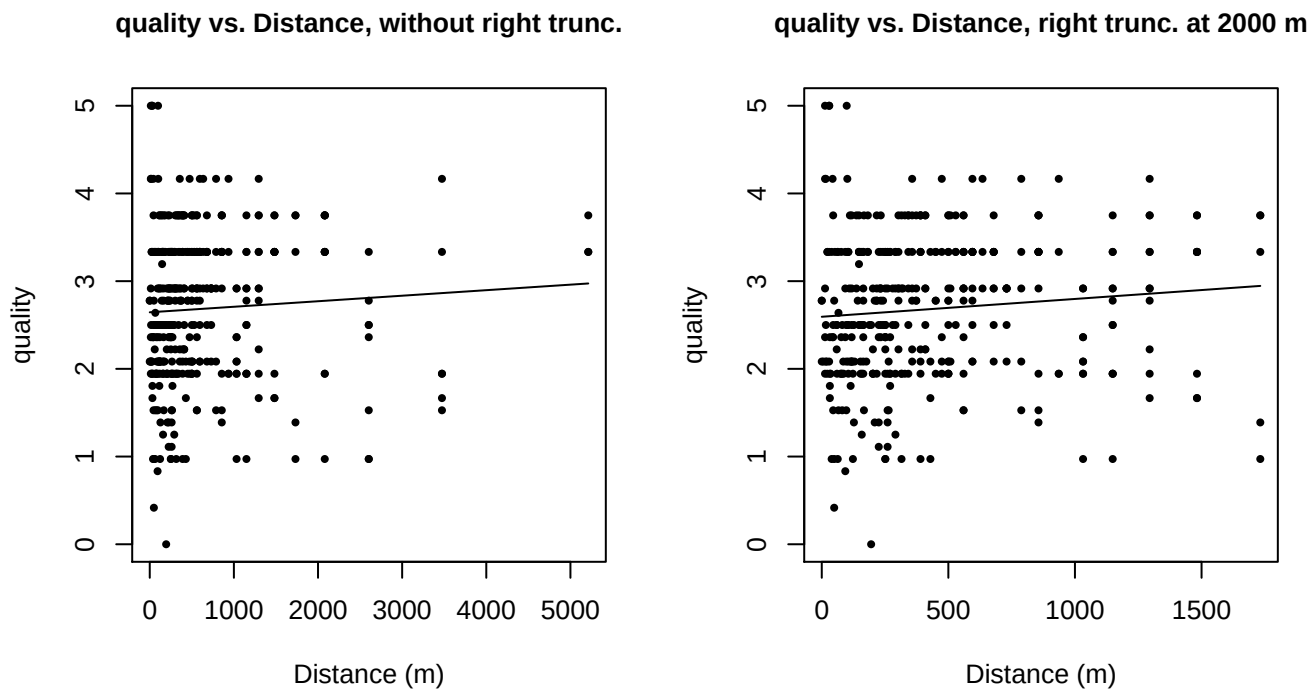

Figure 55: Scatterplots showing the relationship between the survey-specific index of the quality of observation conditions and perpendicular sighting distance, for all sightings (left) and only those not right truncated (right). Low values of the quality index correspond to better observation conditions. The line is a simple linear regression.

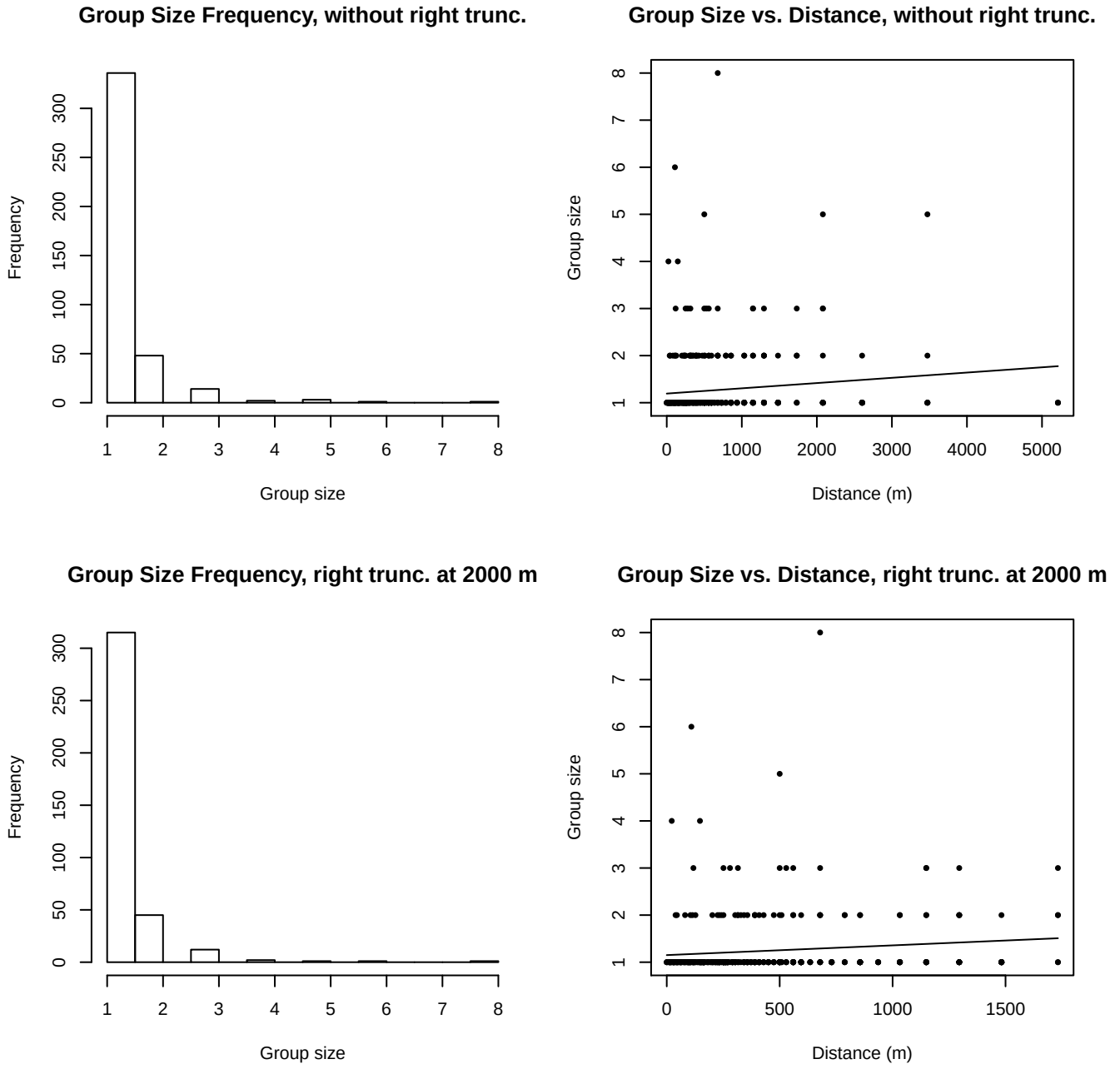

Figure 56: Histograms showing group size frequency and scatterplots showing the relationship between group size and perpendicular sighting distance, for all sightings (top row) and only those not right truncated (bottom row). In the scatterplot, the line is a simple linear regression.

Without Belly Observers - 600 ft

Because this taxon was sighted too infrequently to fit a detection function to its sightings alone, we fit a detection function to the pooled sightings of several other species that we believed would exhibit similar detectability. These "proxy species" are listed below.

Reported By Observer	Common Name	n
Balaenoptera	Balaenopterid sp.	2
Balaenoptera acutorostrata	Minke whale	8

Balaenoptera borealis	Sei whale	0
Balaenoptera borealis/edeni	Sei or Bryde's whale	0
Balaenoptera borealis/physalus	Fin or Sei whale	0
Balaenoptera edeni	Bryde's whale	0
Balaenoptera musculus	Blue whale	0
Balaenoptera physalus	Fin whale	15
Eubalaena glacialis	North Atlantic right whale	2
Eubalaena glacialis/Megaptera novaeangliae	Right or humpback whale	0
Megaptera novaeangliae	Humpback whale	16
Physeter macrocephalus	Sperm whale	10
Total		53

Table 32: Proxy species used to fit detection functions for Without Belly Observers - 600 ft. The number of sightings, n, is before truncation.

The sightings were right truncated at 600m. Due to a reduced frequency of sightings close to the trackline that plausibly resulted from the behavior of the observers and/or the configuration of the survey platform, the sightings were left truncted as well. Sightings closer than 32 m to the trackline were omitted from the analysis, and it was assumed that the the area closer to the trackline than this was not surveyed. This distance was estimated by inspecting histograms of perpendicular sighting distances.

Covariate	Description
beaufort	Beaufort sea state.
size	Estimated size (number of individuals) of the sighted group.

Table 33: Covariates tested in candidate "multi-covariate distance sampling" (MCDS) detection functions.

Key	Adjustment	Order	Covariates	Succeeded	Δ AIC	Mean ESHW (m)
hn				Yes	0.00	293
hr				Yes	1.14	318
hn			beaufort	Yes	1.57	293
hn	cos	3		Yes	1.65	311
hn	herm	4		Yes	1.93	291
hr			beaufort	Yes	1.97	326
hn	cos	2		Yes	1.97	283
hr	poly	2		Yes	3.14	318
hr	poly	4		Yes	3.14	318
hn			size	No		
hr			size	No		
hn			beaufort, size	No		
hr			beaufort, size	No		

Table 34: Candidate detection functions for Without Belly Observers - 600 ft. The first one listed was selected for the density model.

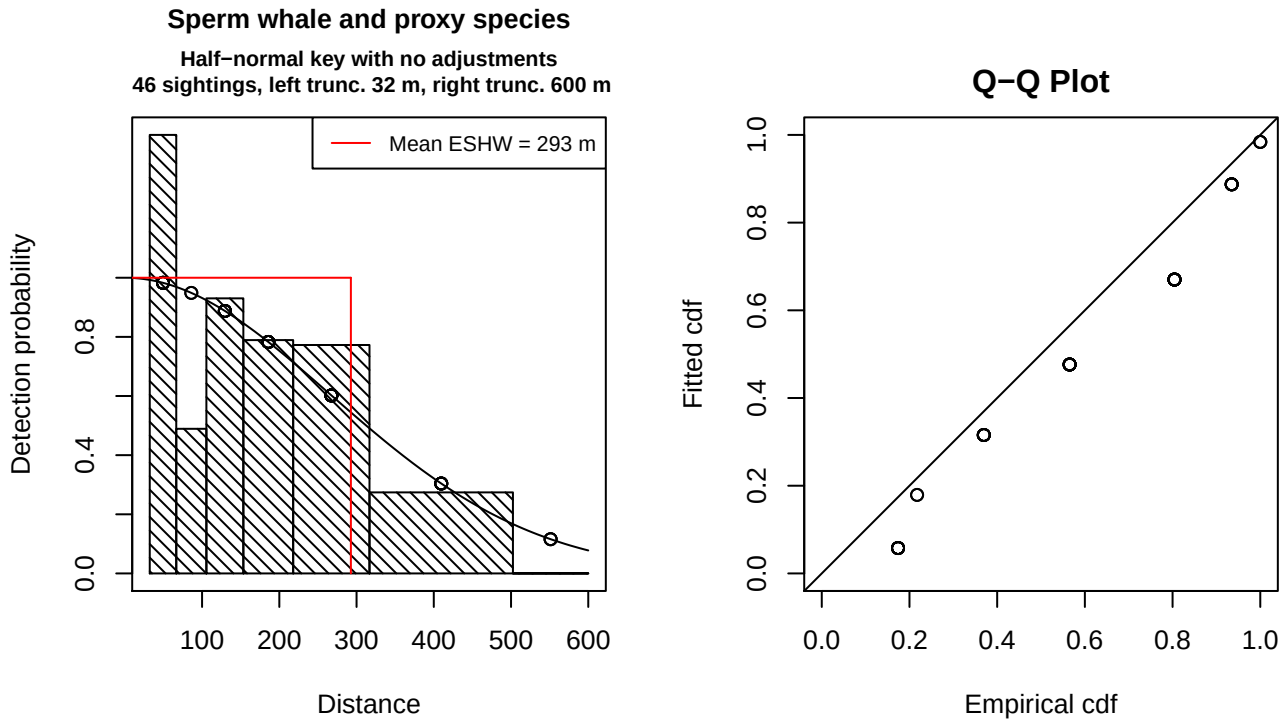

Figure 57: Detection function for Without Belly Observers - 600 ft that was selected for the density model

Statistical output for this detection function:

```
Summary for ds object
Number of observations :  46
Distance range         :  32.24668  -  600
AIC                    :  177.4011

Detection function:
 Half-normal key function

Detection function parameters
Scale Coefficients:
            estimate        se
(Intercept) 5.581559 0.1339955

                     Estimate          SE        CV
Average p            0.487738  0.06208134 0.1272842
N in covered region 94.312922 15.59372100 0.1653402
```

Additional diagnostic plots:

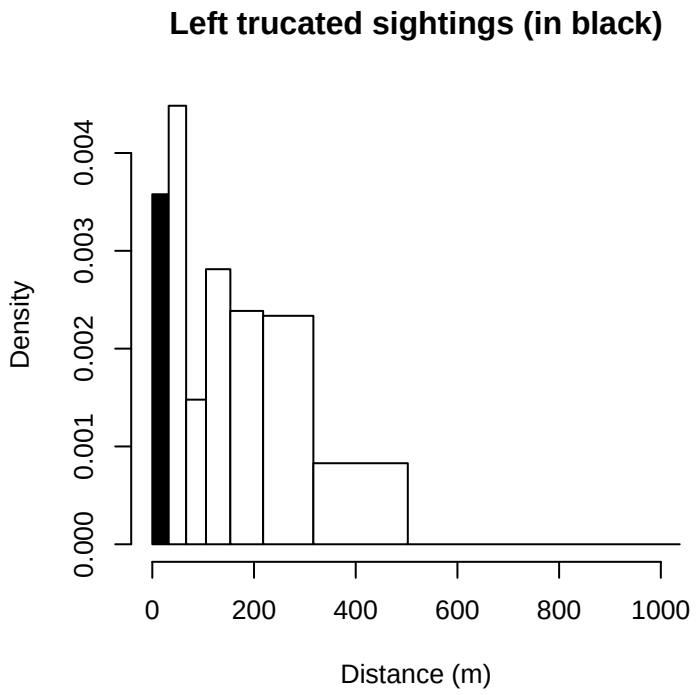

Figure 58: Density of sightings by perpendicular distance for Without Belly Observers - 600 ft. Black bars on the left show sightings that were left truncated.

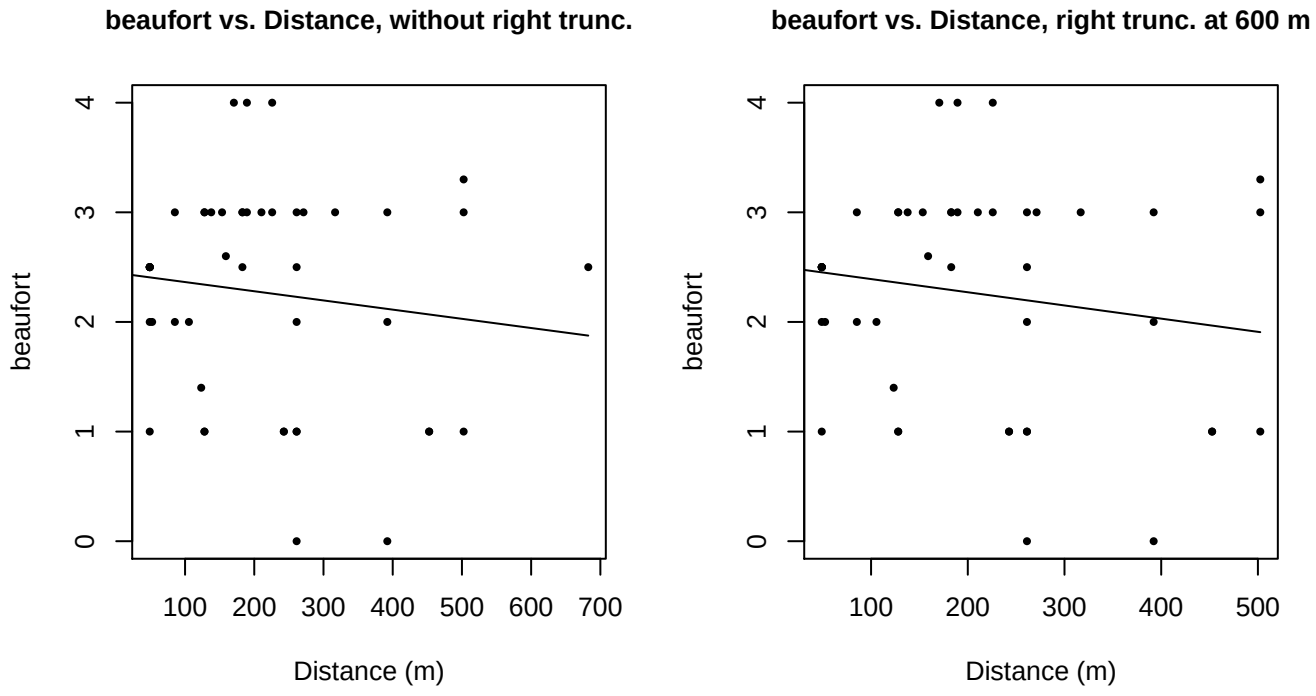

Figure 59: Scatterplots showing the relationship between Beaufort sea state and perpendicular sighting distance, for all sightings (left) and only those not right truncated (right). The line is a simple linear regression.

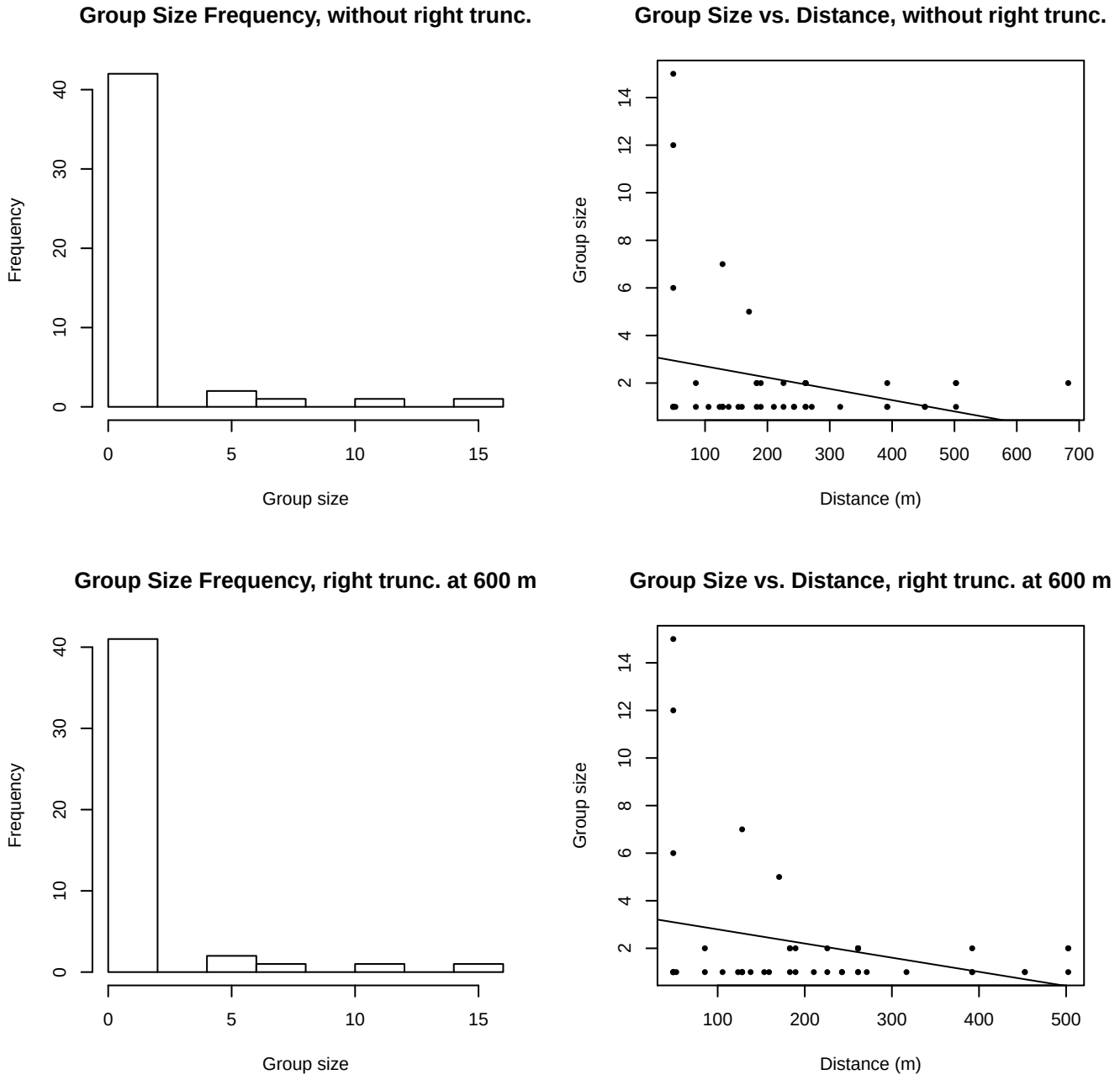

Figure 60: Histograms showing group size frequency and scatterplots showing the relationship between group size and perpendicular sighting distance, for all sightings (top row) and only those not right truncated (bottom row). In the scatterplot, the line is a simple linear regression.

Without Belly Observers - 750 ft

Because this taxon was sighted too infrequently to fit a detection function to its sightings alone, we fit a detection function to the pooled sightings of several other species that we believed would exhibit similar detectability. These "proxy species" are listed below.

Reported By Observer	Common Name	n
Balaenoptera	Balaenopterid sp.	1
Balaenoptera acutorostrata	Minke whale	0

Balaenoptera borealis	Sei whale	0
Balaenoptera borealis/edeni	Sei or Bryde's whale	2
Balaenoptera borealis/physalus	Fin or Sei whale	0
Balaenoptera edeni	Bryde's whale	3
Balaenoptera musculus	Blue whale	0
Balaenoptera physalus	Fin whale	2
Eubalaena glacialis	North Atlantic right whale	0
Eubalaena glacialis/Megaptera novaeangliae	Right or humpback whale	0
Megaptera novaeangliae	Humpback whale	6
Physeter macrocephalus	Sperm whale	37
Total		51

Table 35: Proxy species used to fit detection functions for Without Belly Observers - 750 ft. The number of sightings, n, is before truncation.

The sightings were right truncated at 600m. Due to a reduced frequency of sightings close to the trackline that plausibly resulted from the behavior of the observers and/or the configuration of the survey platform, the sightings were left truncted as well. Sightings closer than 40 m to the trackline were omitted from the analysis, and it was assumed that the the area closer to the trackline than this was not surveyed. This distance was estimated by inspecting histograms of perpendicular sighting distances. The vertical sighting angles were heaped at 10 degree increments, so the candidate detection functions were fitted using linear bins scaled accordingly.

Key	Adjustment	Order	Covariates	Succeeded	Δ AIC	Mean ESHW (m)
hn	cos	2		Yes	0.00	216
hr				Yes	0.59	251
hn	cos	3		Yes	2.31	255
hn	herm	4		Yes	2.46	316
hr	poly	2		Yes	2.59	251
hr	poly	4		Yes	2.59	255
hn				No		

Table 36: Candidate detection functions for Without Belly Observers - 750 ft. The first one listed was selected for the density model.

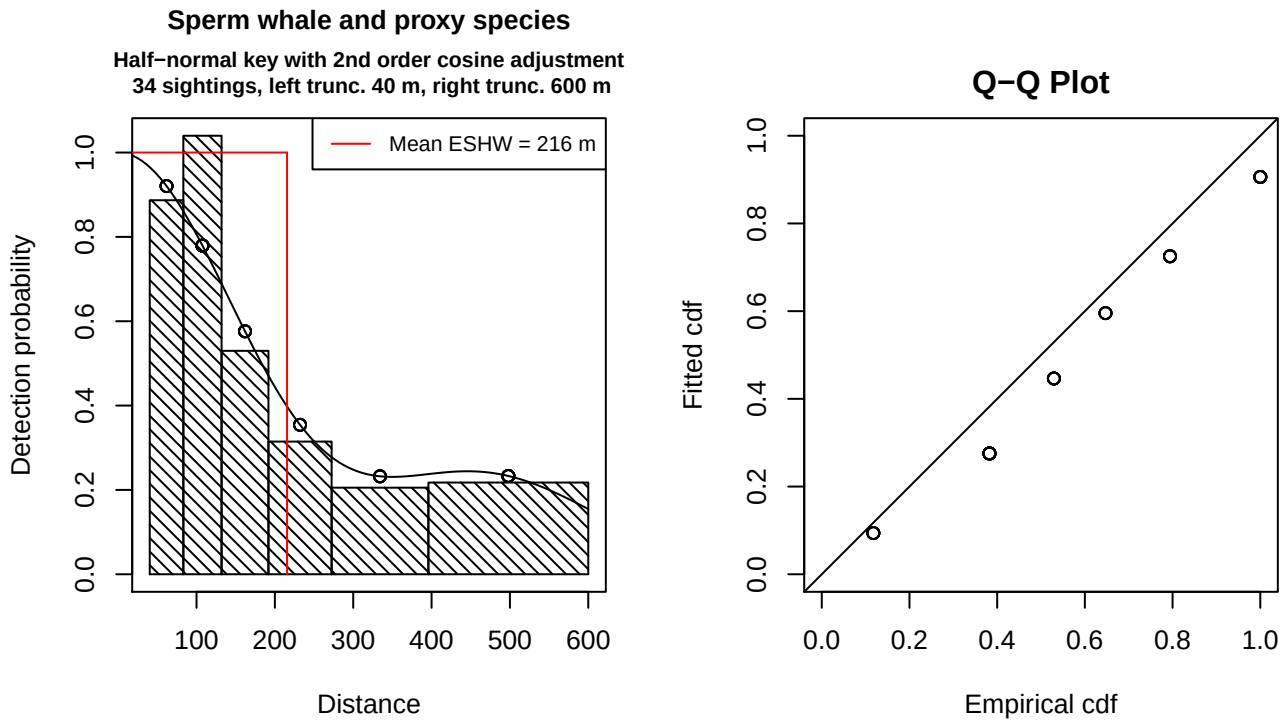

Figure 61: Detection function for Without Belly Observers - 750 ft that was selected for the density model

Statistical output for this detection function:

```
Summary for ds object
Number of observations :  34
Distance range         :  40.30835  -  600
AIC                    :  124.984

Detection function:
 Half-normal key function with cosine adjustment term of order 2

Detection function parameters
Scale Coefficients:
            estimate        se
(Intercept) 5.738325 0.1838281

Adjustment term parameter(s):
              estimate       se
cos, order 2 0.4333819 0.242253


Monotonicity constraints were enforced.
                     Estimate          SE        CV
Average p            0.3592781  0.08709337 0.2424121
N in covered region 94.6342115 26.36346801 0.2785828

Monotonicity constraints were enforced.
```

Additional diagnostic plots:

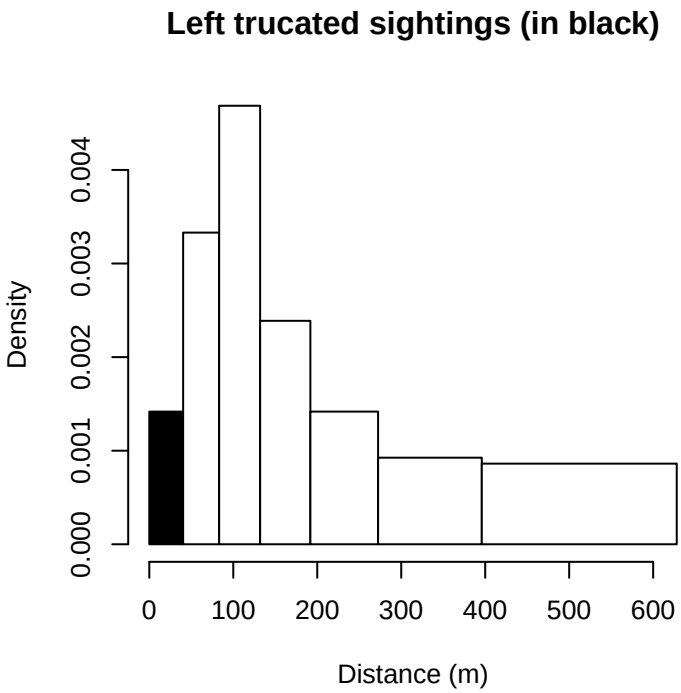

Figure 62: Density of sightings by perpendicular distance for Without Belly Observers - 750 ft. Black bars on the left show sightings that were left truncated.

Without Belly Observers - 1000 ft

Because this taxon was sighted too infrequently to fit a detection function to its sightings alone, we fit a detection function to the pooled sightings of several other species that we believed would exhibit similar detectability. These "proxy species" are listed below.

Reported By Observer	Common Name	n
Balaenoptera	Balaenopterid sp.	1
Balaenoptera acutorostrata	Minke whale	16
Balaenoptera borealis	Sei whale	0
Balaenoptera borealis/edeni	Sei or Bryde's whale	0
Balaenoptera borealis/physalus	Fin or Sei whale	0
Balaenoptera edeni	Bryde's whale	0
Balaenoptera musculus	Blue whale	0
Balaenoptera physalus	Fin whale	32
Eubalaena glacialis	North Atlantic right whale	34
Eubalaena glacialis/Megaptera novaeangliae	Right or humpback whale	0
Megaptera novaeangliae	Humpback whale	30
Physeter macrocephalus	Sperm whale	26
Total		139

Table 37: Proxy species used to fit detection functions for Without Belly Observers - 1000 ft. The number of sightings, n, is before truncation.

The sightings were right truncated at 1500m.

Covariate	Description
beaufort	Beaufort sea state.
quality	Survey-specific index of the quality of observation conditions, utilizing relevant factors other than Beaufort sea state (see methods).
size	Estimated size (number of individuals) of the sighted group.

Table 38: Covariates tested in candidate "multi-covariate distance sampling" (MCDS) detection functions.

Key	Adjustment	Order	Covariates	Succeeded	Δ AIC	Mean ESHW (m)
hr				Yes	0.00	474
hr	poly	4		Yes	0.28	465
hn	cos	2		Yes	0.58	488
hn	cos	3		Yes	1.09	445
hr	poly	2		Yes	1.33	464
hn				Yes	8.94	612
hn	herm	4		Yes	10.79	611
hr			beaufort	No		
hn			beaufort	No		
hr			quality	No		
hn			quality	No		
hr			size	No		
hn			size	No		
hr			beaufort, quality	No		
hn			beaufort, quality	No		
hr			beaufort, size	No		
hn			beaufort, size	No		
hr			quality, size	No		
hn			quality, size	No		
hr			beaufort, quality, size	No		
hn			beaufort, quality, size	No		

Table 39: Candidate detection functions for Without Belly Observers - 1000 ft. The first one listed was selected for the density model.

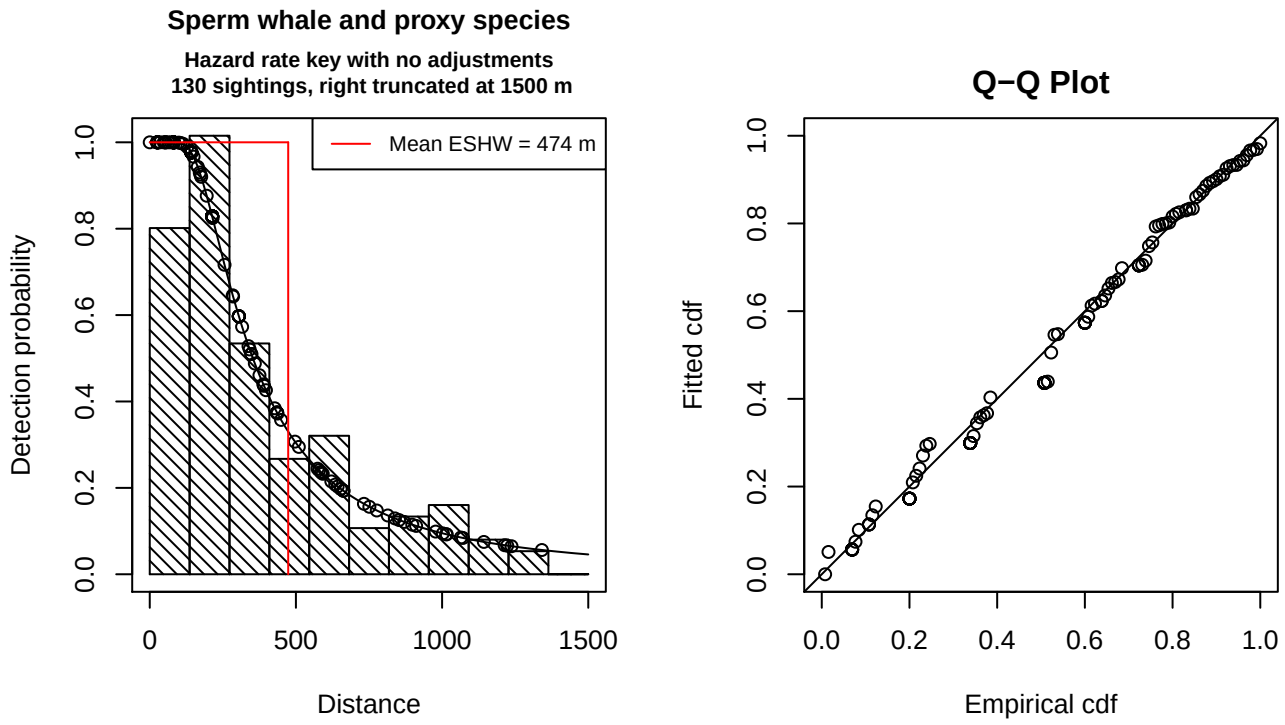

Figure 63: Detection function for Without Belly Observers - 1000 ft that was selected for the density model

Statistical output for this detection function:

```
Summary for ds object
Number of observations :  130
Distance range         :  0  -  1500
AIC                    :  1788.429

Detection function:
 Hazard-rate key function

Detection function parameters
Scale Coefficients:
            estimate        se
(Intercept) 5.668741 0.2097304

Shape parameters:
             estimate        se
(Intercept) 0.6203132 0.1719714

                      Estimate          SE        CV
Average p             0.315735  0.03965146 0.1255846
N in covered region 411.737693 59.71626486 0.1450347
```

Additional diagnostic plots:

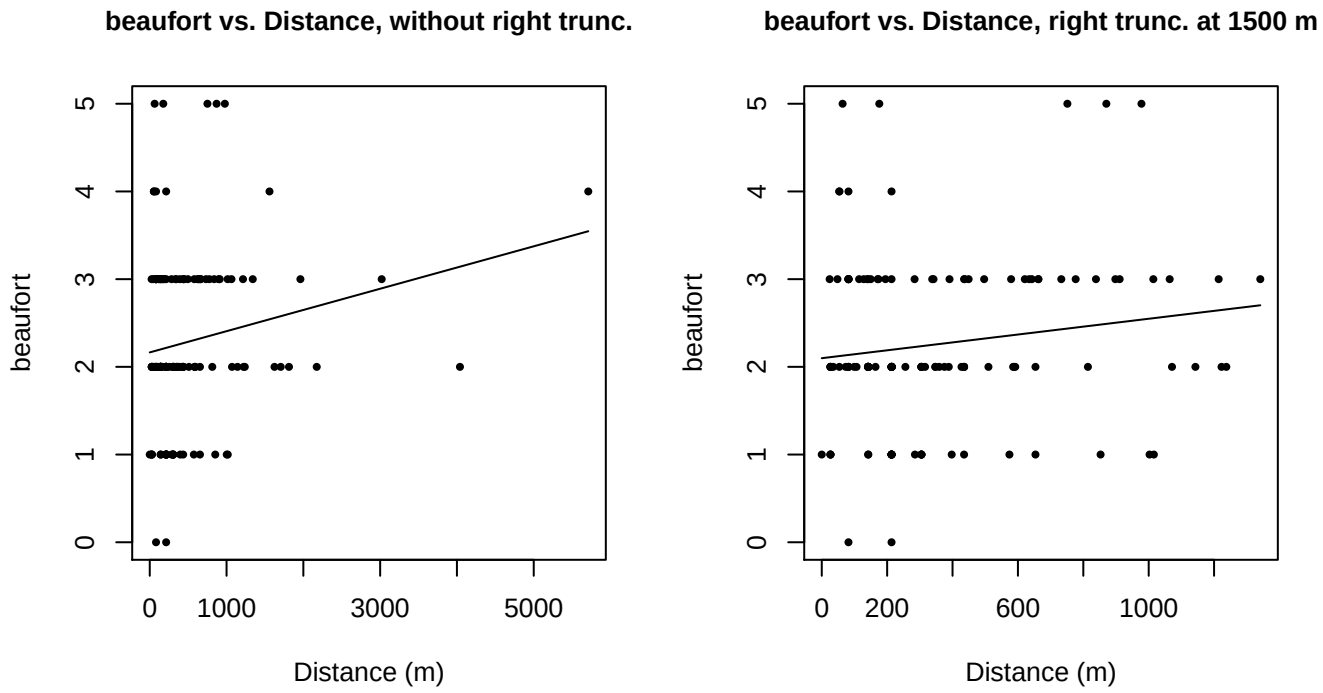

Figure 64: Scatterplots showing the relationship between Beaufort sea state and perpendicular sighting distance, for all sightings (left) and only those not right truncated (right). The line is a simple linear regression.

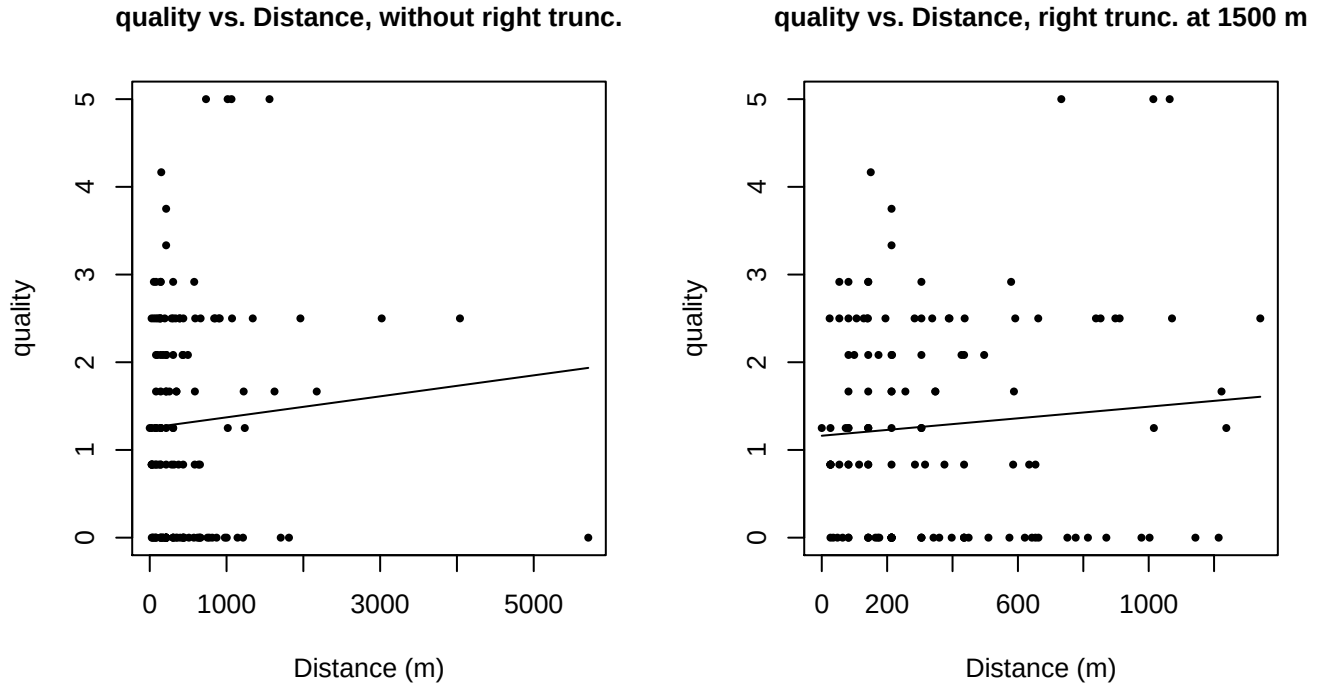

Figure 65: Scatterplots showing the relationship between the survey-specific index of the quality of observation conditions and perpendicular sighting distance, for all sightings (left) and only those not right truncated (right). Low values of the quality index correspond to better observation conditions. The line is a simple linear regression.

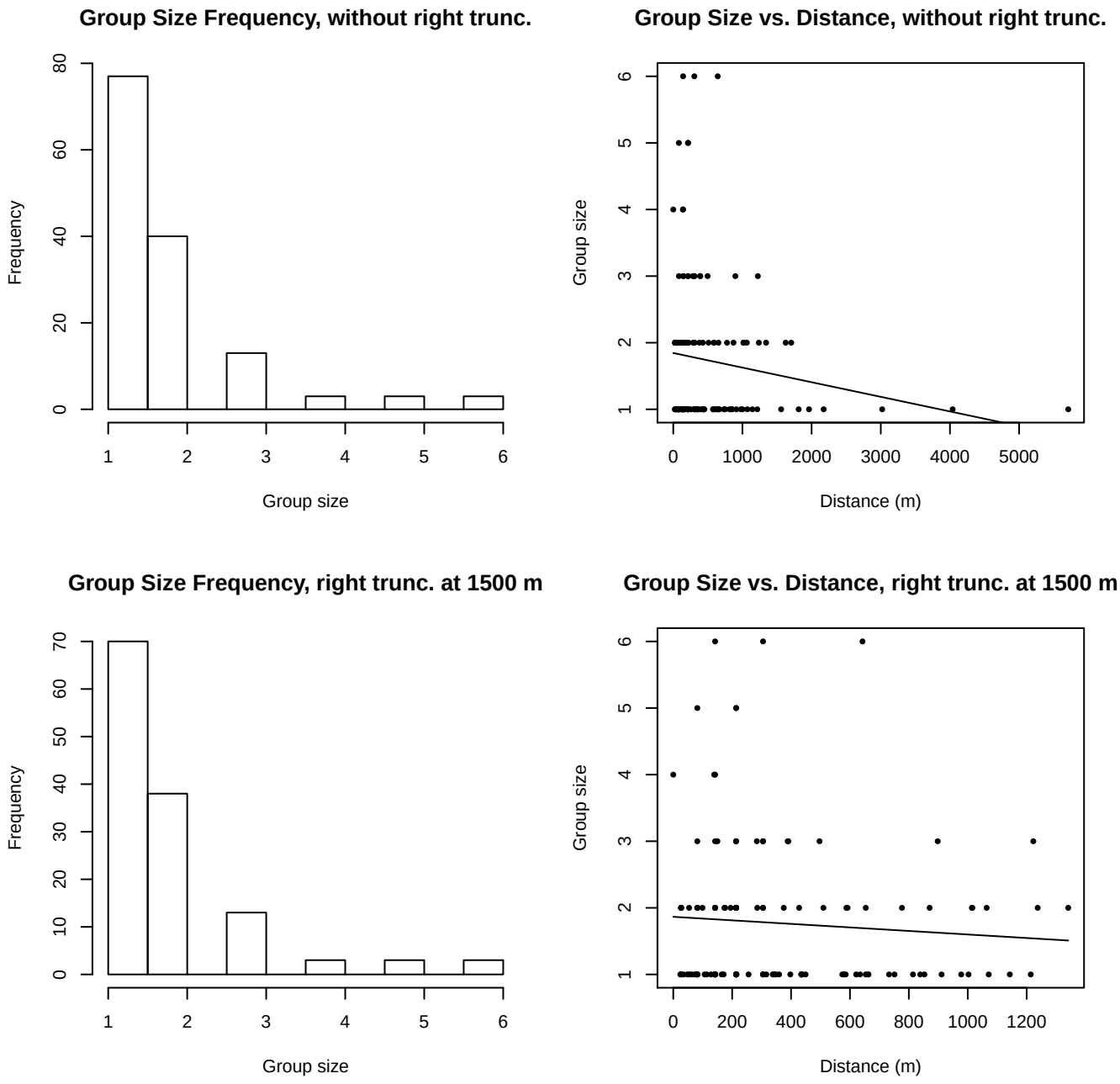

Figure 66: Histograms showing group size frequency and scatterplots showing the relationship between group size and perpendicular sighting distance, for all sightings (top row) and only those not right truncated (bottom row). In the scatterplot, the line is a simple linear regression.

UNCW Aerial Surveys

Because this taxon was sighted too infrequently to fit a detection function to its sightings alone, we fit a detection function to the pooled sightings of several other species that we believed would exhibit similar detectability. These "proxy species" are listed below.

Reported By Observer	Common Name	n
Balaenoptera	Balaenopterid sp.	1
Balaenoptera acutorostrata	Minke whale	15

Balaenoptera borealis	Sei whale	0
Balaenoptera borealis/edeni	Sei or Bryde's whale	0
Balaenoptera borealis/physalus	Fin or Sei whale	0
Balaenoptera edeni	Bryde's whale	0
Balaenoptera musculus	Blue whale	0
Balaenoptera physalus	Fin whale	19
Eubalaena glacialis	North Atlantic right whale	31
Eubalaena glacialis/Megaptera novaeangliae	Right or humpback whale	0
Megaptera novaeangliae	Humpback whale	23
Physeter macrocephalus	Sperm whale	26
Total		115

Table 40: Proxy species used to fit detection functions for UNCW Aerial Surveys. The number of sightings, n, is before truncation.

The sightings were right truncated at 1500m.

Covariate	Description
beaufort	Beaufort sea state.
quality	Survey-specific index of the quality of observation conditions, utilizing relevant factors other than Beaufort sea state (see methods).
size	Estimated size (number of individuals) of the sighted group.

Table 41: Covariates tested in candidate "multi-covariate distance sampling" (MCDS) detection functions.

Key	Adjustment	Order	Covariates	Succeeded	Δ AIC	Mean ESHW (m)
hn	cos	3		Yes	0.00	398
hr	poly	4		Yes	1.33	435
hr				Yes	1.73	441
hr	poly	2		Yes	1.76	432
hn	cos	2		Yes	1.90	448
hn				Yes	7.05	539
hn	herm	4		Yes	8.97	538
hr			beaufort	No		
hn			beaufort	No		
hr			quality	No		
hn			quality	No		
hr			size	No		
hn			size	No		
hr			beaufort, quality	No		

hn	beaufort, quality	No
hr	beaufort, size	No
hn	beaufort, size	No
hr	quality, size	No
hn	quality, size	No
hr	beaufort, quality, size	No
hn	beaufort, quality, size	No

Table 42: Candidate detection functions for UNCW Aerial Surveys. The first one listed was selected for the density model.

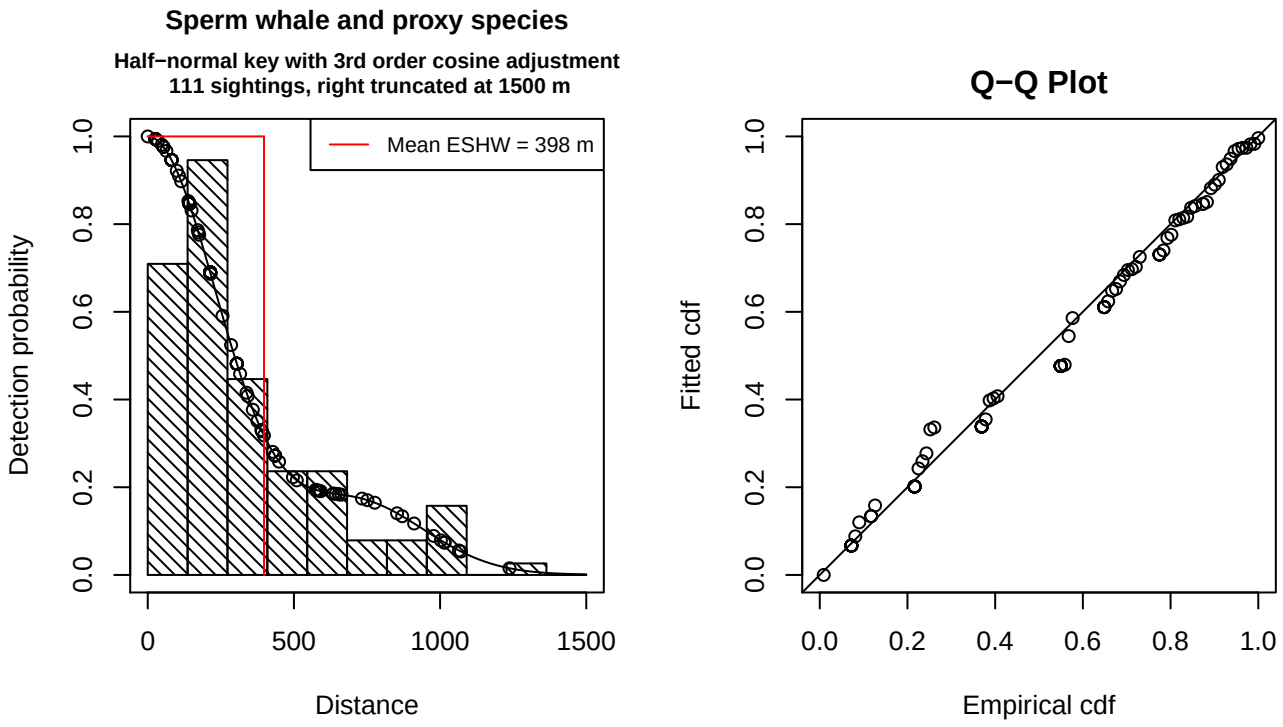

Figure 67: Detection function for UNCW Aerial Surveys that was selected for the density model

Statistical output for this detection function:

```
Summary for ds object
Number of observations :  111
Distance range         :  0  -  1500
AIC                    :  1501.474

Detection function:
 Half-normal key function with cosine adjustment term of order 3

Detection function parameters
Scale Coefficients:
            estimate         se
(Intercept) 6.097794 0.06273553
```

```
Adjustment term parameter(s):
             estimate        se
cos, order 3 0.412894 0.1290932


Monotonicity constraints were enforced.
                       Estimate          SE        CV
Average p             0.2651265  0.02716248 0.1024510
N in covered region 418.6680359 54.77465800 0.1308308

Monotonicity constraints were enforced.
```

Additional diagnostic plots:

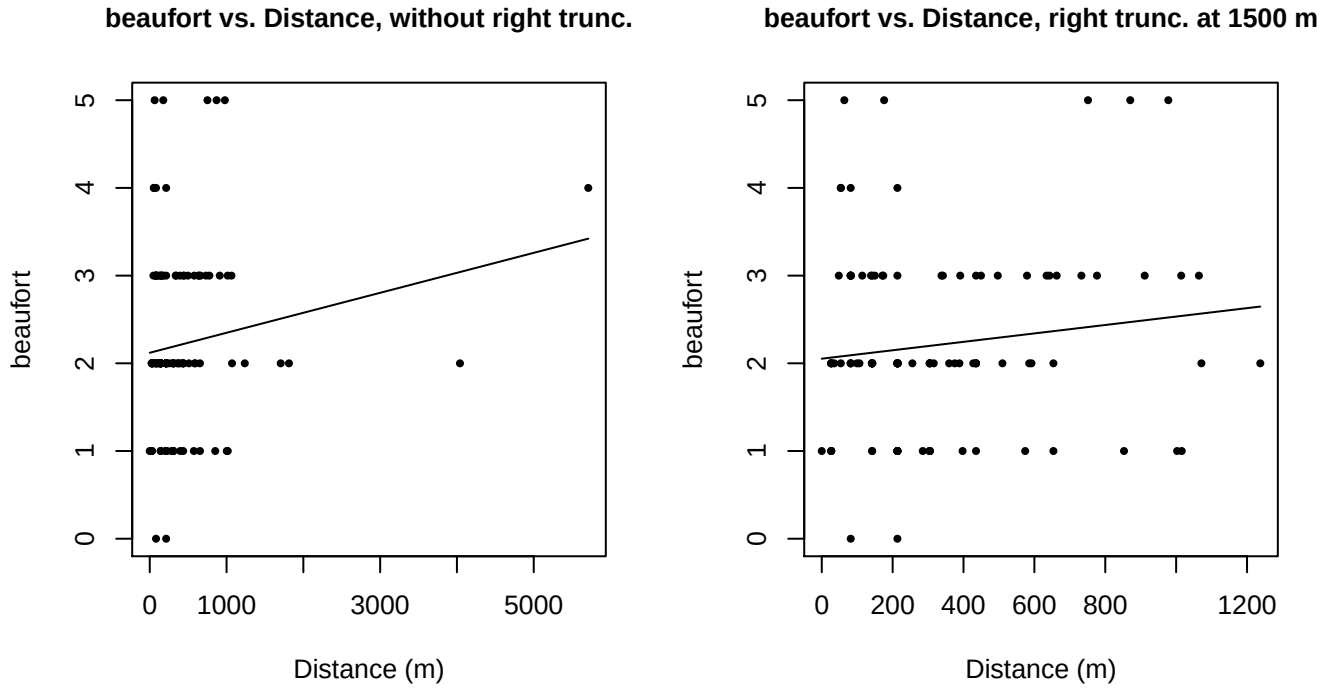

Figure 68: Scatterplots showing the relationship between Beaufort sea state and perpendicular sighting distance, for all sightings (left) and only those not right truncated (right). The line is a simple linear regression.

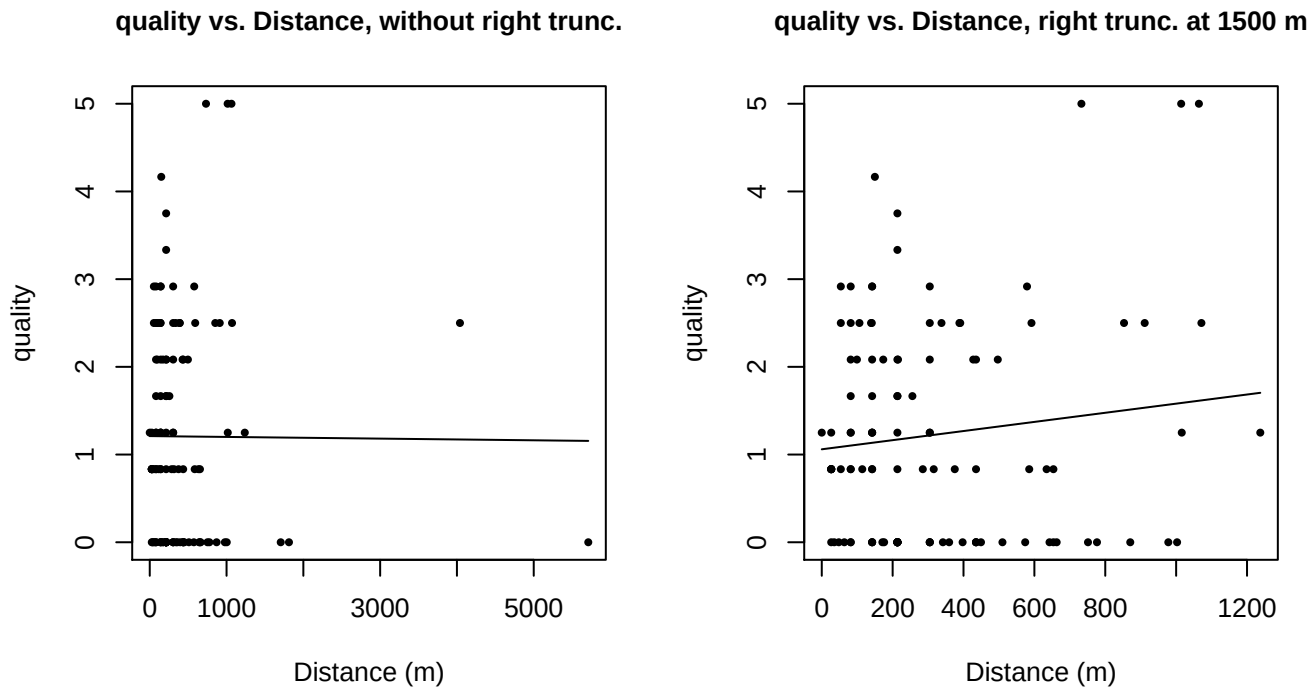

Figure 69: Scatterplots showing the relationship between the survey-specific index of the quality of observation conditions and perpendicular sighting distance, for all sightings (left) and only those not right truncated (right). Low values of the quality index correspond to better observation conditions. The line is a simple linear regression.

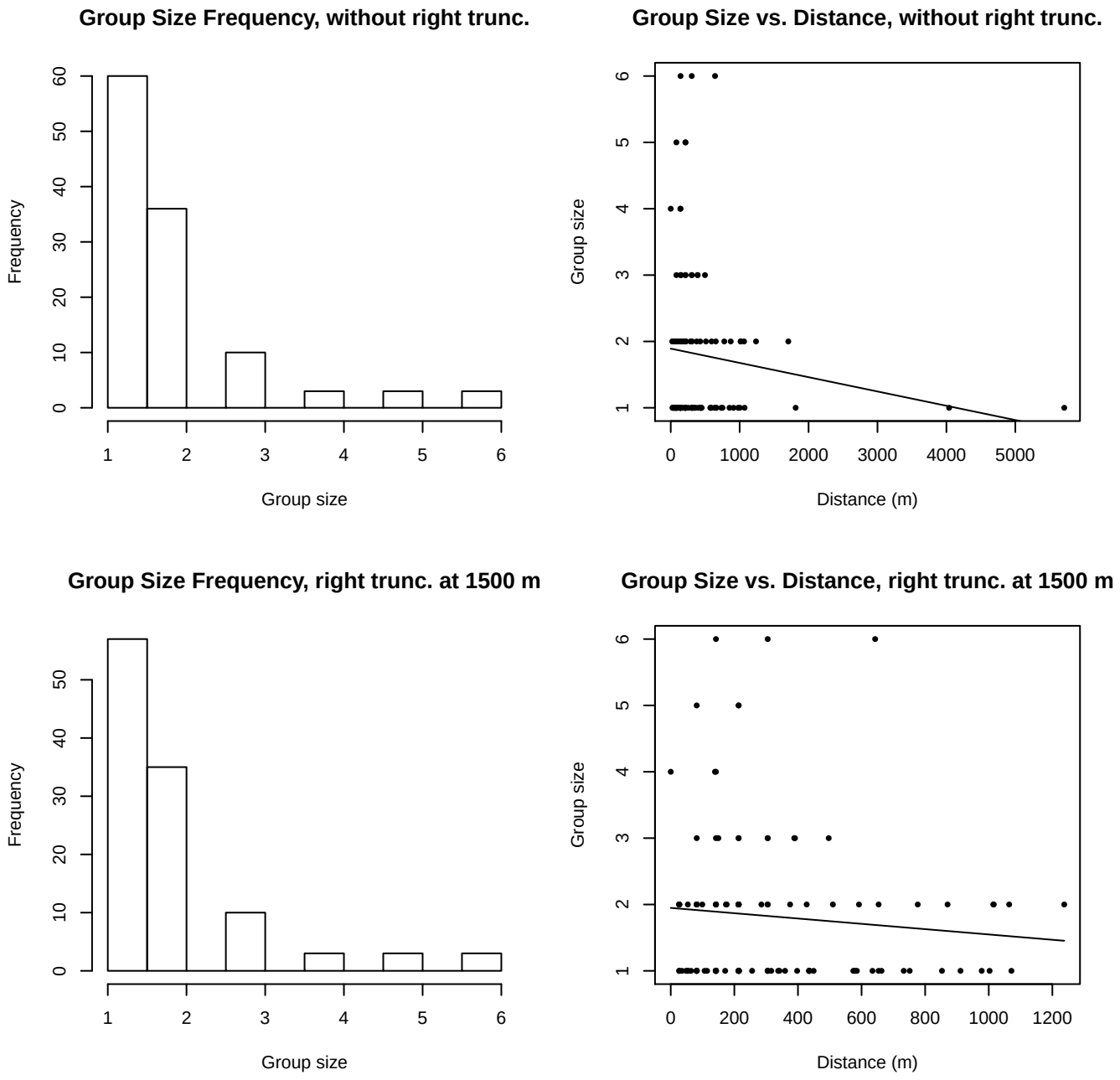

Figure 70: Histograms showing group size frequency and scatterplots showing the relationship between group size and perpendicular sighting distance, for all sightings (top row) and only those not right truncated (bottom row). In the scatterplot, the line is a simple linear regression.

NARWSS Aerial Surveys

The sightings were right truncated at 4000m. Due to a reduced frequency of sightings close to the trackline that plausibly resulted from the behavior of the observers and/or the configuration of the survey platform, the sightings were left truncted as well. Sightings closer than 61 m to the trackline were omitted from the analysis, and it was assumed that the the area closer to the trackline than this was not surveyed. This distance was estimated by inspecting histograms of perpendicular sighting distances. The vertical sighting angles were heaped at 10 degree increments up to 80 degrees and 1 degree increments thereafter, so the candidate detection functions were fitted using linear bins scaled accordingly.

Covariate	Description

beaufort	Beaufort sea state.
quality	Survey-specific index of the quality of observation conditions, utilizing relevant factors other than Beaufort sea state (see methods).

Table 43: Covariates tested in candidate "multi-covariate distance sampling" (MCDS) detection functions.

Key	Adjustment	Order	Covariates	Succeeded	Δ AIC	Mean ESHW (m)
hn				Yes	0.00	1823
hn			beaufort	Yes	1.23	1839
hn			quality	Yes	1.55	1823
hn	cos	3		Yes	1.69	1652
hn	cos	2		Yes	1.94	1759
hn	herm	4		Yes	1.99	1835
hr			beaufort	Yes	2.39	1982
hr			quality	Yes	3.05	1940
hn			beaufort, quality	Yes	3.09	1838
hr				Yes	3.29	2025
hr			beaufort, quality	Yes	4.06	1961
hr	poly	4		Yes	5.29	2024
hr	poly	2		Yes	5.29	2024

Table 44: Candidate detection functions for NARWSS Aerial Surveys. The first one listed was selected for the density model.

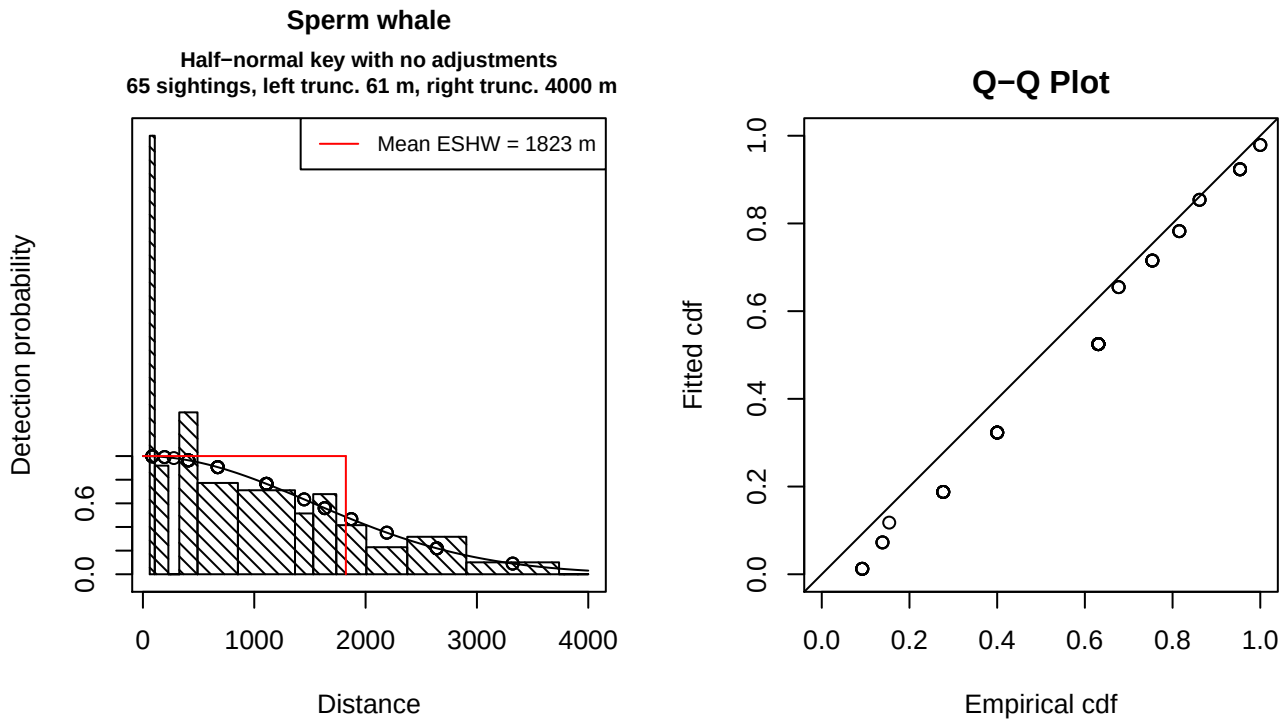

Figure 71: Detection function for NARWSS Aerial Surveys that was selected for the density model

Statistical output for this detection function:

```
Summary for ds object
Number of observations :  65
Distance range         :  61.25319  -  4000
AIC                    :  318.3643

Detection function:
 Half-normal key function

Detection function parameters
Scale Coefficients:
            estimate        se
(Intercept) 7.323696 0.1043268

                     Estimate          SE        CV
Average p            0.455687  0.04592525 0.1007825
N in covered region 142.641774 19.41770611 0.1361292
```

Additional diagnostic plots:

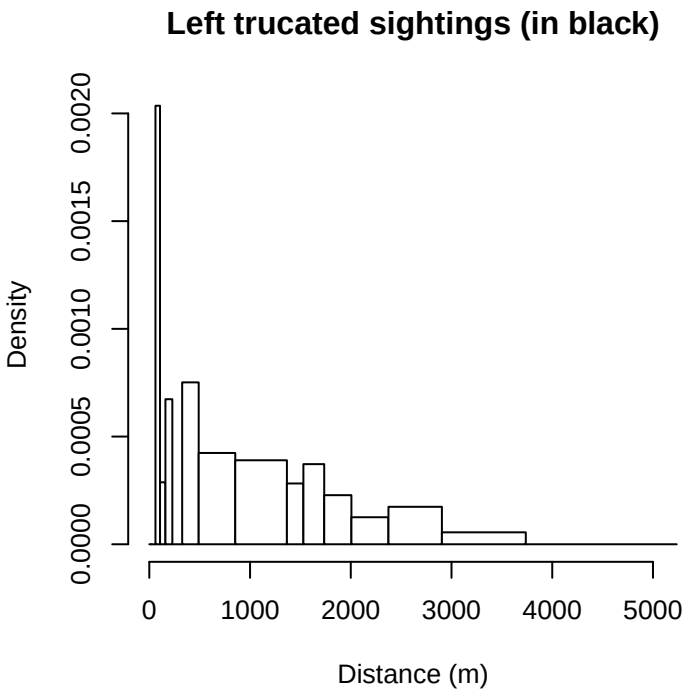

Figure 72: Density of sightings by perpendicular distance for NARWSS Aerial Surveys. Black bars on the left show sightings that were left truncated.

Figure 73: Scatterplots showing the relationship between Beaufort sea state and perpendicular sighting distance, for all sightings (left) and only those not right truncated (right). The line is a simple linear regression.

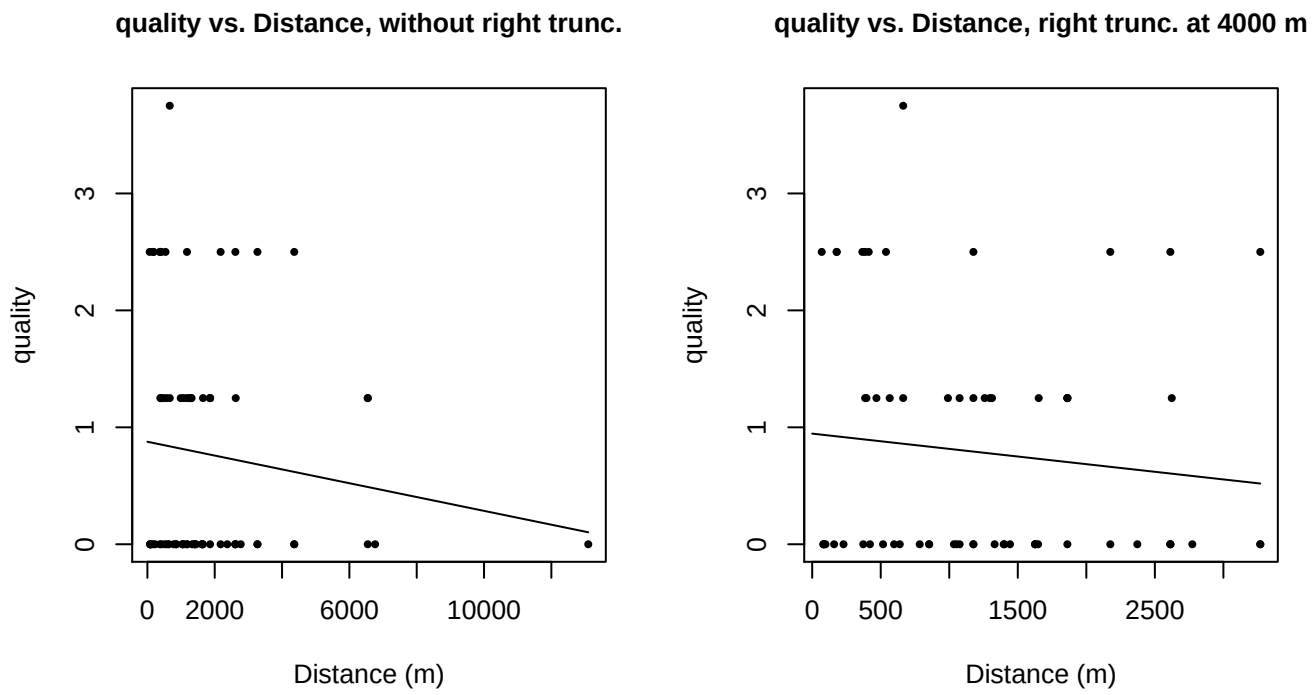

Figure 74: Scatterplots showing the relationship between the survey-specific index of the quality of observation conditions and perpendicular sighting distance, for all sightings (left) and only those not right truncated (right). Low values of the quality index correspond to better observation conditions. The line is a simple linear regression.

g(0) Estimates

Platform	Surveys	Group Size	*g(0)*	Biases Addressed	Source
Shipboard	All	Any	0.53	Both	Barlow and Sexton (1996)
Shipboard	NEFSC Abel-J Binocular Surveys	Any	0.28	Perception	Palka (2006)
Shipboard	NEFSC Endeavor	Any	0.46	Perception	Palka (2006)
Aerial	All	Any	0.172	Availability	Watwood et al. (2006)

Table 45: Estimates of *g(0)* used in this density model.

Palka (2006) provided survey-specific g(0) estimates for two NOAA NEFSC shipboard surveys that used bigeye binoculars: the Abel-J 1998 survey (0.28) and the Endeavor 2004 survey (0.46). These estimates used a dual-team methodology that accounted perception bias but not availability bias. We used the estimates for the lower team, which was the primary team and the one for which we have sightings.

No survey-specific g(0) estimates were available for our other shipboard surveys. For these, we relied on results from Barlow and Sexton's (1996) simulation model, using dive data reported by Watwood et al. (2006). Using DTAGs, Watwood et al. tracked sperm whales in three regions and reported an average dive cycle consisting of a 45 min dive followed by a 9 min surface interval, with sperm whales in the northwest Atlantic averaging 45.7 min and 9.3 min, yielding a total dive cycle of 55 min. Using these data, we consulted Barlow and Sexton (1996), who modeled g(0) for sperm whales observed from shipboard surveys that utilized 25x binoculars. Their estimates accounted for both availability and perception bias. For a 60 min dive cycle, Barlow and Sexton estimated g(0)=0.53. Note that this differs from other publications such as Whitehead (2002) that assumed a 30 min dive cycle, yielding g(0)=0.87. Barlow and Sexton described the 30 minute cycle as typical for mixed groups with calves and the 60 minute cycle as typical for solitary large males. But Watwood et al. reported that their 55 min dive cycle was obtained from groups composed predominantly of females and immature whales, and advised that their results were most relevant for those age/sex classes.

Although Barlow and Sexton cautioned that their results cannot be extrapolated to other survey methods, we utilized their g(0) estimate for naked eye shipboard surveys as well, as no alternative estimate was available in the literature. But this decision turned out to be relatively unimportant because no sperm whales were sighted on the only naked eye cruise we had that occurred within our East Coast study area. We also used this estimate with the European naked eye surveys, which did not publish g(0) estimates. (The European surveys were not used in the East Coast model documented here, but may have been used in the AFTT model. Please consult the AFTT model documentation for more information.)

Finally, we note that Palka's (2006) g(0) estimates that only addressed perception bias were lower than the g(0) estimate we derived from Barlow and Sexton (1996) that addressed both perception and availability bias. This was not expected, and may indicate that the Barlow and Sexton estimate overestimates g(0) in our study area, which would ultimately lead to an underestimation of sperm whale abundance.

No estimate of g(0) was available in the literature for sperm whales sighted on aerial surveys. Sperm whales are long-diving animals (Barlow and Sexton, 1996), thus availability bias is likely to be substantial. Utilizing equation (3) of Carretta et al. (2000) (which follows Barlow et al. 1988), we computed the availability bias component of g(0) from the mean surface and dive intervals (9.3 min and 45.7 min) for sperm whales in the Atlantic Ocean reported by Watwood et al. (2006). We did not obtain an estimate of perception bias, but perception bias for whales is expected to be negligible (Carretta et al. 2000).

Density Models

Sperm whales are widely distributed throughout the North Atlantic (Waring et al. 2014). In our study area, sightings were concentrated north of Cape Hatteras along the continental slope and in deeper waters. In this region, sperm whales have been found to be associated with submarine canyons (Whitehead et al. 1992), the north wall of the Gulf Stream (Waring et al. 1993), and temperature fronts and warm-core eddies (Waring et al. 2001; Griffin 1999). Foraging sperm whales undertake deep, long dives, mainly targeting cephalopods (Watwood et al. 2006), which may aggregate around these physiographic and oceanographic features.

Some authors report a seasonal cycle in distribution within our study area, including seasonal movement on-shelf, possibly to feed (CETAP 1982; Scott and Sadove 1997; Waring et al. 2014). The survey effort available to us only covered the entire study area in summer, making it difficult to model seasonal dynamics with high confidence. CETAP (1982) reported sightings of sperm whales north of Cape Hatteras off the shelf and along the shelf break during all four seasons, and on the shelf during spring, summer, and fall. The NOAA NARWSS aerial surveys observed sperm whales on Georges Bank or its eastern edge during all months of the year except January and November, when surveying was relatively sparse. Acoustic monitoring detected sperm whales every month of the year off the shelf near Onslow Bay, North Carolina (Hodge and Read 2014; Debich et al. 2014). Acoustic monitoring at the shelf break near Jacksonville, Florida detected sperm whales in December although not in other months (Norris et al. 2014; Debich et al. 2013). Finally, Waring et al. (2014) describe sperm whales as occupying the off-shelf waters near either Cape Hatteras or the mid-Atlantic bight during all four seasons.

Together, these studies indicate that sperm whales are present throughout the year but they do not reveal a clear pattern in their distribution. Given that, we modeled sperm whale abundance with a single, year-round model that incorporated all available survey data. Although survey effort off the continental shelf was sparse in non-summer months, we allowed the model to predict off-shelf during all months of the year. These predictions should be viewed with due caution. We recognize that sperm whales exhibit complex social dynamics that affect both their distribution and migration patterns (Waring et al. 2014), but our survey data lacked the data attributes (e.g. sex) to address this, e.g. by fitting separate models to different portions of the population. Nonetheless, we believe our models provide the best spatially-explicit description of sperm whale distribution in the study area at the time of this writing.

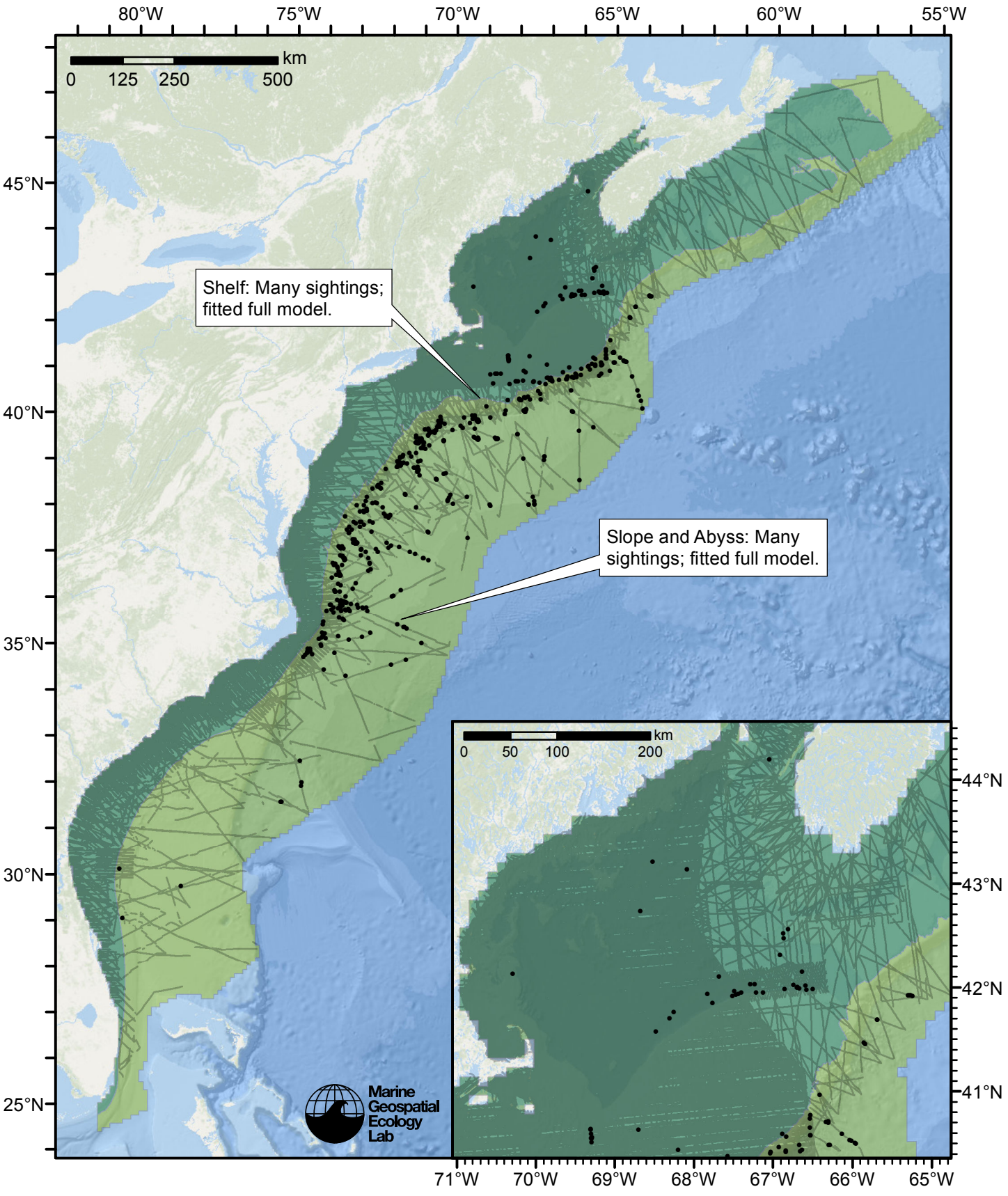

Figure 75: Sperm whale density model schematic. All on-effort sightings are shown, including those that were truncated when detection functions were fitted.

Climatological Model

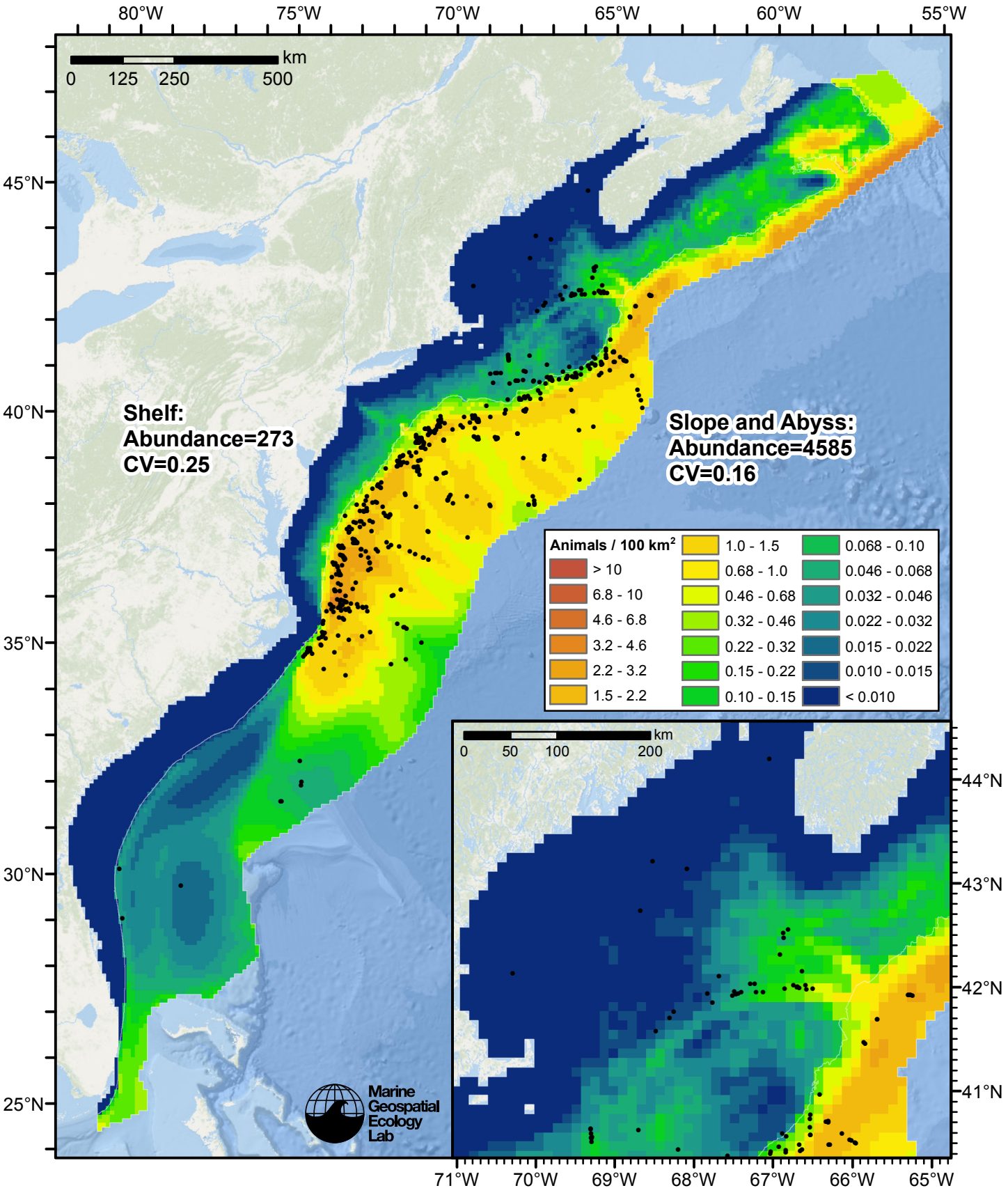

Figure 76: Sperm whale density predicted by the climatological model that explained the most deviance. Pixels are 10x10 km. The legend gives the estimated individuals per pixel; breaks are logarithmic. Abundance for each region was computed by summing the density cells occuring in that region.

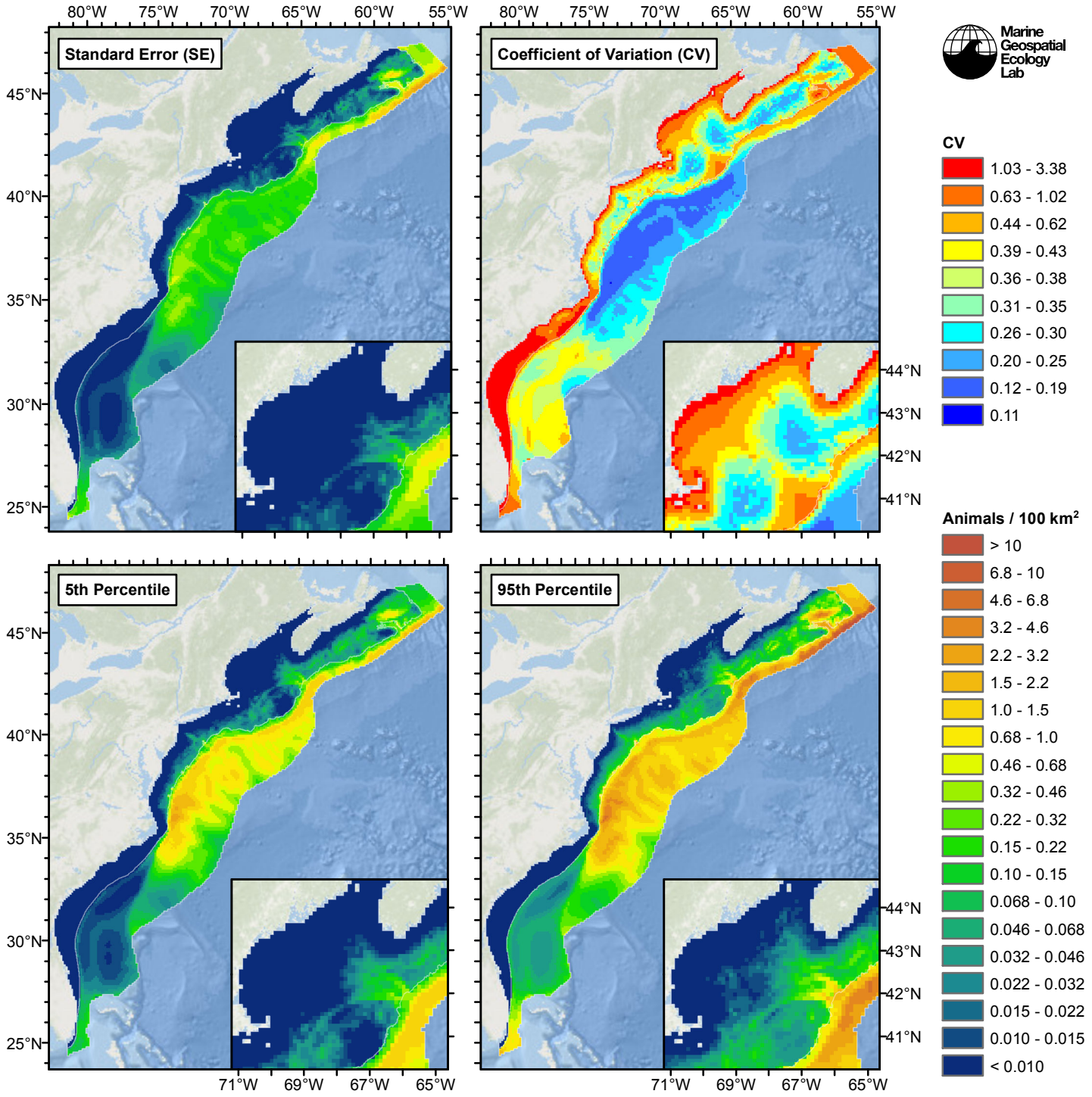

Figure 77: Estimated uncertainty for the climatological model that explained the most deviance. These estimates only incorporate the statistical uncertainty estimated for the spatial model (by the R mgcv package). They do not incorporate uncertainty in the detection functions, g(0) estimates, predictor variables, and so on.

Slope and Abyss

Statistical output

```
Rscript.exe: This is mgcv 1.8-2. For overview type 'help("mgcv-package")'.


Family: Tweedie(p=1.295)
```

```
Link function: log

Formula:
abundance ~ offset(log(area_km2)) + s(log10(Depth), bs = "ts",
    k = 5) + s(I(DistToCanyonOrSeamount/1000), bs = "ts", k = 5) +
    s(ClimSST, bs = "ts", k = 5) + s(I(ClimDistToFront1^(1/3)),
    bs = "ts", k = 5) + s(I(ClimDistToAEddy/1000), bs = "ts",
    k = 5) + s(I(ClimCumVGPM90^(1/3)), bs = "ts", k = 5)

Parametric coefficients:
            Estimate Std. Error t value Pr(>|t|)
(Intercept)  -6.7273     0.1762  -38.18   <2e-16 ***
---
Signif. codes:  0 '***' 0.001 '**' 0.01 '*' 0.05 '.' 0.1 ' ' 1

Approximate significance of smooth terms:
                                   edf Ref.df      F  p-value
s(log10(Depth))                  3.305      4 16.080 2.14e-15 ***
s(I(DistToCanyonOrSeamount/1000)) 1.665      4  9.193 3.07e-10 ***
s(ClimSST)                       3.135      4  5.008 6.26e-05 ***
s(I(ClimDistToFront1^(1/3)))     0.906      4  1.666  0.00462 **
s(I(ClimDistToAEddy/1000))       1.052      4  4.412 9.36e-06 ***
s(I(ClimCumVGPM90^(1/3)))        1.079      4  4.581 3.55e-06 ***
---
Signif. codes:  0 '***' 0.001 '**' 0.01 '*' 0.05 '.' 0.1 ' ' 1

R-sq.(adj) =  0.0425   Deviance explained = 40.7%
-REML = 2250.4  Scale est. = 26.263    n = 17198

All predictors were significant. This is the final model.
Creating term plots.
Diagnostic output from gam.check():

Method: REML   Optimizer: outer newton
full convergence after 14 iterations.
Gradient range [-0.001563729,0.0004442838]
(score 2250.418 & scale 26.26344).
Hessian positive definite, eigenvalue range [0.2162883,1045.422].
Model rank =  25 / 25

Basis dimension (k) checking results. Low p-value (k-index<1) may
indicate that k is too low, especially if edf is close to k'.

                                    k'   edf k-index p-value
s(log10(Depth))                  4.000 3.305   0.806    0.00
s(I(DistToCanyonOrSeamount/1000)) 4.000 1.665   0.778    0.00
s(ClimSST)                       4.000 3.135   0.841    0.24
s(I(ClimDistToFront1^(1/3)))     4.000 0.906   0.846    0.35
s(I(ClimDistToAEddy/1000))       4.000 1.052   0.840    0.15
s(I(ClimCumVGPM90^(1/3)))        4.000 1.079   0.762    0.00

Predictors retained during the model selection procedure: Depth, DistToCanyonOrSeamount, ClimSST,
ClimDistToFront1, ClimDistToAEddy, ClimCumVGPM90

Predictors dropped during the model selection procedure: Slope, DistTo125m, ClimTKE, ClimDistToCEddy
```

Model term plots

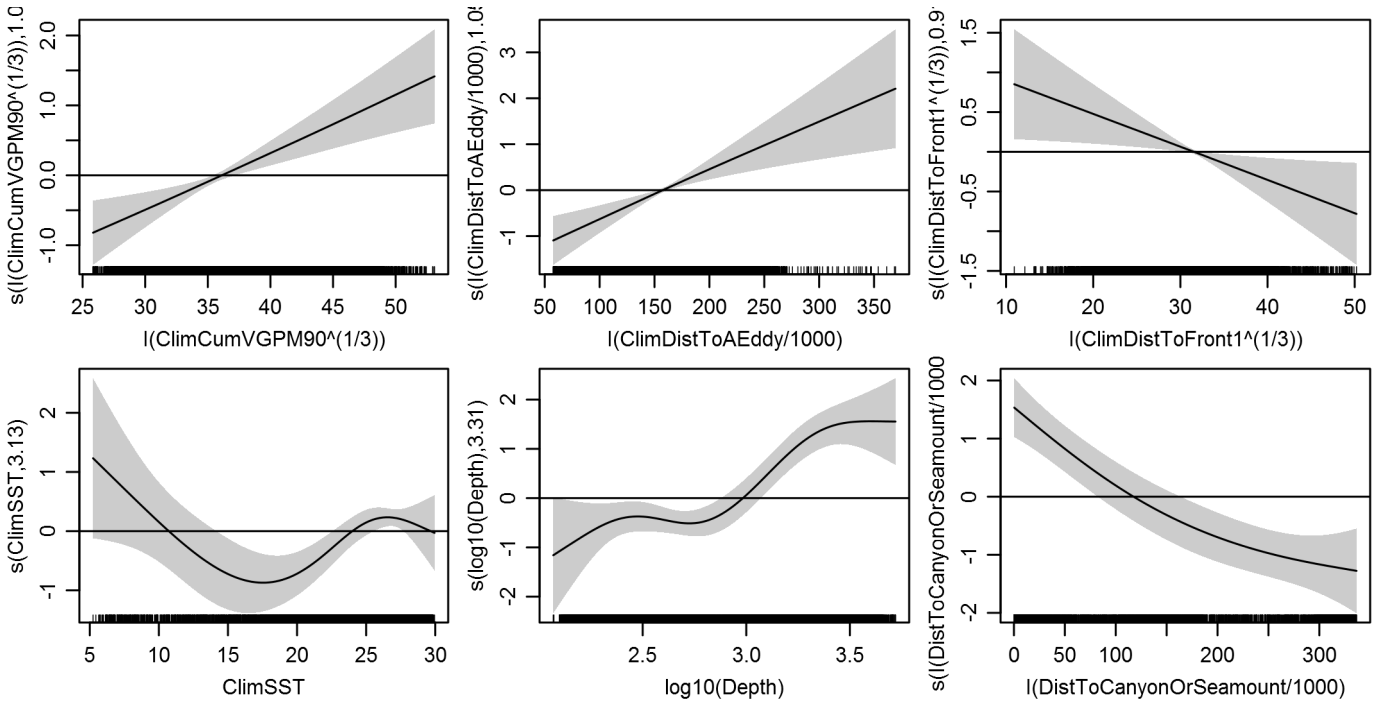

Diagnostic plots

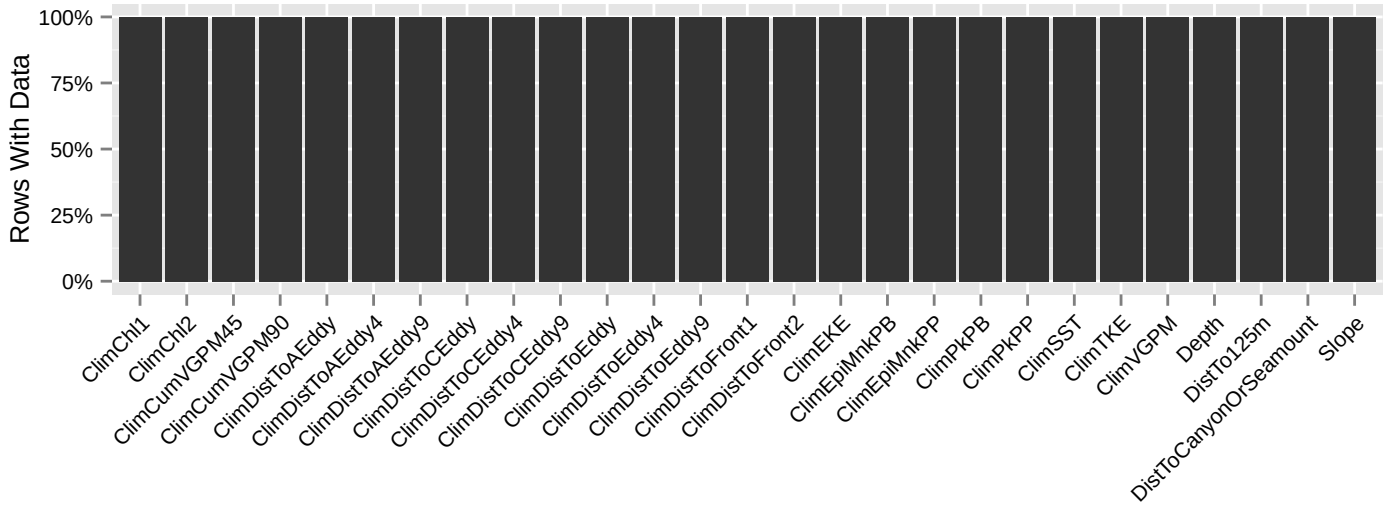

Figure 78: Segments with predictor values for the Sperm whale Climatological model, Slope and Abyss. This plot is used to assess how many segments would be lost by including a given predictor in a model.

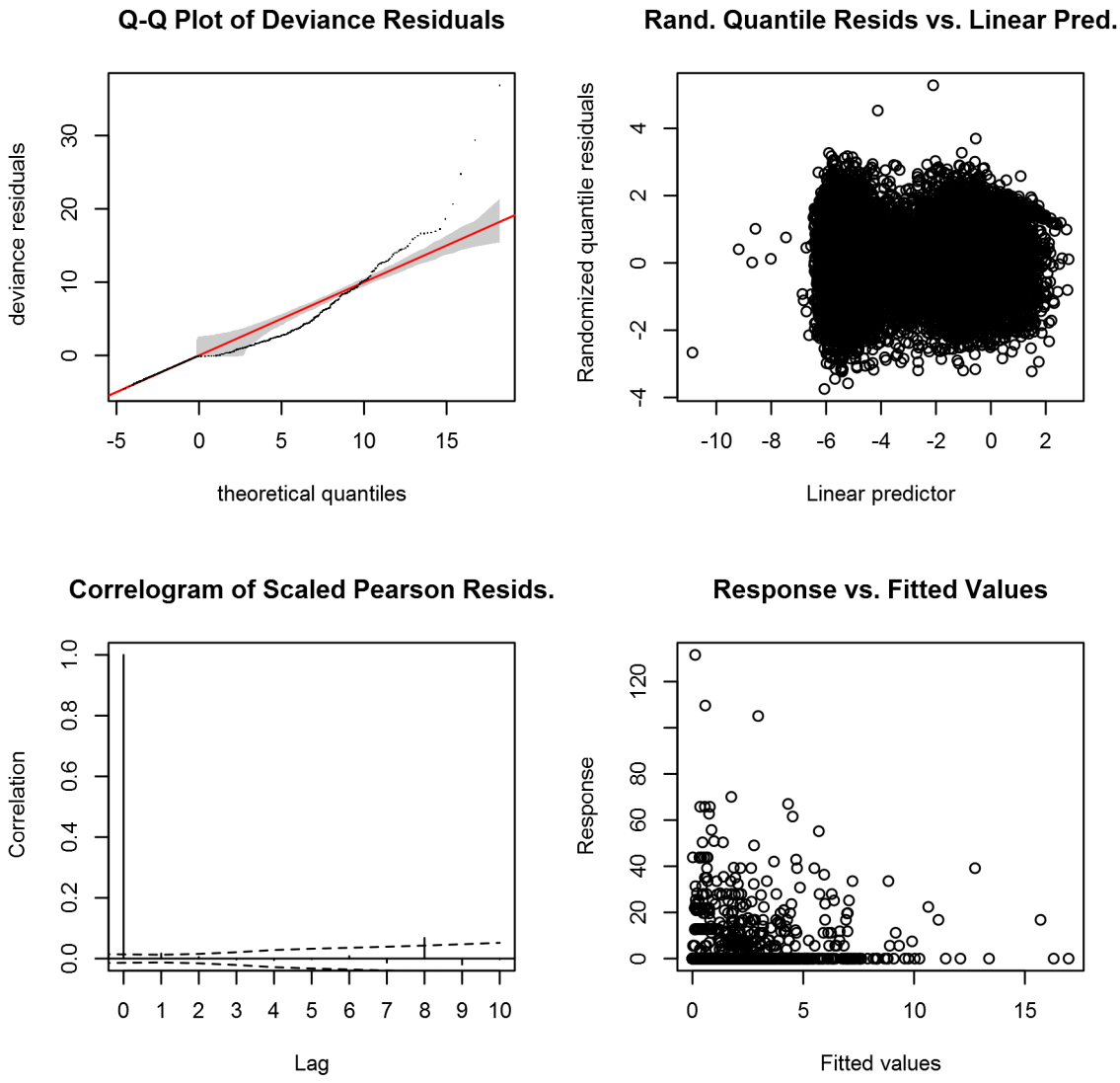

Figure 79: Statistical diagnostic plots for the Sperm whale Climatological model, Slope and Abyss.

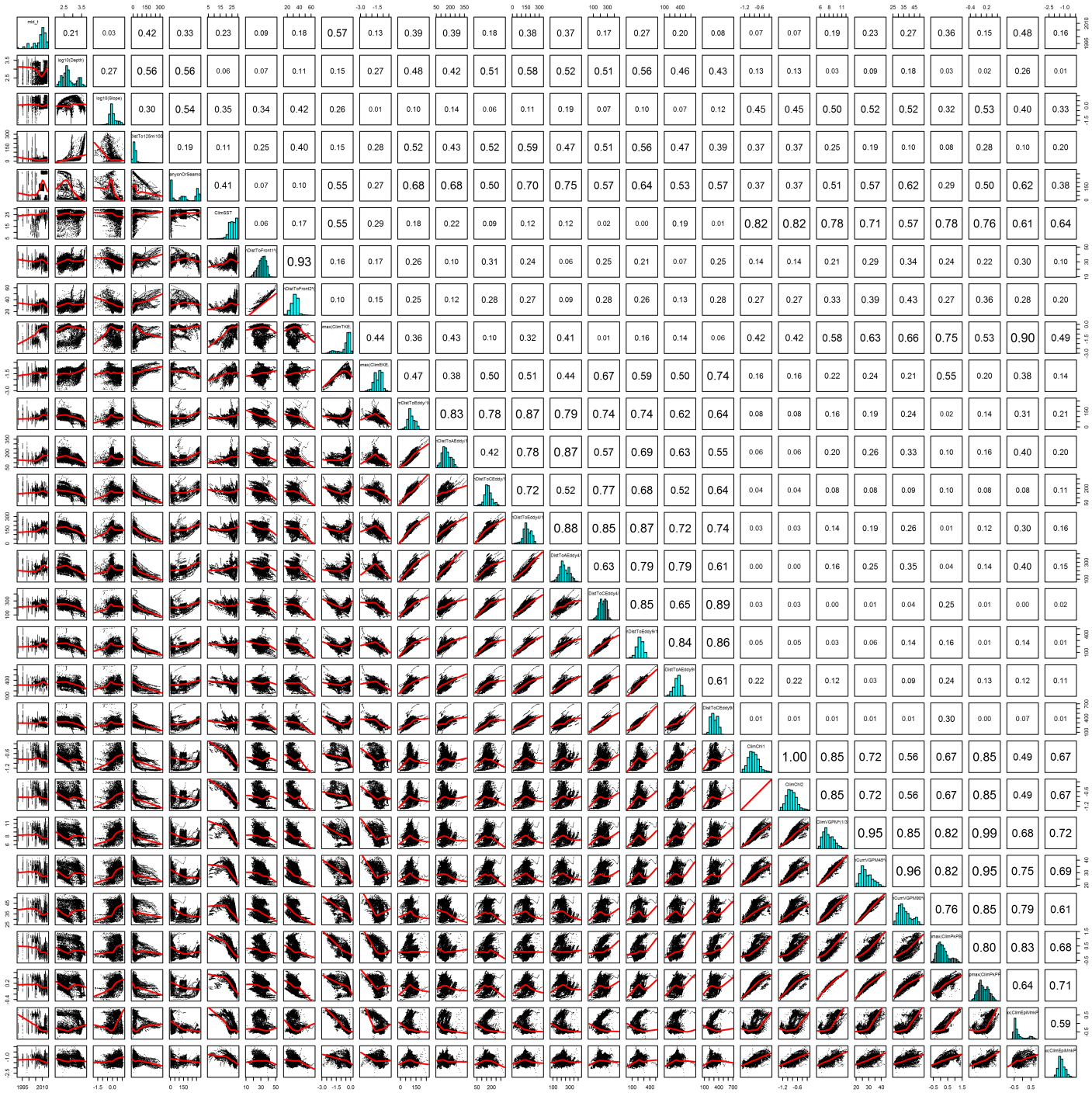

Figure 80: Scatterplot matrix for the Sperm whale Climatological model, Slope and Abyss. This plot is used to inspect the distribution of predictors (via histograms along the diagonal), simple correlation between predictors (via pairwise Pearson coefficients above the diagonal), and linearity of predictor correlations (via scatterplots below the diagonal). This plot is best viewed at high magnification.

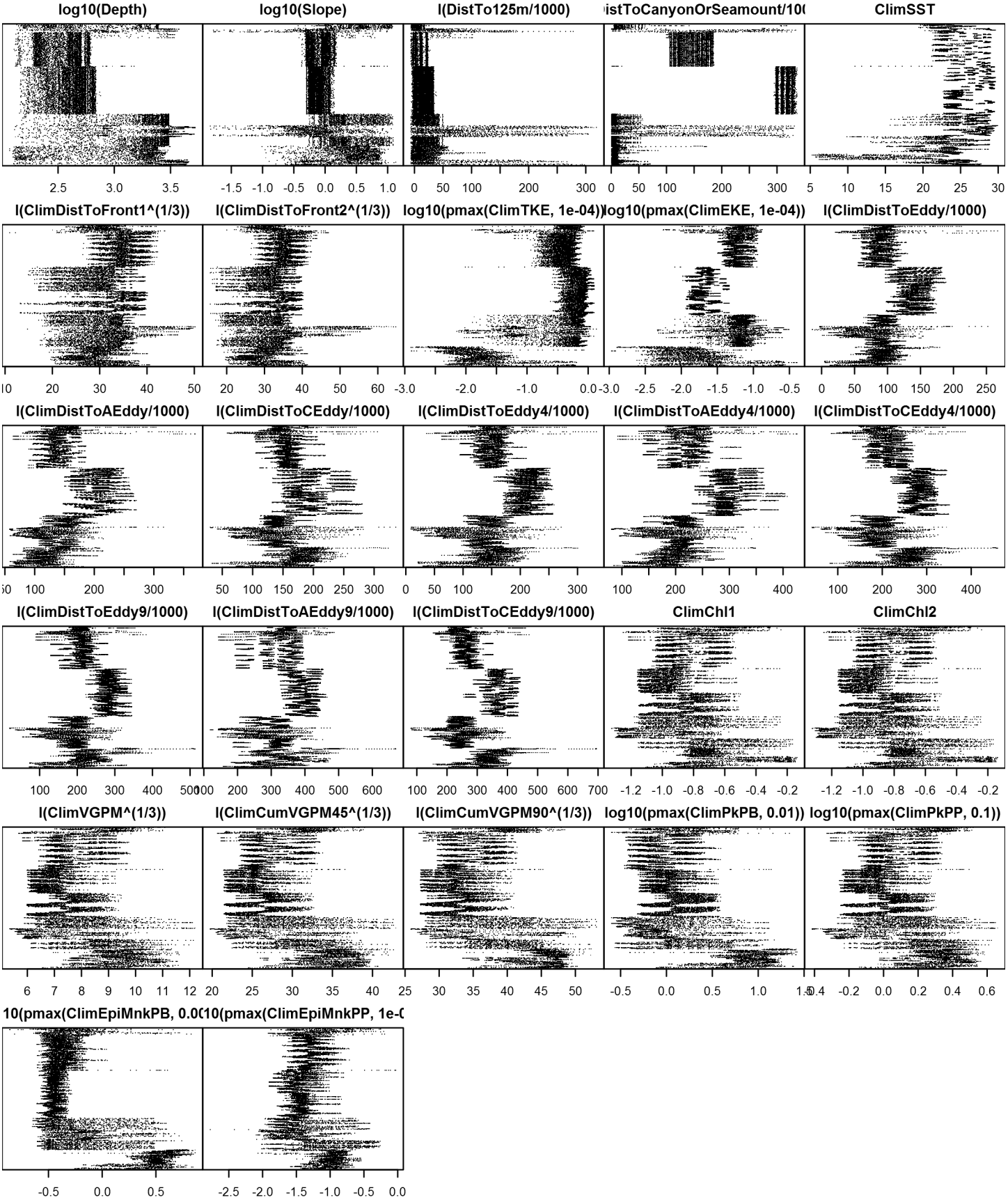

Figure 81: Dotplot for the Sperm whale Climatological model, Slope and Abyss. This plot is used to check for suspicious patterns and outliers in the data. Points are ordered vertically by transect ID, sequentially in time.

Shelf

Statistical output

```
Rscript.exe: This is mgcv 1.8-2. For overview type 'help("mgcv-package")'.


Family: Tweedie(p=1.155)
Link function: log

Formula:
abundance ~ offset(log(area_km2)) + s(sqrt(DistToShore/1000),
    bs = "ts", k = 5) + s(log10(Slope), bs = "ts", k = 5) + s(I(DistToCanyonOrSeamount/1000),
    bs = "ts", k = 5) + s(log10(pmax(ClimPkPB, 0.01)), bs = "ts",
    k = 5)

Parametric coefficients:
            Estimate Std. Error t value Pr(>|t|)
(Intercept) -11.5896     0.5074  -22.84   <2e-16 ***
---
Signif. codes:  0 '***' 0.001 '**' 0.01 '*' 0.05 '.' 0.1 ' ' 1

Approximate significance of smooth terms:
                                   edf Ref.df      F  p-value
s(sqrt(DistToShore/1000))         2.4750      4  3.814 0.000375 ***
s(log10(Slope))                   1.0313      4  5.558 1.23e-06 ***
s(I(DistToCanyonOrSeamount/1000)) 1.2504      4 13.764 2.57e-14 ***
s(log10(pmax(ClimPkPB, 0.01)))    0.9824      4  4.379 1.22e-05 ***
---
Signif. codes:  0 '***' 0.001 '**' 0.01 '*' 0.05 '.' 0.1 ' ' 1

R-sq.(adj) =  0.00498   Deviance explained = 30.8%
-REML =  517.1  Scale est. = 34.387    n = 87038

All predictors were significant. This is the final model.
Creating term plots.
Diagnostic output from gam.check():

Method: REML   Optimizer: outer newton
full convergence after 13 iterations.
Gradient range [-0.0003041872,1.227789e-06]
(score 517.1037 & scale 34.38704).
Hessian positive definite, eigenvalue range [0.3923094,406.457].
Model rank =  17 / 17

Basis dimension (k) checking results. Low p-value (k-index<1) may
indicate that k is too low, especially if edf is close to k'.

                                   k'   edf k-index p-value
s(sqrt(DistToShore/1000))         4.000 2.475   0.574       0
s(log10(Slope))                   4.000 1.031   0.633       0
s(I(DistToCanyonOrSeamount/1000)) 4.000 1.250   0.605       0
s(log10(pmax(ClimPkPB, 0.01)))    4.000 0.982   0.570       0

Predictors retained during the model selection procedure: DistToShore, Slope,
DistToCanyonOrSeamount, ClimPkPB

Predictors dropped during the model selection procedure: Depth, DistTo125m, ClimSST,
ClimDistToFront1, ClimEKE
```

Model term plots

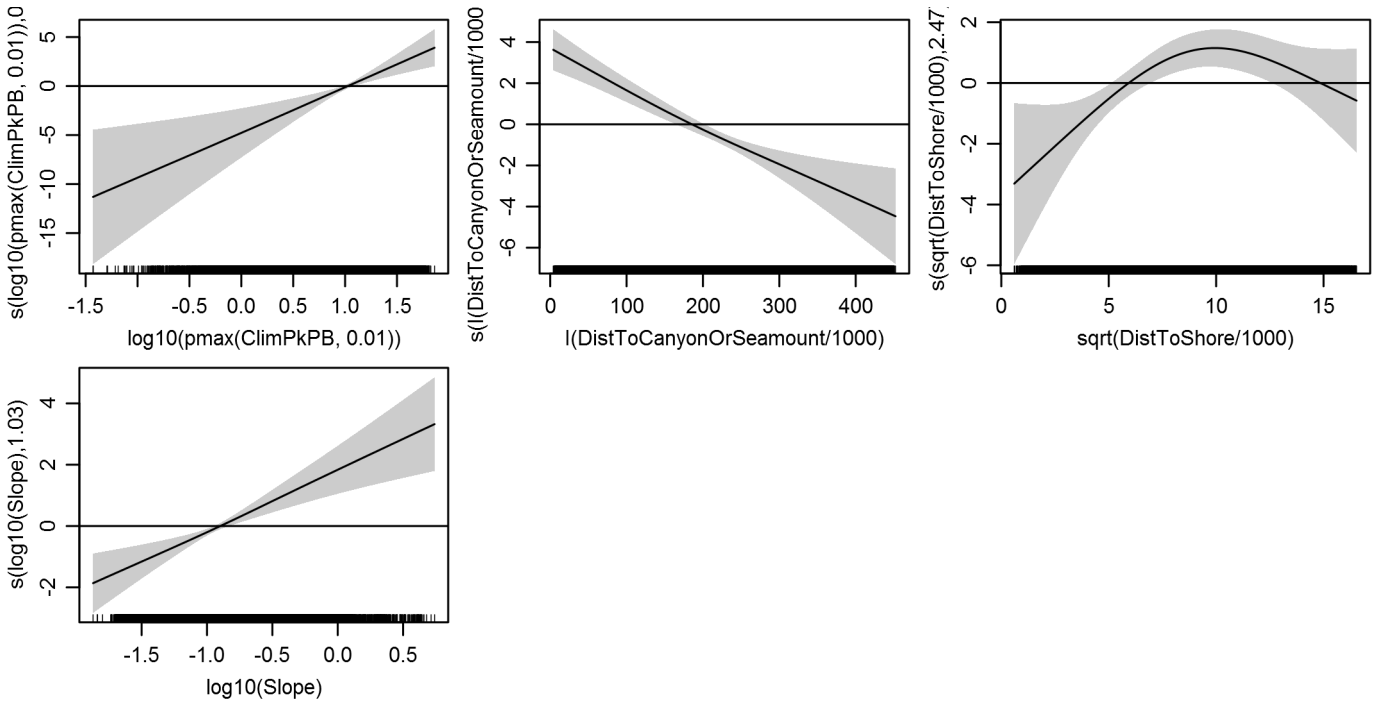

Diagnostic plots

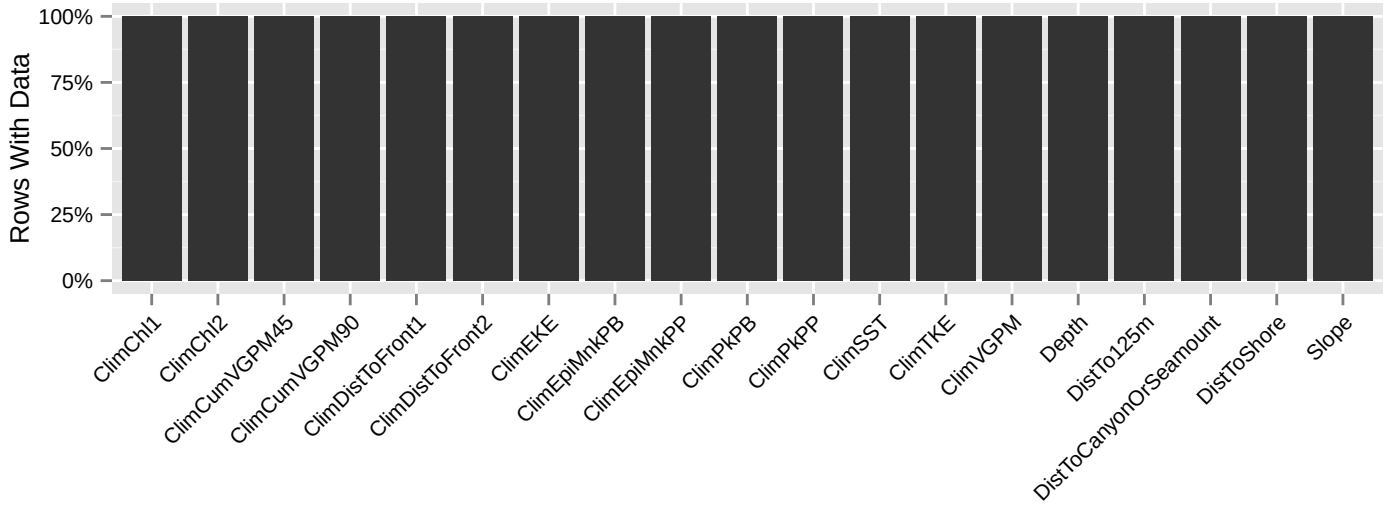

Figure 82: Segments with predictor values for the Sperm whale Climatological model, Shelf. This plot is used to assess how many segments would be lost by including a given predictor in a model.

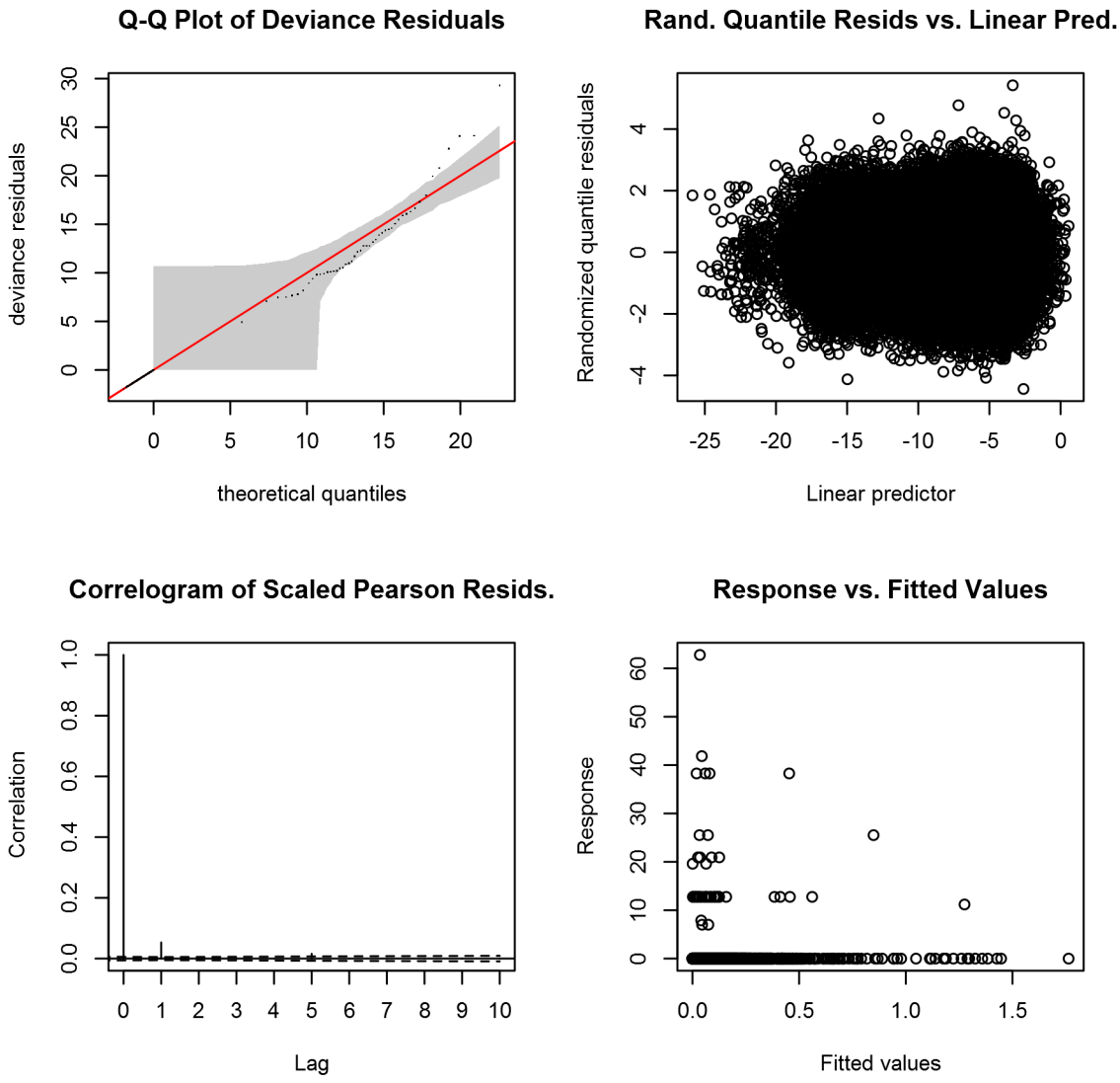

Figure 83: Statistical diagnostic plots for the Sperm whale Climatological model, Shelf.

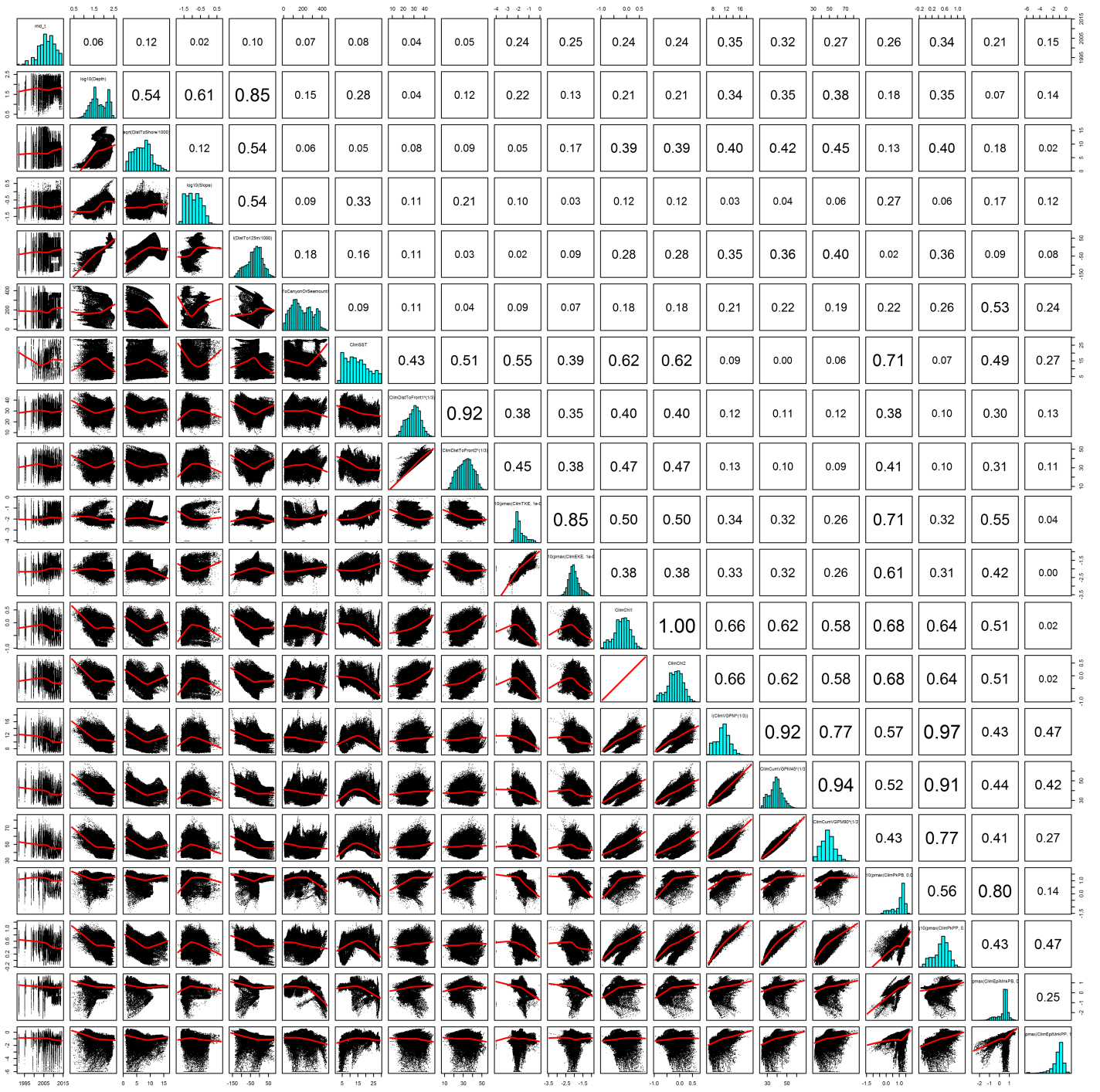

Figure 84: Scatterplot matrix for the Sperm whale Climatological model, Shelf. This plot is used to inspect the distribution of predictors (via histograms along the diagonal), simple correlation between predictors (via pairwise Pearson coefficients above the diagonal), and linearity of predictor correlations (via scatterplots below the diagonal). This plot is best viewed at high magnification.

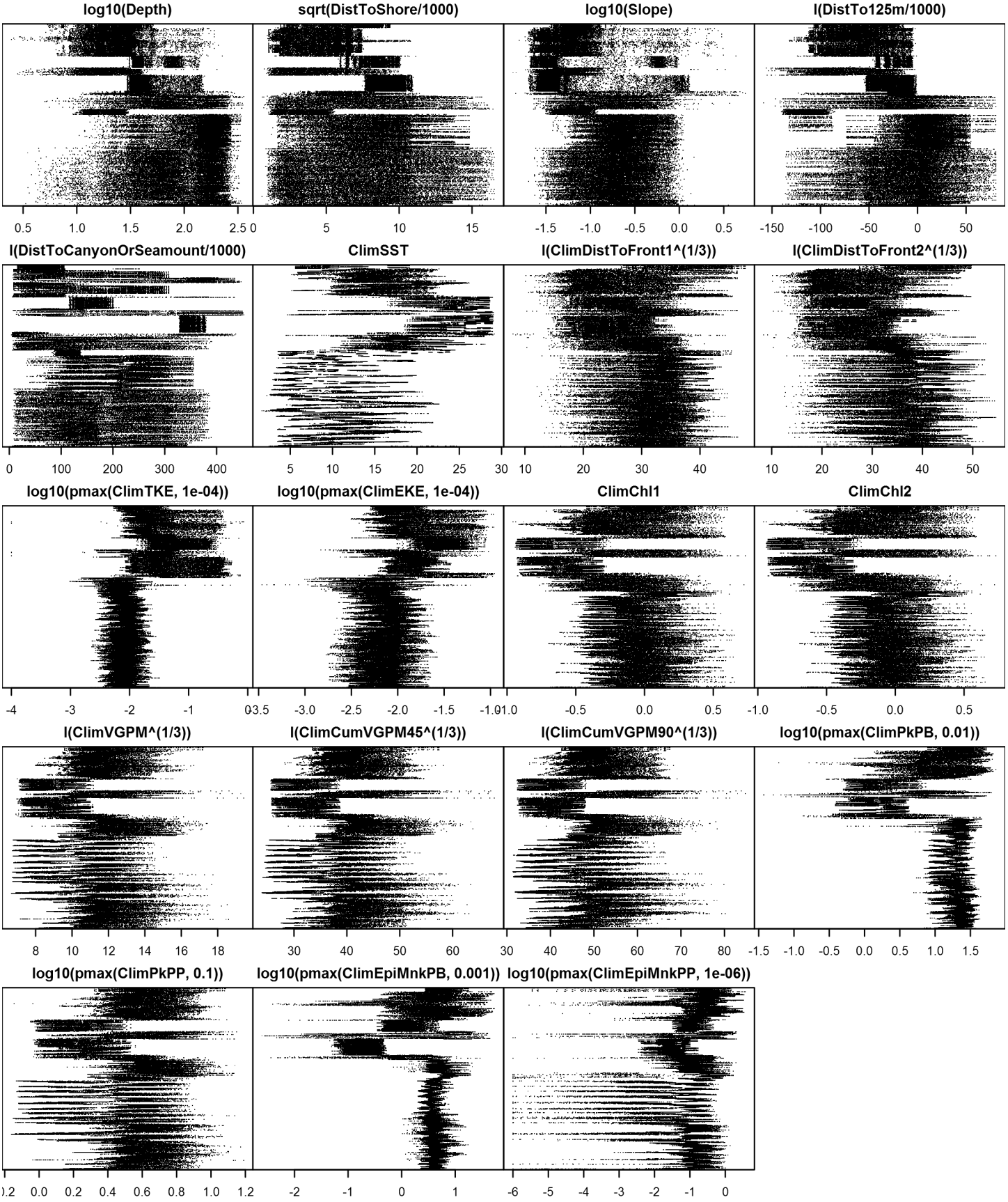

Figure 85: Dotplot for the Sperm whale Climatological model, Shelf. This plot is used to check for suspicious patterns and outliers in the data. Points are ordered vertically by transect ID, sequentially in time.

Contemporaneous Model

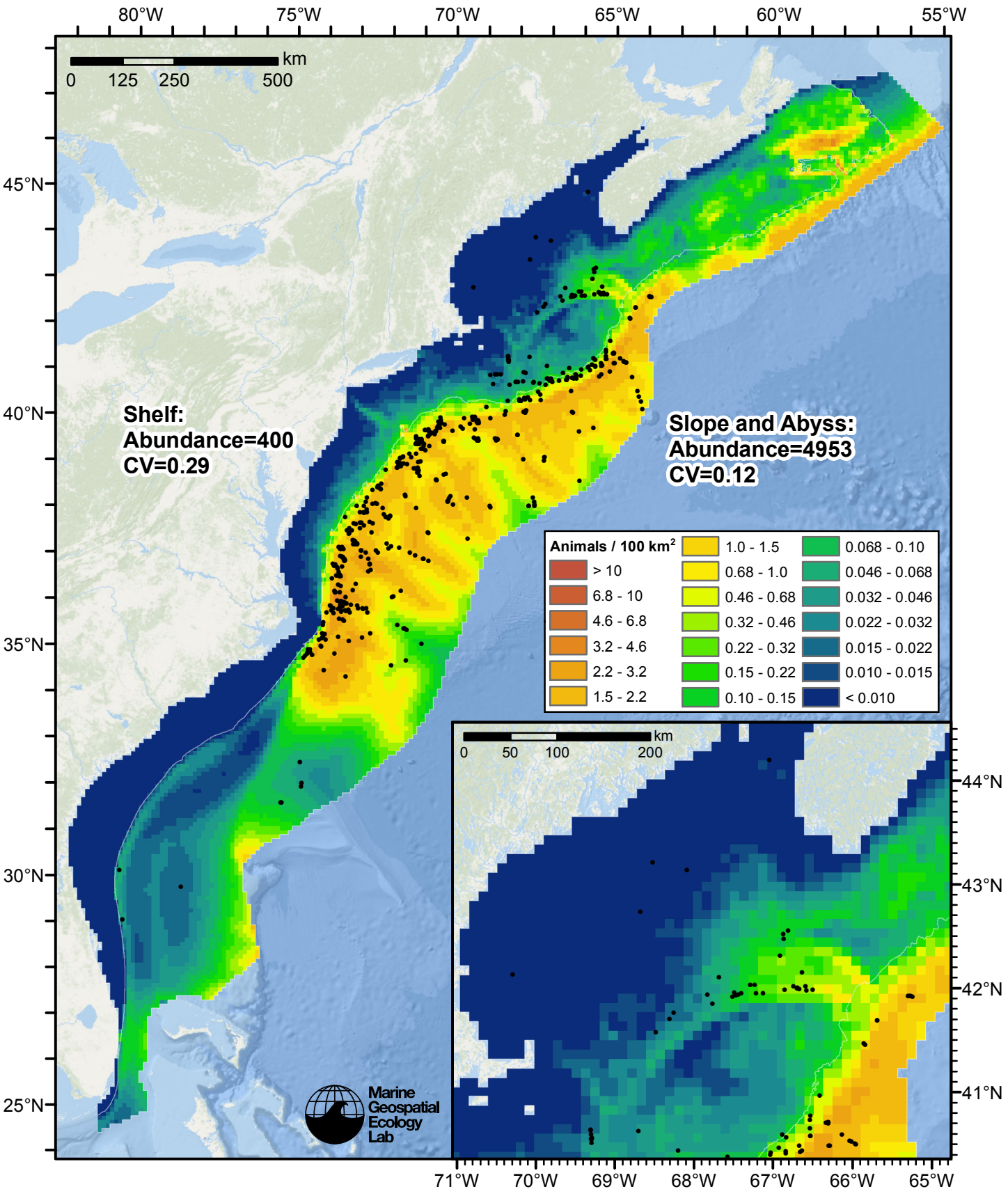

Figure 86: Sperm whale density predicted by the contemporaneous model that explained the most deviance. Pixels are 10x10 km. The legend gives the estimated individuals per pixel; breaks are logarithmic. Abundance for each region was computed by summing the density cells occuring in that region.

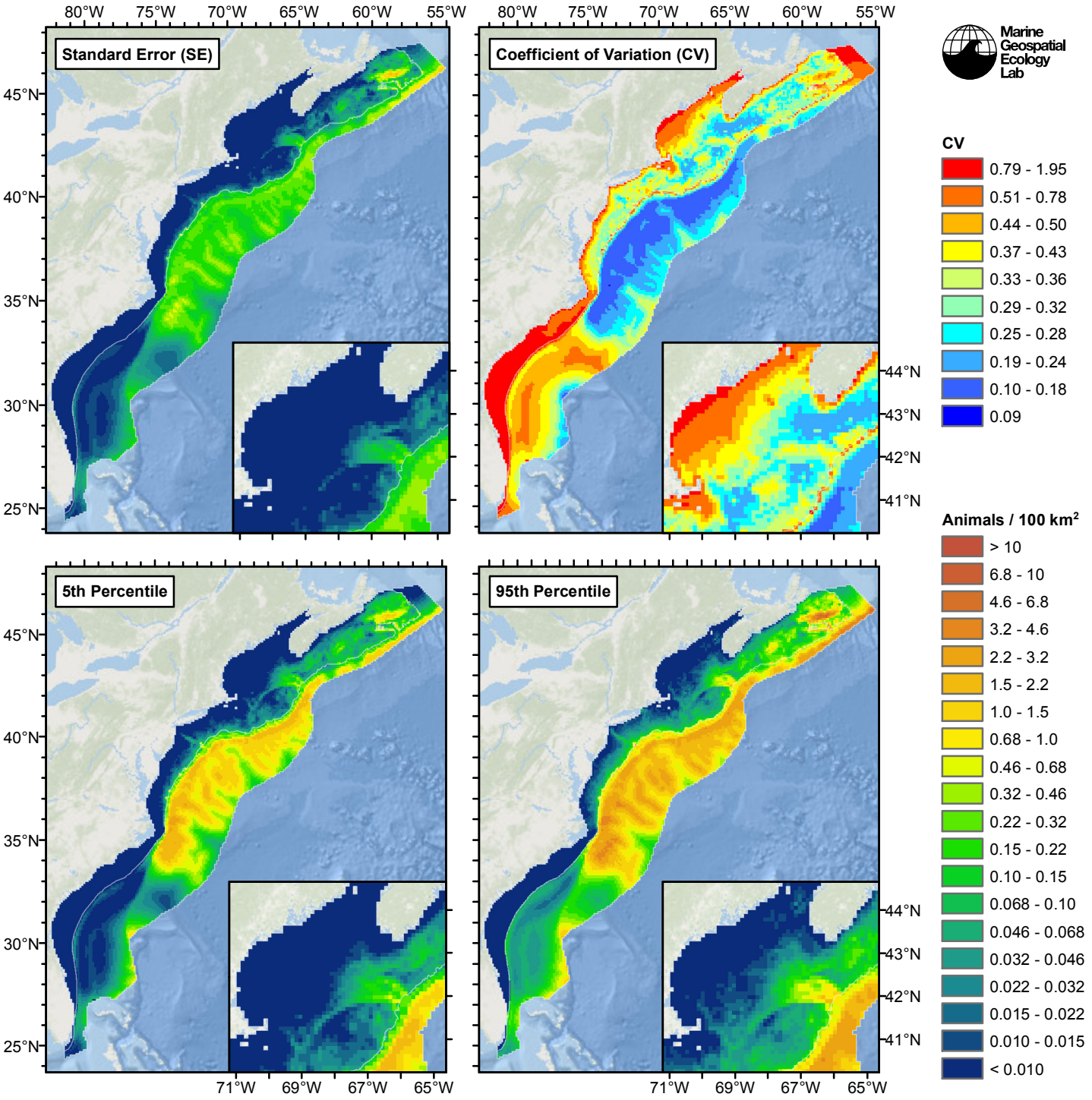

Figure 87: Estimated uncertainty for the contemporaneous model that explained the most deviance. These estimates only incorporate the statistical uncertainty estimated for the spatial model (by the R mgcv package). They do not incorporate uncertainty in the detection functions, g(0) estimates, predictor variables, and so on.

Slope and Abyss

Statistical output

```
Rscript.exe: This is mgcv 1.8-2. For overview type 'help("mgcv-package")'.


Family: Tweedie(p=1.294)
```

```
Link function: log

Formula:
abundance ~ offset(log(area_km2)) + s(log10(Depth), bs = "ts",
    k = 5) + s(I(DistToCanyonOrSeamount/1000), bs = "ts", k = 5) +
    s(SST, bs = "ts", k = 5) + s(I(DistToFront1^(1/3)), bs = "ts",
    k = 5) + s(I(DistToCEddy9/1000), bs = "ts", k = 5)

Parametric coefficients:
            Estimate Std. Error t value Pr(>|t|)
(Intercept)  -6.8016     0.1806  -37.67   <2e-16 ***
---
Signif. codes:  0 '***' 0.001 '**' 0.01 '*' 0.05 '.' 0.1 ' ' 1

Approximate significance of smooth terms:
                                    edf Ref.df      F  p-value
s(log10(Depth))                  3.6190      4 12.603 2.78e-11 ***
s(I(DistToCanyonOrSeamount/1000)) 2.4667      4 20.519  < 2e-16 ***
s(SST)                           0.9644      4  3.329 0.000157 ***
s(I(DistToFront1^(1/3)))         1.0791      4  5.568 1.44e-06 ***
s(I(DistToCEddy9/1000))          3.2452      4  5.224 6.11e-05 ***
---
Signif. codes:  0 '***' 0.001 '**' 0.01 '*' 0.05 '.' 0.1 ' ' 1

R-sq.(adj) =  0.0411   Deviance explained = 41.1%
-REML = 2227.1  Scale est. = 25.866    n = 16939

All predictors were significant. This is the final model.
Creating term plots.
Diagnostic output from gam.check():

Method: REML   Optimizer: outer newton
full convergence after 15 iterations.
Gradient range [-0.0001657223,0.000220557]
(score 2227.122 & scale 25.86577).
Hessian positive definite, eigenvalue range [0.3403835,1036.881].
Model rank =  21 / 21

Basis dimension (k) checking results. Low p-value (k-index<1) may
indicate that k is too low, especially if edf is close to k'.

                                   k'   edf k-index p-value
s(log10(Depth))                 4.000 3.619   0.797    0.00
s(I(DistToCanyonOrSeamount/1000)) 4.000 2.467   0.808    0.00
s(SST)                          4.000 0.964   0.859    0.19
s(I(DistToFront1^(1/3)))        4.000 1.079   0.876    0.71
s(I(DistToCEddy9/1000))         4.000 3.245   0.868    0.38

Predictors retained during the model selection procedure: Depth, DistToCanyonOrSeamount, SST,
DistToFront1, DistToCEddy9

Predictors dropped during the model selection procedure: Slope, DistTo125m, TKE, DistToAEddy9
```

Model term plots

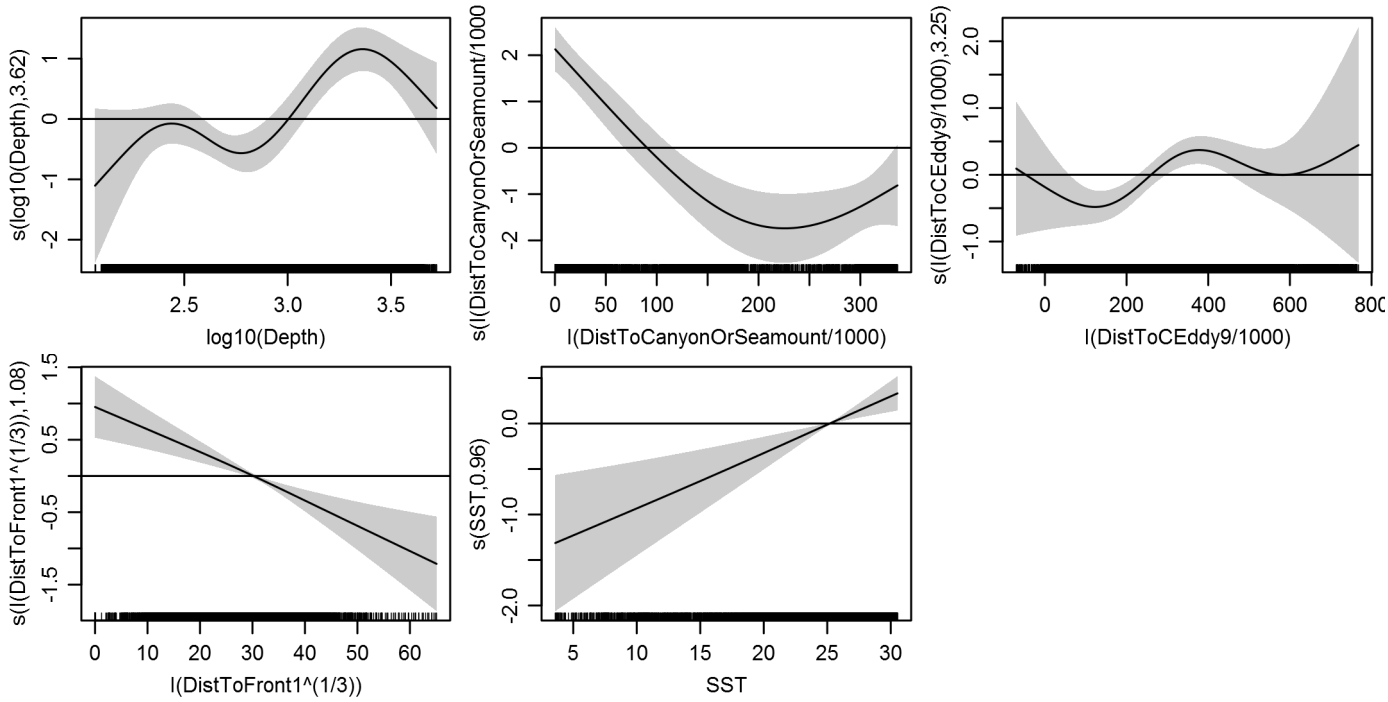

Diagnostic plots

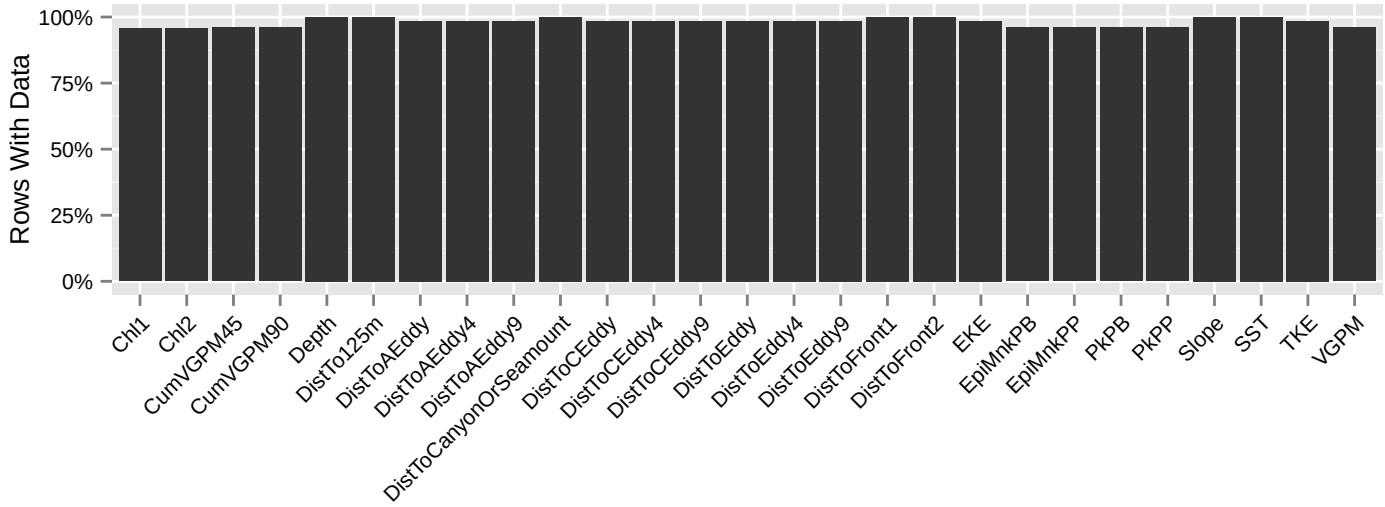

Figure 88: Segments with predictor values for the Sperm whale Contemporaneous model, Slope and Abyss. This plot is used to assess how many segments would be lost by including a given predictor in a model.

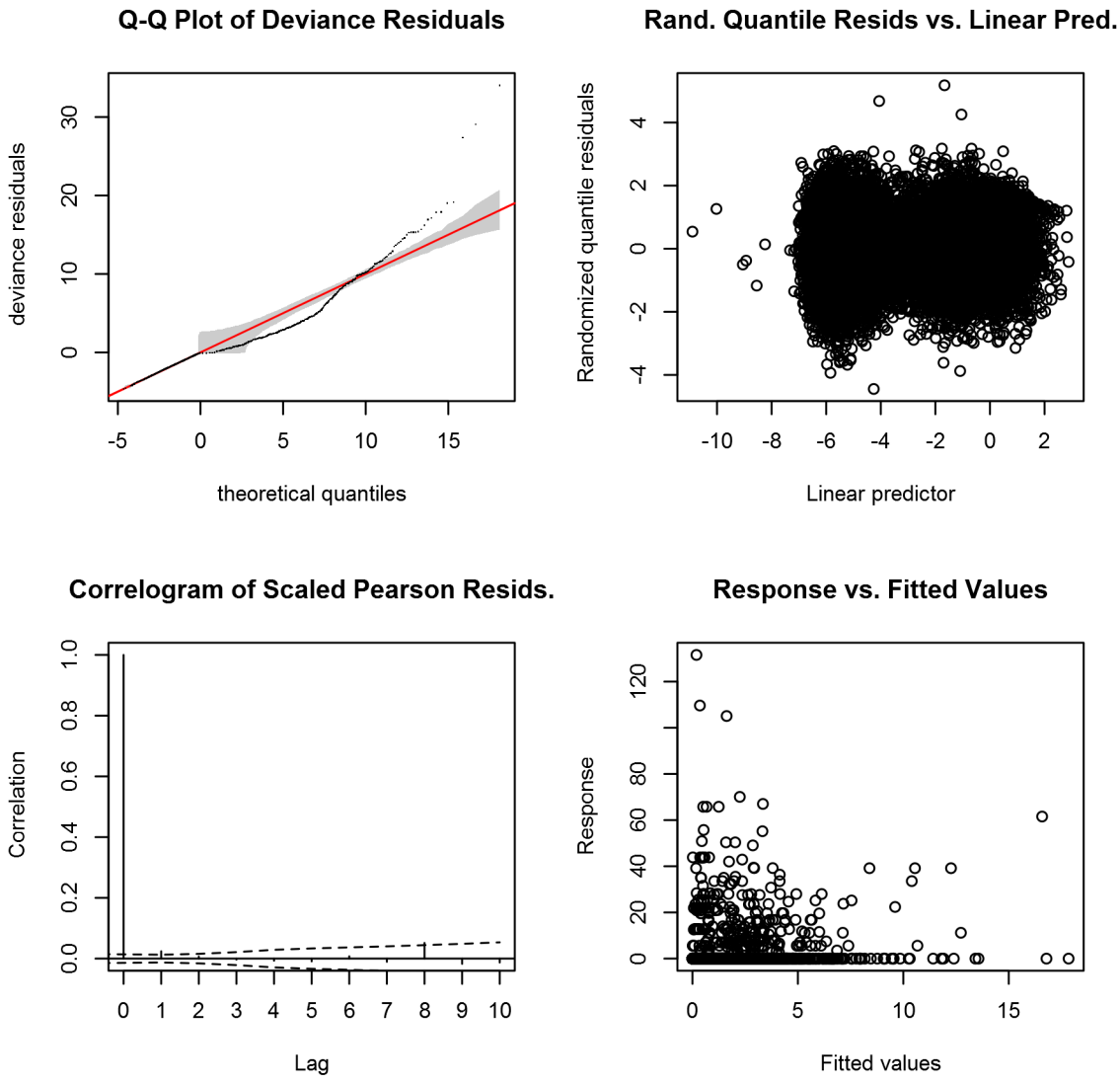

Figure 89: Statistical diagnostic plots for the Sperm whale Contemporaneous model, Slope and Abyss.

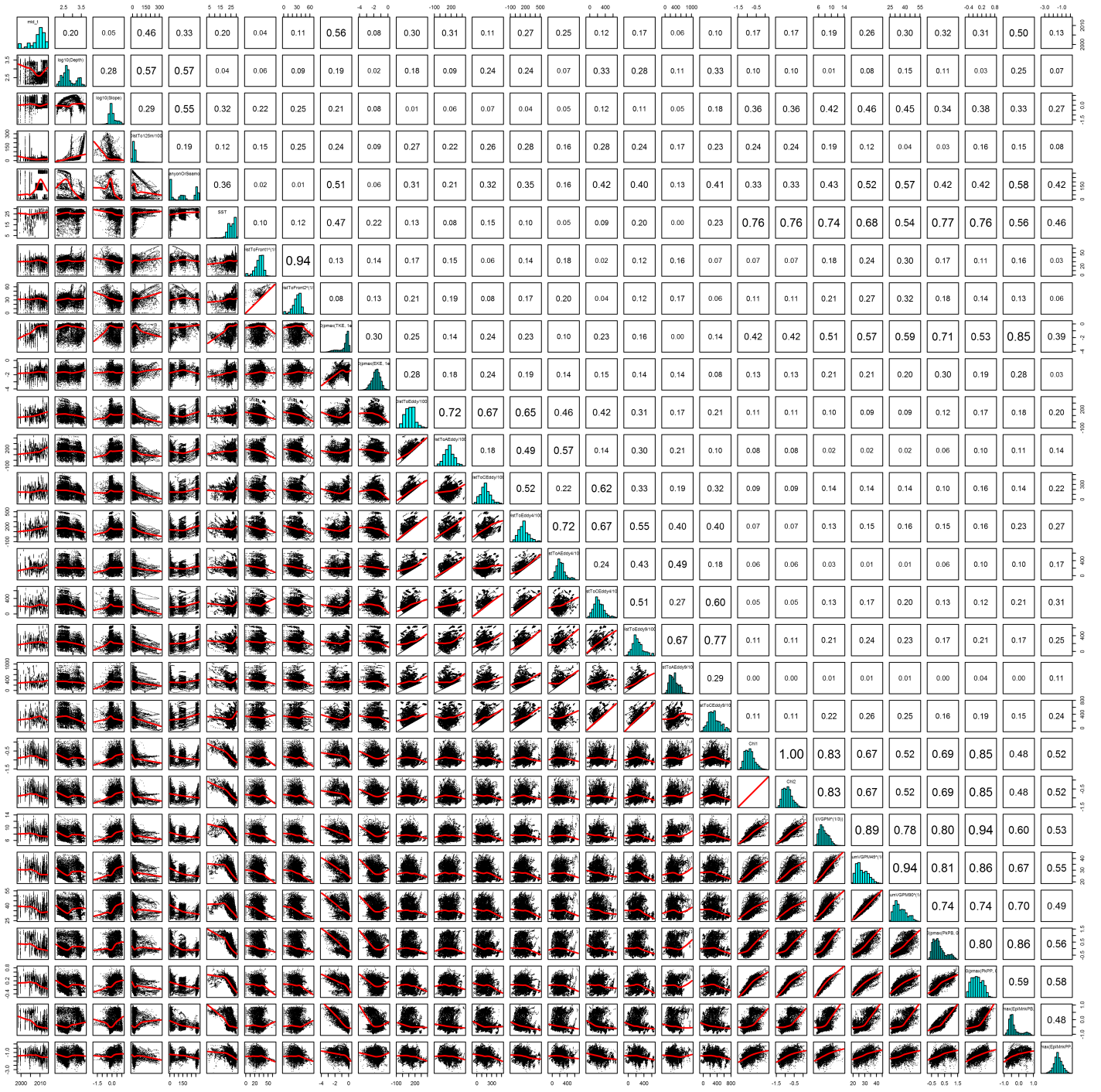

Figure 90: Scatterplot matrix for the Sperm whale Contemporaneous model, Slope and Abyss. This plot is used to inspect the distribution of predictors (via histograms along the diagonal), simple correlation between predictors (via pairwise Pearson coefficients above the diagonal), and linearity of predictor correlations (via scatterplots below the diagonal). This plot is best viewed at high magnification.

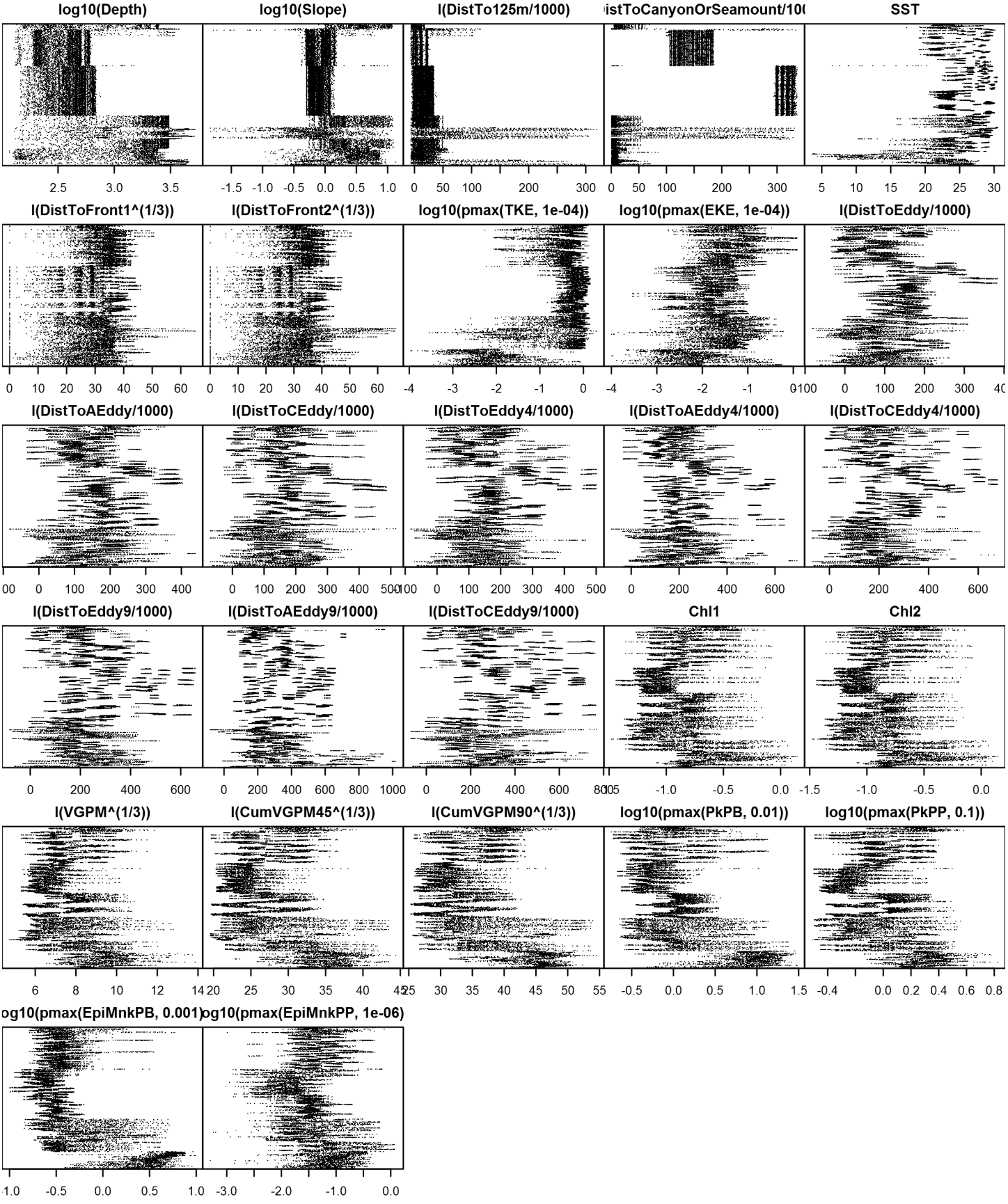

Figure 91: Dotplot for the Sperm whale Contemporaneous model, Slope and Abyss. This plot is used to check for suspicious patterns and outliers in the data. Points are ordered vertically by transect ID, sequentially in time.

Shelf

Statistical output

```
Rscript.exe: This is mgcv 1.8-2. For overview type 'help("mgcv-package")'.


Family: Tweedie(p=1.152)
Link function: log

Formula:
abundance ~ offset(log(area_km2)) + s(log10(Depth), bs = "ts",
    k = 5) + s(log10(Slope), bs = "ts", k = 5) + s(I(DistToCanyonOrSeamount/1000),
    bs = "ts", k = 5) + s(log10(pmax(EKE, 1e-04)), bs = "ts",
    k = 5) + s(log10(pmax(PkPB, 0.01)), bs = "ts", k = 5)

Parametric coefficients:
            Estimate Std. Error t value Pr(>|t|)
(Intercept) -11.4775     0.4598  -24.96   <2e-16 ***
---
Signif. codes:  0 '***' 0.001 '**' 0.01 '*' 0.05 '.' 0.1 ' ' 1

Approximate significance of smooth terms:
                                   edf Ref.df      F  p-value
s(log10(Depth))                  0.995      4  2.772 0.000498 ***
s(log10(Slope))                  1.022      4  4.366 1.41e-05 ***
s(I(DistToCanyonOrSeamount/1000)) 1.241      4 16.770  < 2e-16 ***
s(log10(pmax(EKE, 1e-04)))       1.010      4  3.299 0.000176 ***
s(log10(pmax(PkPB, 0.01)))       0.948      4  2.836 0.000391 ***
---
Signif. codes:  0 '***' 0.001 '**' 0.01 '*' 0.05 '.' 0.1 ' ' 1

R-sq.(adj) =  0.000939   Deviance explained = 31.3%
-REML = 501.25  Scale est. = 33.869    n = 83417

All predictors were significant. This is the final model.
Creating term plots.
Diagnostic output from gam.check():

Method: REML   Optimizer: outer newton
full convergence after 12 iterations.
Gradient range [-0.0001535581,0.0001097937]
(score 501.2517 & scale 33.86853).
Hessian positive definite, eigenvalue range [0.3079212,398.51].
Model rank =  21 / 21

Basis dimension (k) checking results. Low p-value (k-index<1) may
indicate that k is too low, especially if edf is close to k'.

                                   k'   edf k-index p-value
s(log10(Depth))                 4.000 0.995   0.934    0.00
s(log10(Slope))                 4.000 1.022   0.941    0.04
s(I(DistToCanyonOrSeamount/1000)) 4.000 1.241   0.931    0.01
s(log10(pmax(EKE, 1e-04)))      4.000 1.010   0.938    0.00
s(log10(pmax(PkPB, 0.01)))      4.000 0.948   0.933    0.00

Predictors retained during the model selection procedure: Depth, Slope, DistToCanyonOrSeamount, EKE,
PkPB
```

```
Predictors dropped during the model selection procedure: DistToShore, DistTo125m, SST, DistToFront1
```

Model term plots

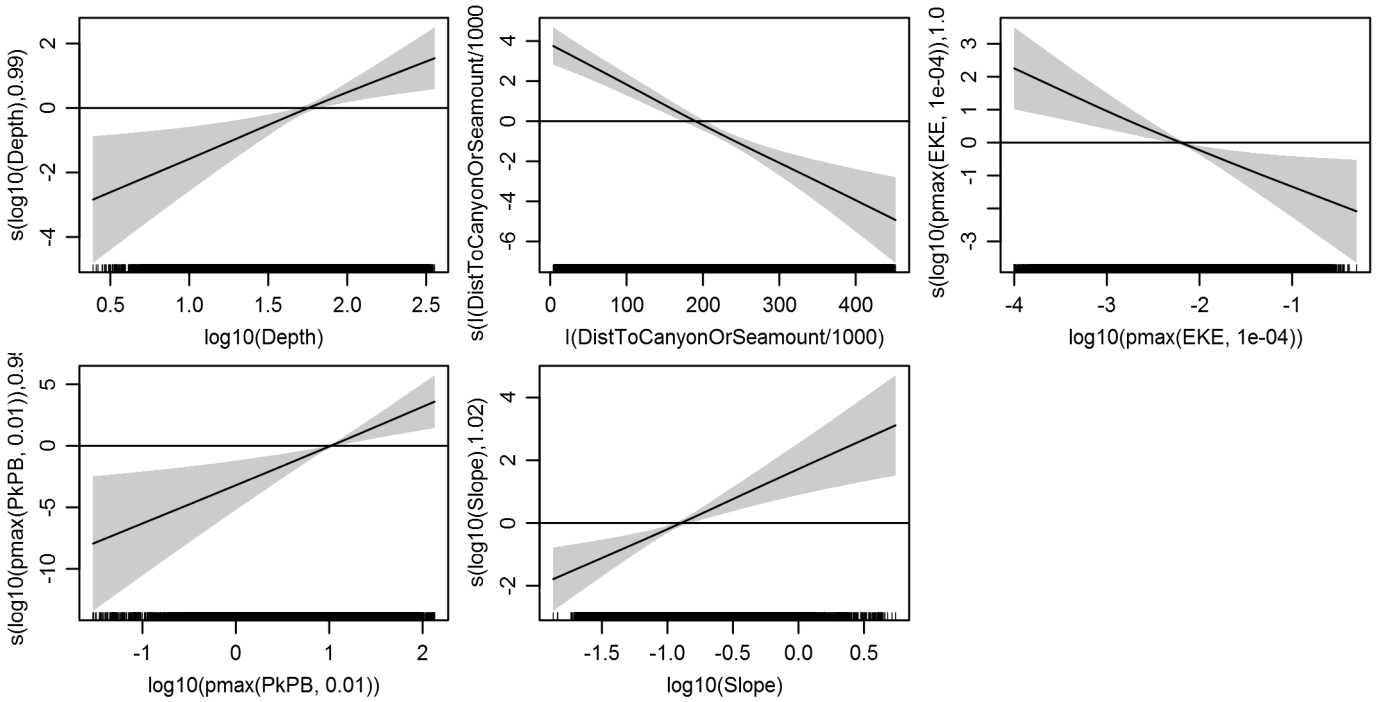

Diagnostic plots

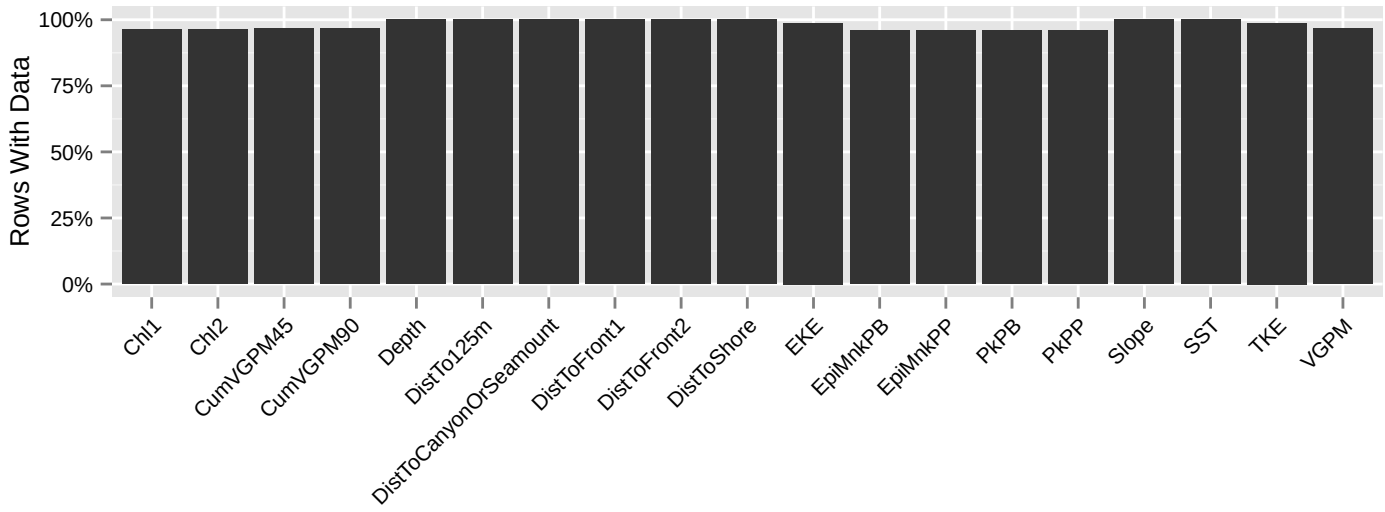

Figure 92: Segments with predictor values for the Sperm whale Contemporaneous model, Shelf. This plot is used to assess how many segments would be lost by including a given predictor in a model.

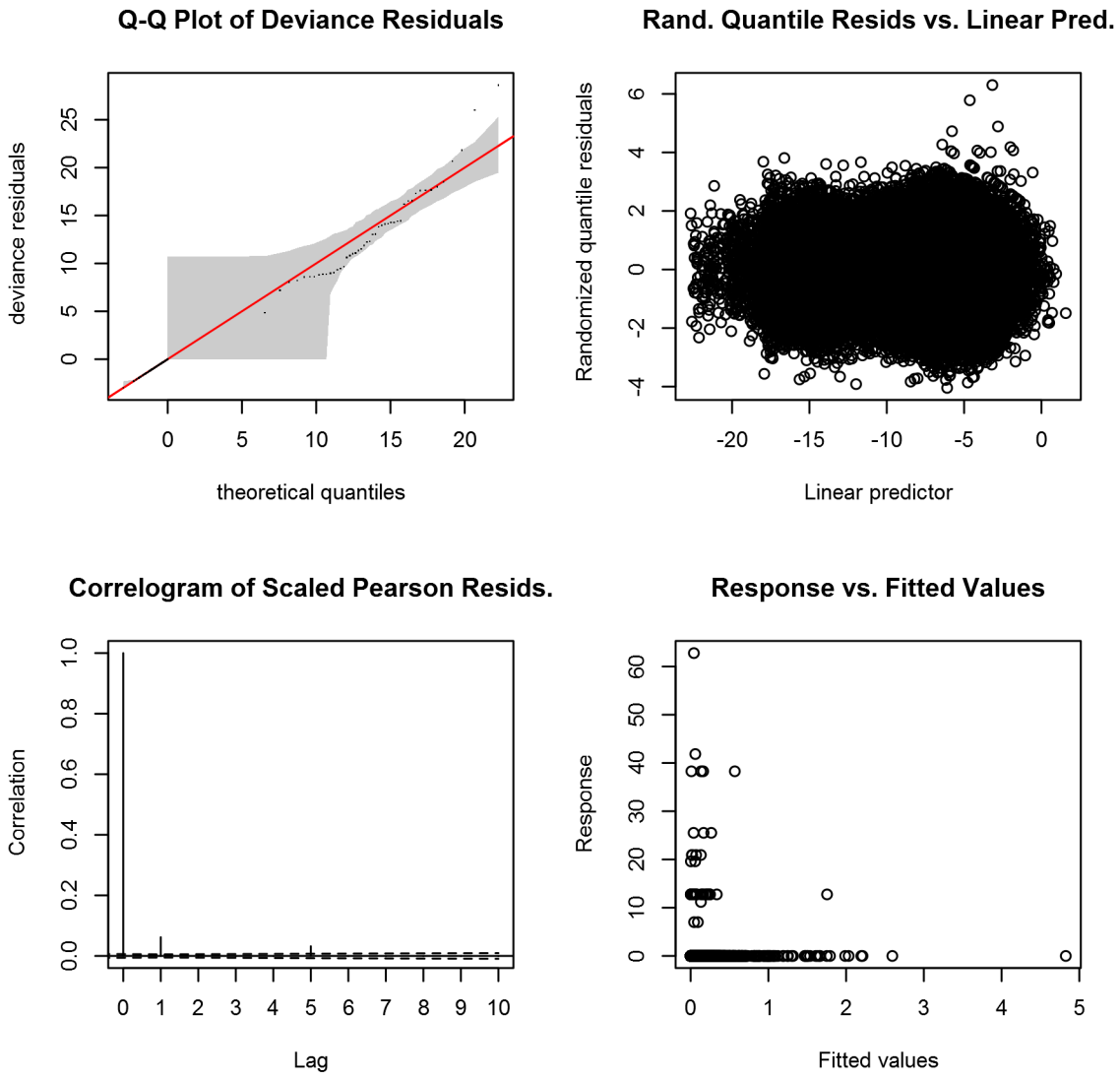

Figure 93: Statistical diagnostic plots for the Sperm whale Contemporaneous model, Shelf.

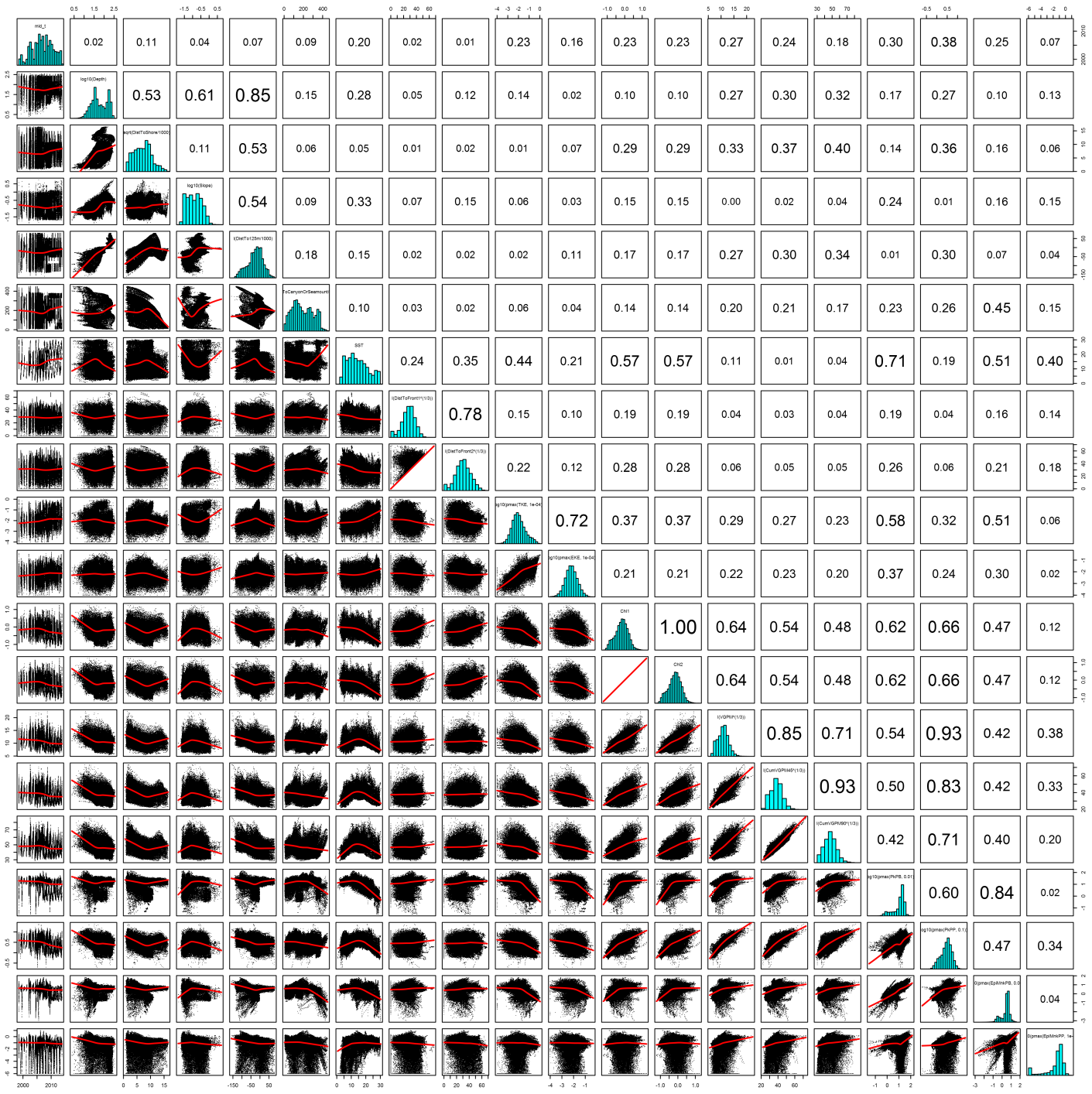

Figure 94: Scatterplot matrix for the Sperm whale Contemporaneous model, Shelf. This plot is used to inspect the distribution of predictors (via histograms along the diagonal), simple correlation between predictors (via pairwise Pearson coefficients above the diagonal), and linearity of predictor correlations (via scatterplots below the diagonal). This plot is best viewed at high magnification.

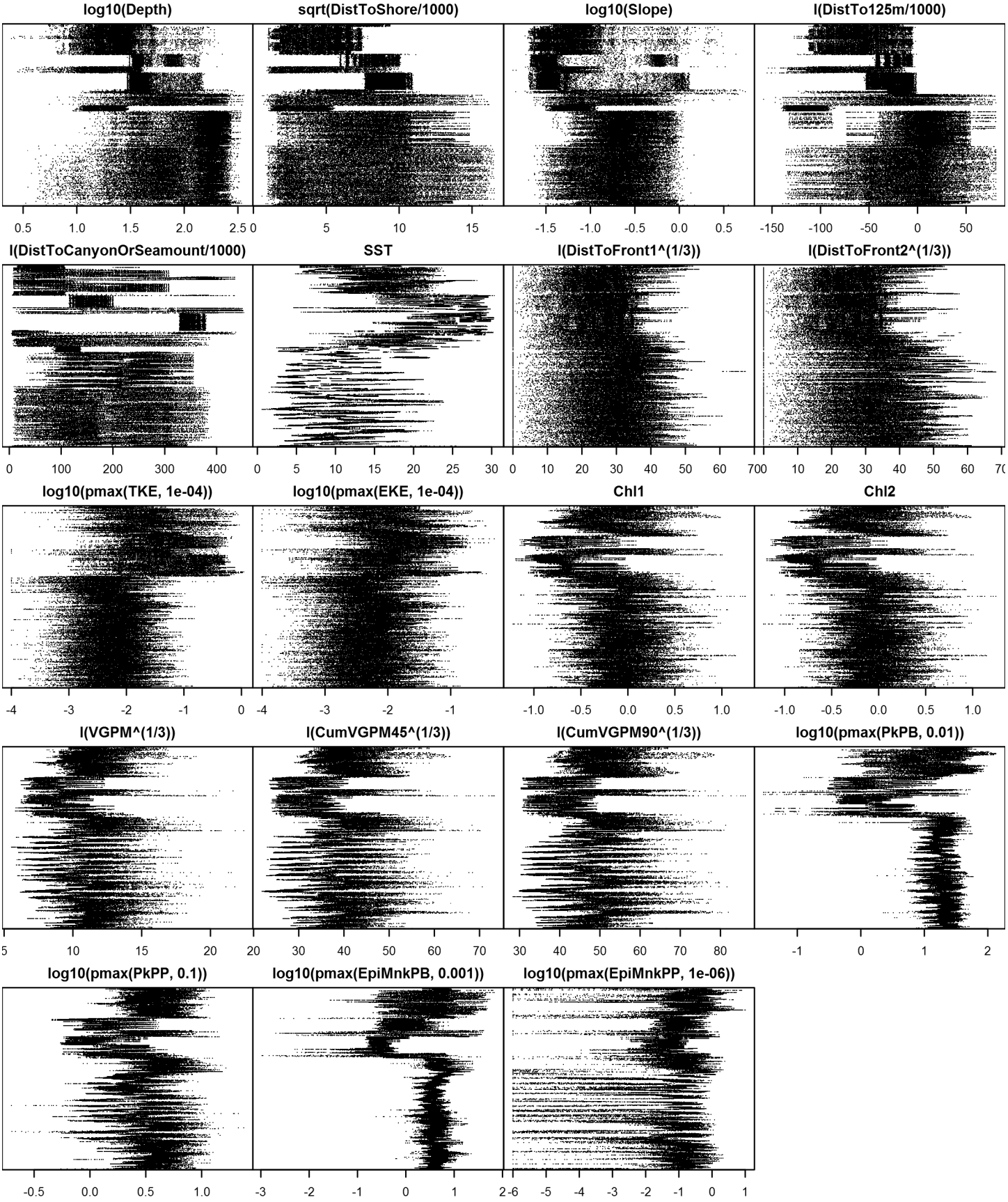

Figure 95: Dotplot for the Sperm whale Contemporaneous model, Shelf. This plot is used to check for suspicious patterns and outliers in the data. Points are ordered vertically by transect ID, sequentially in time.

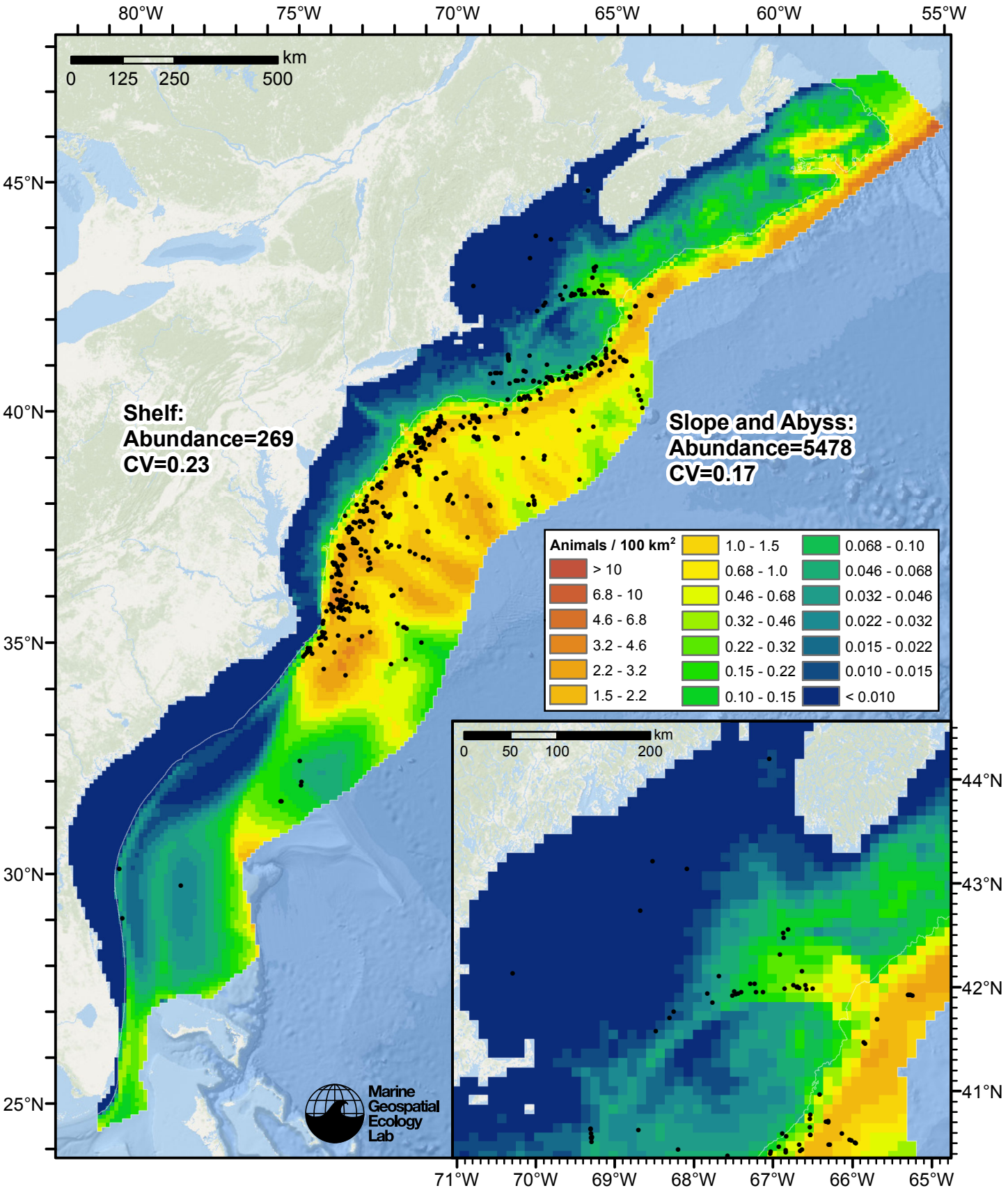

Figure 96: Sperm whale density predicted by the climatological same segments model that explained the most deviance. Pixels are 10x10 km. The legend gives the estimated individuals per pixel; breaks are logarithmic. Abundance for each region was computed by summing the density cells occuring in that region.

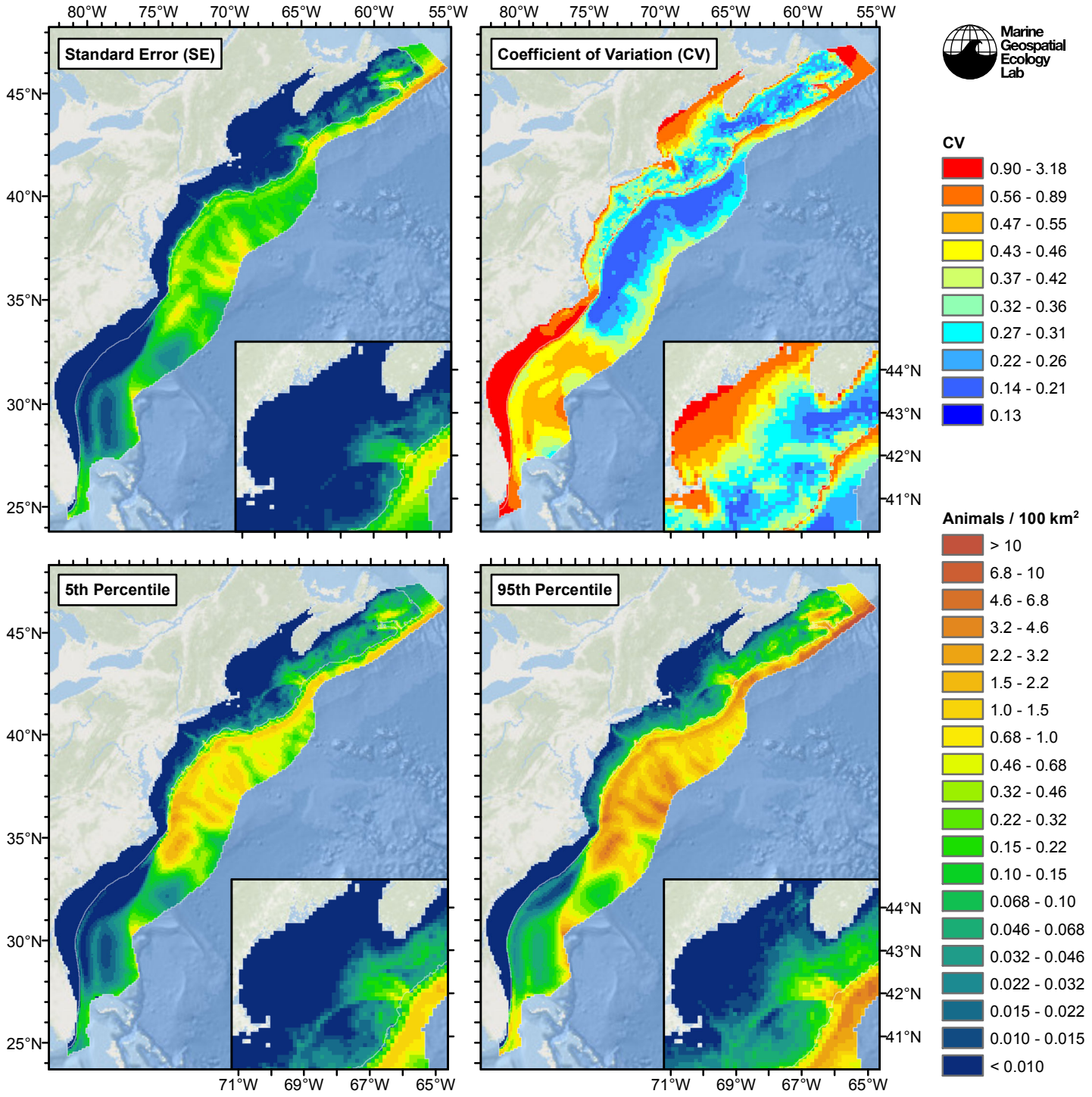

Figure 97: Estimated uncertainty for the climatological same segments model that explained the most deviance. These estimates only incorporate the statistical uncertainty estimated for the spatial model (by the R mgcv package). They do not incorporate uncertainty in the detection functions, g(0) estimates, predictor variables, and so on.

Slope and Abyss

Statistical output

```
Rscript.exe: This is mgcv 1.8-2. For overview type 'help("mgcv-package")'.


Family: Tweedie(p=1.297)
```

```
Link function: log

Formula:
abundance ~ offset(log(area_km2)) + s(log10(Depth), bs = "ts",
    k = 5) + s(I(DistTo125m/1000), bs = "ts", k = 5) + s(I(DistToCanyonOrSeamount/1000),
    bs = "ts", k = 5) + s(ClimSST, bs = "ts", k = 5) + s(I(ClimDistToFront1^(1/3)),
    bs = "ts", k = 5) + s(log10(pmax(ClimEKE, 1e-04)), bs = "ts",
    k = 5) + s(I(ClimDistToAEddy/1000), bs = "ts", k = 5)

Parametric coefficients:
            Estimate Std. Error t value Pr(>|t|)
(Intercept)   -6.920      0.193  -35.86   <2e-16 ***
---
Signif. codes:  0 '***' 0.001 '**' 0.01 '*' 0.05 '.' 0.1 ' ' 1

Approximate significance of smooth terms:
                                    edf Ref.df      F  p-value
s(log10(Depth))                  3.7144      4 14.086 1.11e-12 ***
s(I(DistTo125m/1000))            0.8956      4  1.750 0.003057 **
s(I(DistToCanyonOrSeamount/1000)) 2.0325      4 17.360  < 2e-16 ***
s(ClimSST)                       3.5259      4  6.545 6.17e-06 ***
s(I(ClimDistToFront1^(1/3)))     1.0505      4  4.733 5.11e-06 ***
s(log10(pmax(ClimEKE, 1e-04)))   0.9267      4  1.893 0.003103 **
s(I(ClimDistToAEddy/1000))       0.9616      4  2.545 0.000665 ***
---
Signif. codes:  0 '***' 0.001 '**' 0.01 '*' 0.05 '.' 0.1 ' ' 1

R-sq.(adj) =  0.0419   Deviance explained = 41.7%
-REML = 2226.8  Scale est. = 25.874    n = 16939

All predictors were significant. This is the final model.
Creating term plots.
Diagnostic output from gam.check():

Method: REML   Optimizer: outer newton
full convergence after 14 iterations.
Gradient range [-0.0005097222,0.0002790447]
(score 2226.811 & scale 25.87359).
Hessian positive definite, eigenvalue range [0.3131816,1025.231].
Model rank =  29 / 29

Basis dimension (k) checking results. Low p-value (k-index<1) may
indicate that k is too low, especially if edf is close to k'.

                                   k'   edf k-index p-value
s(log10(Depth))                 4.000 3.714   0.686    0.00
s(I(DistTo125m/1000))           4.000 0.896   0.767    0.02
s(I(DistToCanyonOrSeamount/1000)) 4.000 2.033   0.692    0.00
s(ClimSST)                      4.000 3.526   0.767    0.02
s(I(ClimDistToFront1^(1/3)))    4.000 1.050   0.785    0.24
s(log10(pmax(ClimEKE, 1e-04)))  4.000 0.927   0.765    0.02
s(I(ClimDistToAEddy/1000))      4.000 0.962   0.771    0.04

Predictors retained during the model selection procedure: Depth, DistTo125m, DistToCanyonOrSeamount,
ClimSST, ClimDistToFront1, ClimEKE, ClimDistToAEddy

Predictors dropped during the model selection procedure: Slope, ClimDistToCEddy
```

Model term plots

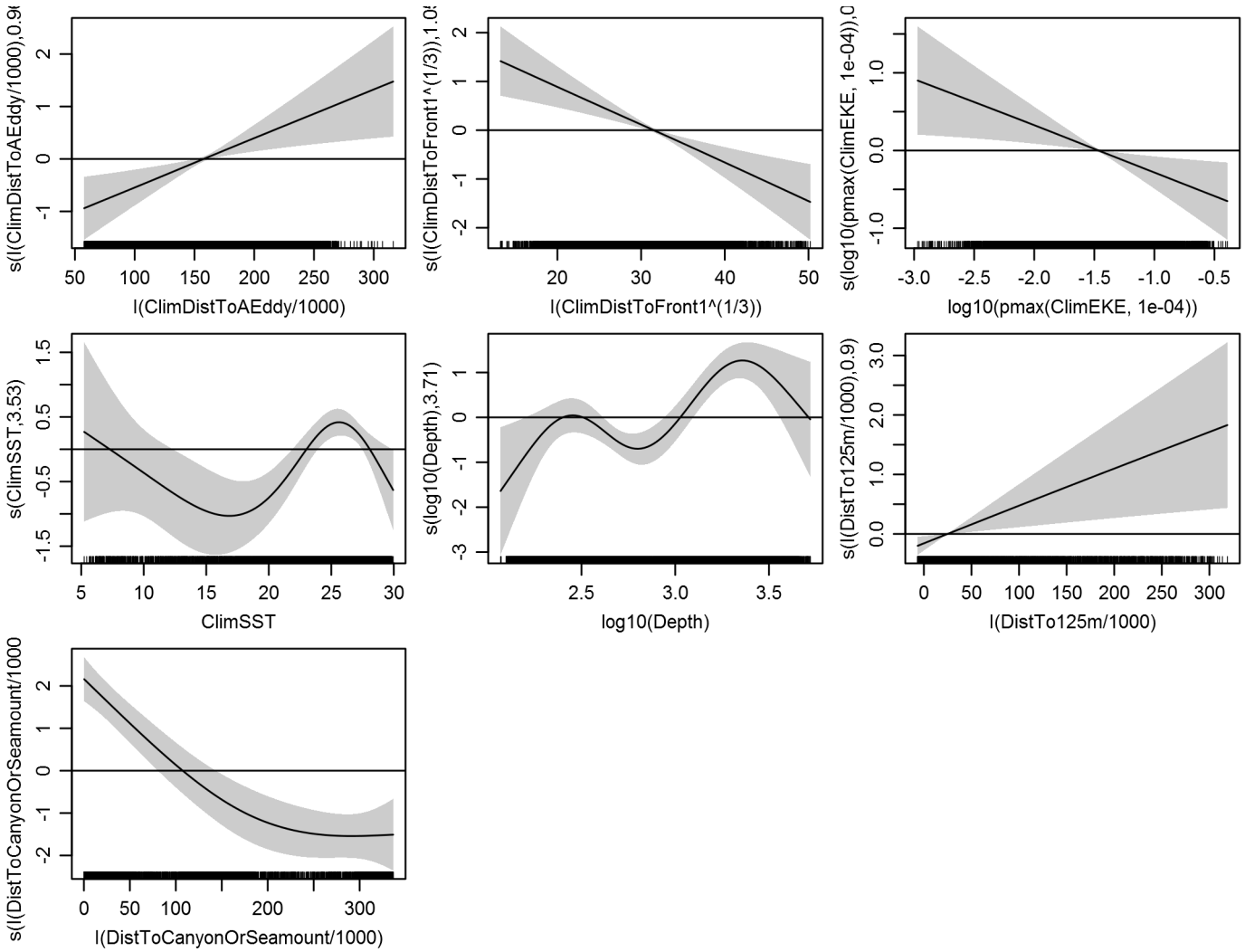

Diagnostic plots

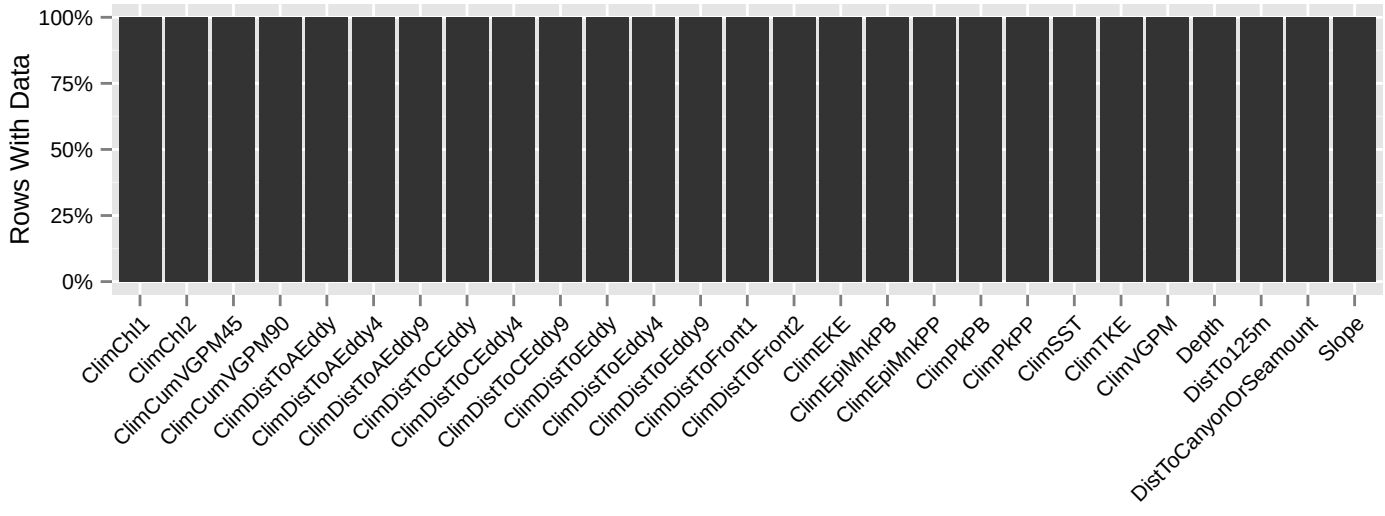

Figure 98: Segments with predictor values for the Sperm whale Climatological model, Slope and Abyss. This plot is used to assess how many segments would be lost by including a given predictor in a model.

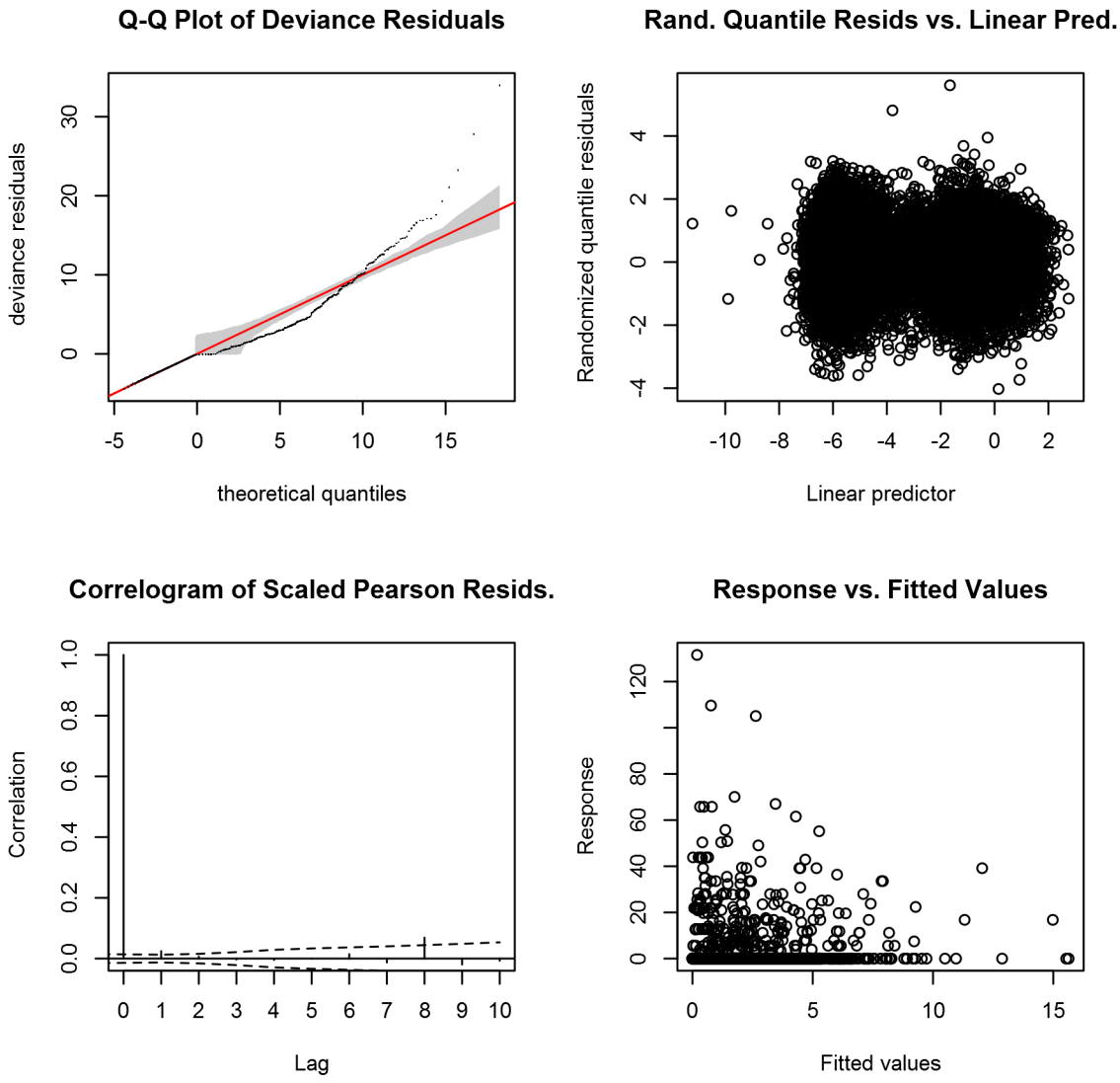

Figure 99: Statistical diagnostic plots for the Sperm whale Climatological model, Slope and Abyss.

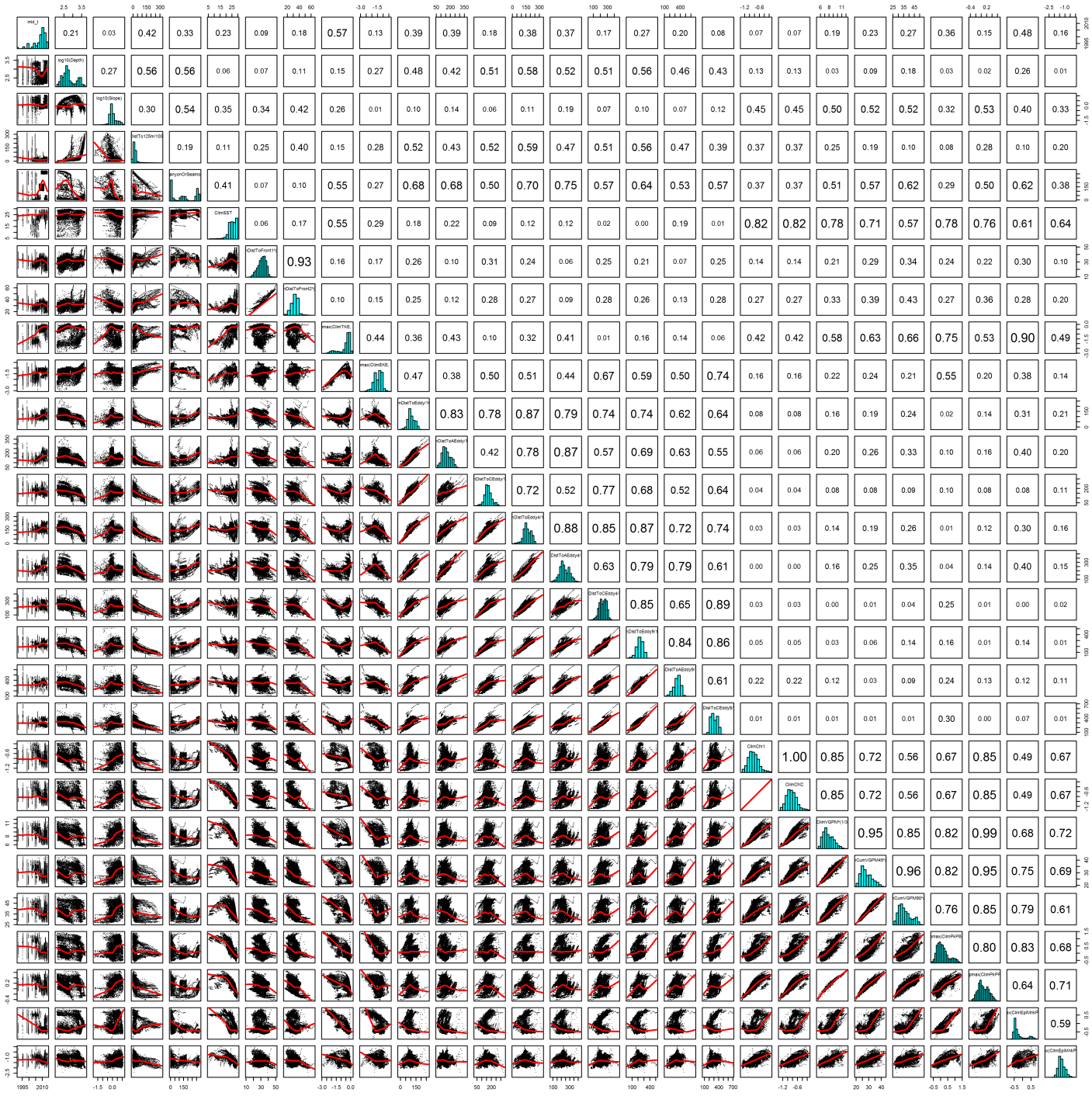

Figure 100: Scatterplot matrix for the Sperm whale Climatological model, Slope and Abyss. This plot is used to inspect the distribution of predictors (via histograms along the diagonal), simple correlation between predictors (via pairwise Pearson coefficients above the diagonal), and linearity of predictor correlations (via scatterplots below the diagonal). This plot is best viewed at high magnification.

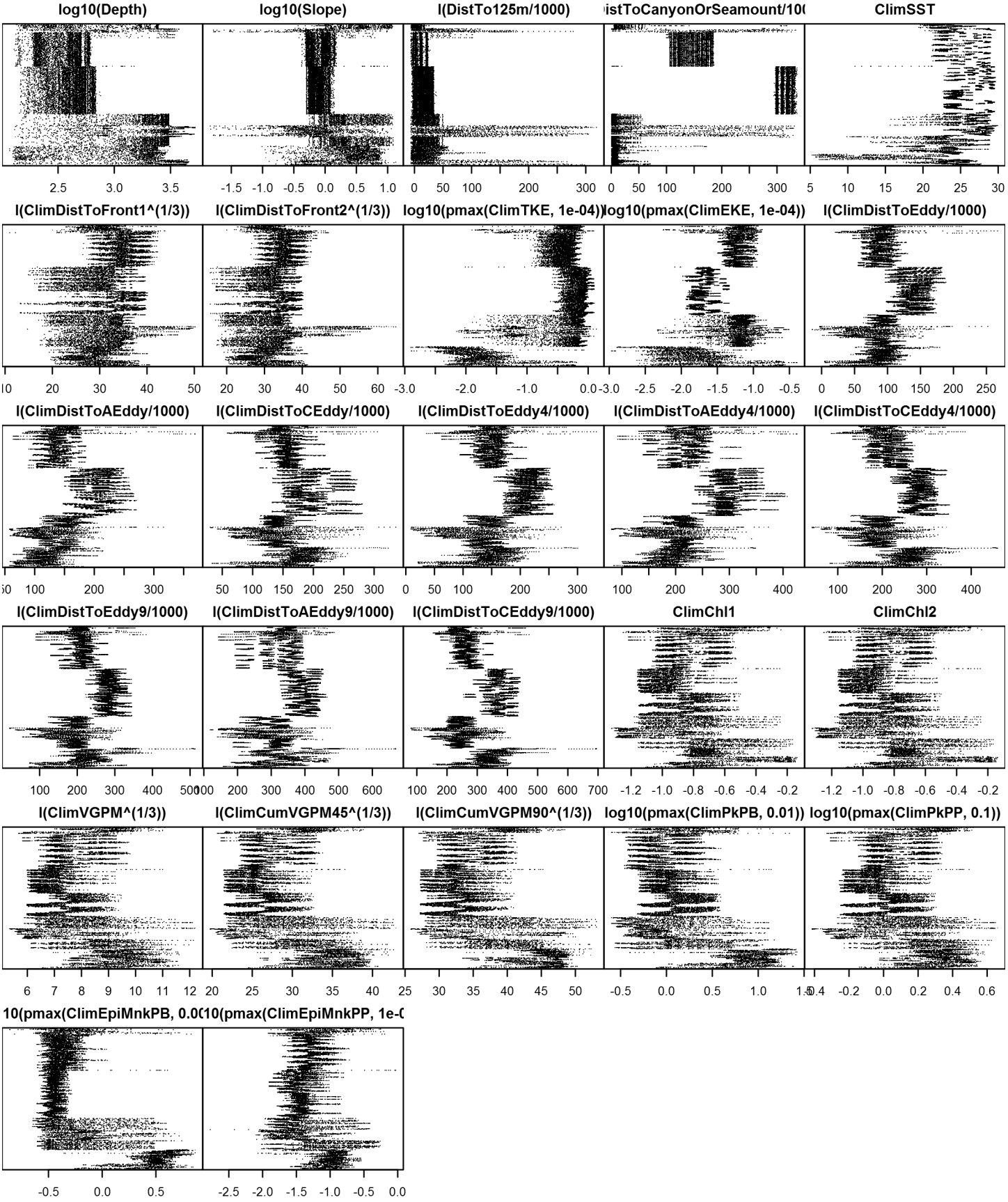

Figure 101: Dotplot for the Sperm whale Climatological model, Slope and Abyss. This plot is used to check for suspicious patterns and outliers in the data. Points are ordered vertically by transect ID, sequentially in time.

Shelf

Statistical output

```
Rscript.exe: This is mgcv 1.8-2. For overview type 'help("mgcv-package")'.


Family: Tweedie(p=1.156)
Link function: log

Formula:
abundance ~ offset(log(area_km2)) + s(log10(Depth), bs = "ts",
    k = 5) + s(log10(Slope), bs = "ts", k = 5) + s(I(DistToCanyonOrSeamount/1000),
    bs = "ts", k = 5) + s(log10(pmax(ClimPkPB, 0.01)), bs = "ts",
    k = 5)

Parametric coefficients:
            Estimate Std. Error t value Pr(>|t|)
(Intercept) -11.6733     0.5064  -23.05   <2e-16 ***
---
Signif. codes:  0 '***' 0.001 '**' 0.01 '*' 0.05 '.' 0.1 ' ' 1

Approximate significance of smooth terms:
                                   edf Ref.df      F  p-value
s(log10(Depth))                 1.0231      4  2.775 0.000525 ***
s(log10(Slope))                 0.9885      4  3.392 0.000116 ***
s(I(DistToCanyonOrSeamount/1000)) 1.2865      4 19.799  < 2e-16 ***
s(log10(pmax(ClimPkPB, 0.01)))  0.9923      4  4.720 5.65e-06 ***
---
Signif. codes:  0 '***' 0.001 '**' 0.01 '*' 0.05 '.' 0.1 ' ' 1

R-sq.(adj) =  0.00494   Deviance explained = 29.3%
-REML = 505.57  Scale est. = 35.05     n = 83417

All predictors were significant. This is the final model.
Creating term plots.
Diagnostic output from gam.check():

Method: REML   Optimizer: outer newton
full convergence after 13 iterations.
Gradient range [-3.330147e-07,4.115323e-07]
(score 505.5674 & scale 35.05021).
Hessian positive definite, eigenvalue range [0.1948333,398.9656].
Model rank =  17 / 17

Basis dimension (k) checking results. Low p-value (k-index<1) may
indicate that k is too low, especially if edf is close to k'.

                                   k'   edf k-index p-value
s(log10(Depth))                 4.000 1.023   0.444       0
s(log10(Slope))                 4.000 0.989   0.457       0
s(I(DistToCanyonOrSeamount/1000)) 4.000 1.286   0.375       0
s(log10(pmax(ClimPkPB, 0.01)))  4.000 0.992   0.368       0

Predictors retained during the model selection procedure: Depth, Slope, DistToCanyonOrSeamount,
ClimPkPB

Predictors dropped during the model selection procedure: DistToShore, DistTo125m, ClimSST,
ClimDistToFront1, ClimEKE
```

Model term plots

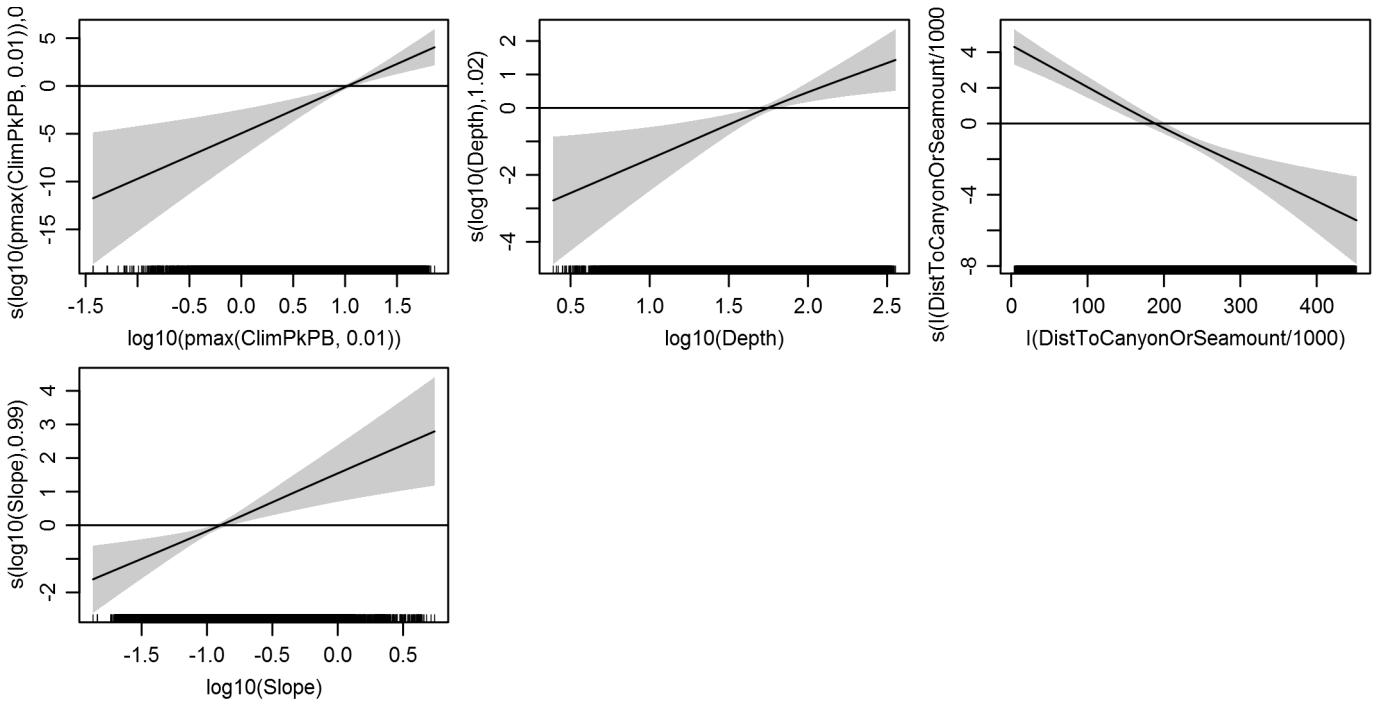

Diagnostic plots

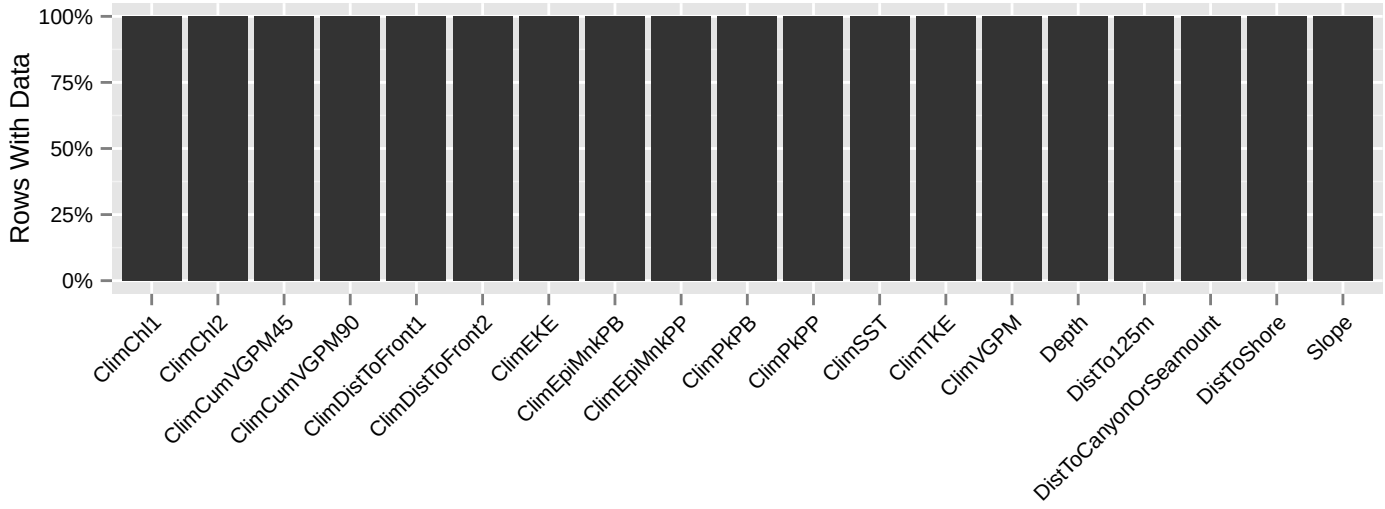

Figure 102: Segments with predictor values for the Sperm whale Climatological model, Shelf. This plot is used to assess how many segments would be lost by including a given predictor in a model.

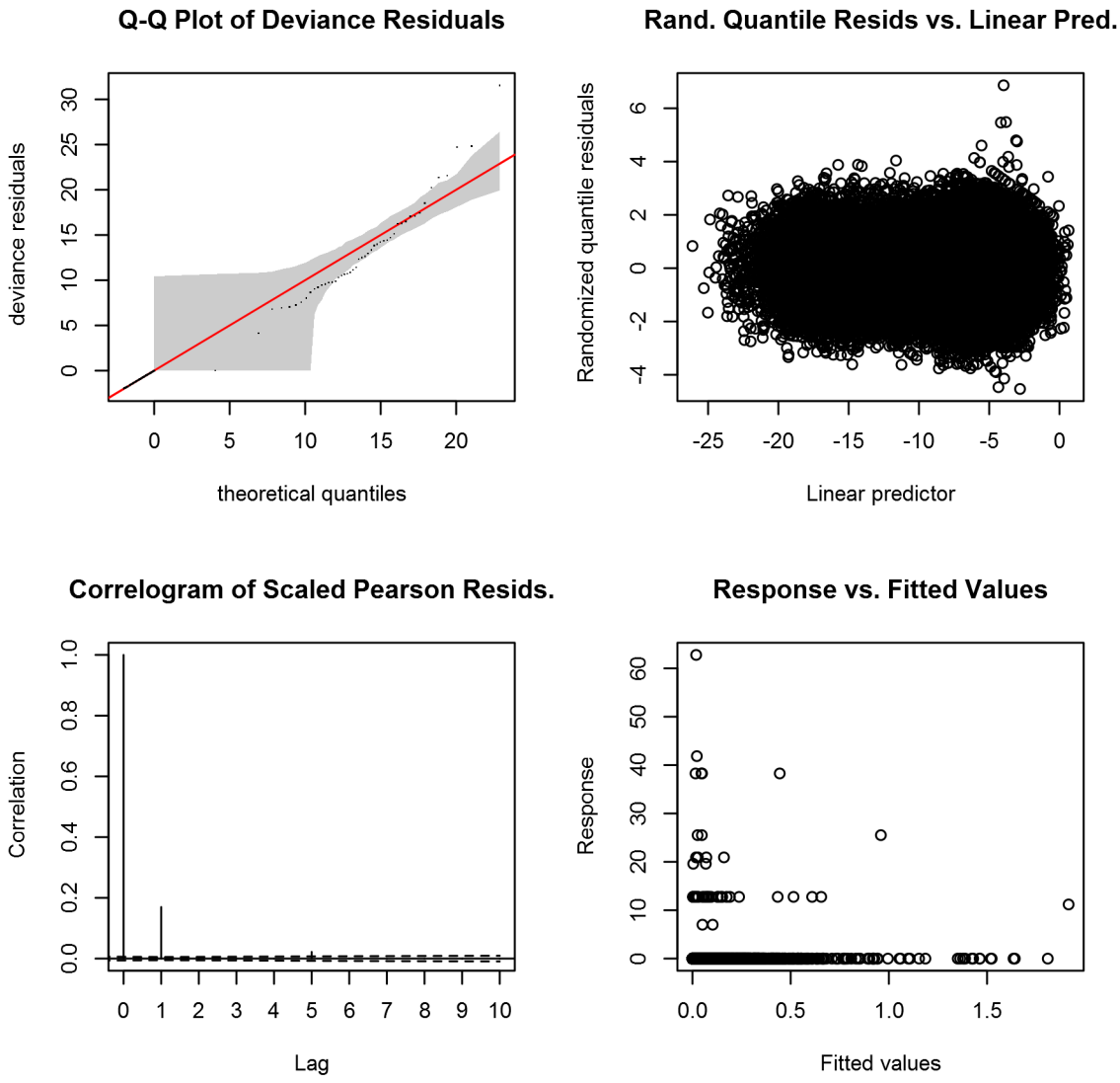

Figure 103: Statistical diagnostic plots for the Sperm whale Climatological model, Shelf.

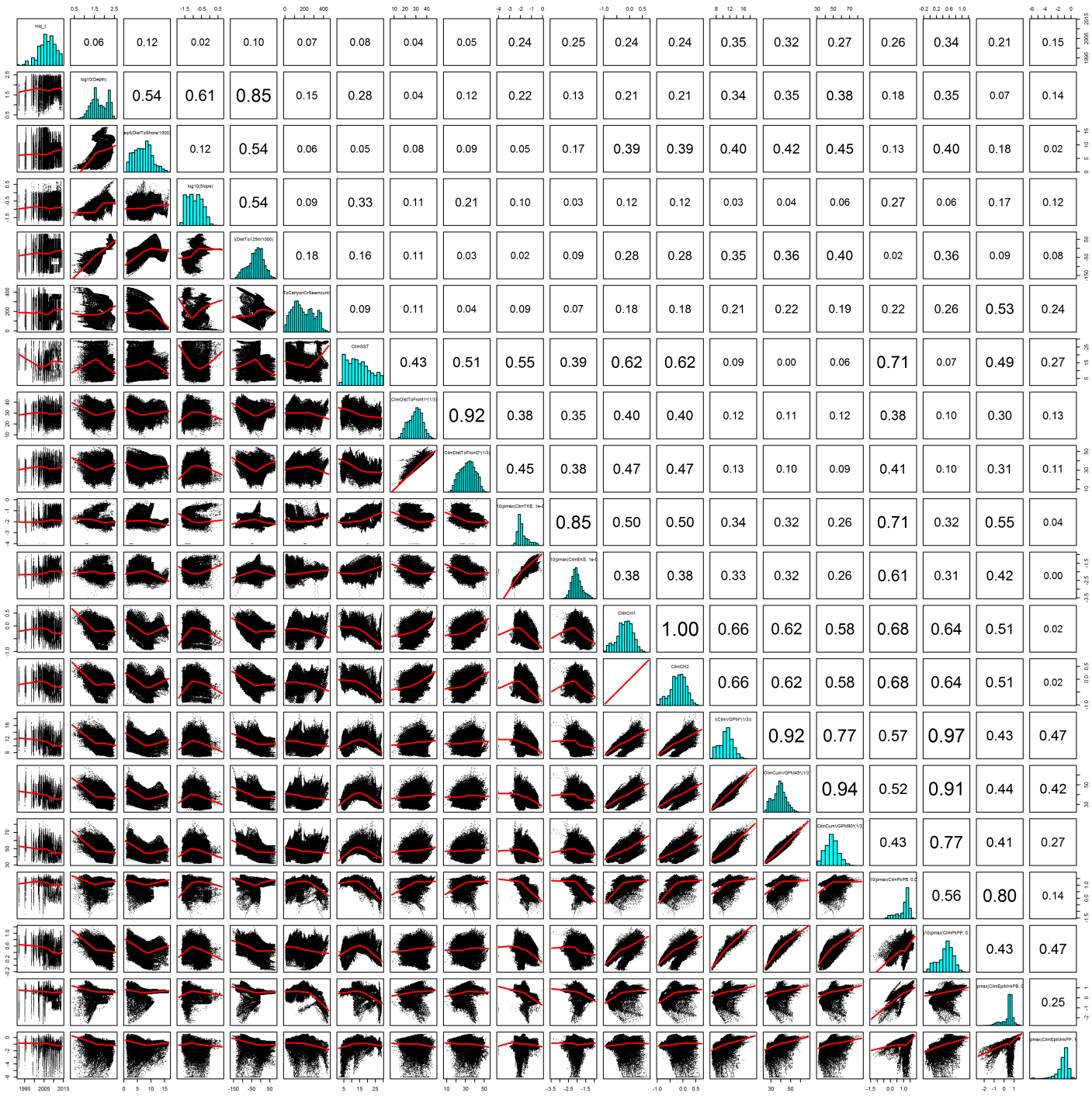

Figure 104: Scatterplot matrix for the Sperm whale Climatological model, Shelf. This plot is used to inspect the distribution of predictors (via histograms along the diagonal), simple correlation between predictors (via pairwise Pearson coefficients above the diagonal), and linearity of predictor correlations (via scatterplots below the diagonal). This plot is best viewed at high magnification.

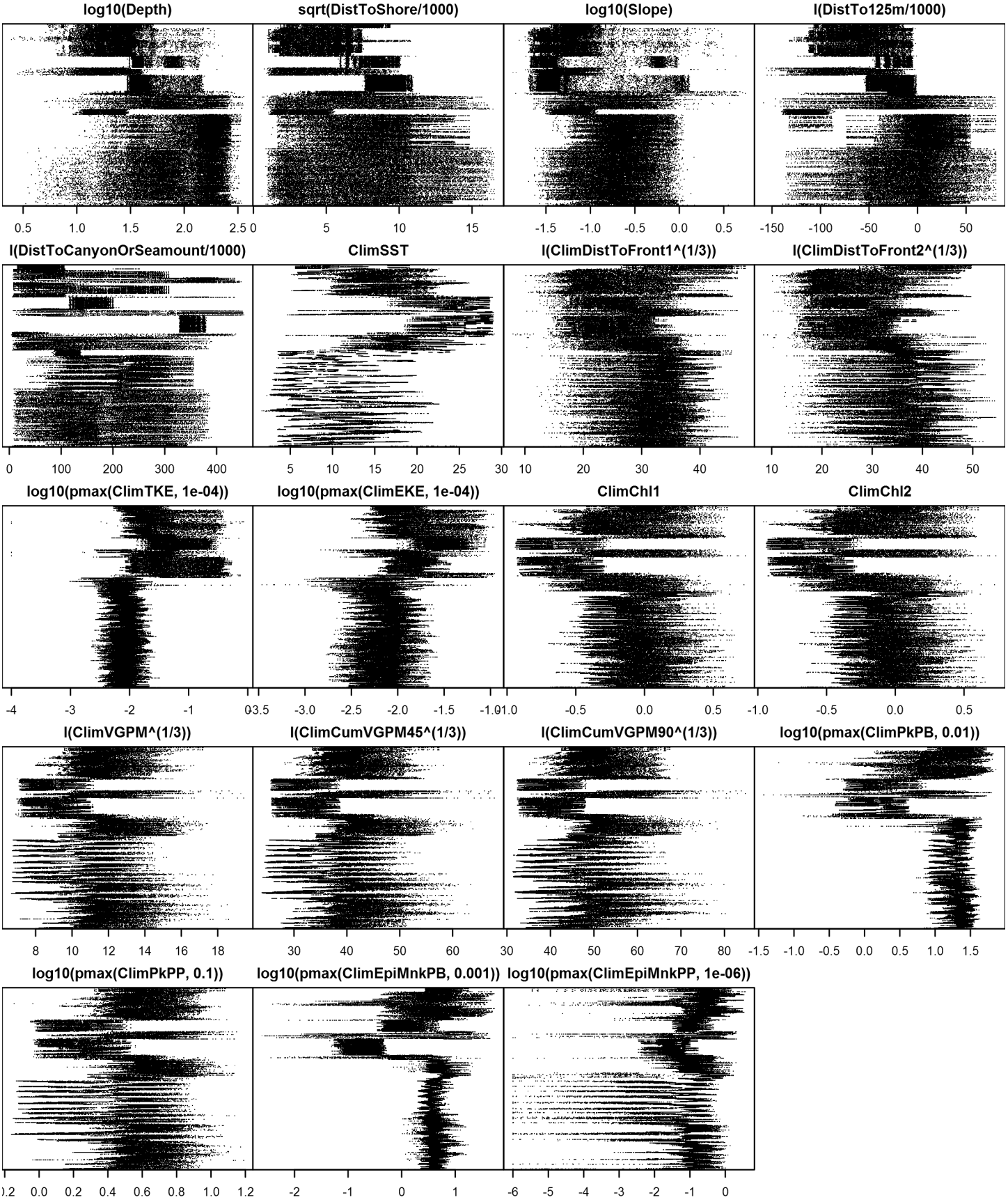

Figure 105: Dotplot for the Sperm whale Climatological model, Shelf. This plot is used to check for suspicious patterns and outliers in the data. Points are ordered vertically by transect ID, sequentially in time.

Model Comparison

Spatial Model Performance

The table below summarizes the performance of the candidate spatial models that were tested. For each subregion, the first model contained only physiographic predictors. Subsequent models added additional suites of predictors of based on when they became available via remote sensing.

For each model, three versions were fitted; the % Dev Expl columns give the % deviance explained by each one. The "climatological" models were fitted to 8-day climatologies of the environmental predictors. Because the environmental predictors were always available, no segments were lost, allowing these models to consider the maximal amount of survey data. The "contemporaneous" models were fitted to day-of-sighting images of the environmental predictors; these were smoothed to reduce data loss due to clouds, but some segments still failed to retrieve environmental values and were lost. Finally, the "climatological same segments" models fitted climatological predictors to the segments retained by the contemporaneous model, so that the explantory power of the two types of predictors could be directly compared. For each of the three models, predictors were selected independently via shrinkage smoothers; thus the three models did not necessarily utilize the same predictors.

Predictors derived from ocean currents first became available in January 1993 after the launch of the TOPEX/Poseidon satellite; productivity predictors first became available in September 1997 after the launch of the SeaWiFS sensor. Contemporaneous and climatological same segments models considering these predictors usually suffered data loss. Date Range shows the years spanned by the retained segments. The Segments column gives the number of segments retained; % Lost gives the percentage lost.

Predictors	Climatol % Dev Expl	Contemp % Dev Expl	Climatol Same Segs % Dev Expl	Segments	% Lost	Date Range
Slope and Abyss:						
Phys	38.1			17198		1992-2013
Phys+SST	40.1	39.5	40.1	17198	0.0	1992-2013
Phys+SST+Curr	40.7	41.1	41.7	16939	1.5	1995-2013
Phys+SST+Curr+Prod	40.7	39.5	40.2	16520	3.9	1998-2013
Shelf:						
Phys	29.1			87038		1992-2014
Phys+SST	29.1	29.1	29.1	87038	0.0	1992-2014
Phys+SST+Curr	26.3	28.3	26.1	85972	1.2	1995-2013
Phys+SST+Curr+Prod	30.8	31.3	29.3	83417	4.2	1998-2013

Table 46: Deviance explained by the candidate density models.

Abundance Estimates

The table below shows the estimated mean abundance (number of animals) within the study area, for the models that explained the most deviance for each model type. Mean abundance was calculated by first predicting density maps for a series of time steps, then computing the abundance for each map, and then averaging the abundances. For the climatological models, we used 8-day climatologies, resulting in 46 abundance maps. For the contemporaneous models, we used daily images, resulting in 365 predicted abundance maps per year that the prediction spanned. The Dates column gives the dates to which the estimates apply. For our models, these are the years for which both survey data and remote sensing data were available.

The Assumed g(0)=1 column specifies whether the abundance estimate assumed that detection was certain along the survey trackline. Studies that assumed this did not correct for availability or perception bias, and therefore underestimated abundance. The In our models column specifies whether the survey data from the study was also used in our models. If not, the study

provides a completely independent estimate of abundance.

Dates	Model or study	Estimated abundance	CV	Assumed g(0)=1	In our models
1992-2014	Climatological model	4859	0.15	No	
1998-2013	Contemporaneous model*	5353	0.12	No	
1992-2014	Climatological same segments model	5747	0.16	No	
Jun-Aug 2011	Central Virginia to lower Bay of Fundy (Waring et al. 2014)	1593	0.36	No	No
Jun-Aug 2011	Central Florida to central Virginia (Waring et al. 2014)	695	0.39	No	No
Jun-Aug 2011	Central Florida to lower Bay of Fundy, combined	2288	0.28	No	No
Jun-Aug 2004	Maryland to Bay of Fundy (Waring et al. 2006)	2607	0.57	No	Yes
Jun-Aug 2004	Florida to Maryland (Waring et al. 2006)	2197	0.47	No	Yes
Jun-Aug 2004	Florida to Bay of Fundy (Waring et al. 2006; Palka 2006)	4804	0.38	No	Yes
Jul-Sep 1998	Maryland to Gulf of St. Lawrence (only on-shelf in Nova Scotia) (Waring et al. 2006)	2848	0.49	No	Yes
Jul-Aug 1998	Florida to Maryland (Waring et al. 2006)	1181	0.51	Yes	Yes
Jul-Sep 1998	Florida to Gulf of St. Lawrence, combined	4029	0.38	Yes/No	Yes

Table 47: Estimated mean abundance within the study area. We selected the model marked with * as our best estimate of the abundance and distribution of this taxon. For comparison, independent abundance estimates from NOAA technical reports and/or the scientific literature are shown. Please see the Discussion section below for our evaluation of our models compared to the other estimates. Note that our abundance estimates are averaged over the whole year, while the other studies may have estimated abundance for specific months or seasons. Our coefficients of variation (CVs) underestimate the true uncertainty in our estimates, as they only incorporated the uncertainty of the GAM stage of our models. Other sources of uncertainty include the detection functions and g(0) estimates. It was not possible to incorporate these into our CVs without undertaking a computationally-prohibitive bootstrap; we hope to attempt that in a future version of our models.

Density Maps

Climatological Model

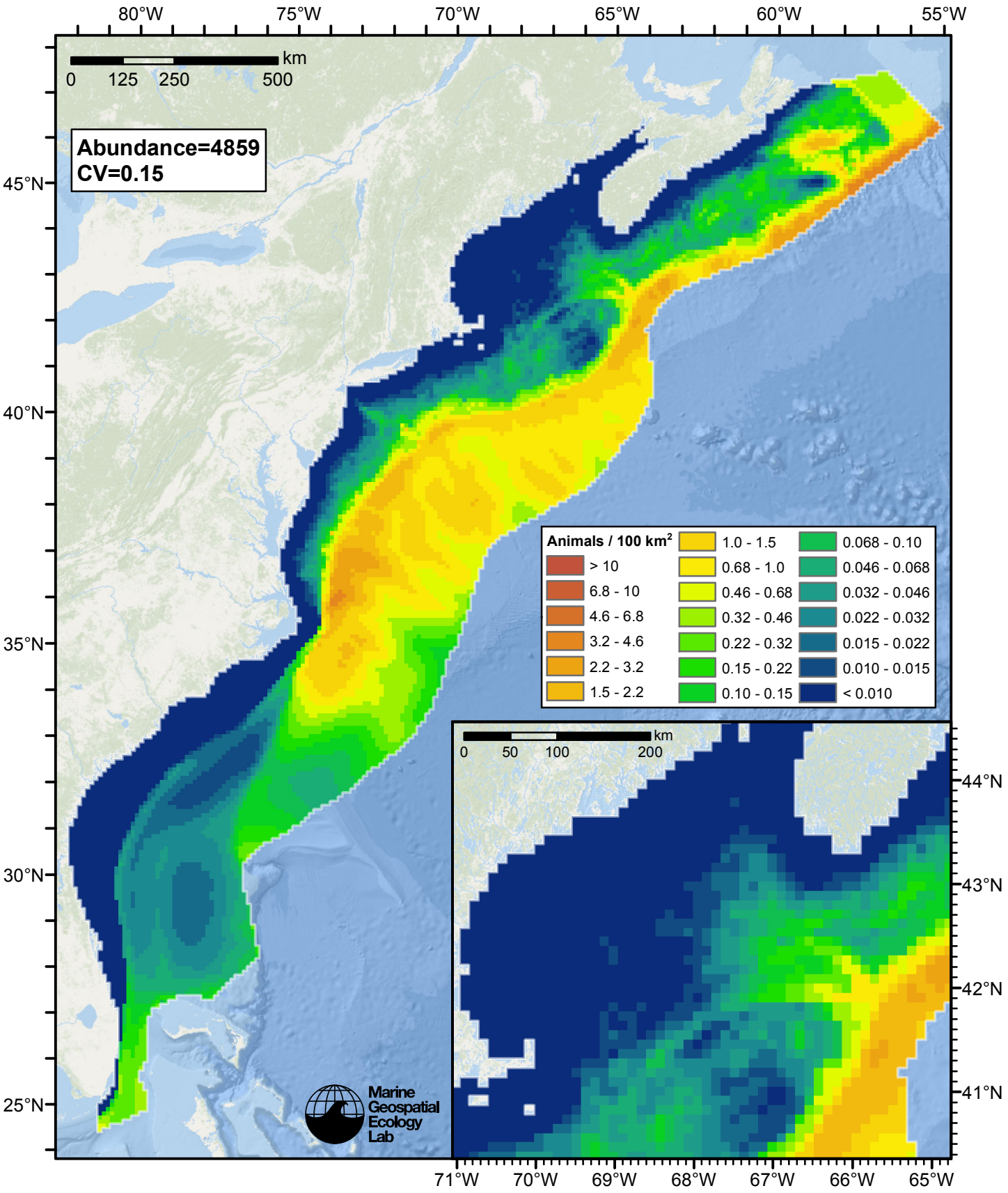

Figure 106: Sperm whale density and abundance predicted by the climatological model that explained the most deviance. Regions inside the study area (white line) where the background map is visible are areas we did not model (see text).

Contemporaneous Model

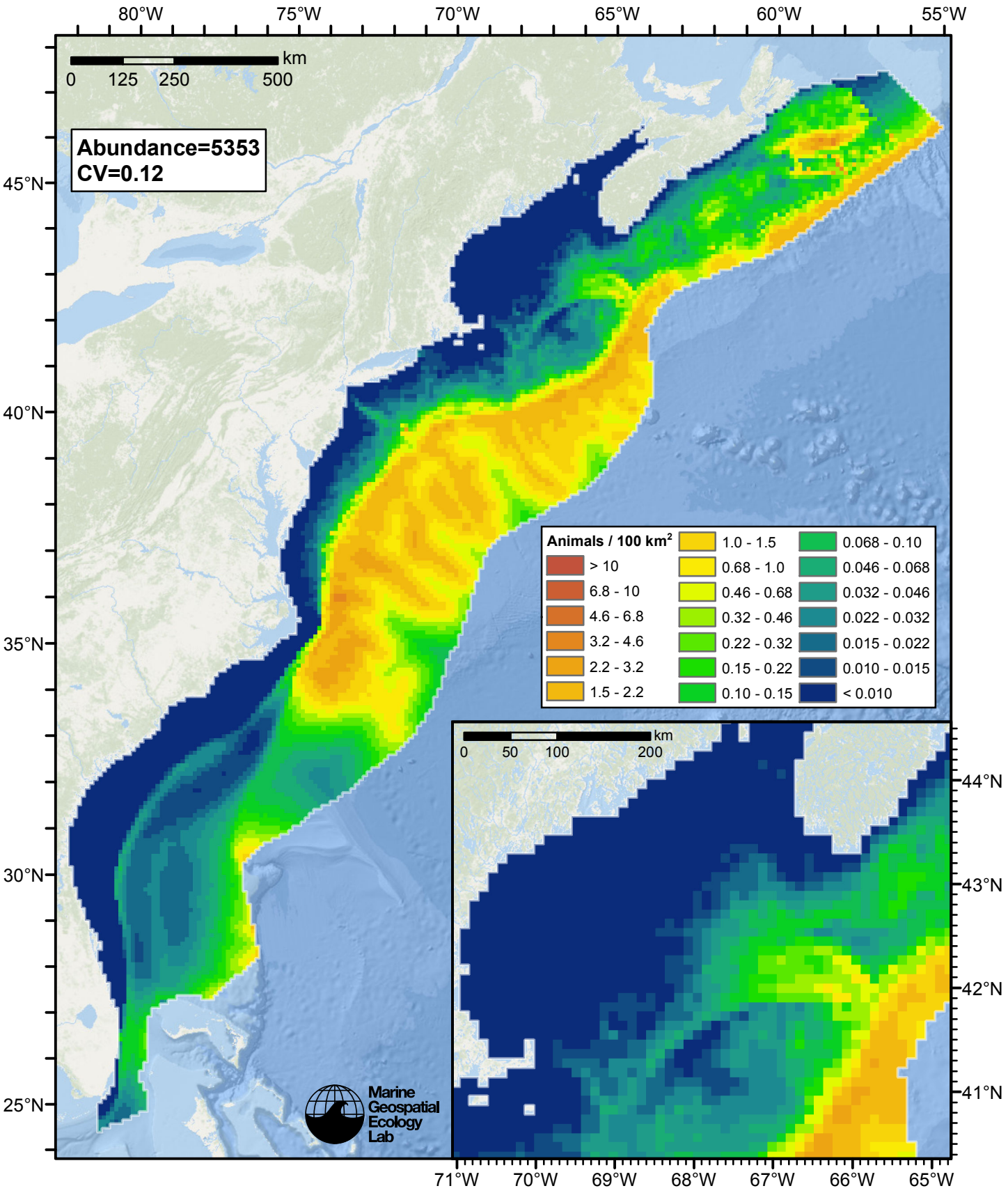

Figure 107: Sperm whale density and abundance predicted by the contemporaneous model that explained the most deviance. Regions inside the study area (white line) where the background map is visible are areas we did not model (see text).

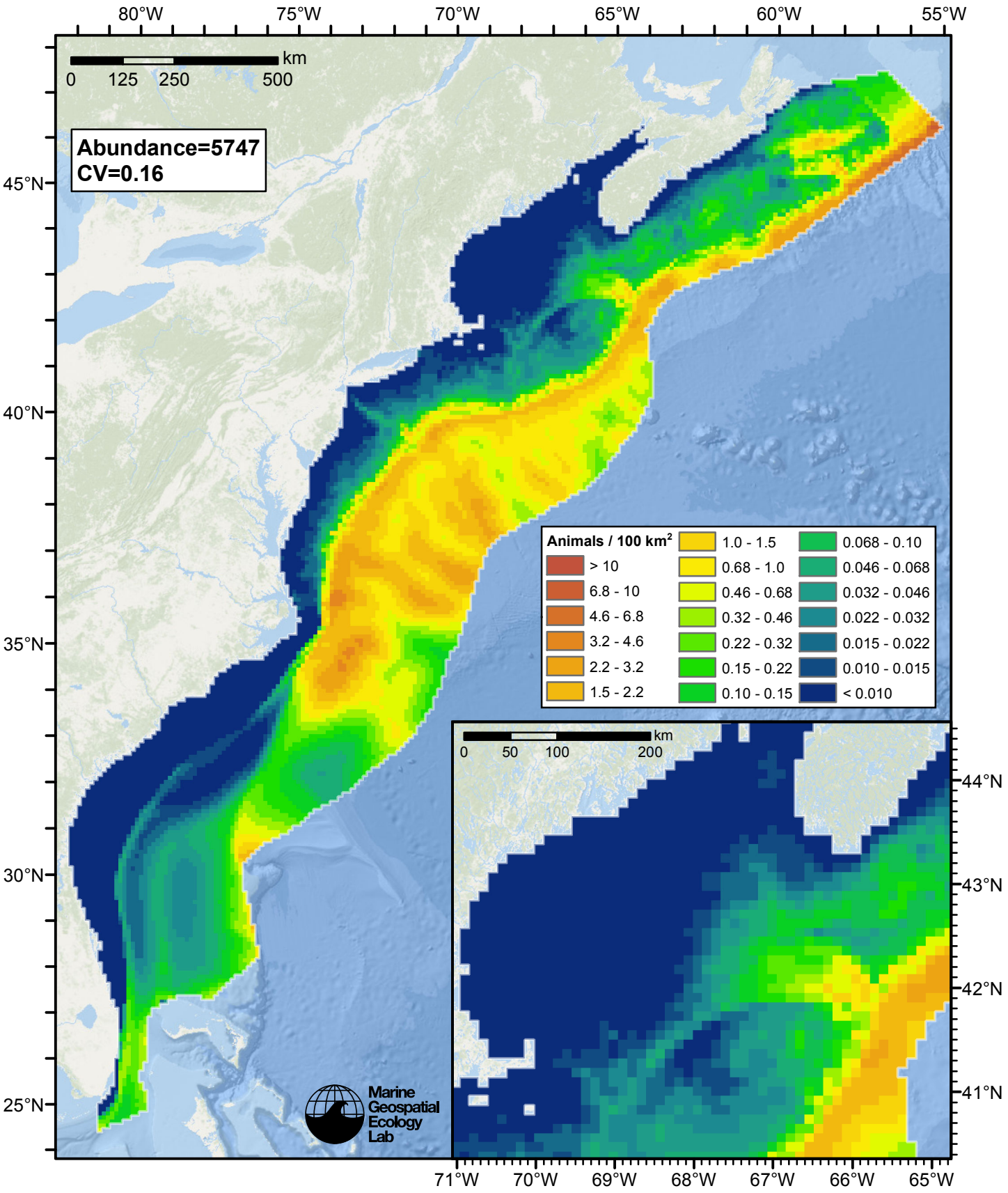

Figure 108: Sperm whale density and abundance predicted by the climatological same segments model that explained the most deviance. Regions inside the study area (white line) where the background map is visible are areas we did not model (see text).

Temporal Variability

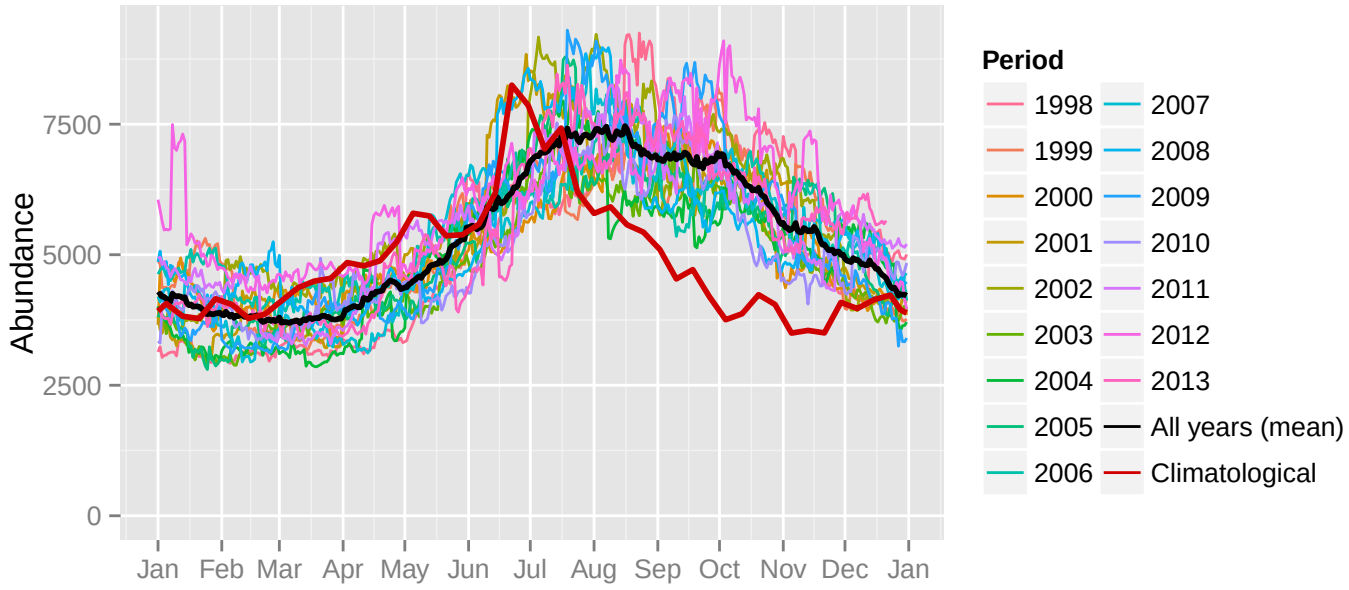

Figure 109: Comparison of Sperm whale abundance predicted at a daily time step for different time periods. Individual years were predicted using contemporaneous models. "All years (mean)" averages the individual years, giving the mean annual abundance of the contemporaneous model. "Climatological" was predicted using the climatological model. The results for the climatological same segments model are not shown.

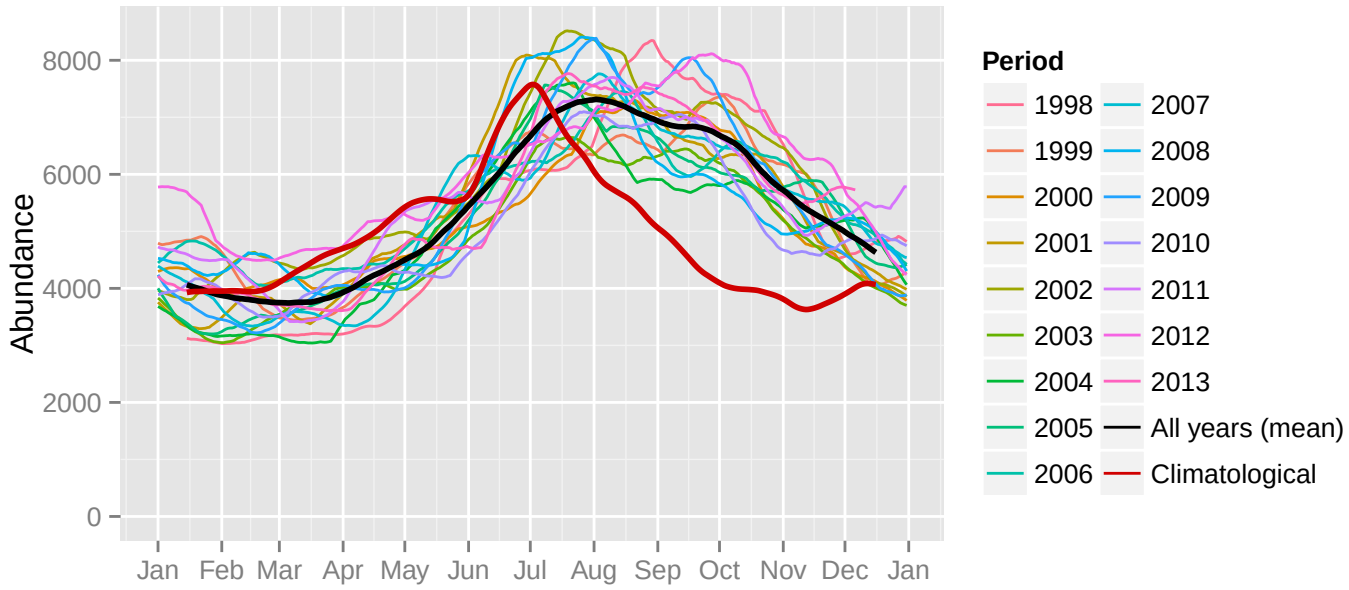

Figure 110: The same data as the preceding figure, but with a 30-day moving average applied.

Climatological Model

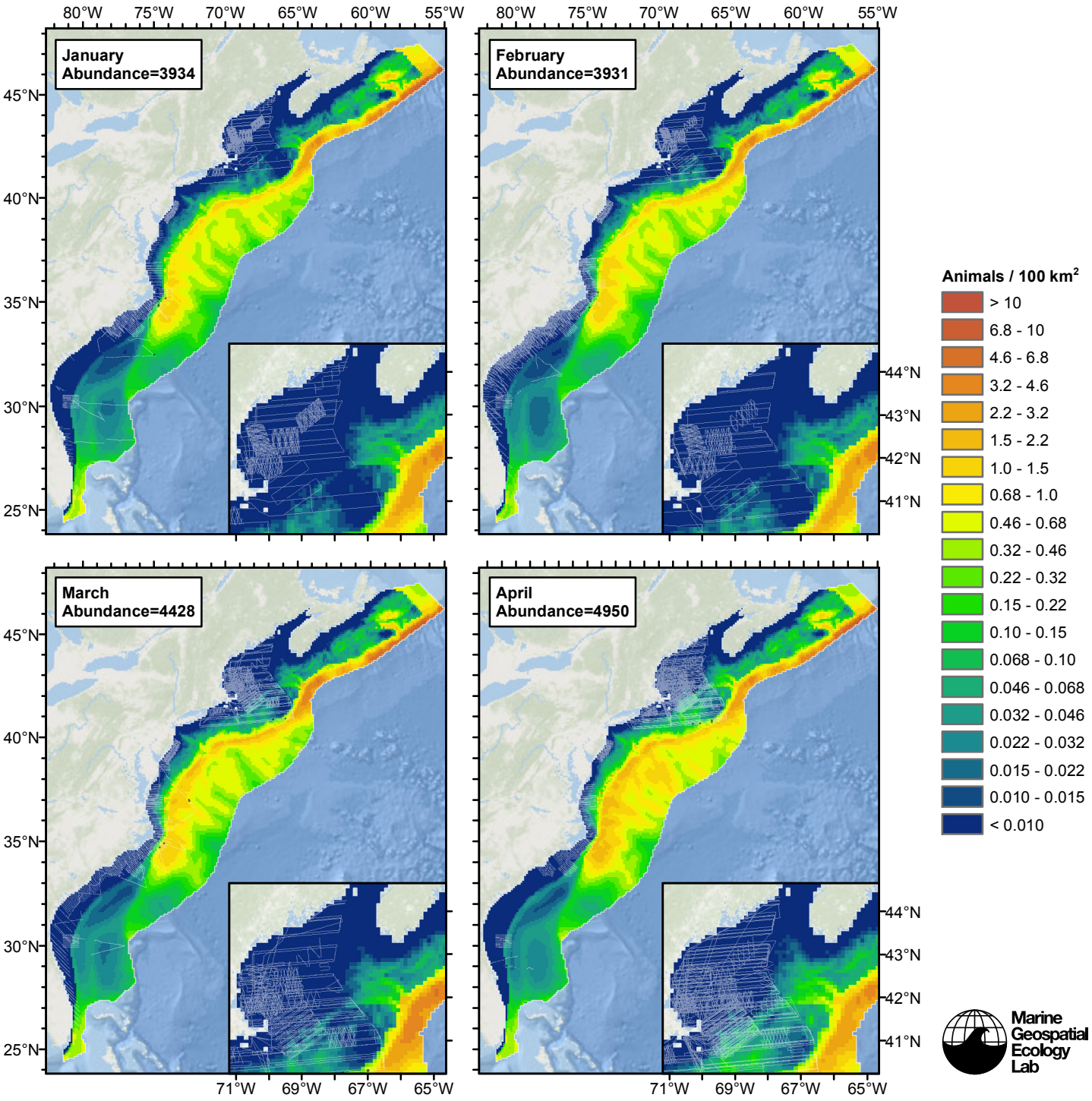

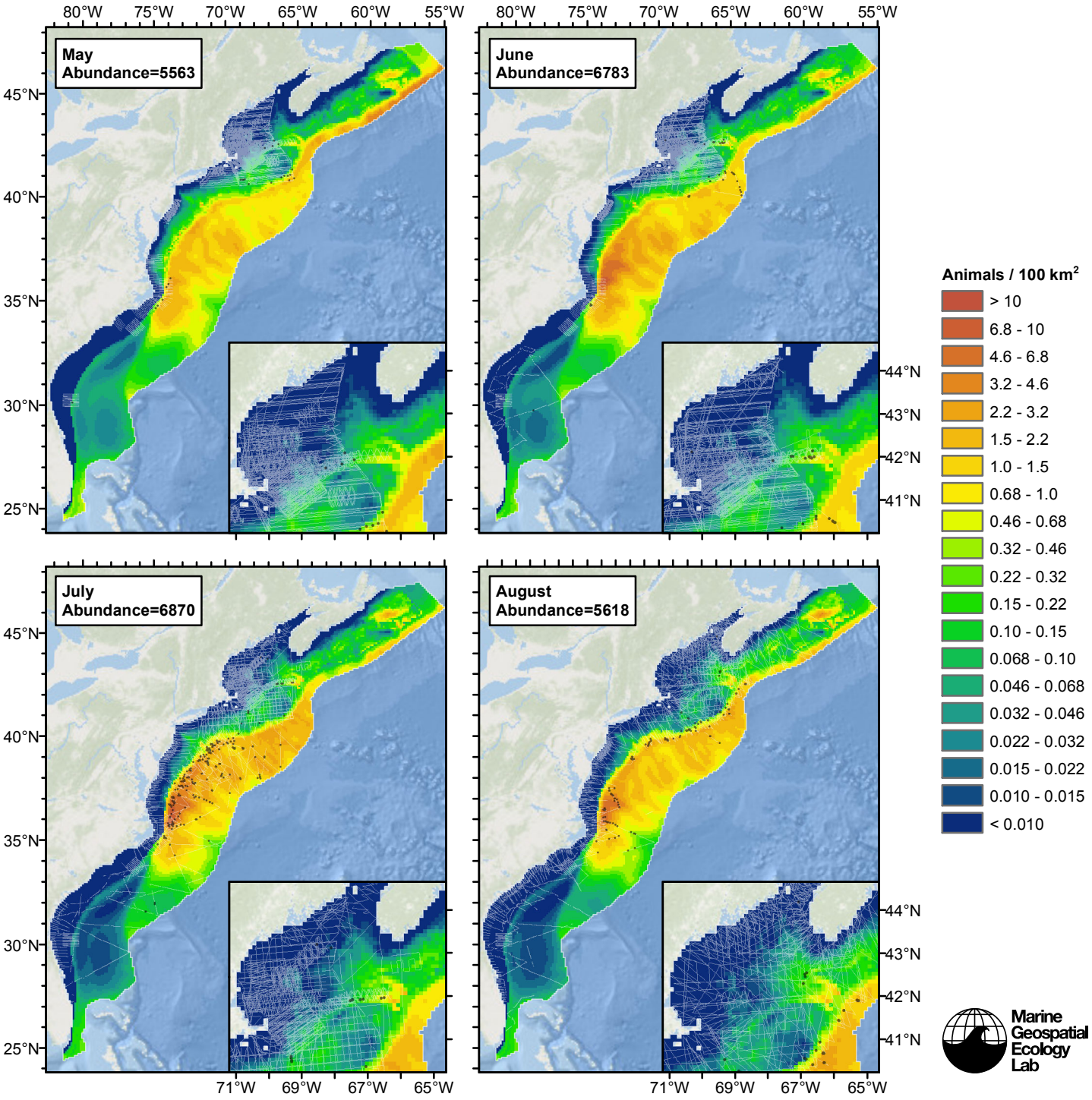
May
Abundance=5563
June
Abundance=6783
July
Abundance=6870
August
Abundance=5618
80°W
75°W
70°W
65°W
60°W
55°W
45°N
40°N
35°N
30°N
25°N
44°N
43°N
42°N
41°N
71°W
69°W
67°W
65°W
Animals / 100 km²
> 10
6.8 - 10
4.6 - 6.8
3.2 - 4.6
2.2 - 3.2
1.5 - 2.2
1.0 - 1.5
0.68 - 1.0
0.46 - 0.68
0.32 - 0.46
0.22 - 0.32
0.15 - 0.22
0.10 - 0.15
0.068 - 0.10
0.046 - 0.068
0.032 - 0.046
0.022 - 0.032
0.015 - 0.022
0.010 - 0.015
< 0.010
Marine
Geospatial
Ecology
Lab

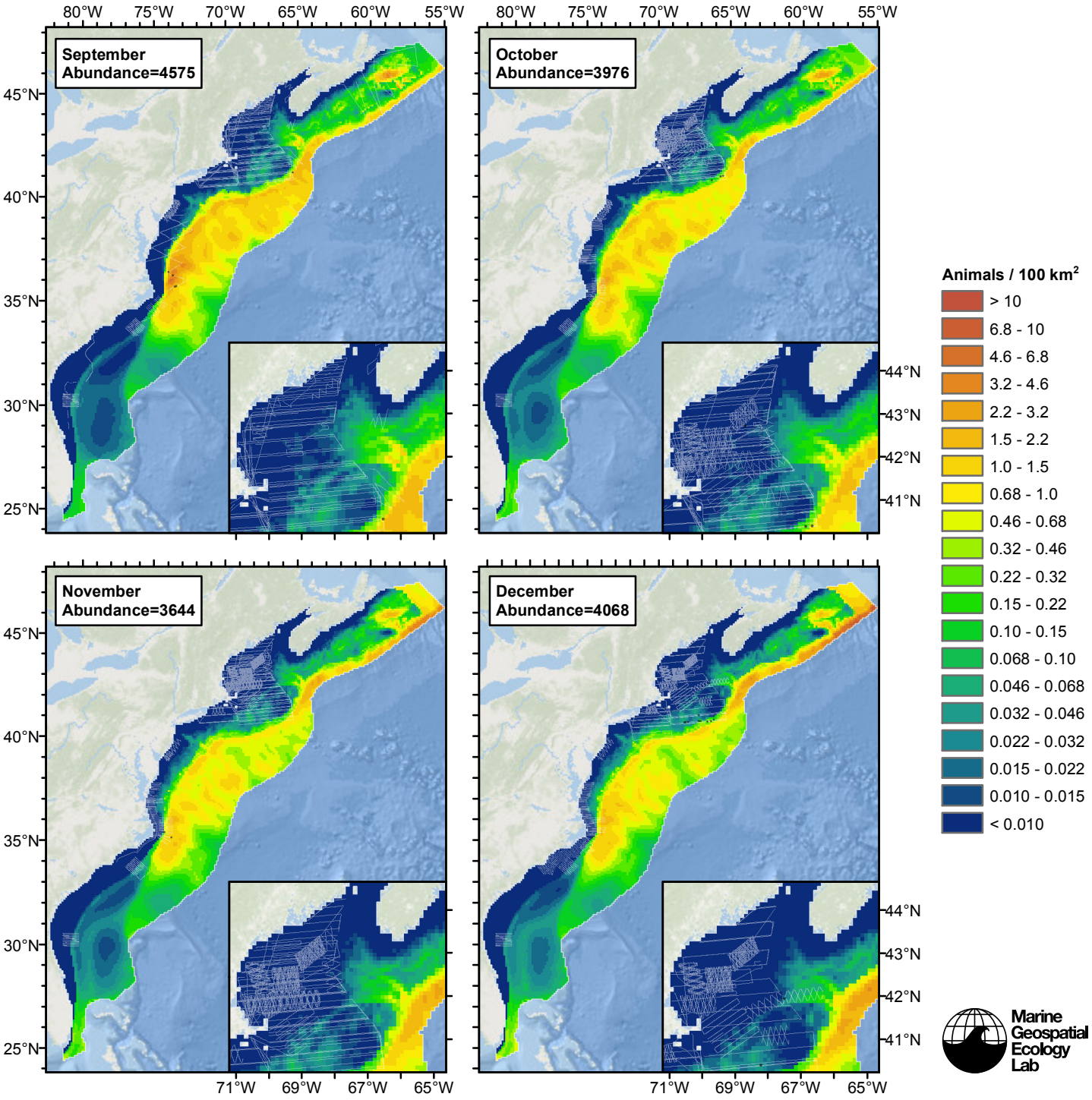
September
Abundance=4575
October
Abundance=3976
November
Abundance=3644
December
Abundance=4068
80°W
75°W
70°W
65°W
60°W
55°W
45°N
40°N
35°N
30°N
25°N
44°N
43°N
42°N
41°N
71°W
69°W
67°W
65°W
Animals / 100 km²
> 10
6.8 - 10
4.6 - 6.8
3.2 - 4.6
2.2 - 3.2
1.5 - 2.2
1.0 - 1.5
0.68 - 1.0
0.46 - 0.68
0.32 - 0.46
0.22 - 0.32
0.15 - 0.22
0.10 - 0.15
0.068 - 0.10
0.046 - 0.068
0.032 - 0.046
0.022 - 0.032
0.015 - 0.022
0.010 - 0.015
< 0.010
Marine
Geospatial
Ecology
Lab

Contemporaneous Model

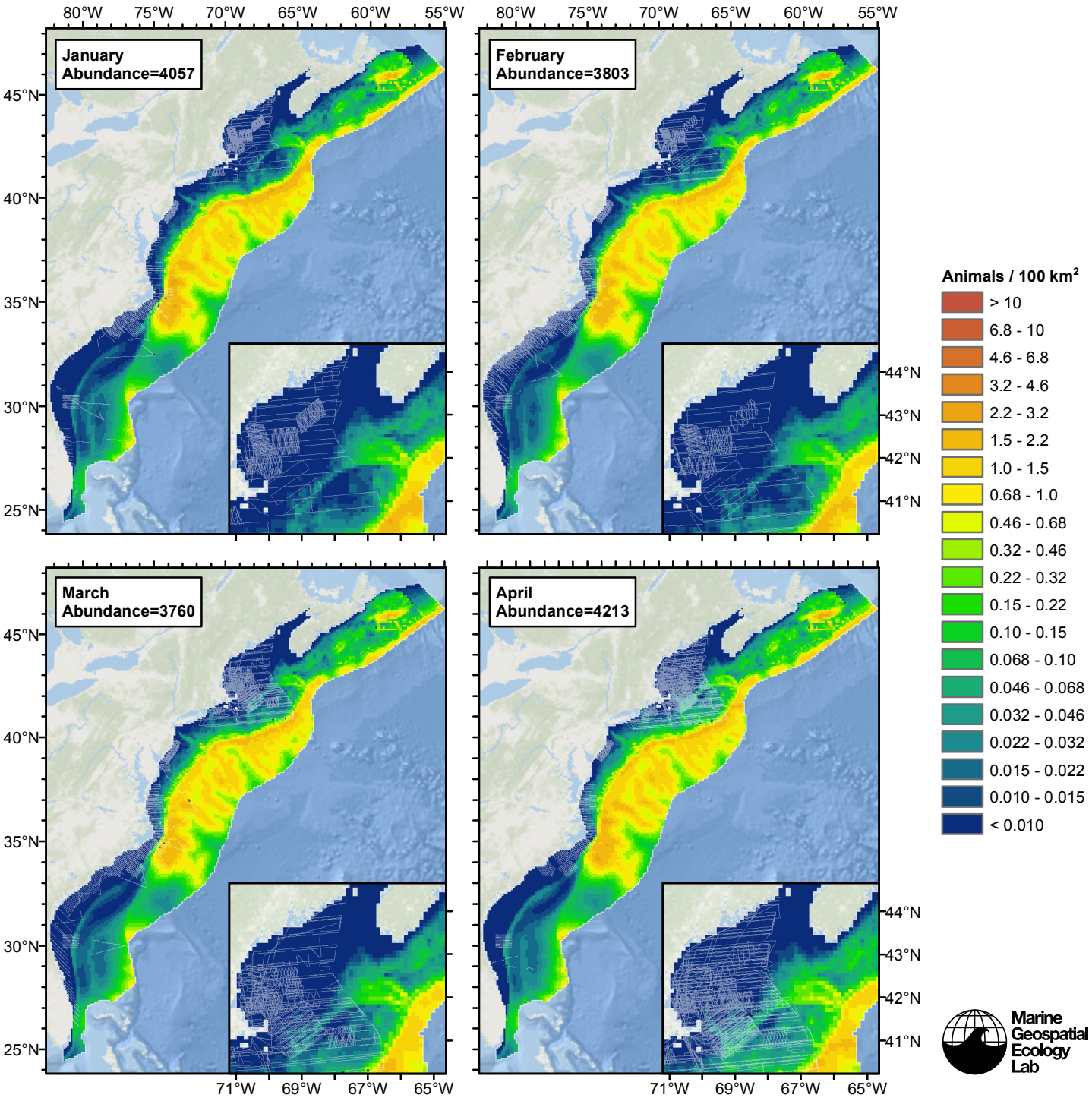

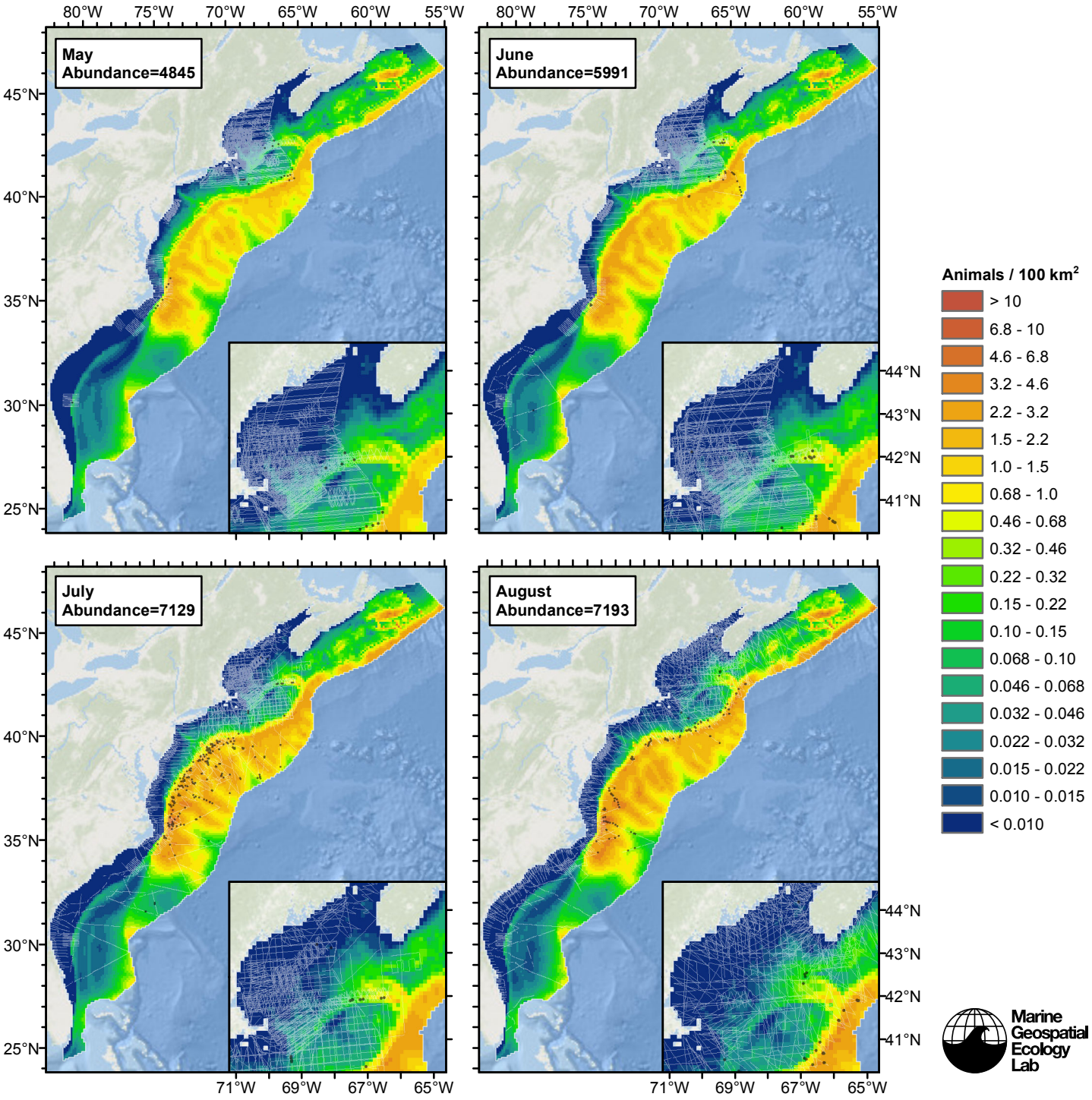
May
Abundance=4845
June
Abundance=5991
July
Abundance=7129
August
Abundance=7193
80°W
75°W
70°W
65°W
60°W
55°W
45°N
40°N
35°N
30°N
25°N
44°N
43°N
42°N
41°N
71°W
69°W
67°W
65°W
Animals / 100 km²
> 10
6.8 - 10
4.6 - 6.8
3.2 - 4.6
2.2 - 3.2
1.5 - 2.2
1.0 - 1.5
0.68 - 1.0
0.46 - 0.68
0.32 - 0.46
0.22 - 0.32
0.15 - 0.22
0.10 - 0.15
0.068 - 0.10
0.046 - 0.068
0.032 - 0.046
0.022 - 0.032
0.015 - 0.022
0.010 - 0.015
< 0.010
Marine
Geospatial
Ecology
Lab

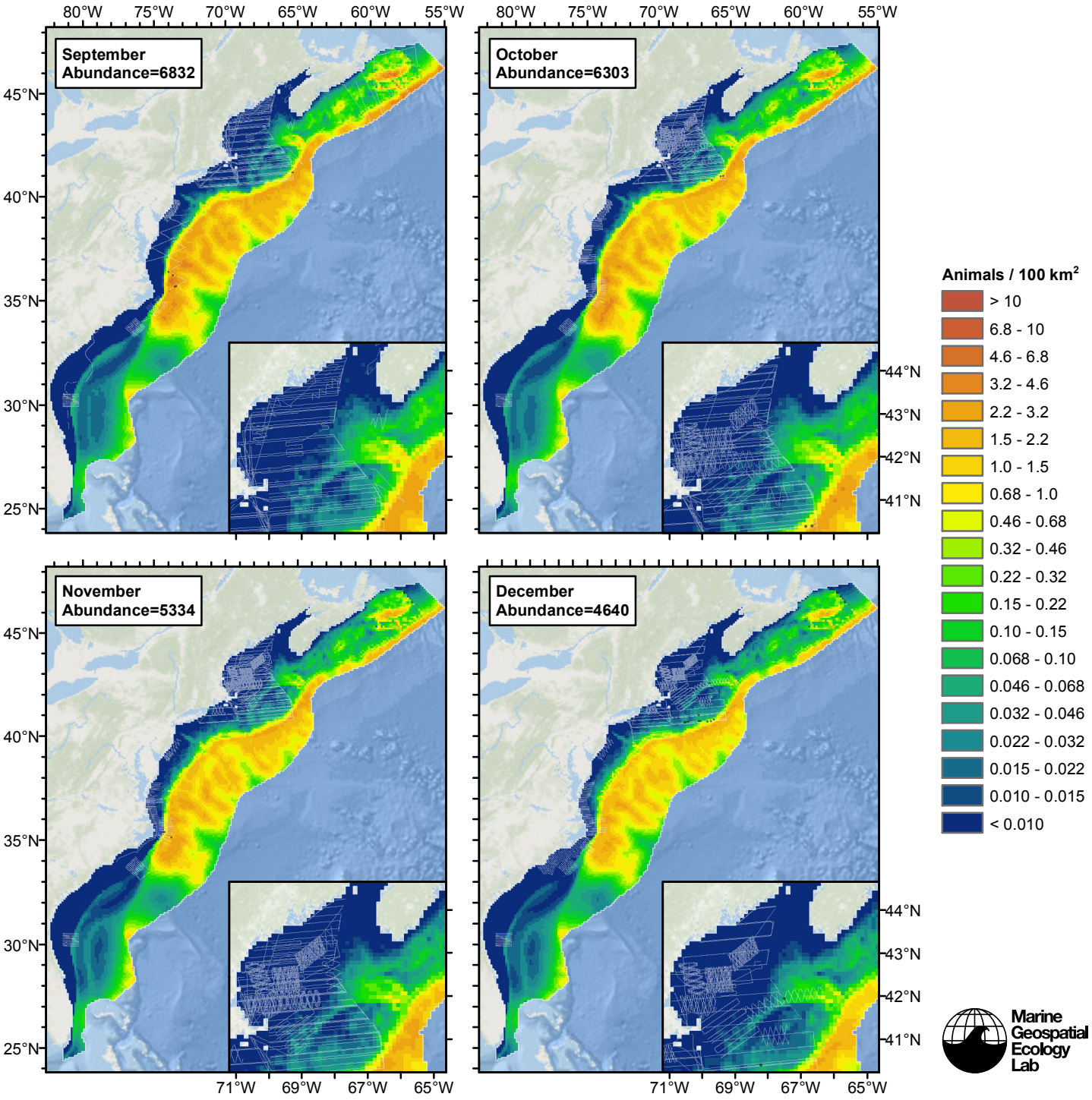
September
Abundance=6832
October
Abundance=6303
November
Abundance=5334
December
Abundance=4640
80°W
75°W
70°W
65°W
60°W
55°W
45°N
40°N
35°N
30°N
25°N
44°N
43°N
42°N
41°N
71°W
69°W
67°W
65°W
Animals / 100 km²
> 10
6.8 - 10
4.6 - 6.8
3.2 - 4.6
2.2 - 3.2
1.5 - 2.2
1.0 - 1.5
0.68 - 1.0
0.46 - 0.68
0.32 - 0.46
0.22 - 0.32
0.15 - 0.22
0.10 - 0.15
0.068 - 0.10
0.046 - 0.068
0.032 - 0.046
0.022 - 0.032
0.015 - 0.022
0.010 - 0.015
< 0.010
Marine
Geospatial
Ecology
Lab

Climatological Same Segments Model

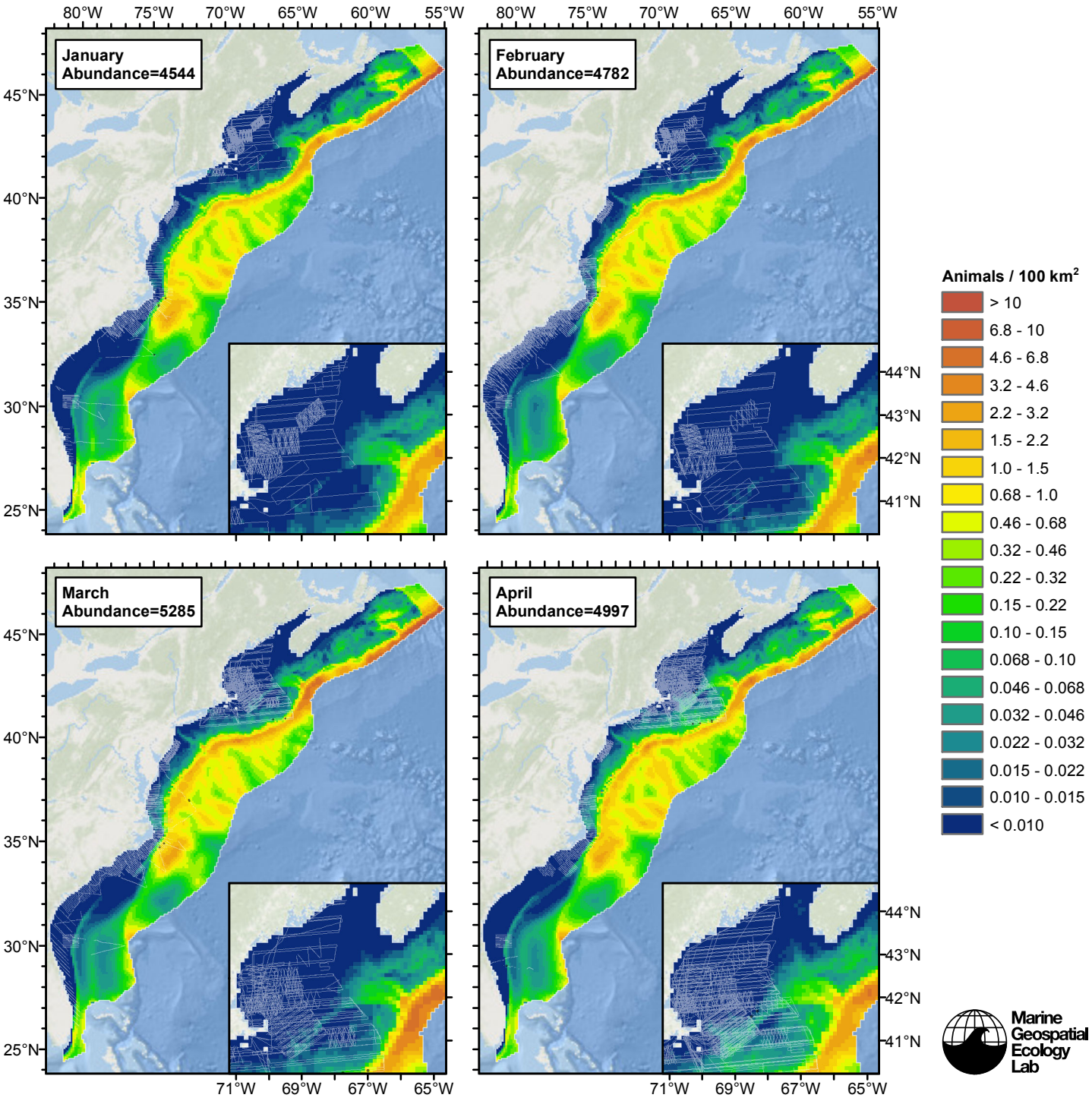

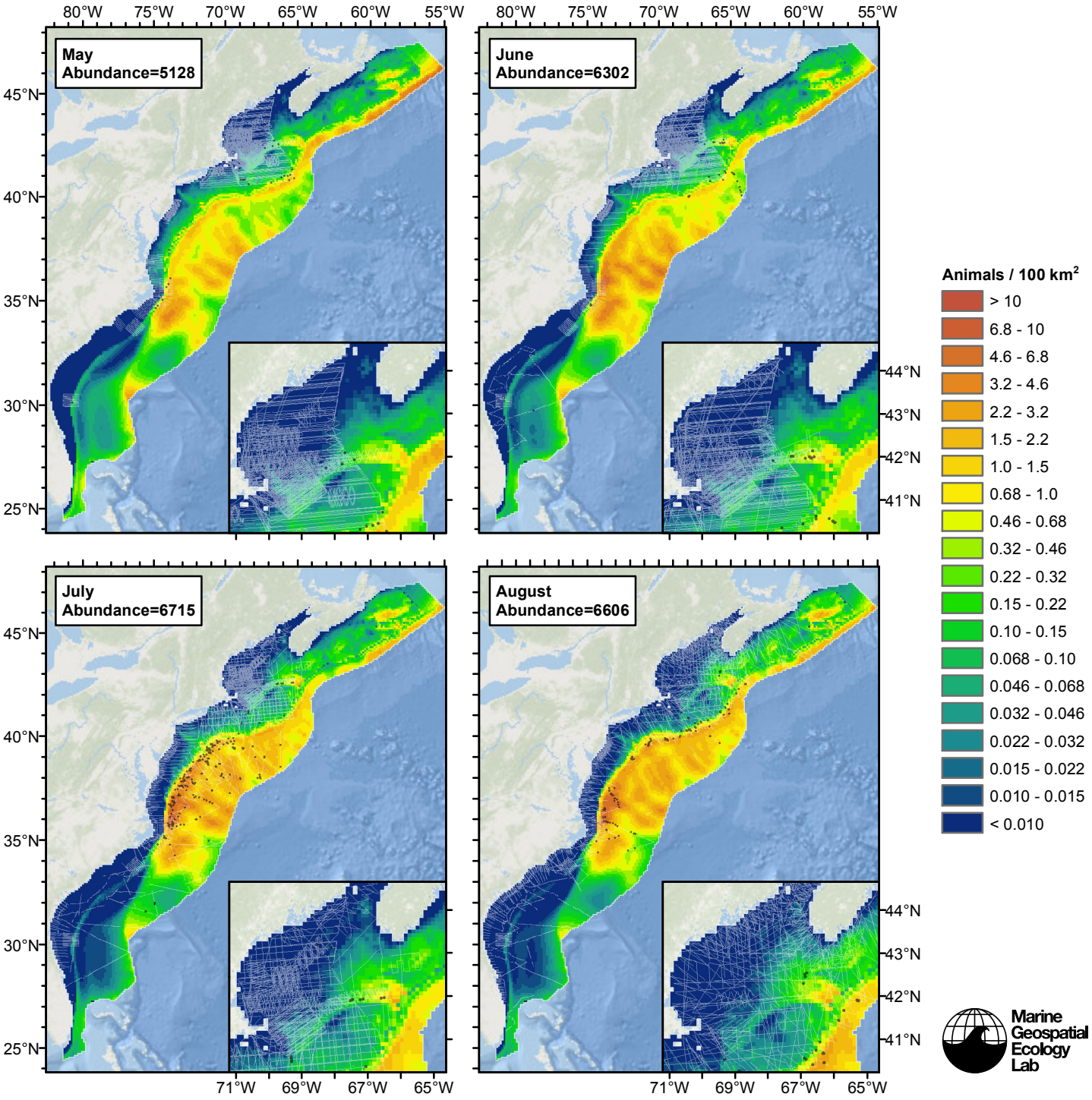
May
Abundance=5128
June
Abundance=6302
July
Abundance=6715
August
Abundance=6606
80°W
75°W
70°W
65°W
60°W
55°W
45°N
40°N
35°N
30°N
25°N
44°N
43°N
42°N
41°N
71°W
69°W
67°W
65°W
Animals / 100 km²
> 10
6.8 - 10
4.6 - 6.8
3.2 - 4.6
2.2 - 3.2
1.5 - 2.2
1.0 - 1.5
0.68 - 1.0
0.46 - 0.68
0.32 - 0.46
0.22 - 0.32
0.15 - 0.22
0.10 - 0.15
0.068 - 0.10
0.046 - 0.068
0.032 - 0.046
0.022 - 0.032
0.015 - 0.022
0.010 - 0.015
< 0.010
Marine
Geospatial
Ecology
Lab

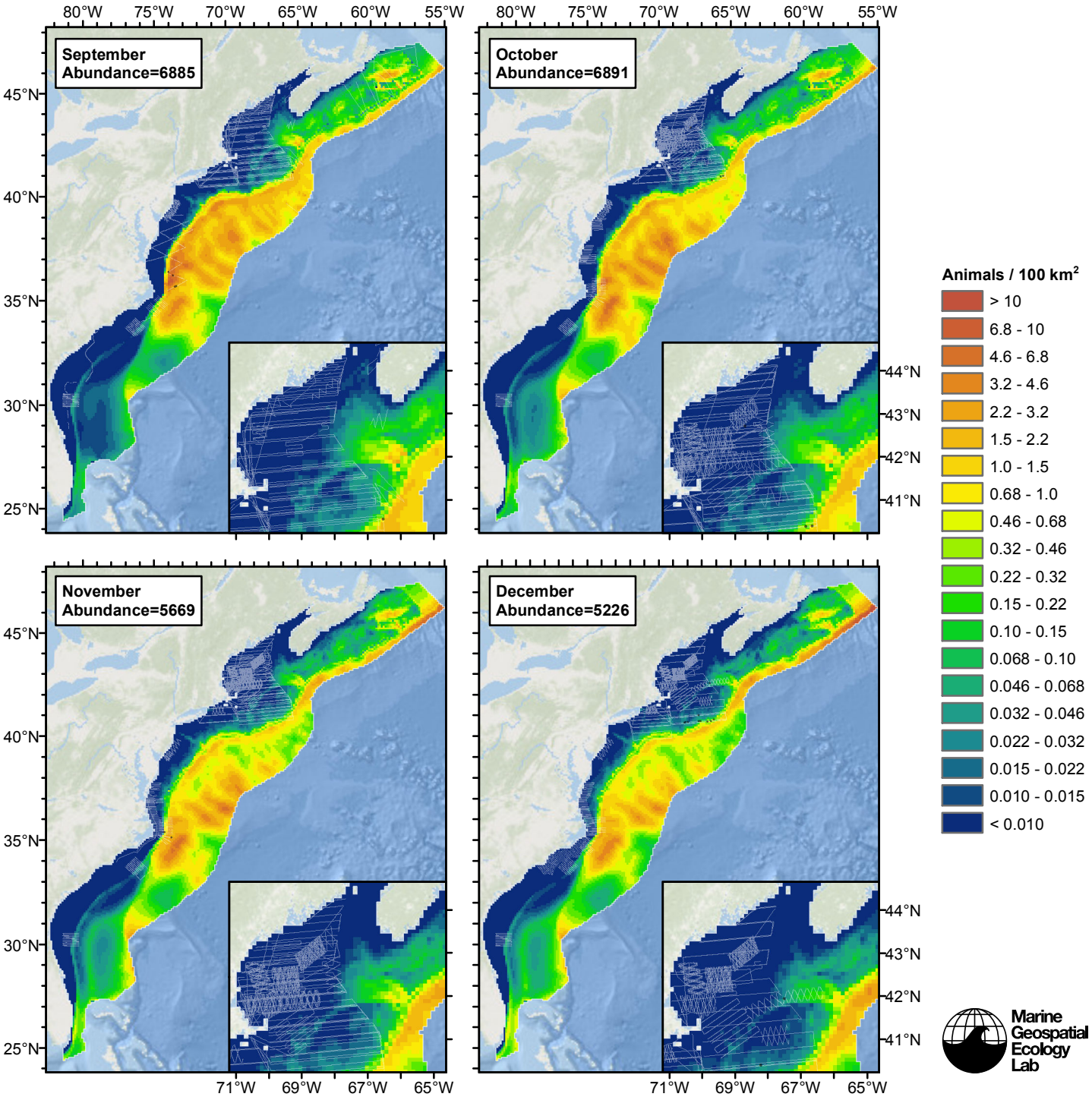

Discussion

The large majority of sperm whales were sighted in the Slope and Abyss region of our study area. Here, the climatological models achieved slightly better fits than the contemporaneous models, explaining 0.5-1.2% more deviance, suggesting that climatological predictors are slightly more suitable for modeling sperm whales in this region. In the Shelf region, where sperm whales were much less frequently sighted, the contemporaneous models achieved better fits, explaining up to 2.2% more deviance.

All of the models predicted high abundance along the shelf break and near submarine canyons, consistent with what has been reported in the literature. All of the models reproduced Waring et al.'s (2014) description of sperm whales residing of Cape Hatteras in the winter, then expanding their distribution northward in the summer. The climatological models, despite

achieving better fits, predicted what we believe to be an implausible seasonal cycle in the far north of the study area, in a narrow strip off the shelf of Nova Scotia. Here, predicted abundance is highest in winter months, roughly November-May, and lowest in summer months, June-October (see Temporal Variability section above). This seems contrary to the pattern suggested for the mid-Atlantic by Waring et al. Also, this strip off the Nova Scotia shelf is an area of high standard error in the climatological models (Figures 77, 97), probably due to receiving relatively low survey effort.

The contemporaneous models did not predict this suspicious seasonal pattern or exhibit as high standard error in the region. Instead they predicted a high-in-summer, low-in-winter pattern, similar to that predicted for the mid-Atlantic region. Although we do not find the pattern displayed by the climatological models to be impossible–it could happen if sperm whales north of the study area retreat south to Nova Scotia to overwinter– we find the contemporaneous model's predictions more plausible. For this reason, we selected the contemporaneous model's predictions as our best estimate of sperm whale distribution and abundance.

The model predicted a seasonal variation in abundance, ranging from about 3750 in March to about 7200 in August. Waring et al. (2014) reported that the center of sperm whale distribution shifts north in spring and summer, then south in winter. Wong and Whitehead (2014) reported that sperm whales were more prevalent around Kelvin Seamount, just east of our study area, in spring (April-June) compared to winter (November-March). Our model is consistent with these findings that sperm whale abundance is higher in summer than winter. To reflect that finding, we recommend that our monthly predictions be used for federal regulatory purposes and marine spatial planning applications. However we caution that off-shelf regions have been relatively poorly surveyed in non-summer seasons, and that sperm whales exhibit complex social dynamics that may impede attempts to model the entire population as a single unit, as we have done. We strongly recommend additional surveying be performed in non-summer months off the shelf to better reveal seasonal patterns in sperm whale abundance.

We note in passing that in the Slope and Abyss region, the inclusion of productivity predictors failed to improve the models. In the climatological model that considered all segments, all of the productivity predictors were discarded during model selection. In the other two models, productivity predictors were not discarded, but the models that included them explained less deviance than those that did not. This suggests that those predictors were not important enough to mitigate the incremental difficulty in modeling the subset of segments for which those predictors were available.

In the Shelf region, this situation did not occur; the inclusion of productivity predictors improved all models, explaining 3.0-4.5% more deviance. For the contemporaneous and climatological same segments models, this result must be viewed cautiously, as the models that considered productivity predictors used a subset of the segments used by the models that did not consider productivity predictors. But for the climatological model that used all segments, the explained deviance statistic is directly comparable between models that considered different predictors. In this case, the inclusion of productivity predictors resulted in models that explained 4.5% more deviance, a clear improvement.

References

Barlow J, Oliver CW, Jackson TD, Taylor BL (1988) Harbor Porpoise, Phocoena phocoena, Abundance Estimation for California, Oregon, and Washington: II. Aerial Surveys. Fishery Bulletin 86: 433-444.

Barlow J, Sexton S (1996) The effect of diving and searching behavior on the probability of detecting track-line groups, g(0), of long-diving whales during line transect surveys. NOAA National Marine Fisheries Service, Southwest Fisheries Center Administrative Report LJ-96-14. 21 pp.

CETAP (1982) A characterization of marine mammals and turtles in the mid-and north Atlantic areas of the US outer continental shelf. Final Report. Bureau of Land Management, Washington, DC. Ref. AA551-CT8-48.

Carretta JV, Lowry MS, Stinchcomb CE, Lynn MS, Cosgrove RE (2000) Distribution and abundance of marine mammals at San Clemente Island and surrounding offshore waters: results from aerial and ground surveys in 1998 and 1999. Administrative Report LJ-00-02, available from Southwest Fisheries Science Center, P.O. Box 271, La Jolla, CA USA 92038. 44 p.

Debich AJ, Baumann-Pickering A, Sirovic A, Buccowich JS, Gentes ZE, et al. (2014) Passive Acoustic Monitoring for Marine Mammals in the Cherry Point OPAREA 2011-2012. MPL Technical Memorandum #545. Marine Physical Laboratory, Scripps Institution of Oceanography, University of California San Diego, La Jolla, California. 83 p. Available online: http://www.navymarinespeciesmonitoring.us/index.php/download_file/view/660/

Debich AJ, Baumann-Pickering A, Sirovic A, Kerosky SA, Roche LK, et al. (2013) Passive Acoustic Monitoring for Marine Mammals in the Jacksonville Range Complex 2010-2011. MPL Technical Memorandum #541. Marine Physical Laboratory, Scripps Institution of Oceanography, University of California San Diego, La Jolla, California. 57 p. Available online: http://www.navymarinespeciesmonitoring.us/index.php/download_file/view/465/

Griffin RB (1999) Sperm whale distributions and community ecology associated with a warm-core ring of Georges Bank. Marine Mammal Science 15: 33-51.

Hodge L, Reed A (2014) Passive Acoustic Monitoring for Marine Mammals in Onslow Bay (multiple documents). Reports by the Duke University Marine Laboratory, Beaufort, North Carolina. Available online: http://www.navymarinespeciesmonitoring.us/reading-room/atlantic/ under Technical Reports.

Norris TF, Oswald JO, Yack TM, Ferguson EL (2014) An Analysis of Marine Acoustic Recording Unit (MARU) Data Collected off Jacksonville, Florida in Fall 2009 and Winter 2009-2010. Final Report. Submitted to Naval Facilities Engineering Command (NAVFAC) Atlantic, Norfolk, Virginia, under Contract No. N62470-10-D-3011, Task Order 021, issued to HDR Inc., Norfolk, Virginia. Prepared by Bio-Waves Inc., Encinitas, CA. 21 November 2012. Revised January 2014.

Palka DL (2006) Summer Abundance Estimates of Cetaceans in US North Atlantic Navy Operating Areas. US Dept Commer, Northeast Fish Sci Cent Ref Doc. 06-03: 41 p.

Scott TM, Sadove SS (1997) Sperm whale, Physeter macrocephalus, sightings in the shallow shelf waters off Long Island, New York. Marine Mammal Science 13: 317-321.

Waring GT, Fairfield CP, Ruhsam CM, Sano M (1993) Sperm whales associated with Gulf Stream features off the northeastern USA shelf. Fisheries Oceanography 2: 101-105.

Waring GT, Hamazaki T, Sheehan D, Wood G, Baker S (2001) Characterization of beaked whale (Ziphiidae) and sperm whale (Physeter macrocephalus) summer habitat in shelf-edge and deeper waters off the northeast U.S. Marine Mammal Science 17: 703-717.

Waring GT, Josephson E, Fairfield CP, Maze-Foley K, ds. (2006) U.S. Atlantic and Gulf of Mexico Marine Mammal Stock Assessments – 2005. NOAA Tech Memo 194.

Waring GT, Josephson E, Maze-Foley K, Rosel PE, eds. (2014) U.S. Atlantic and Gulf of Mexico Marine Mammal Stock Assessments – 2013. NOAA Tech Memo NMFS NE 228; 464 p.

Watwood SL, Miller PJO, Johnson M, Madsen PT, Tyack PL (2006) Deep-diving foraging behaviour of sperm whales (Physeter macrocephalus). Journal of Animal Ecology 75:814-825.

Whitehead H (2002) Estimates of the current global population size and historical trajectory for sperm whales. Mar Ecol Prog Ser. 242: 295-304.

Whitehead H, Brennan S, Grover D (1992) Distribution and behaviour of male sperm whales on the Scotian Shelf, Canada. Canadian Journal of Zoology 70: 912-918.

Wong SNP, Whitehead H (2014) Seasonal occurrence of sperm whales (Physeter macrocephalus) around Kelvin Seamount in the Sargasso Sea in relation to oceanographic processes. Deep Sea Research Part I 91: 10-16.